CANADIAN THESES

THÈSES CANADIENNES

Canada

TC –

IS   0-315-23243-9

CANADIAN THESES ON MICROFICHE SERVICE – SERVICE DES THÈSES CANADIENNES SUR MICROFICHE

PERMISION TO MICROFILM – AUTORISATION DE MICROFILMER

• Please print or type – Écrire en lettres moulées ou dactylographier

AUTHOR – AUTEUR

Full Name of Author – Nom complet de l'auteur

Monty Leigh Proctor

Date of Birth – Date de naissance

Dec. 27, 1960

Canadian Citizen – Citoyen canadien

☑ Yes Oui   ☐ No Non

Country of Birth – Lieu de naissance

Canada

Permanent Address – Résidence fixe

*3211-112 Avenue
Edmonton, Alberta
T5W 0M1*

THESIS – THÈSE

Title of Thesis – Titre de la thèse

Steam Injection Experiments in a Scaled Physical Model.

Degree for which thesis was presented
Grade pour lequel cette thèse fut présentée

M. Sc. (Petroleum Engineering)

Year this degree conferred
Année d'obtention de ce grade

1985

University – Université

University of Alberta

Name of Supervisor – Nom du directeur de thèse

Dr. S.M. Farouq Ali

AUTHORIZATION – AUTORISATION

Permission is hereby granted to the NATIONAL LIBRARY OF CANADA to **microfilm this thesis and to lend or sell copies of the film.**

The author reserves other publication rights, and neither the thesis nor extensive extracts from it may be printed or otherwise reproduced without the author's written permission.

L'autorisation est, par la présente, accordée à la BIBLIOTHÈQUE NATIONALE DU CANADA de **microfilmer** cette thèse et de **prêter** ou de **vendre des exemplaires du film.**

L'auteur se réserve les autres droits de publication; ni la thèse ni de longs extraits de celle-ci ne doivent être imprimés ou autrement reproduits sans l'autorisation écrite de l'auteur.

▶ ATTACH FORM TO THESIS – VEUILLEZ JOINDRE CE FORMULAIRE À LA THÈSE ◀

Signature
Monty Proctor

Date
October 15, 1985

NL-91 (r 84/03)

Canada

THE UNIVERSITY OF ALBERTA

STEAM INJECTION EXPERIMENTS IN A SCALED PHYSICAL MODEL

by

MARTY L. PROCTOR

A THESIS

SUBMITTED TO THE FACULTY OF GRADUATE STUDIES AND RESEARCH

IN PARTIAL FULFILMENT OF THE REQUIREMENTS FOR THE DEGREE

OF MASTER OF SCIENCE

IN

PETROLEUM ENGINEERING

DEPARTMENT OF MINERAL ENGINEERING

EDMONTON, ALBERTA

FALL, 1985

THE UNIVERSITY OF ALBERTA

RELEASE FORM

NAME OF AUTHOR

    MARTY L. PROCTOR

TITLE OF THESIS

    STEAM INJECTION EXPERIMENTS IN A SCALED PHYSICAL MODEL

DEGREE FOR WHICH THESIS WAS PRESENTED   MASTER OF SCIENCE

YEAR THIS DEGREE GRANTED   FALL, 1985

       Permission is hereby granted to THE UNIVERSITY OF ALBERTA LIBRARY to reproduce single copies of this thesis and to lend or sell such copies for private, scholarly or scientific research purposes only.

       The author reserves other publication rights, and neither the thesis nor extensive extracts from it may be printed or otherwise reproduced without the author's written permission.

(SIGNED) ....

PERMANENT ADDRESS:

3711 - 112 Avenue

Edmonton, Alberta

T5W 0M1

DATED October 2, 1985

THE UNIVERSITY OF ALBERTA

FACULTY OF GRADUATE STUDIES AND RESEARCH

The undersigned certify that they have read, and
recommend to the Faculty of Graduate Studies and Research,
for acceptance, a thesis entitled STEAM INJECTION
EXPERIMENTS IN A SCALED PHYSICAL MODEL submitted by MARTY L.
PROCTOR in partial fulfilment of the requirements for the
degree of MASTER OF SCIENCE in PETROLEUM ENGINEERING.

....
                    Supervisor

....

....

....

Date... October 2, 1985

To My Parents, John and Gayle,
and to My Wife, Pam,
For Their Endless Support and Encouragement.

ABSTRACT

This research was directed toward a study of steam injection processes and was comprised of experiments conducted in a scaled physical model, under a wide variety of conditions.

A large part of the work was devoted to the design and construction of the scaled model apparatus used to conduct the steam injection experiments. The apparatus was designed to represent one-quarter of an eight hectare (twenty acre) five-spot pattern and the scaling was based upon low pressure scaling criteria.

A number of steamflood experiments were carried out to show the use of the apparatus and the efficacy of the processes under investigation. The main target of the experimental studies was the Aberfeldy heavy oil reservoir of the Lloydminster area. This reservoir is characterized by a viscous oil (1275 mPa·s at reservoir temperature) and thin pay. Bottom water is present in parts of the reservoir. To examine the recovery potential of the Aberfeldy prototype, several types of experiments were conducted, including continuous steamfloods in homogeneous packs, a continuous steamflood in a bottom water pack, slug runs in homogeneous packs, and a steamflood following a waterflood.

The steam slug runs in the model representing the Aberfeldy reservoir, which entailed the injection of a small volume of steam followed by the continuous injection of cold water, gave favorable results, generally better than the continuous steamflood runs. Judging from these experiments,

the steam slug process would appear to be a viable recovery technique for the Aberfeldy reservoir.

As expected, bottom water had a very detrimental effect on the efficiency of a conventional steamflood, with oil recovery in one run being one-tenth of the recovery experienced in the continuous steamflood experiments. A steamflood following a waterflood in the Aberfeldy model without bottom water, produced a low incremental recovery of 5.9% of the original oil in place (8.1% of the waterflood residual oil saturation).

The possibility of steamflooding a conventional oil reservoir, to improve the ultimate oil recovery, appears to warrant further investigation. Experiments conducted in a model of a light oil prototype yielded the highest oil recovery of all experiments carried out in this research. Recoveries of 36% of the original oil in place were predicted for a prototype thickness of eleven meters. Future experiments designed to examine the steamflood recovery response from a conventional oil reservoir should include an examination of the effect of oil saturation, because reservoirs of this type will normally be waterflooded first.

ACKNOWLEDGEMENTS

Table of Contents

List of Tables

List of Figures

List of Plates

xviii

1. INTRODUCTION

Steam injection has been widely successful in North America for the recovery of heavy oil. It currently accounts for over 78% of all oil produced in the world by enhanced recovery methods[1]. The form of steam injection which has had greatest success in Canada (Cold Lake) is cyclic steam stimulation, although recoveries are limited to less than 20%.

The emphasis in this work was on steamflooding, which is normally the second stage process after cyclic steam stimulation. In California heavy oil reservoirs, steamflooding has resulted in oil recoveries of as much as 77% (San Ardo), with 55-60% being commonplace (Kern River).

Steamflooding is dependent on achieving communication between injection and production wells. This is more difficult to achieve in Canadian heavy oil reservoirs than in California because of low reservoir temperatures which preclude primary production, and because of excessive heat losses in thin formations. However, steamflooding is now succeeding in Lloydminster reservoirs which were previously considered to be unsuitable for this method of enhanced recovery.

Other studies[2,3] have shown that steamflooding may be a viable method of recovering waterflood residual oil from light oil or moderately viscous oil reservoirs. Farouq Ali[2] suggests that the product of the rock porosity and the oil saturation must be greater than 0.10 for a steamflood project to be economically successful. He lists several conventional oil fields in Alberta and Saskatchewan as

possible candidates for steamflood operations based on data from the Energy Resources Conservation Board of Alberta. These fields include Acheson, Fenn-Big Valley, Golden Spike, Pembina, Red Water, Turner Valley, Wizard Lake, and Steelman.

Generally, the occurrence of bottom water and/or gas cap zones, common in Alberta and Saskatchewan heavy oil reservoirs, have been regarded as being additionally unfavorable factors in steamflood operations, leading to poor volumetric sweep efficiency. However, experience has shown that gravity drainage is an important factor in thermal in situ recovery of bitumen and heavy oil. This experience suggests ways in which the high water saturation zones (bottom water) and existing or induced gas caps may be utilized, possibly in association with steam additives, to promote cost effective steam drives in marginal reservoirs.

2. OBJECTIVES OF THIS STUDY

The principal objectives of this investigation were as follows:

1. To design and fabricate a low pressure, scaled steamflood model to simulate a selected field (Aberfeldy) in Saskatchewan with the provision of the following:

   i. Injection and production equipment, and material to simulate adjacent formations.

   ii. Facility for steam generation and steam quality control.

   iii. Equipment for rapid cooling of the model for establishing the initial conditions in accordance with the scaling criteria.

   iv. Facility for data acquisition, processing, and plotting.

2. To conduct a series of steamflood experiments to examine model performance under a wide variety of operating conditions, in particular the following:

   i. Base steamflood in a model saturated with 100% water to observe temperature distributions and to refine operational procedures.

   ii. Waterflood at room temperature and at low temperature to establish the base oil recovery.

   iii. Continuous steamfloods in a model simulating the Aberfeldy reservoir (hereafter referred to as the Aberfeldy model).

   iv. Continuous steamfloods in a model simulating a light oil reservoir.

3

v.   Continuous steamfloods in a model simulating a reservoir containing an oil much more viscous than the Aberfeldy prototype oil.

vi.   Experiments designed to examine the effect of the production interval on steamflood recovery.

vii.   Steamflood experiments designed to examine the effect of bottom water on steamflood recovery.

viii.   Experiments involving a steam slug driven by cold water.

The purpose of the above runs was to judge the model capability for a variety of experiments, and also to examine a broad range of steamfloods to determine the processes which merit a closer look in the near future.

3. LITERATURE REVIEW

Several in-depth reviews detailing the current state of steamflood technology are presented in the literature.[','] Farouq Ali[4] gives a comprehensive description of the theories that have been proposed to explain the mechanics of steam advance in an oil-bearing formation.

Models (both physical and numerical) have been used to gain a better understanding of the physical processes involved in a steamflood operation. Models have also been extensively employed as predictive tools to help design the best recovery program for a particular field. This chapter presents a survey of the experimental approaches to steam injection and a brief description of the types of experiments that have been conducted. The agreement between model and prototype results will also be examined. Finally, the role of numerical simulation in conjunction with physical models will be discussed.

3.1 Experimental Approaches to Steam Injection

Experiments of many types have been conducted in physical models to examine thermal recovery processes. These include straightforward steamflood studies which investigate relevant operating parameters such as steam injection rate and pressure, steam quality, pattern size and type, and reservoir thickness, to name a few. Other steam injection studies have been conducted in laboratory models to examine recovery from reservoirs with specific attributes such as bottom water, gas caps, shale breaks, extremely high oil viscosity, or with substantial waterflood residual oil

saturation.

Physical models representing prototype reservoirs can be of three types: (1) scaled, (2) partially scaled, or (3) unscaled. A fully scaled model would be extremely desirable because the experimental results could be directly applied to a field situation and used to predict reservoir response to various recovery schemes. However, it is difficult to achieve an exactly scaled model. Relaxing some of the scaling criteria to give a partially scaled model may alleviate some of the scaling problems, but then the possibility exists that incomplete scaling will produce errors in the results. The other option is to forego scaling altogether and to focus on a particular aspect of the reservoir in an attempt to obtain qualitative information about a distinct recovery mechanism. The great majority of laboratory investigations have utilized this type of model, as discussed in the next section.

3.1.1 Unscaled Physical Models

Unscaled models have been used extensively in petroleum research. Typically, the materials and operating conditions for the unscaled model are chosen to represent an element of the prototype being studied, and although the models are not scaled (and thus quantitative predictions are not possible), the unscaled experiments can provide important information with respect to the processes at work in the prototype.

One of the earliest laboratory studies dealing with steam injection was conducted by Willman et al.[7] This work provided much useful information on the mechanisms involved

in a steamflood operation. The experiments were carried out using linear cores saturated with refined oils and crudes having varying viscosities and steam distillation properties. Of particular significance, the study obtained oil recoveries by steam injection as much as 100% greater than oil recoveries by waterflood. The improved oil recovery by steam injection was attributed to (1) thermal expansion of the oil, (2) viscosity reduction, and (3) steam distillation. The procedures used for predicting the performance of a steam drive were based on the Marx-Langenheim' equations and thus the same assumptions were applied. Important limitations are inherent as a result of the assumptions of frontal displacement of oil by steam and equal heat losses to cap and base rock.

Ozen and Farouq Ali' conducted experiments on linear, consolidated cores under isothermal conditions and found that the steam drive can be an effective process to recover waterflood residual oil. They also performed an experiment which indicated that the injection of a small volume of a light hydrocarbon, such as naphtha, prior to steam injection would increase the ultimate oil recovery. Ozen and Farouq Ali' were among the first to study the role of heat losses in laboratory studies of steam injection.

Baker'° conducted an experimental study of heat flow in steamflooding by using steam to displace water in a plane-radial fluid-flow model. The heat losses to the cap and base rocks were calculated using thermocouple data and it was found that heat losses were not dependent on injection rate but were a function of time alone for a given

reservoir thickness and thermal diffusivity. However, he did find that the volume of the hot water zone ahead of the steam did depend on the injection rate and that this hot water zone contained a significant portion of the injected heat. Baker also reports that considerable gravity override was observed in his experiments. In a later study, again using the radial flow model, Baker[11] obtained a more detailed definition of the steam front which enabled him to provide a quantitative measure of the steam zone volume and gravity override.

El-Saleh and Farouq Ali[12] conducted an experimental study of oil recovery by a steam slug driven by a cold waterflood in a linear porous medium using several types of oil and various steam-slug sizes. They found that the steam displacement process was more efficient in the case of light oils than for heavier ones and that oil recovery increased with an increase in the steam slug size. Hong[13] and Ault, Johnson and Kamilos,[14] recently presented papers which discussed the application of a waterflood to reservoirs which have been subject to steam-drive operations. Hong's[13] work was based on numerical simulations while Ault et al.[14] present actual field performance data.

Two large elemental models, used to simulate steam injection and other recovery processes as applied to the oil sands, are described by Redford, Flock, Peters, and Lee.[15] One of the two models consists of a 6-inch by 6-foot steel pipe with a 1/4-inch cement lining and an outer 4-inch layer of magnesia for insulation. The model was fitted with many thermocouples and pressure transducers and used a data

acquisition system for collecting all necessary information during a run. It could be packed with any oil sand of interest and inclined to represent the desired angle of dip. This model has been used extensively in many steam injection studies and is still in operation at the University of Alberta.

Redford et al.[5] also described a second model which was built at the Alberta Research council. It consists of a 1.5m diameter cell equipped with an elaborate data acquisition and analysing system which includes approximately 1500 thermocouples, pressure transducers, and flow measurement devices as well as extensive control equipment. The Alberta Research Council also conducts experiments in two similar, but smaller (45 cm cell and a 23.6 cm cell) models. These models have been used for a variety of experiments employing steam and other fluids in oil sand recovery experiments and are still in use today.

Flock and Lee[4] carried out an investigation involving a steamflood displacement of a medium gravity crude oil using the 6-foot steel pipe described by Redford et al.[5] The tube was packed with unconsolidated sand from the Lloydminster field and saturated with a medium gravity crude oil. It was noted that the temperature distribution within the porous system resulting from injecting steam into a core with a waterflood residual oil saturation was similar to the temperature distribution observed when steam displaced a water saturated porous medium. The authors found agreement between their work and the work of Baker.[10,11]

Flock and Lee[16] suggest that these results indicate that steam can be used as a tertiary recovery process in medium gravity crude oil reservoirs that have been previously waterflooded. They obtained as much as a 40% increase in oil recovery by injecting steam into a previously waterflooded core. However, with the model being insulated as described above, the experimental environment was adiabatic and as such, the effects of heat losses to cap and base rock were not considered. Thus, as the authors indicate, the results obtained from these experiments must be treated with care when considering applying them to a prototype.

Farouq Ali and Abad[17] performed experiments to obtain qualitative information on the effect of three solvents injected into a three-dimensional elemental model in conjunction with steam. They found that bitumen recovery was determined by the solvent used, the volume of the solvent, and the placement of the solvent. It was found that when the solvent was injected into the producing well, followed by steam injection into the injection well, recovery was much higher than when both solvent and steam were injected into the same well. Their results indicated that smaller solvent slugs are more effective in bitumen recovery than large slugs. They suggest that an optimum combination of the solvent and steam slug sizes exists which will maximize bitumen recovery. They also found that recovery tends to increase with a decrease in steam injection rate, down to some minimum optimal rate.

Lee[18] observed results similar to those of Farouq Ali and Abad[17] from his adiabatic experiments conducted using a 6-foot linear elemental model; i.e. that sweep efficiency improved with higher injection rate and lower pressure. In addition he performed experiments to investigate the effect of reservoir dip on oil recovery and found that downdip steam injection was always more efficient than updip steam injection. He observed that the downdip displacement was more piston-like whereas in the updip injection case, the upward channelling of steam left behind a substantial amount of unswept oil. In another series of experiments with the model in a horizontal position, Lee[18] compared various locations of the injection interval and found that injection into the lower portion of the tube gave better oil recovery than injection into the upper portion.

The models described thus far were essentially unscaled, elemental models. The general purpose of models of this type is to provide insight into the fluid-rock interactions under appropriate conditions of temperature, pressure, and, when additives are used, chemical environment. The limitations of these models result from the fact that they are not scaled and therefore cannot be used for quantitative prototype predictions.

3.1.2 Scaled or Partially Scaled Physical Models

A model which could accurately predict the production response of a reservoir under steam stimulation would be highly desirable. Scaled model experiments have been carried out to study the effect of variations in operational

parameters such as injection rate, production pressure, slug size, completion intervals, flood pattern and size, steam additives, reservoir heterogeneities, and steam quality. These models may also be used to calibrate numerical models or provide some insight into the effects of parameters which may not be properly incorporated into a numerical simulator.

Farouq Ali and Redford[1][9] present a comprehensive review of the approaches used in scaling steam injection processes. They state that the design of a scaled physical model is based on the Principle of Similarity* and is characterized by the same ratios of dimensions, forces, velocities, temperature differences, and concentration differences as those occurring in the prototype.

In general, two types of scaling methods can be used to model thermal recovery processes; (1) high pressure and (2) low pressure (or vacuum). Each of these will be discussed and a comparison of the two will be made.

3.1.2.1 High Pressure Scaled Model Studies

There have been several notable studies dealing with scaling thermal recovery methods as applied to high pressure scaled models. Geertsma, Croes, and Schwarz[21] derived the dimensionless groups for scaling the displacement process involving the injection of hot water with the objective of increasing recovery from reservoirs containing viscous crudes. (They also derived the scaling groups for the conventional water drive and a solvent injection process). Pujol and Boberg[22] developed one of the best known sets of

_____

*The authors refer the readers to a book by Johnstone and Thring[20] for a discussion of the Principle of Similarity.

scaling criteria applicable to multidimensional steam injection. Their work has been utilized by several experimenters in scale model studies. Niko and Troost[23] derived scaling criteria for cyclic steam stimulation in a radial, two phase (oil-steam) system. Other noteworthy studies which deal with high pressure model scaling criteria include the work of Perkins and Collins[24], Demetre, Bentsen and Flock[25], Greenkorn[26], Loomis and Crowell[27], Bentsen[28], Rapoport[29], and Leverett, Lewis and True[30]. Several experimental studies have employed high pressure model scaling criteria, some of which will be discussed below.

Pursley[31] applied the Pujol-Boberg[22] scaling criteria to simulate reservoir conditions existing at Cold Lake, Alberta using several three-dimensional models. For the steam drive studies, high pressure scaled models were constructed to represent one-eighth of a five spot pattern for a prototype having a thickness of 42.7 m (140 feet) and a depth of 457.3 m (1500 feet). Models representing 0.5-, 4, and 8-hectare (1.25-, 10-, and 20-acre) patterns were used. The prototype oil viscosity was approximately 100 000 mPa·s and in some experiments the reservoir contained a bottom water zone and/or a gas cap. The model fluids were the same as the reservoir fluids but due to the scaling criteria, the porous medium for the model was different (200 times more permeable than the prototype). The author states that the objective of the model studies was to determine whether the bottom water zone or the gas cap could be used during a steam drive operation. A water zone was created by inverting the model, scraping out a layer of oil-saturated

sand, and replacing it with water saturated sand. A gas cap was installed by slowly injecting gas into the model, while removing a corresponding volume of oil, and allowing the gas to distribute over the top of the model by gravity segregation. He also incorporated impermeable tight streaks in his model (when required) by placing thin sheets of silicone or concrete into the pack at appropriate positions.

With bottom water present, Pursley[31] found that recovery was significantly higher because the steam tended to override and contact a greater portion of the oil sand. He suggested that a steam drive through a bottom water zone would be feasible if good vertical permeability exists and if heating close to the base of the oil sand can be achieved. However, he found that thicker water sands had the adverse effect of significantly delaying oil production. Based on results of runs with a gas cap present, he suggested that steam injection through the gas cap may provide a better approach in cases where the oil sand is separated from the bottom water layer by an impermeable material. In other experiments, the effect of permeability was examined. Pursley[31] found that increasing the model permeability from 400 darcys to 1200 darcys had little effect on oil recovery. He also found that lowering the quality of the injected steam decreases recovery at corresponding values of steam injected, but on the basis of heat injected, the recoveries were similar. Pursley[31] also reported on experiments concerning pattern size, steam bank size, additives to steam, and tertiary wet combustion studies.

Ehrlich[32] conducted experiments in a three-dimensional model, scaled according to the Pujol-Boberg[22] scaling criteria, to study steam displacement in the Wabasca Grand Rapids 'A' sand. The model represented one-quarter of a 0.08 hectare (0.2 acre) five-spot pattern for a prototype reservoir with a 9-10.7m (30-35 feet) thick pay zone and with oil viscosity of approximately 5×10^6 mPa·s. Based on this study, the author found that the residual oil saturation behind a steam front is about 20% of the pore volume regardless of the initial oil saturation. He suggested that the areal sweep efficiency of a steam front is high because of the low effective steam mobility. He found that vertical sweep efficiency was low because of steam override and the oil-steam ratio is low when override occurs. Ehrlich[32] also found that the use of caustic along with steam does not improve recovery despite the success of caustic emulsifiers used as additives with hot waterfloods.

Huygen[33] used a three-dimensional, high pressure (7MPa) model packed with Berea sand to examine the steamflood recovery of eight different crudes. (The model considers only heat flow in the scaling calculations). Huygen[33] prepared a correlation using exponential curves to predict oil production and steam sweep data based on values of initial oil saturation, specific gravity, viscosity at 38°C, distillation residue at steam temperature, steam-to-oil viscosity ratio, and the viscosity ratio multiplied by the steam/water specific volume ratio. In a later study, Huygen and Lowry[34] performed experiments to study steamflooding in the presence of a bottom water zone. The bottom water was

installed in their model by the same method used by Pursley.[31] They observed that the bottom water acted as a pressure sink which counteracted gravity segregation of the steam. They also reported that if the steam injection rate is high enough, no gravity override occurs and much of the formation is swept layer by layer, resulting in a high oil recovery. However, they state that a too high injection rate wastes steam and a too low rate promotes override, and thus, an optimum rate exists. The authors conclude that a bottom water zone provides the steam injectivity missing in immobile tar sands but soaks up heat and oil, making the process inefficient when thicker bottom water layers exist. They found that heating of the oil sand by conduction through the water layer is slow. They also observed the displacement of the heated tar to be parallel to the steam front and through the bottom water zone, rather than ahead of the steam.

Singhal[35] and Lo[34] employed Pujol-Boberg[22] scaling criteria in their scaled model studies. Their experiments were carried out in a scaled model apparatus which was operated at pressures in the range of 100-117 kPa (14.5-17 psi), and thus the apparatus may be considered to be an intermediate pressure scaled model. The authors observed that the hot condensate zone ahead of the steam zone exhibited severe fingering and channelling which resulted in early water breakthrough but that the steam zone did not exhibit fingering. Consistent with other studies, the authors observed severe gravity override as well as underrunning of hot condensate fluid. They also report that

oil recovery increased with both increased steam injection rate and with increased steam quality. They suggest, based on experimental results, that waterflooding a reservoir after steamflooding will recover as much as 5% more oil.

3.1.2.2 Low Pressure Scaled Model Studies

Scaled physical models employing vacuum scaling criteria were first proposed by Stegemeier, Laumbach, and Volek.[37] They demonstrated that materials differing from those found in the prototype reservoir can be used in the vacuum model system and that such a model can accurately predict field response. As this is the scaling method applied to the physical model used in this study, extensive details of the scaling criteria of Stegemeier et al. are presented in a later chapter.

Stegemeier et al.[37] report that they performed scaled experiments to design or to provide operational assistance for several of Shell's steam drive projects including Tatums[38], Coalinga[39], Slocum[40], Mt. Poso[41], Peace River[42], Yorba Linda[43] and Midway Sunset.[37] They provide results from two of their large model studies, the Mt. Poso and Midway Sunset fields, as examples of the type of information which may be derived from vacuum model studies.

The Mt. Poso study conducted by Stegemeier et al.[37] included a series of about fifty experiments which demonstrated that steam override would be a significant factor in the field, causing oil and water to be displaced downdip by gravity. They found that heating downdip improved the oil-steam ratio but that only part of the

reservoir was depleted. In some runs, the effect of prototype oil saturation distribution within the reservoir was investigated and it was found that a high oil saturation mid-dip, or especially updip, improved the displacement process over a uniform saturation distribution. The results of these experiments led the authors to recommend conditions for a successful steamflood at Mt. Poso. A study of the Midway Sunset field included experiments to compare the results of steamflooding and a steam soak process.

Prats[42] conducted numerous experiments using vacuum models employing Stegemeier et al.'s[37] scaling criteria. His study was focused on the Peace River, Alberta oil sand deposit where a bottom water layer exists. Five prototypes were examined and Prats concluded that each prototype reservoir required a unique operating strategy in order to obtain the optimal recovery. Many operational variables were examined including steam quality, injection rates, completion interval, pressure levels, and heat scavenging by injecting water after the steam drive. Many of the runs were conducted with a high water saturation present in the lower part of the model. This zone of high water saturation was established by creating a temperature gradient in the model (with the bottom being significantly hotter) and injecting water through selected wells with bottom completions. The injected water preferentially displaced oil from the lower layer of the model. After the desired initial oil saturation profile was established, the temperature gradient was maintained for one or two days to allow the model to reach horizontal and vertical

equilibrium.

Doscher[44] constructed a vacuum model based on the scaling criteria of Stegemeier et al.[37] with a slight modification. Doscher developed scaling parameters from similarities in an integral form, based on a study by Yortsos[45], rather than a differential form as used by Stegemeier et al.[37] Doscher and Huang[46] used this model to investigate the steam drive performance in a Kern River type heavy oil field. Experiments were conducted to study the effect of injection rate, bottom water, steam quality, oil viscosity, and reservoir permeability. Based on the experiments conducted for a particular prototype, they concluded that an optimum steam injection rate exists, above and below which, performance decreases. They suggested that production rate is a linear function of steam quality, and a function of the square root of the oil viscosity at steam temperature.

Doscher and Ghassemi[47] performed experiments on the vacuum model described above[44] and determined that the viscosity of the crude oil is a very important parameter which affects the efficiency of the steam drive process. They also conducted experiments to examine the effect of reservoir thickness on the steam drive efficiency. Although little evidence is presented in the paper, they suggest the possibility of the oil-steam ratio in thin reservoirs being as high as, or even higher than in thick reservoirs. This is contrary to the prediction made by analytic models which indicate that the oil-steam ratio will vary directly as a function of reservoir thickness. It seems likely that

excessive heat losses would limit the economic viability of a steam drive process in thin formations.

3.1.2.3 High Pressure vs. Low Pressure Scaled Models

Each of the two model types has distinct advantages and disadvantages. Because high pressure models often employ the same fluids as the prototype, they are considered to provide a better scaling of rock-fluid interactions such as permeability, relative permeability, and capillary pressure alterations. Stegemeier et al.[37] note that the Clausius-Clapeyron relation is more accurately matched at subatmospheric pressures and low temperatures; thus the modeling of temperature distribution is better in the vacuum model. This affects the viscosity distribution, internal energy distribution, and the steam zone pressure gradient, all of which are thought to be important aspects of the thermal recovery process. It is generally accepted that the vacuum model is less expensive to construct, safer to operate, and is able to turn out results quicker than the high pressure model. It is interesting to note that although Prats[42] had both types of models available to him, after considering the relative advantages and disadvantages of each, he chose to conduct his experiments in a vacuum model.

On the negative side, neither the high pressure nor the low pressure scaled model account for compressibility effects. More importantly, neither model is able to use prototype fluids and porous media if proper scaling is to be maintained. Kimber and Farouq Ali[44] found that if prototype

fluids and porous media are used in a high pressure model, the geometric similarity must be distorted in the vertical dimension. This would also affect other scaling parameters. Doscher and Huang[44] point out that physical scaling fails badly when chemical reactivity, capillary pressure, or physical adsorption play important roles in the process, but they state that in the steam drive these phenomena are not important.

Prats[42] and others suggest that the main factor which may not be scaled in the vacuum model is the relative permeability. (This would also be true of the high pressure model, but to a lesser extent.) In a discussion at the Canada-Venezuala oil sands symposium of 1977[49] Prats stated that it is not known whether the relative permeabilities are scaled and gave several factors which contribute to the problem. The most important is that it is not known how to obtain a single set of three-phase relative permeability curves which will be applicable for a given prototype reservoir under the anticipated operating conditions. In addition, he says it is not known how to make up a set of relative permeability properties for the laboratory scaled models. For these reasons, he suggests that it is not possible to determine how well or how poorly relative permeabilities are matched in the scaled models.

In general, it is believed that the high and low pressure scaled models provide a reasonable description of the phenomena involved in the steam drive process. A later section gives some examples of the ability of the scaled models to predict the field response to steam stimulation.

3.1.3 Studies of Thin, Bottom Water Reservoirs

Kasraie and Farouq Ali[50] discuss the mechanisms involved in thermal stimulation of bottom water reservoirs. Based on their survey of existing field and laboratory data, the authors conclude that a water zone thicker than about one-fifth of the oil zone would make cyclic steam stimulation uneconomical.

As mentioned in previous sections, a few experimental studies have been undertaken to examine oil recovery by steam injection into reservoirs underlain by water. However, none of these studies were directed toward reservoirs of the Aberfeldy type; i.e. thin reservoirs, often associated with relatively thick bottom water zones and/or a gas cap.

The Peace River reservoirs, modeled by Prats[42] contain a substantial oil saturation (45%) in conjunction with the "bottom water" layer; thus injection into the bottom water zone still produces an economically acceptable amount of oil. The Cold Lake reservoir studied by Pursley[31] has a pay thickness of 140 feet (42.7 m) and the Wabasca reservoir studied by Huygen and Lowry[34] has a thin bottom water zone relative to the total pay thickness. Both have viscosities in the order of 10^5 mPa·s. Thus, the results of these studies may not be representative of the Aberfeldy reservoir. Similarly, only limited work has been reported with respect to steamflooding thin oil reservoirs (e.g. Doscher and Ghassemi[47]).

A numerical simulation study was recently reported by Singh, Malcolm, and Heidrick[51]. Their objective was to

evaluate steam injection and steam injection with additives into reservoirs with bottom water. The project encompassed a number of numerical simulations which were run to determine the effects of bottom water thickness, carbon dioxide injected along with the steam, blocking agents, and injection-production strategy. They concluded that the injection of carbon dioxide alone, followed by steam injection would result in improved production. They note that there is no data available concerning the application of additives for the thermal recovery of bitumen from reservoirs with bottom water. The results given are of a very general nature, and do not give any definite guidelines for producing bottom water reservoirs.

3.2 Agreement Between Experimental and Field Results

With regard to unscaled experiments, there is little likelihood of obtaining the same oil recovery or oil production rate as in the field. However, some studies have shown that field values of the residual oil saturation to steam are similar to laboratory values. The residual oil saturation to steam is dependent upon the the ultimate oil displacement by steam, and depends less on mass/heat transfer effects.

Stegemeier et al.[37] observed excellent agreement between their scaled model studies and field responses for the Mount Poso steam drive model. present a plot of the predicted versus the actual field performance, which demonstrates the accuracy of the scaled model predictions. Prats[42] gives a comparison of the full-scale vs. actual

response for the Peace River scaled model studies in a table and again, close agreement is observed. This is particularly interesting in the case of the Peace River study because the in situ oil viscosity is very high, while in the model, the prototype oil was represented by a relatively light oil.

3.3 Role of Numerical Simulation

Numerical simulation of steam injection processes is at a stage where simpler situations can be simulated. The principle limitations are (1) the grid size, which limits simulation to that of an element of symmetry of a pattern, and that too, with limited definition; and (2) process representation, which means that some of the processes involved in thermal stimulation are still unclear, particularly the rock-fluid interactions. Often, unrealistic assumptions are put into a simulator to obtain a history match; for example, using a rock compressibility factor which is several orders of magnitude higher than the real compressibility ('spongy rock' effect[52]) to compensate for a parameter which is not implemented (or possibly not understood).

In spite of these deficiencies, numerical simulators can be valuable tools to complement physical model studies. They can provide fast predictions which may be used to assess the relative role of variables in a given steam process. With adequate information available for history matching, numerical simulators may be modified to provide accurate predictions of reservoir response to changes in

operational strategy, thus precluding the need for physical models. However, if production data is limited or nonexistent, the use of a numerical simulator in conjunction with a scaled physical model would provide the most reliable prediction.

4. SCALING THE STEAM DRIVE PROCESS FOR A VACUUM MODEL

This chapter will outline some of the details of the scaling method which was used in this study. The assumptions underlying the scaling procedure are listed and two of the major assumptions are discussed. To demonstrate the application of this scaling method, the details of the calculations used to model the Aberfeldy reservoir and the associated operating parameters will be presented.

4.1 Vacuum Model Scaling Parameters

The scaled model used in this study was designed based on the scaling rules of Stegemeier, Laumbach, and Volek.[37] Their scaling rules were derived by rewriting the equations governing the steam injection process into dimensionless form and then determining a set of similarity parameters by inspectional analysis. Engineering judgement was used to reduce the set of similarity parameters to a set of scaling parameters which could generally be matched between the scaled model and the field prototype. These scaling parameters are presented in Table 1.

The assumptions made by Stegemeier et al.[37] in the derivation of the scaling parameters, are reproduced below:

1. Three phases may exist consisting of an oleic phase, an aqueous phase, and a steam vapour phase (no volatile hydrocarbons).

2. There is no partitioning into or out of the oil phase (dead oil).

3. Rock compressibility and thermal expansion are negligible.

Table 1. Scaling Parameters for Steam Processes.

Number	Parameter	Name of Parameter
1	$\dfrac{P_r}{\rho_r\, g_r\, L_r}$	Poiseuille number divided by Stokes number.
2	$\left\{\dfrac{f_{sr}\, L_{vr}}{C_r\, T_r} + 1\right\} \cdot A$	Modified Jacob number + 1.
3	$\dfrac{f_{sr}\, \mu_{sr}\, \rho_r}{\mu_r\, \rho_{sr}}$	Ratio of steam pressure gradient to oil pressure gradient.
4	$\dfrac{k_{hr}\, t_r}{\phi_r\, S_r\, \rho_r\, C_r\, L_r{}^2} \cdot A$	Fourier number or Peclet number.
5	$\dfrac{\phi_r\, S_r\, \mu_r\, L_r}{k_r\, \rho_r\, g_r\, t_r}$	Stokes Number
6	$\dfrac{w_r\, t_r}{\rho_r\, \phi_r\, S_r\, L_r{}^3}$	Poiseuille number divided by modified Poiseuille number.

After Stegemeier, Laumbach, and Volek[3,7]

Subscript 'r' indicates that the variable is a reference quantity used to obtain a dimensionless term.

4. Darcy's and Fourier's equations are valid.

5. Capillary pressure effects are negligible.

6. The system is in local thermodynamic equilibrium.

7. Kinetic energy, potential energy, and viscous dissipation energy are negligible compared with the thermal energy.

8. The enthalpy and internal energy are essentially equal for the oleic phase and for the aqueous phase, and are linear functions of the temperature.

9. The difference between the steam enthalpy and internal energy can be neglected.

10. The time rate of change of the specific steam enthalpy in the steam zone is negligible.

11. The internal energy of the rock is a linear function of the temperature.

12. The saturated steam temperature is the maximum temperature in any location.

13. Relative permeabilities depend exclusively on the saturations.

14. The residual oil saturation to steam and the connate water saturation are constant and uniform throughout the model.

15. Critical saturation for steam flow is assumed to be zero.

16. The changes in the density of the immovable water and residual oil are negligible.

In view of the above assumptions, some degree of error in the results is inevitable. In particular, strict scaling would require that the capillary pressure and the relative

permeability relationships be the same functions of saturation in the model as in the prototype. In addition, a practical limitation results from the possible problems associated with finding model materials and fluids with the properties necessary to satisfy the scaling groups.

The failure to scale the capillary pressure is thought to be acceptable because of the high crude oil viscosity in the prototype reservoir. Demetre et al.[25] found that in the case of large values of mobility ratio, the breakthrough recovery is only a weak function of the capillary number, provided the displacement is stable. Bentsen[28] states that the mobility ratio dominates the displacement process in a linear system and therefore it is possible to eliminate the requirement that the relative permeabilities (or their ratio) be the same in the model and in the prototype, under certain circumstances. The paper deals with a linear displacement process, but the author suggests that more complex problems may be handled in an analogous manner.

As mentioned in the literature review, Prats[49] states that the three-phase relative permeability curves applicable to the prototype under the anticipated operating conditions cannot be determined. Similarly, it is not known how to make up a set of relative permeability properties for the laboratory model. This problem makes it difficult to know whether the relative permeability relationships are scaled or are not scaled. Despite this limitation, Prats[49] obtained good agreement between the model and field results in his Peace River scaled model study, as noted earlier.

Justification for the assumptions made in deriving the scaling rules is further (and perhaps better) provided by the agreement between laboratory model results and actual field operations. (Examples were given in the literature review.)

4.2 Designing the Aberfeldy Scaled Model

Three models were built to represent the Aberfeldy prototype, one with a scaling factor of 173.2 to 1, and two with scaling factors of 400 to 1 (one of which represented a reservoir twice as thick as the other). Each model was designed to simulate one quarter of a five-spot pattern and as such, each had one injection well and one production well, at diagonally opposite corners. Because of the work involved in preparing for a run, and the cleaning necessary after a run, the smallest model was used for the preliminary runs until familiarity with the equipment was established.

The thin pay zone of the Aberfeldy reservoir requires that the scaled model representing it be very thin also, particularly for a model with a scaling factor of 400 to 1. Thus the second small model was built with an exaggerated vertical height to give better insight into the effects of bottom water and steam override in the model experiments. However, because the best predictions can be made with a model as large as is practical, the large model was used for the majority of the runs. This is the model that will be discussed in the example calculations presented in the following sections.

4.2.1 Prototype Data

The first step in designing a physical model to simulate a field system is to determine the characteristics which will be used to describe the prototype reservoir. The following values were chosen to represent the Aberfeldy prototype:

Well Spacing: 8 hectare (20 Acre), 5 spot pattern

Net Pay Thickness: 11 meters.

Gross Pay Thickness: Varies from 10 to 13 meters.

Porosity: 0.31

Permeability: 2000 md

Thermal Conductivity: 1.2 Btu/hr·ft·°F (0.002077 KW/m·K)

Heat Capacity: 2.2217 KJ/Kg·K

Initial Saturation: S_o=0.75, S_g=0.02, S_w=0.23

Steamflood Residual Oil Saturation: S_{or}=0.15

Oil Viscosity: 1275 mPa·s at 23.9°C, 560 mPa·s at 32.2°C, 90 mPa·s at 65.6°C, 12.5 mPa·s at 135.0°C, and 1.29 mPa·s at 301.7°C

Water Viscosity: 0.891 mPa·s at 25.8°C

Gas Viscosity: 0.013 mPa·s at 23.3°C and 0.016 mPa·s at 134.4°C

Specific Gravity of Gas: 0.55

Initial Reservoir Pressure: 3.45 MPa

Initial Reservoir Temperature: 23.3°C

Steam Injection Pressure: 1.900 MPa

Steam Injection Rate: 100-150 m³/day

Steam Quality: 0.70 (Actually it is 0.80 to 0.85 but a lower value was used to allow for wellbore heat loss.)

4.2.1 Prototype Data

The first step in designing a physical model to simulate a field system is to determine the characteristics which will be used to describe the prototype reservoir. The following values were chosen to represent the Aberfeldy prototype:

Well Spacing: 8 hectare (20 Acre), 5 spot pattern

Net Pay Thickness: 11 meters.

Gross Pay Thickness: Varies from 10 to 13 meters.

Porosity: 0.31

Permeability: 2000 md

Thermal Conductivity: 1.2 Btu/hr·ft·°F (0.002077 KW/m·K)

Heat Capacity: 2.2217 KJ/Kg·K

Initial Saturation: S_o=0.75, S_g=0.02, S_w=0.23

Steamflood Residual Oil Saturation: S_{or}=0.15

Oil Viscosity: 1275 mPa·s at 23.9°C, 560 mPa·s at 32.2°C, 90 mPa·s at 65.6°C, 12.5 mPa·s at 135.0°C, and 1.29 mPa·s at 301.7°C

Water Viscosity: 0.891 mPa·s at 25.8°C

Gas Viscosity: 0.013 mPa·s at 23.3°C and 0.016 mPa·s at 134.4°C

Specific Gravity of Gas: 0.55

Initial Reservoir Pressure: 3.45 MPa

Initial Reservoir Temperature: 23.3°C

Steam Injection Pressure: 1.900 MPa

Steam Injection Rate: 100-150 m³/day

Steam Quality: 0.70 (Actually it is 0.80 to 0.85 but a lower value was used to allow for wellbore heat loss.)

Depth of Reservoir: 522.4 m

Bottom Water: Varies from 0 to 6.9 m.

Pressure Range: The pressure range is usually bounded on the upper side by the fracture gradient of the reservoir and on the lower side by the bottomhole production pressure. For calculation purposes, a back pressure on the formation of 0.345 MPa (50 psia) was assumed.

$$\therefore (P_p)_p = 0.345 \text{ MPa}$$

4.2.2 Length Scale Determination

The length scale is determined by pressure-temperature relations and by constraints placed on the size of the physical model. Stegemeier et al.[37] state that the best match of the pressure-temperature relation for saturated steam can be obtained by making the length scaling factor, $\gamma(L)$, as small as possible, and thus the model should be as large as possible. The limits are that the model must be of a size suitable for a laboratory and small enough to ensure that the run time is not prohibitive.

In this project, the model represents 1/4 of an 8 hectare, 5-spot pattern. The model is 81.3 cm (32 in) square and 6.4 cm (2.5 in) thick. This produces a length scaling factor of 173.2 in 3 dimensions.

$$\therefore L_p/L_m = \gamma(L) = 173.2 \quad \ldots (1)$$

4.2.3 Model Pressure Scaling

For prototype pressures of the order of 0.345 MPa (50 psia) and for typical length scales, Stegemeier et al.[37] state that the pressure-temperature relation at saturation can best be matched if one selects as low a value for the model production pressure as is possible. From a practical standpoint, the lowest value that can be maintained due to vacuum pump limitations and vapour pressure considerations is about 7 kPa (1 psia).

$$\therefore (P_p)_m = 6.895 \text{ kPa (1 psia)}$$

With the above value for the model production pressure chosen, model pressure scaling is calculated from scaling parameter (1) in Table 1.

$$\gamma(\Delta P) = \frac{(P-P_p)_p}{(P-P_p)_m} = \frac{\rho_p \ g_p \ L_p}{\rho_m \ g_m \ L_m} \quad \ldots(2)$$

To this point, the density ratio is the only unknown in the above equation. The first time through the scaling calculations it is necessary to assume a value of $\gamma(\rho_r)$, the density ratio, which was found to be approximately equal to 0.9, and using this, a relationship between P_m and P_p can be developed from Equation (2) as follows:

$$\gamma(\Delta P) = \frac{(P-P_p)_p}{(P-P_p)_m} = (0.9)(1.0)(173.2)$$

$$P_m = (P_p)_m + 0.0064152 \ P_p - 0.0064152 \ (P_p)_p$$

$$P_m = 0.006895 - (0.0064152)(0.34475) + 0.0064152 \ P_p$$

$$\therefore P_m = 0.004683 + 0.006415 \ P_p \quad \ldots(3)$$

where P_m is the model pressure corresponding to a prototype

pressureP_p, with P_m and P_p both in MPa. Refer to Table 2 for a tabulation of the corresponding values.

4.2.4 Model Temperature Scaling

Stegemeier et al.[37] state that the best match between prototype and model oil viscosity curves is obtained by making the model temperature range as large as possible. As a practical limitation, the minimum initial model temperature is about 3°C. Thus $(T_o)_m$ = 3°C. To scale the temperature, corresponding temperatures at only one other point are required.

Stegemeier et al.[37] suggest that it is best to take a value from the middle of the pressure range for finding the temperature difference ratio because most of the oil will be produced when these temperatures are significant. Further, they state that the lower part of the pressure-temperature relation for saturated steam is difficult to fit.

Using prototype and model temperatures corresponding to a prototype pressure of 2.00 MPa (see Table 2), the value for the temperature ratio can be determined as follows:

$$\frac{\Delta T_p}{\Delta T_m} = \frac{(T-T_o)_p}{(T-T_o)_m} = \frac{(212.42-23.30)}{(57.03-3.0)} \quad ...(4)$$

$$\frac{\Delta T_p}{\Delta T_m} = 3.5 \quad ...(5)$$

If this ratio is constant over the temperature range (Stegemeier et al.[37] state that it must be in order to have the proper proportion of energy stored as internal energy), a model temperature relation can be developed as follows:

Table 2: Prototype and Model Scaling Values.

Prototype Values							Model Values										
P (MPa)	Ts (C)	hw (kJ/kg)	CwΔT (kJ/kg)	Lv (kJ/kg)	ρs (kg/m3)	μs (cp)	P (MPa)	Ts (C)	Tsc (C)	hw (kJ/kg)	CwΔT (kJ/kg)	Lv (kJ/kg)	ρs (kg/m3)	μs (cp)	fs	μom/μop (cp/cp)	wa/wi
3.45	241.73	1045.9	947.84	1757.9	17.2322	0.0173	0.02682	86.47	65.40	274.07	261.50	2342.59	0.17100	0.01090	0.06965	7.0195	0.8854
3.00	233.90	1008.4	910.64	1795.7	14.9970	0.0170	0.02393	83.92	63.24	264.69	252.12	2349.28	0.15110	0.01080	0.07319	7.3253	0.8827
2.50	223.99	962.11	864.33	1841.0	12.5031	0.0166	0.02072	80.77	60.40	252.80	240.23	2356.40	0.13520	0.01060	0.07750	7.2644	0.8793
2.00	212.42	908.79	811.01	1890.7	10.0371	0.0162	0.01751	57.03	57.10	238.99	228.42	2365.72	0.11290	0.01040	0.08230	7.4558	0.8776
1.50	198.32	844.89	747.11	1947.3	7.5890	0.0156	0.01431	52.84	53.06	222.12	209.55	2373.60	0.08820	0.01020	0.08792	7.8512	0.8765
1.00	179.91	762.61	665.03	2015.3	5.1430	0.0149	0.01110	47.61	47.80	200.15	187.58	2386.99	0.07816	0.01000	0.09474	6.6411	0.8758
0.50	151.86	640.23	542.45	2108.5	2.6674	0.0140	0.007891	41.15	39.77	166.61	154.04	2403.94	0.06170	0.00970	0.10440	4.9637	0.8754
0.34475	138.34	562.00	464.22	2149.7	0.5322	0.0133	0.006895	38.50	35.91	150.48	137.91	2409.19	0.04556	0.00950	0.10790	1.4290	0.8751

$$T_m - (T_o)_m = \frac{T_p - (T_o)_p}{3.5}$$

$$\therefore T_m = 0.286 \, T_p - 3.657 \quad ...(6)$$

The model values calculated from Equation (6) are given in Table 2 and are designated T_{sc} to denote that they are calculated values.

As seen in Table 2, the calculated values, T_{sc}, do not correspond exactly to the saturated steam values, T_s. Stegemeier et al.[37] state that better scaling is obtained by allowing the error to occur at the lower temperatures. They note that the portion of the pressure-temperature saturation relation which is most difficult to match is the part pertaining to low prototype pressures, which often are not encountered.

4.2.5 Scaling the Steam Quality

Stegemeier et al.[37] use parameter (2) in Table 1 to calculate the model steam quality.

$$\left(\frac{f_{sr} \, L_{vr}}{C_r \, T_r} + 1\right) * A \quad ...(7)$$

When $\phi \Delta S$ is not matched, and if it is assumed that cap and base rock heating are dominant, as is often the case in steam drive processes (particularly in thin reservoirs), 'A' is replaced by $\phi S_r (\rho_r c_r / \rho_{cr} c_{cr})$. Thus the equation to calculate the model steam quality is given by:

$$f_{sm} = (\frac{C_w \Delta T}{L_v})_m \{(\frac{f_s L_v'}{C_w \Delta T}+1)_p \ [\frac{(\phi_p \Delta S_p)}{(\phi_m \Delta S_m)} \cdot \frac{(\rho_p C_p)}{(\rho_m C_m)} \cdot \frac{(\rho_{cm} C_{cm})}{(\rho_{cp} C_{cp})}] -1\} \quad ..(8)$$

It was assumed that a porosity of 0.32 would be obtained in the model; i.e. $\phi_m = 0.32$, and it was assumed that the change in oil saturation within the model would be 0.85; i.e. $\Delta S_m = 0.85$. In the prototype, with $\Delta S = 1 - S_{or} - S_{wc}$, and $S_{or} = 0.15$, the change in oil saturation is 0.62; i.e. $\Delta S_p = 0.62$.

Values of model steam quality at various pressures have been calculated using Equation (8) and are presented in Table 2.

The proportion of injected water and steam required to obtain the desired model steam quality were calculated based upon the premise that the enthalpy rate of the two inlet streams combined must equal the required enthalpy rate of the wet steam injected into the model, plus any heat losses.

$$\therefore w_{ss}h_{ss} + w_a h_a = (w_{ss} + w_a)(f_{sm}L_v + c_w \Delta T) + Q_{loss} \quad ...(15)$$

where w_s and w_a are the mass rates of flow of the superheated steam and the aqueous phase respectively; h_{ss} and h_a are the entering superheated steam enthalpy and quality control water enthalpy respectively, and Q_{loss} is the rate of heat loss.

Equation (13) can be rearranged as follows:

$$\frac{w_a}{w_{wi}} = \frac{h_{ss} - f_s L_v - c_w \Delta T - (Q_{loss}/w_{wi})}{h_{ss} - h_{wa}} \quad ...(16)$$

where w_{wi} is the total mass rate injected $(=w_{ss} + w_a)$ (calculated in a later section) and $h_{wa} = h_f$ at 23°C which is

equal to 96.52 KJ/Kg. Assuming that the steam temperature is 120°C, the quality control water temperature is 23°C, and $Q_{loss}=0$, the values of h_{ss} were calculated and found to vary with model pressure as shown in Table 3.[53]

Using these values for h_{ss} and substituting other known values into Equation (16) gives values of w_a/w_{wi} at various pressures. These values are tabulated in Table 2.

4.2.6 Scaling the Model Oil Viscosity

Parameter (3) in Table 1. was used to scale the oil viscosity. From parameter (3), Stegemeier et al.[37] obtained the following relation:

$$\frac{\mu_{o_m}}{\mu_{o_p}} = [\ \frac{(f_{sm})}{(f_{sp})} \cdot \frac{(\mu_{sm})}{(\mu_{sp})} \cdot \frac{(\rho_{sp})}{(\rho_{sm})} \cdot \frac{(\rho_{o_m})}{(\rho_{o_p})}\ ] \ ...(9)$$

Known quantities were substituted into Equation (9) and values of model viscosity were calculated for various pressures. These are presented in Table 2.

Determining the Time Scale

Stegemeier et al.[37] developed the following equation from parameter (4) in Table 1.

$$\frac{t_m}{t_p} = \frac{(k_{hp})}{(k_{hm})} \cdot \frac{(\rho_{cm}c_{cm})}{(\rho_{cp}c_{cp})} \cdot (\frac{L_m}{L_p})^2 \ ...(10)$$

This assumes that the temperature distribution was more significant in the cap and base rock than in the reservoir (which is the same assumption made to determine the model steam quality).

The thermal conductivity for granite is 2.81 kcal/(m·hr·deg C).[54]

Table 3. Steam Enthalpy at Various Model Pressures

Model Pressure (MPa)	Steam Enthalpy (KJ/Kg)
0.006895	2726.00
0.007891	2725.92
0.01110	2725.59
0.01431	2725.25
0.01751	2724.92
0.02072	2724.59
0.02393	2724.25
0.02682	2723.95

$$\therefore k_{hm} = 0.003266 \text{ KW/m·K}$$

The heat capacity of the prototype, M_p, is given by the following equation:

$$M_p = \phi\rho_o c_o S_o + \phi\rho_w c_w S_w + (1-\phi)(\rho_r c_r)$$

Substituting the prototype data and taking $\rho_r = 2.14$ g/cm³ [55] gives:

$$M_p = (\rho_r c_r)_p = 2.1803 \text{ KJ/Kg·K}$$

Similarly, the heat capacity in the model, M_m, can be calculated as follows:

$$M_m = (\rho_r c_r)_m = 2.3824 \text{ KJ/Kg·K}$$

Substituting the above values into the time scale equation (Equation (10)), the time scale was found to be:

$$t_m/t_p = 12.1836 \text{ min/year} \quad \ldots(11)$$

4.2.8 Model Permeability Scaling

By modifying parameter (5) of Table 1, Stegemeier et al.[37] developed the following equation:

$$\frac{k_m}{k_p} = \left[\frac{(\phi_m \Delta S_m)}{(\phi_p \Delta S_p)} \cdot \frac{(L_m)}{(L_p)} \cdot \frac{(\mu_m)}{(\mu_p)} \cdot \frac{(\rho_p)}{(\rho_m)} \cdot \frac{(t_p)}{(t_m)} \right] \quad \ldots(12)$$

A single representative value of μ_m/μ_p must be chosen because μ_m/μ_p and the expression for k_m/k_p are temperature dependent. Stegemeier et al.[37] state that values from the lower portion of Table 2 should be weighted most heavily, thus, for the scaling of the Aberfeldy prototype, a value corresponding to a prototype pressure of 1.00 MPa was chosen. By substituting values already determined and the prototype data into Equation (12), a value for the model permeability was found to be,

$$k_m = 4216.5 \text{ darcies.}$$

4.2.9 Injection and Production Rate Scaling

Stegemeier et al.[37] used parameter (6) in Table 1 to develop the following equation:

$$\frac{w_m}{w_p} = [\ \frac{(\rho_{om})}{(\rho_{op})} \cdot \{\frac{L_m}{L_p}\}^3 \cdot \frac{(\phi_m \Delta S_m)}{(\phi_p \Delta S_p)} \cdot \frac{(t_m)}{(t_p)}\ ] \ ...(13)$$

Substituting values into Equation (13) gives,

$$w_m/w_p = 9.0728 \ \frac{cm^3/min}{m^3/day} \ ...(14)$$

where the volumetric rates are at standard conditions.

Thus, to simulate an injection rate of 100 m³/day in the prototype, the model injection rate was 1/4 of 907.3 cm³/min, which is 226.8 cm³/min.

4.2.10 Well Scaling

Direct geometric scaling of the wells is not practical for a model of this size. The 'slit well' technique presented by Stegemeier, Lambauch, and Volek[37] was used to scale the wells. The width of the slit is determined by the following equation:

$$w = 2\pi r \qquad \text{where } w = \text{slit width.} \ ...(17)$$
$$r = \text{scaled radius of the well.}$$

Using the length scale of 173.2 for this model, and assuming that the prototype wells are 6 inches in diamater, the scaled diameter of the model wells would be 6/173.2 = 0.03464". With this, the width of the model well slit can be calculated.

Q

$$w = \frac{2\pi(0.03464")}{2} = 0.1088"$$

The wells in the model were constructed in a manner such that the injection and production interval could be altered with relative ease. For most of the experiments conducted in this study, the injection and production intervals were positioned in the same manner as described by Singhal.[35] In the injection well there were four slots opposite the lower portion of the well and in the production well there were eight slots over the length of the well.

Table 4 presents a summary of the important experimental parameters which were calculated in this chapter.

Table 4.   Summary of the Scaling Calculations for the
             Aberfeldy Model.

Length Scale: $\gamma(L) = L_p/L_m = 173.2$

Pressure Relation: $P_m = 0.004683 + 0.006415\ P_p$ (MPa)

Temperature Relation: $T_m = 0.286\ T_p - 3.657$ (C)

Time Scale: $t_m/t_p = 12.18$ min/year

Permeability: prototype = 2 darcies,

                       model = 4216.5 darcies

Injection and Production Rate Scales:

$$\frac{w_m}{w_p} = 9.0728\ \frac{cm^3/min}{m^3/day}$$

5. EXPERIMENTAL APPARATUS AND PROCEDURE

This chapter contains a description of the equipment and materials used in the study. Details concerning the model operation are presented, including a discussion of the procedures involved in packing and saturating the model, and conducting the experiments. A schematic diagram of the apparatus used in this research is given in Figure 1. The main components of this apparatus are the physical model, the steam injection system, the model cart and cold storage unit, and the data aquistion system.

5.1 Physical Model

Plate 1 shows the model apparatus in an inclined position with the cap and base rocks in place. In this plate, a spare model is shown in front of the apparatus to illustrate what the porous media of the model was contained in.

All of the models used in this project were designed to represent one-quarter of a 281.55m x 281.55m x 11m thick five-spot pattern, with an area of 8 ha (20 acres). The model used for the bulk of the experiments was constructed with the dimensions of 81.28cm x 81.28cm x 6.35cm thick (32in. x 32in. x 2.5in.) which resulted in a three-dimensional length scale of 173.2. Because the experiments were conducted under vacuum conditions in order to satisfy the scaling groups, a severe load was induced on the large surface area of the models. Thus, it was necessary to construct the models from a strong material, suitable for withstanding this type of loading. Another

44

Figure 1.

Schematic Diagram of Apparatus.
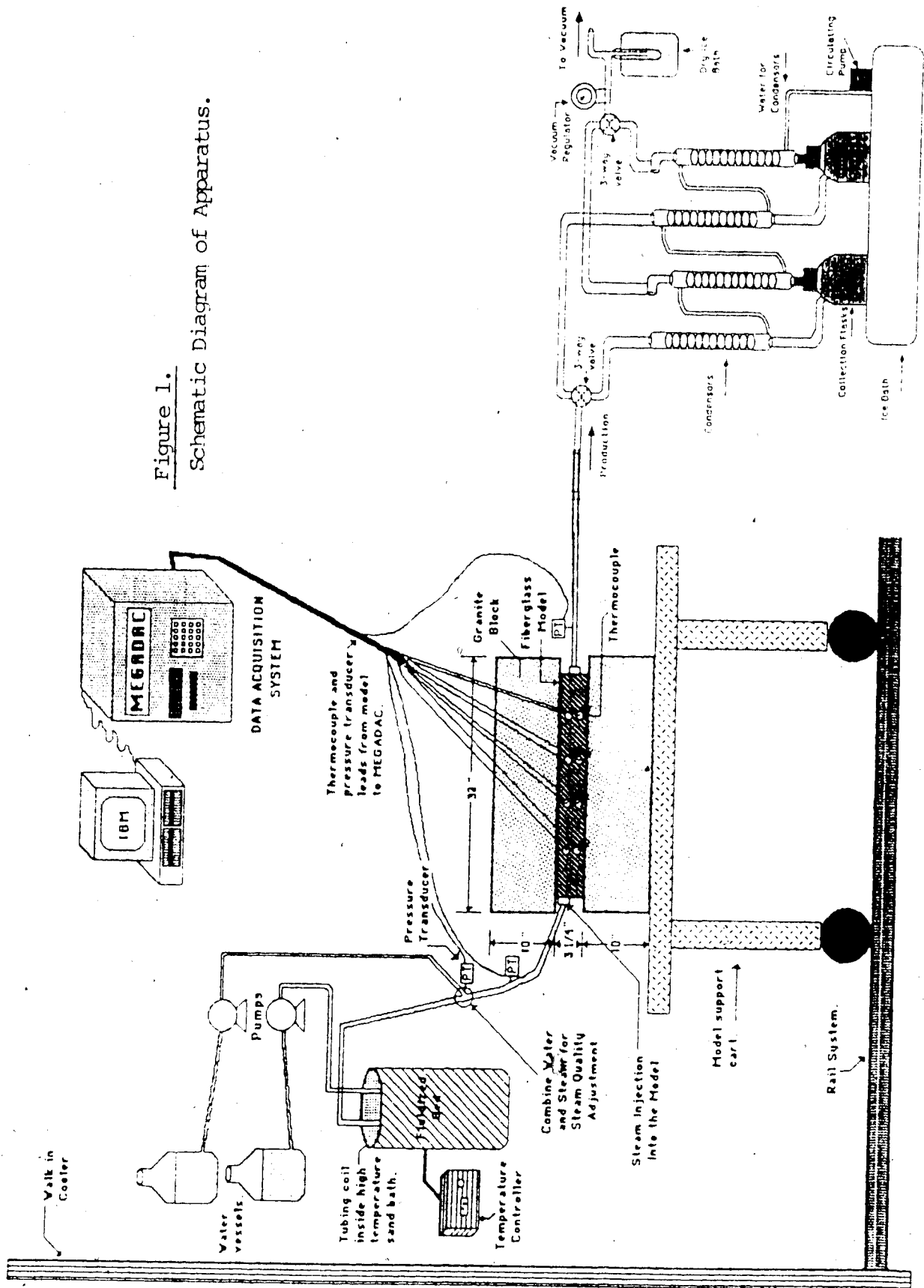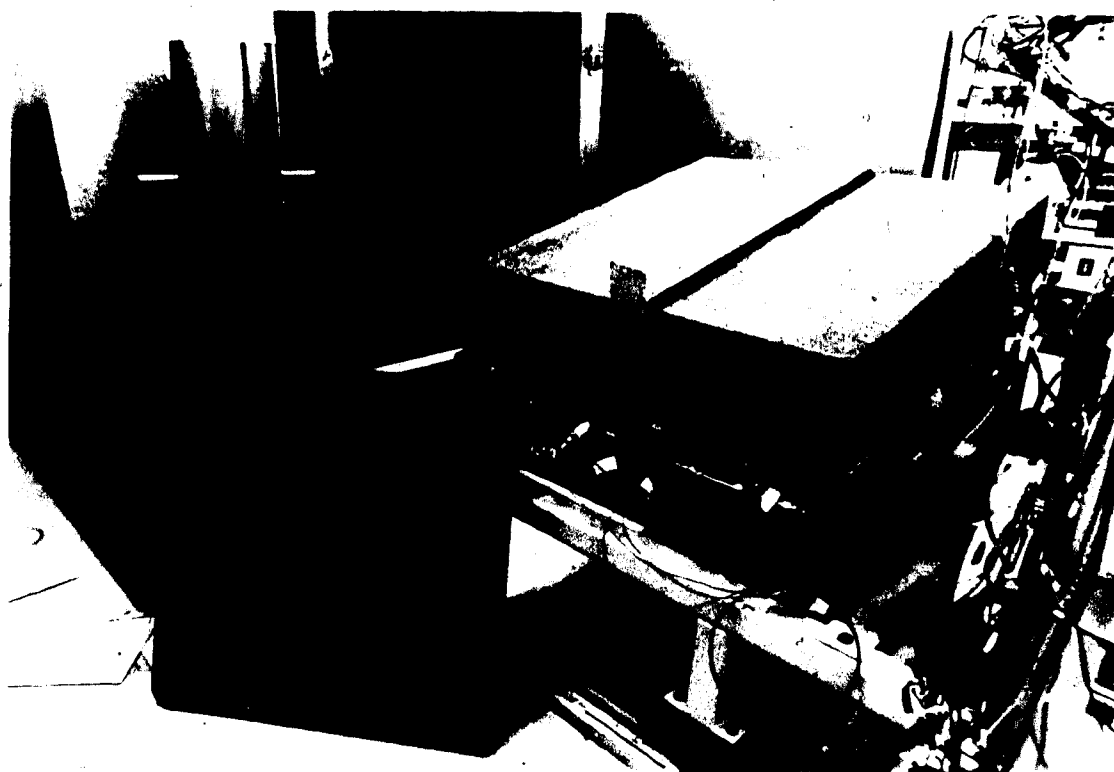
Plate 1: Model Assembly in Inclined Position.

consideration in the model construction was the heat transfer coefficient of the model material, which should be as low as possible. Additionally, because several models were to be used in this work, it was necessary to choose a material which was inexpensive and relatively easy to machine. For these reasons, fiberglass was chosen as the model material. The models were constructed of molded fiberglass, with wall thicknesses of 1.9 cm (0.75 inches). A local company* was able to build the models according to the desired specifications.

The cap and base rocks of the model consisted of granite blocks, each with the dimensions of 91.4cm x 91.4cm x 21.6cm thick (36in x 36in x 8.5in thick)†. Heat losses from the lateral boundaries of the model were minimized by applying a two inch layer of cellular neoprene to all exposed surfaces.

5.1.1 Model Wells

Important components of the model were the injection and production wells. These were constructed out of aluminum rod and set into diagonally opposite corners of the molded fiberglass model as seen in Plate 1. The wells were designed to allow a gate device to be inserted into them which enabled the experimenter to selectively choose the injection and production intervals.

----

*Triple M Fiberglass, 8135 Wagner Road, Edmonton, Alberta. Cost = $400 ea.
†DoAll Edmonton Ltd., 9743-45th Ave., Edmonton, 436-0373.

5.1.2 Porous Media

The scaling groups required that the model permeability be of the order of 4200 darcies. To obtain this high permeability, glass beads with a diameter of approximately 3 mm (6-8 mesh) were purchased.* Because of the high cost of these beads, it was necessary to clean them following\ every run so that they could be re-used. A degreasing solution† was first used to remove most of the oil, then a laboratory detergent was applied by hand to the beads. The beads were dried in a five foot stainless steel tube which can be seen to the left of the cooler doorway in Plate 1.

Thirty-one thermocouples were placed within the model to measure temperatures for the purpose of recording the heat fronts through the model. A diagram given as Figure 2 illustrates the thermocouple positions within the model.

5.1.3 Steam Injection System

The steam used in the experiments was obtained by combining a stream of superheated steam with a stream of room temperature water. A low pressure boiler comprised of a fluidized bath** with a 100 foot (30.5 m) length of stainless steel tubing coiled inside was used to generate the superheated steam. By maintaining the superheated steam at a temperature of 120°C, the desired steam quality was obtained.

----

*Canasphere Industries Ltd., 3344-58th Ave. S.E., Calgary, Alberta. Cost = $9.25/lb.
†Slik No. 5 degreaser, supplied by Baroid of Canada, Ltd., Calgary, Alta., 263-8740. Cost = $2.40/litre.
**Techne Incorporated, 3700 Brunswick Pike, Princeton, New Jersey. Cost = $5400.

Side View

This view shows
the relative position
of the upper and lower
thermocouples.

36"

8 1/2"

3 1/2"

8 1/2"

2"

Granite
Block

Thermocouple
Ports
(Note The Two
Layers.)

Fiberglass
Model

Top View

This view illustrates
the approximate position
of the top layer of
thermocouples.

PRODUCTION
WELL

32"

32"

THERMOCOUPLE
LEADS

INJECTION
WELL
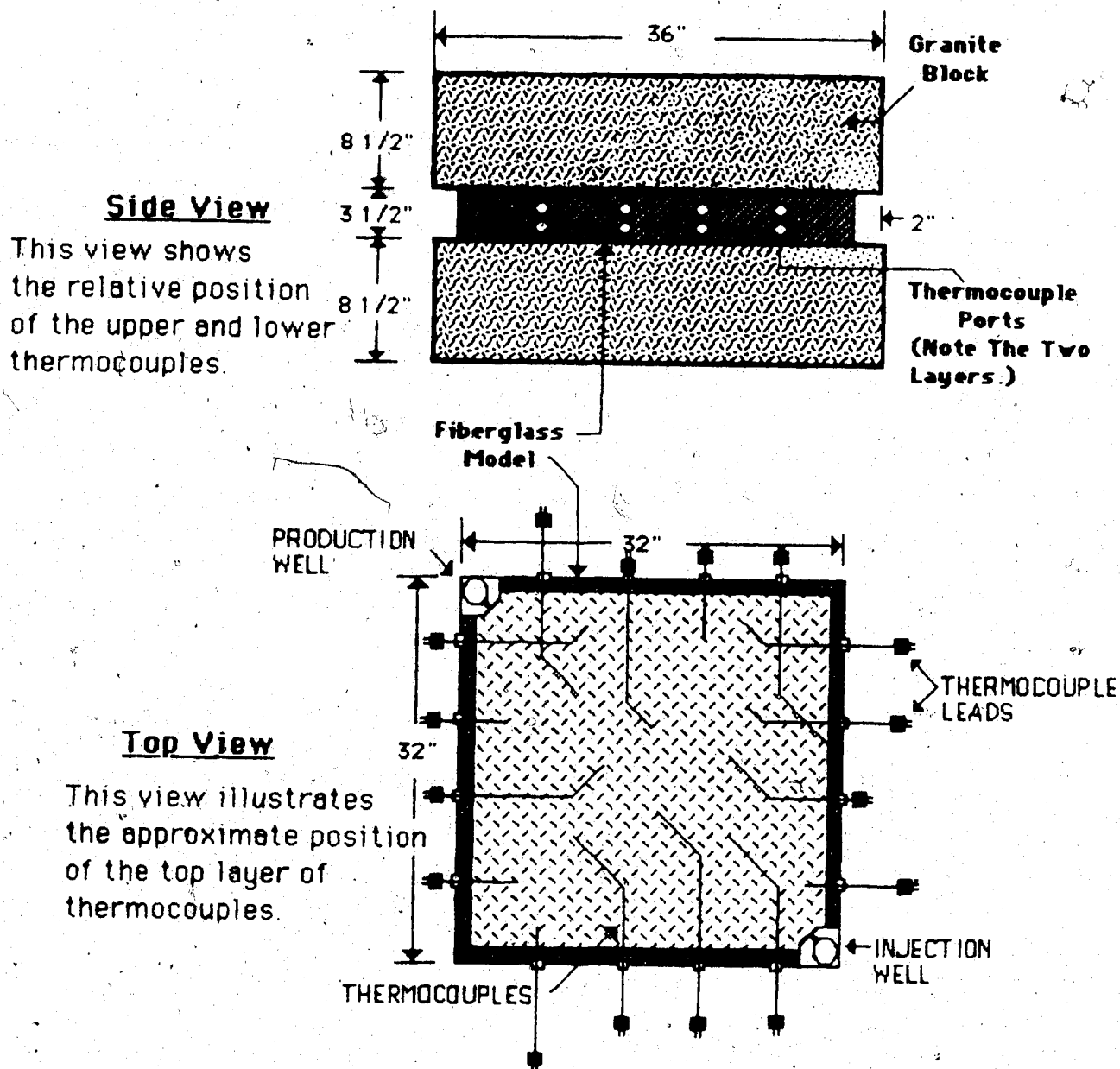
THERMOCOUPLES

Figure 2. Diagram of Model Illustrating Thermocouple
Positions

Plate 2 shows the main components of the steam injection system. The boiler assembly can be seen in the left portion of the plate. The two Milroyal controlled volume pumps used to pump de-aired, distilled water to the steam generator and to the water-steam mixing point are shown on the shelf of the table in the center part of Plate 2. Some of the stainless steel tubing and fittings required for the steam injection system are also visible in this plate.

5.1.4 Model Cart, Cold Storage

A unique design was employed in the construction of many components of the experimental apparatus. The model support cart is a good example of this. A shaft was welded into the support area for the model and this shaft was connected by a rack and pinion to a gear box. The gear box had a tremendous mechanical advantage so that the entire 4000 pound model apparatus could be rotated with ease to improve the efficiency of the saturation process and to allow the simulation of a dipping reservoir in future runs. The cart was set on castors which rolled on tracks to facilitate the movement of the model in and out of the cold storage room.

A walk-in cooler was used to cool the model to the initial temperature, as required by the scaling groups. A local company* custom built and installed the 8' x 10' x 7'h walk-in cooler.

----

*Alberta Zero-Temp Industries Ltd., 11440-81st Street, Edmonton, Alberta. Cost = $5387.
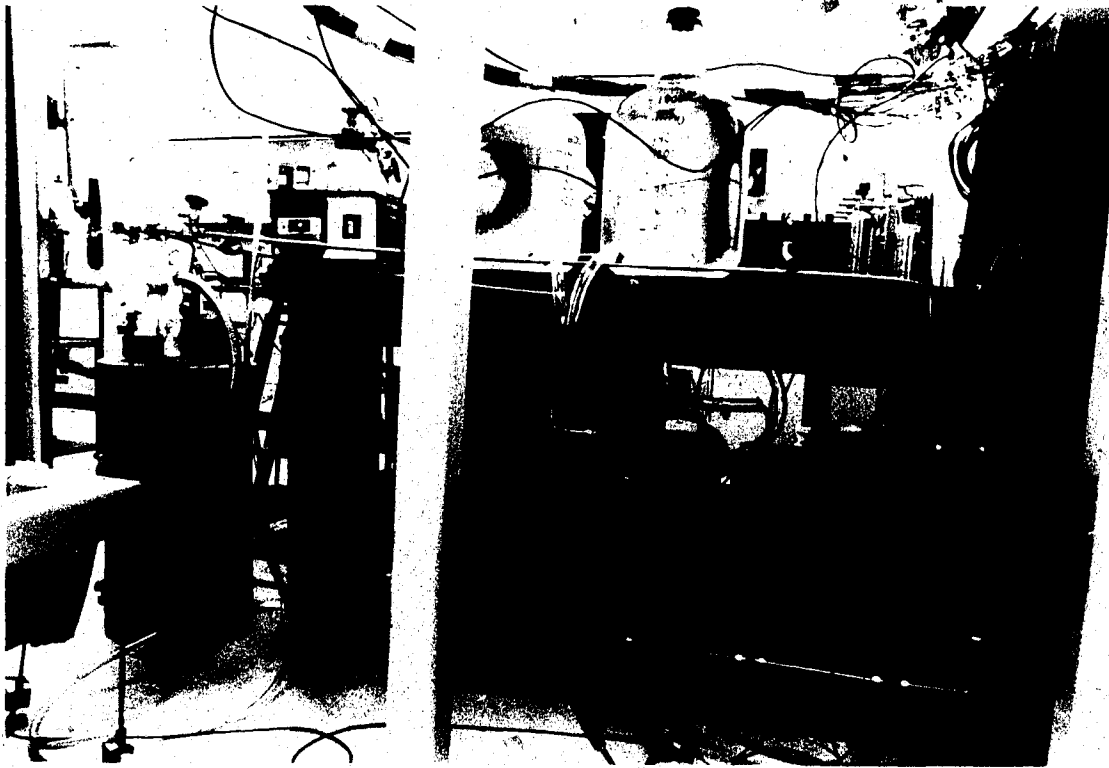
Plate 2: Steam Injection System.

Plate 3. Model Cart and Cold Storage Unit.

Plate 3 shows the model apparatus on the cart, ready to roll into the cooler. Notice the tracks on the floor for moving the cart in and out of the cold ·storage room. The structure shown in the foreground was used to remove the upper granite block to facilitate packing and cleaning operations.

5.1.5 Data Acquisition System

In order to obtain as much information as possible from each experiment, thermocouples* and pressure transducers† were placed in the system to measure temperature and pressure, respectively. A MEGADAC data acquisition unit from Optim Electronics Corporation** was used to collect data during the experimental runs. The MEGADAC was capable of reading up to 128 input channels and these channels could be scanned at a rate as slow as one sample per 30 minutes and as fast as 20000 samples per second. One outstanding feature of this unit was that it could be configured with an IBM Personal Computer and, using the software supplied with the MEGADAC, the IBM PC could control the data acquisition system and process the experimental results.

The IBM PC acted as an interactive interpreter between the data acquisition unit and the experimenter. It prompted the experimenter to send information to the MEGADAC which

----

*Thermo Electric (Canada) Ltd., 8425 Argyll Road, Edmonton, Alberta. Cost = $72.99 (TC and wire).
†Validyne Engineering Corporation, 8626 Wilbur Avenue, Northridge, California.
**Optim Electronics Corporation, Middlebrook Tech Park, 12401 Middlebrook Road, Germantown, Maryland. Cost = $26,000.

then performed the desired operation and returned the result to the IBM PC. In addition to these controlling capabilities, the software provided many other features, including graphing of results. A system with such capabilities was essential for this project because the actual run time was very short. The MEGADAC unit and the IBM PC running the OPTIM User's Software are shown in Plate 4.

5.1.6 Collection System

Operating the experiments under vacuum conditions introduced special considerations into the design of a collection system. The pore volume of the model was too large to allow the use of a single container to collect the produced fluids and very little information could be obtained from a single sample. Therefore, the system used two flasks to collect the produced fluids and these flasks were arranged so that they could be isolated from the vacuum and emptied individually. Because the vacuum was applied through the produced fluids collection system, it was expected that some vapourization of the produced fluids would occur. For this reason, the collection system included a series of condensers and cold traps to collect and retain all of the produced fluids. Figure 3 shows the configuration of the collection system.

The initial production temperature is low (approximately 3°C), so in order to prevent clogging within the production lines, the early production stream was warmed by flowing hot tap water through the first series of
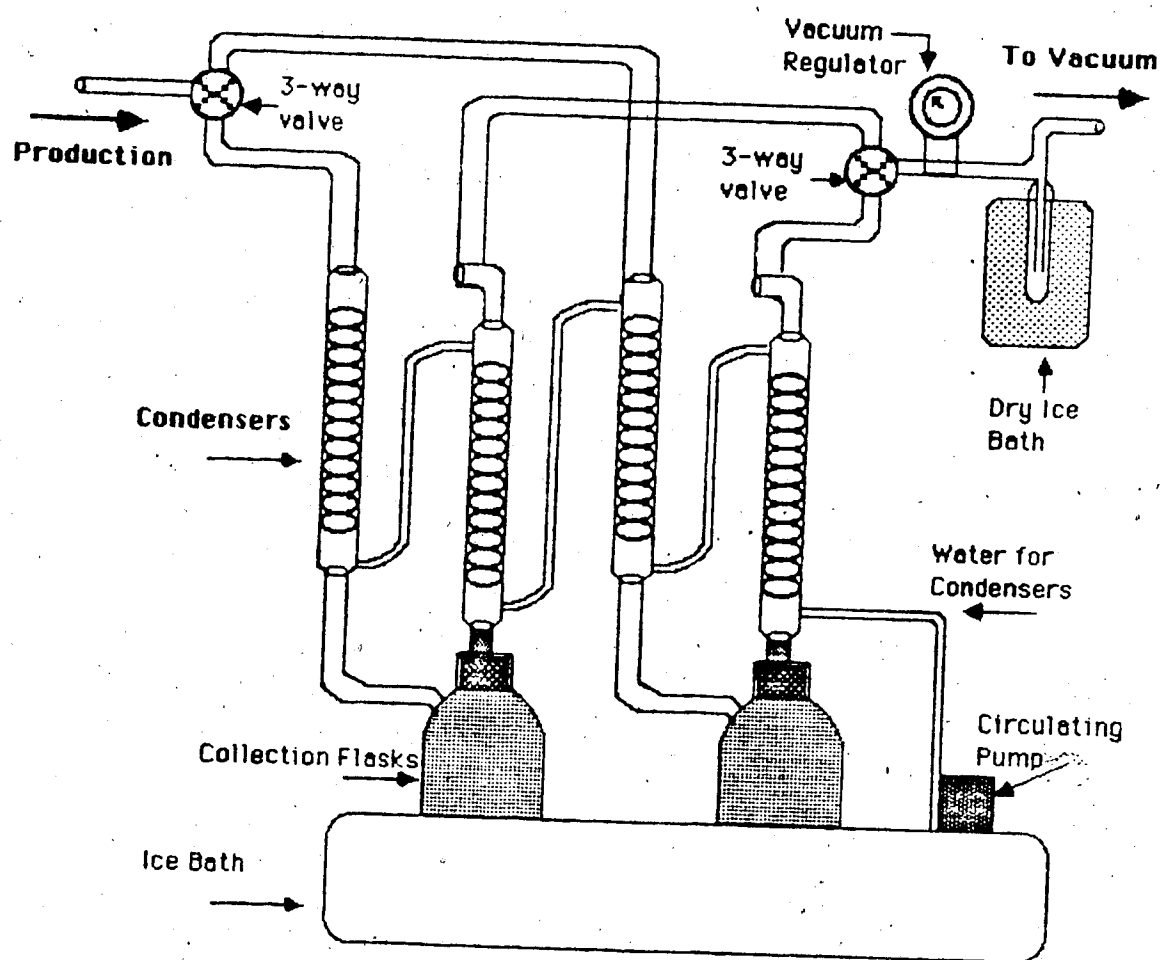
Figure 3. Produced Fluids Collection System

Plate 4: Data Aquisition System.

condensers. However, after injecting approximately half a pore volume of steam, the production temperature was considerably higher. The hot water previously running through the first series of condensers was then replaced by ice water so that the produced fluids were completely condensed.

Because the vacuum was applied through the collection system, it was expected that some of the liquid would be vapourized again, after reaching the production flasks. For this reason, another set of ice water condensers and finally a carbon dioxide cold trap were included in the collection system.

5.1.7 Model Fluids

5.1.7.1 Oil for the Aberfeldy Model

A table detailing the relationship between the required model oil viscosity and the Aberfeldy prototype oil viscosity was presented in a previous chapter as Table 2. Using values from the upper part of this table, which Stegemeier, Laumbach, and Volek[37] indicate are the most accurate, an average value of the ratio of model oil viscosity to prototype oil viscosity was found to be 7.26. If the prototype versus model temperature relation, given by Equation (6), is applied to this viscosity relationship, the values presented in Table 5 can be obtained.

To obtain the desired temperature - viscosity profile for the model oil, a refined MCT 30 base oil, Faxam 100,

Table 5. Temperature vs. Oil Viscosity for the Aberfeldy
Prototype Oil and the Model Oil

Prototype Temperature (C)	Prototype Oil Viscosity (mPa·s)	Model Temperature (C)	Ideal Model Oil Viscosity (mPa·s)
23.9	1275	3.2	9256.5
32.2	560	5.6	4065.6
65.6	90	15.1	653.4
135.0	12.5	35.0	90.75
301.7	1.29	82.6	9.37

supplied by Imperial Oil Limited* was used. A temperature - viscosity profile comparing the ideal curve and the curve given by the Faxam 100 oil is presented as Figure 4. The inclusion of the temperature scaling relationship creates a distortion in the ideal model oil curve which cannot be represented by a real oil. However, the Faxam 100 does provide a reasonable match.

5.1.7.2 Models Oils for the Heavy Oil and the Light Oil Experiments

In addition to the Aberfeldy model experiments, runs were conducted with a higher viscosity oil (11000 mPa·s at room temperature) which represented a prototype oil with reservoir temperature oil viscosity of approximately 13000 mPa·s, and runs were conducted with a lower viscosity oil (50 mPa·s at room temperature) which represented a prototype oil with reservoir temperature oil viscosity of approximately 25 mPa·s. Tables 6 and 7 show the temperature - viscosity relationship of both of these oils, in prototype terms.

5.2 Model Packing and Saturation

5.2.1 Model Packing Procedure

Due to the size and shape of the model used, packing methods such as tamping or vibrating are not practical. Therefore, a 'particle distributor' was employed to pack the glass

----

*McEwen's Fuels & Fertilizers Ltd., ESSO Bulk Plant Agent, 3704 92nd Ave., Edmonton, Alberta.

Table 6. Temperature vs. Oil Viscosity for the Heavy Oil

Model Temperature (C)	Ideal Model Oil Viscosity (mPa·s)	Prototype Temperature (C)	Prototype Oil Viscosity (mPa·s)
3.18	95000	23.9	13085.4
5.55	81000	32.2	11157.0
15.10	36000	65.6	4958.7
35.00	7600	135.0	1046.8
82.63	4500	301.7	619.8

Table 7. Temperature vs. Oil Viscosity for the Light Oil

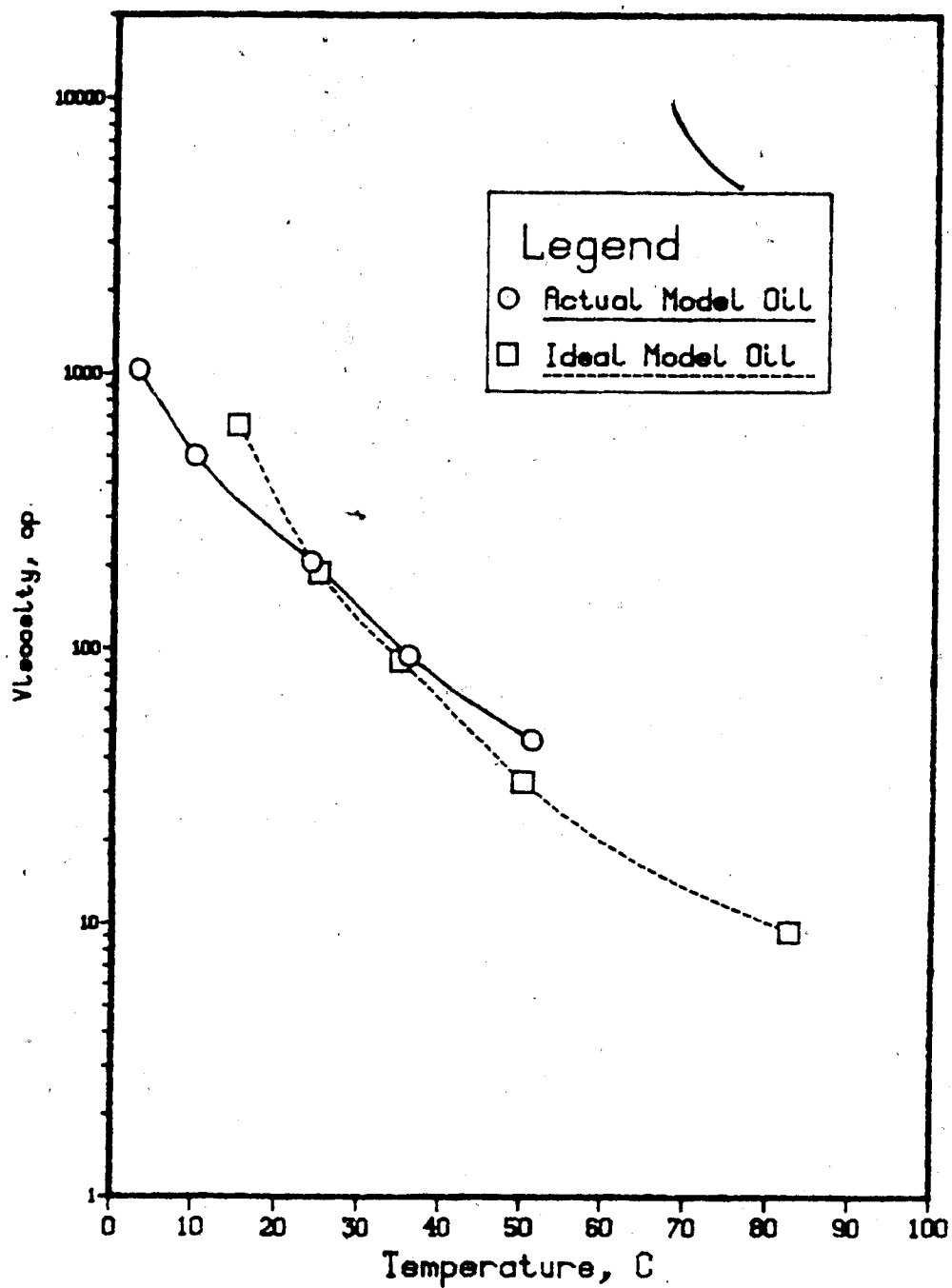| Model Temperature (C)	MCT 10 Oil Viscosity (mPa·s)	Prototype Temperature (C)	Prototype Oil Viscosity (mPa·s)
3.0	185.5	23.3	25.6
11.0	96.8	51.2	13.3
32.0	33.1	124.7	4.6
49.0	17.6	184.1	2.42

Figure 4. Temperature-Viscosity Profile for the Ideal and the Actual Model Oil

beads in the model. This method of packing was first proposed by Currie and Gregory[54] and later modified by the Gulf Research & Development Company as reported in a paper by Wygal.[57]

It is claimed that the particle distributor can be used to obtain packs which are mechanically stable with uniform properties throughout, and which may be accurately reproduced. The tamping and vibrating method of packing is said to create packs which are usually non-uniform or unstable.

The success of the particle distributor is a result of the beads hitting the pack singly after being evenly distributed by a set of sieves. Part of the energy of the falling bead is transferred to the surface beads which are thereby knocked into more stable positions. As the pack grows, the surface reportedly appears fluid and alive for a depth of two or three particle diameters.

The particle distributor is easily made. For this project, it was constructed using five wire mesh screens with 5/8 inch openings. The screens were enclosed in a plywood box designed to fit over the large model. A diagram of the particle distributor is given in Figure 5. The model was packed by allowing the beads to pass through a metering board onto the screens at a uniform rate. After passing a sufficient number of beads through the particle distributor and into the model, the particle distributor was removed and the excess beads were trimmed off the model surface. The porosities of the bead packs were consistently of the order of 33%, with very little variation.

5/8" Mesh
Screens

2"

26"

32"

Plywood Box
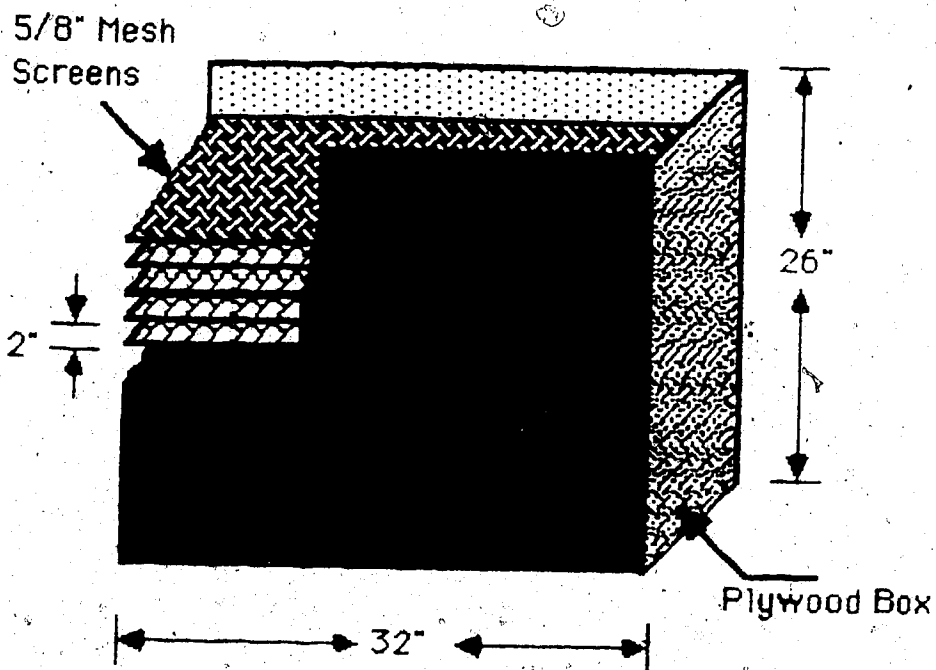
Wygal Particle Distributor

Figure 5. Model Packing Device

5.2.2 Model Saturation

After packing the model with glass beads, a Teflon sheet was placed above the model and a thin layer of silicone was applied between the Teflon sheet and the fiberglass model to provide a vacuum tight seal. A rubber sheet was placed on top of the Teflon sheet to ensure that complete contact was made between the porous media and the upper granite block, which was then set in place above the model, and the entire apparatus was tilted.

Six large saturation ports were incorporated into the model (three on each of two opposing sides) to improve the efficiency of the saturation process. With the apparatus in a tilted position, fluids entered the model from the downdip end and thus the fluid flow into the model proceeded with a gravity stabilized front. To begin the saturation process, a vacuum was applied at the updip end and de-aired, distilled water was pulled into the model through the saturation ports at the downdip end. This continued until the model was completely saturated with water. The amount of water taken into the system was carefully measured and the model porosity was calculated using this water volume.

Valves were installed at the injection and production points. When the model was completely saturated with water, these valves were closed so that a vacuum was maintained within the model, and the water injection lines were replaced by oil injection lines. Next, oil was drawn into the model by a method similar to that described for the water. The amount of oil taken into the model was measured so that the initial oil saturation could be determined.

The above saturation procedure worked well for the Aberfeldy model oil (Faxam-100) and the light oil (MCT-10), but the heavy oil required a modification of the above procedure. It was necessary to warm the heavy oil to about 75°C before attempting to pull it into the model. Even then, the saturation process required ten hours, more than seven of which were needed just to pull the oil into the model.

After saturation was complete, the apparatus was rolled into the cooler to bring the model to the low initial temperature required by the scaling groups. Cooling the large model to 3°C took between 24 and 36 hours.

5.2.2.1 Preparing the Bottom Water Model

Run 15 was a continuous steamflood in a model representing a portion of the Aberfeldy reservoir which was underlain by water. The water layer in the model was established by packing the lower layer of the model with beads and then introducing the volume of water necessary to create the desired bottom water thickness. The original intention was to create a layer of water one inch thick (2/5 of the reservoir thickness). An average final porosity of the bead pack was assumed to be 33% (based on the experience of previous runs). Thus the pore volume of the model would be 0.33 times 42005 cm³ (the total volume of the empty model) which equals 13862 cc. Therefore, 2/5 of this was expected to make up the desired one-inch bottom-water layer. This volume of water was added to the packed model, and the model was placed in a level position in a freezer to freeze

the bottom water into place.

To complete the saturation procedure for this run, a vacuum was applied and 9490 cm³ of de-aired water was pulled into the upper part of the model. Some thawing of the frozen water layer may have occurred in this step, but because the water saturation procedure was relatively quick, the amount of thawing was probably minimal. (The thawing at this point could be further reduced in future runs by saturating with ice cold water.)

Next, oil was drawn into the model to displace the liquid water. The volume of water displaced during this phase of the saturation process was 11520 cc, which indicates a significant amount of thawing occurred in the frozen layer. Calculations based on the assumption that the oil saturation in the oil zone was 92% (which was typical of many runs), indicated that the bottom water layer was 0.43 inches thick (17.2% of the total formation thickness).

5.3 Conducting the Experiments

During the time the model was cooling, other work was performed in preparation for the run. The injection bottles were filled with distilled water and a vacuum was applied to remove any gas which was trapped in the water. All injection and production lines were inspected for leaks and adjusted or replaced if necessary. The thermocouples external to the model were also inspected and replaced if necessary. In addition, all of the pressure transducers were checked or calibrated prior to each run. Just before the model was taken from the cooler, the collection system

was prepared by filling the upper vacuum cold trap with dry ice and obtaining hot water and ice for the condensers.

When the model apparatus had cooled to the initial temperature, as dictated by the scaling calculations, it was rolled out of the cooler and the thermocouple and pressure transducer leads were attached. The data acquisition unit was monitored to ensure that all of the thermocouples and pressure transducers were functioning properly and giving reasonable readings. The injection and production lines were then attached and the steam bypass valve was opened. Steam was flowed through the bypass line until it had stablized at the temperature required for the run, typically 65°C.

With all of the preparatory work complete, the data acquisition unit was reset for the new experiment and the production and injection valves were opened simultaneously. The MEGADAC was programmed to scan each thermocouple and pressure transducer once every thirty seconds. The data was printed continuously and was also saved on the IBM hard disk drive.

The produced fluids were collected in two, 2000 cm³ flasks, which were emptied into a series of 2000 cm³ graduated cylinders. In this way, instantaneous oil and water recovery could be observed as a function of each two litres of total production. Steam injection was continued until one and a half to two pore volumes had been injected, unless problems were encountered.

5.4 Data Analysis

Following the run, a table of instantaneous and cumulative production as functions of the number of pore volumes of steam injected was prepared. Several plots were generated for each run to analyze the data. These included the following:

* A plot of cumulative recovery vs. pore volumes of steam injected.

* A plot of the instantaneous oil and water recovery as a function of pore volumes of steam injected.

* A plot of the instantaneous oil-steam ratio as a funtion of the cumulative oil production.

* Temperature profiles at 0.25, 0.50, 0.75, and 1.00 pore volumes of steam injected.

In addition to these plots, some others were generated to compare the production response resulting from varying recovery schemes and experimental conditions.

6. EXPERIMENTAL RESULTS AND DISCUSSION

Twenty-two experimental runs were attempted as part of this work. The initial conditions for each of these experiments are presented in Table 8. The successful experiments were of the following types:

1. Preliminary runs on a small model. These runs were conducted to gain familiarity with the apparatus and to ensure that all the components were operating satisfactorily.

2. Continuous steamflood conducted in a model saturated with water only. This run was conducted to observe the heat flow within the model and to gain experience with the large model.

3. Continuous steamfloods conducted in a model representing the Aberfeldy reservoir.

4. Continuous steamfloods conducted in a model designed to represent a light oil prototype.

5. Continuous steamfloods conducted in a model saturated with an oil much more viscous (9250 mPa·s at m temperature) than the oil used to represent the Aberfeldy crude.

6. Steamflood following a waterflood. This run was conducted to examine the recovery of waterflood residual oil by steam injection and to analyze the ability of the vacuum model to simulate such a process.

7. Continuous steamflood conducted in the Aberfeldy model with a bottom water zone.

8. Steam slug runs. These runs were conducted to examine the possibility of driving a small slug of steam by the

TABLE 8: INITIAL CONDITIONS FOR EXPERIMENTS

Run#	Vol Water Inj to Sat (cc)	Porosity (%)	Vol Oil Inj to Sat (cc)	Swi (%)	Sol (%)	Initial Temp. (C)	Oil Type	Run Type
1								Preliminary Run
2								Preliminary Run
3*								Preliminary Run
4	13590	32.4	0.00	100.00	0.00	23.0	(Water)	Continuous Steamflood
5	14180	33.8	12300	13.26	86.74	2.5	Faxam-100	Continuous Steamflood
6	13990	33.3	12160	15.51	84.49	1.9	Faxam-100	Continuous Steamflood
7A	13040	31.0	11420	9.59	90.41	3.0	Faxam-100	Cold Waterflood
7B						23.9	Faxam-100	Room Temperature Waterflood
7C						2.7	Faxam-100	Continuous Steamflood
8	15080	35.9				3.0	Heavy Oil	Unsuccessful Run
9	13800	32.9	12100	12.32	87.68	4.0	Heavy Oil	Continuous Steamflood
10	12700		11680	8.00	92.00	4.0	Faxam-100	Continuous Steamflood
11	12945		11040	14.72	85.28	3.0	MCT-10	Unsuccessful Run
12	14050	30.1	12535	10.78	89.22	3.0	MCT-10	Continuous Steamflood
13	12660	33.1	11670	7.82	92.18	3.0	MCT-10	Continuous Steamflood
14	13910	35.9	12550	9.78	90.22	3.0	Faxam-100	Unsuccessful Run
15	13136	32.4	11520	12.30	87.70	3.0	Faxam-100	Steamflood on Bottom Water Model
16	13620	32.9	12730	6.53	93.47	3.0	Faxam-100	Unsuccessful Run
17	13820	33.0	12800	7.38	92.62	3.0	Faxam-100	Cold Water Slug Run
18	13880	33.3	12770	8.00	92.00	3.0	Faxam-100	Cold Water Slug Run
19	13970	32.1	12785	8.48	91.52	3.0	Faxam-100	Cold Water Slug Run
20	13510	32.5	12620	6.59	93.41	3.0	Faxam-100	Unsuccessful Run
21	13660	34.1	12890	5.64	94.36	3.0	Faxam-100	Unsuccessful Run
22	14310		12800	10.55	89.45	3.0	Faxam-100	Hot Waterflood
AVERAGE	13676	32.8	12257	9.84	90.16			

Faxam-100 represents Aberfeldy prototype. (Viscosity = 268 cp at 23 C)
Heavy Oil (Viscosity = 9256.5 cp at 24 C)
MCT-10 represents a light oil prototype. (Viscosity = 60 cp at 23 C)

* Note: The Heavy Oil was too thick at room temperature to saturate the model.

continuous injection of cold water.

9. Hot water slug run. This run was conducted to determine whether steam injectivity could be improved by initially injecting hot water.

The data analysis following each run included the preparation of a table showing all of the important experimental parameters and a listing of the production as a function of steam or water injection. Plots of cumulative recovery versus pore volumes of steam injected, plots of instantaneous oil and water production as a function of cumulative injection, plots of instantaneous oil-steam ratios, and plots comparing the recoveries of several runs were also included in the data analysis. In addition, temperature profiles were generated for each run at increments of 0.10 pore volumes (water equivalent) of steam or water injected.

6.1 Model Design and Operation

Extensive details concerning the scaling of the steam injection process, the equipment included in the apparatus, and procedures used to conduct the experiments were presented in previous chapters. A brief summary of the model design and operation is presented in this section.

Three models were constructed for this project to represent the Aberfeldy prototype; two with length scaling factors of 400 to 1 (one twice as thick as the other) and one relatively large model with a length scaling factor of 173.2 to 1. Each model was designed to simulate one quarter of a five-spot pattern and as such, each had one injection

well and one production well in diagonally opposite corners. The smallest model was used for the preliminary experiments (Runs 1-3) because the degree of work involved in preparing for and conducting these experiments was proportionally less than the work necessary for the larger model experiments.

Most of the experiments were conducted in the large scale model. This model had dimensions of 81.28cm x 81.28cm x 6.35cm thick (32in. x 32in. x 2.5in.) which, when used to represent the Aberfeldy prototype (8 hectare pattern, 11m thick), resulted in a three-dimensional geometric length scaling factor of 173.2. It was constructed out of molded fiberglass and was fitted with 31 thermocouples, placed in two layers within the model. Figure 2 gives a sketch of the model and indicates the position of the thermocouples within the model. The model wells were fabricated from aluminum and were designed to allow a gate device to be inserted into them so that the injection and production intervals could be selectively chosen as required.

In preparation for a run, the model was packed with 3 mm (6-8 mesh) glass beads which gave a permeability of approximately 4200 darcies. A Teflon sheet was sealed to the top of the fiberglass model with silicone and a vacuum was applied to the pack. When the silicone had set sufficiently, so that the vacuum was maintained in the model, the model pack became extremely rigid, and was ready to saturate. The model was saturated in an inclined position with the fluids entering the model from the downdip end through specially designed saturation ports. It was crucial that a vacuum be maintained during the entire

saturation process.

With oil and water saturation complete, two clamping devices were attached to the model to help maintain the vacuum in the event that the internal pressure momentarily exceeded atmospheric during the run. The model was then rolled into the cold storage unit and left to cool for 24 to 36 hours. During this time, the distilled water used for the run was de-aired (and cooled if necessary). The injection pumps were calibrated and all other components of the apparatus were inspected and calibrated if required.

When the model had reached the desired initial temperature (3°C) as dictated by the scaling calculations, it was rolled out of the cooler and the thermocouple and pressure transducer leads were attached and the injection and production lines were put in place. When the steam had stabilized at the desired temperature and the data acquisition unit had been programmed for a new experiment, the run was started. For a typical steam injection the steam entered the model at a temperature of about 65°C and at a flow rate of 230 cm³/min.

The first few minutes of each run were the most critical. For a successful run, oil production was almost immediate; however, as shown in Table 8, not all runs were successful. A common problem with the runs was that the initial steam injectivity could not be attained for the flow rates dictated by the scaling criteria. In a few cases (Runs 11, 14, and 16) this resulted in overpressuring the model to the point where even the clamping device could not maintain the vacuum seal and thus, the run was aborted.

Runs 20 and 21 were spoiled when plugging of the production lines by silicone was not detected prior to the runs.

The heavy oil runs (Runs 8 and 9) posed a special problem with respect to the saturation process. Before the vacuum could successfully draw the heavy oil into the model, the oil had to be warmed to about 75°C and even then, seven hours were required to pull the oil into the model.

In general, the packing and saturating procedures were trouble-free (except for Run 8, as discussed). However, Table 8 shows that there was some variation in the porosity and the initial oil and water saturation of the bead packs. Note that the average porosity of the bead packs was 32.8% and that the porosities ranged from 30.1% (Run 13) to 35.9% (Runs 8 and 15). Also note that the average initial oil saturation was 89.5% and that this varied from 84.49% (Run 6) to 94.36% (Run 21).

The variations in the porosities and saturations may be due to incomplete water and oil saturation within the model. (Recall that the porosity was also determined by the volume of water taken up during the saturation process.) In all runs, the saturation process included the injection of water or oil to the point where it was first observed in the production lines on the side of the model opposite the injection ports; then an additional 2000 cm³ was injected. However, this extra 2000 cm³ only represents an extra 15% of the model pore volume, which, in view of the observed variations in porosity and saturation values, may not be adequate to ensure complete saturation.

6.1.1 Operational Difficulties

Because this project entailed the design and construction of the entire apparatus, several modifications were necessary in the early stages. These included improving the saturation procedure, modifying the collection system, and incorporating better data reduction techniques. However, at the completion of the preliminary runs, most of the necessary improvements had been made.

Some problems could not be remedied with as much success. As noted previously, injectivity problems at the beginning of some runs prevented the continuous injection of steam at the design flow rate. It was occasionally necessary to turn off the injection pumps while maintaining the vacuum at the production end in order to lower the pressure within the model. It is felt that these brief periods without steam injection did not significantly affect the experimental results.

The lack of precise control over the temperature of the steam generating bath posed some difficulties. The boiler was occasionally unable to maintain the necessary temperature and as a result, the steam quality may have been slightly lower than it was designed to be for a few runs. The hot water slug run (Run 22) did not proceed as planned because the steam generator was not capable of increasing temperature during the run. The plan was to begin the run with hot water at an injection temperature of about 40°C and gradually increase the temperature to a steam temperature of 65°C.

6.1.2 Interpretation of Temperature Profiles

A commercially available contouring package* was used to generate temperature profiles for the experiments. Because of the large number of these profiles, they were placed in Appendix A, and organized according to run number.

Each line within a temperature profile represents a particular isotherm; that is, each line passes through points of equal temperature within the model. Because two layers of thermocouples existed within the model, it was possible to present isotherms for each of the two layers, which helped to determine the mechanism of the steam drive occurring within the model. To facilitate interpretation, the upper isotherms were drawn in blue, and the lower isotherms were drawn in red, and each were drawn with a distinct line type so that reproduction in black and white would not prevent the necessary interpretation. If the heat front advanced more rapidly in the upper part of the model, the temperature profiles would show the upper isotherms advancing more rapidly (the isotherm for a specific temperature would extend further in the upper layer), and similarly, if the heat front advanced more rapidly in the lower portion of the model, the temperature profiles would show the lower isotherms advancing more rapidly.

Asymmetrical advance of the isotherms may have been indicative of irregularities in the advance of the heat front, and possible reasons are discussed in later sections. However, some deviations in the isotherms were a result of

----

*DISSPLA, a proprietary software product of Integrated Software Systems Corporation, 10505 Sorrento Valley Road, San Diego, Ca.

problems with the contouring package. Instances where an isotherm curved over itself, or where two isotherms crossed, were due to imperfections in the software package, and should be overlooked. Likewise, in some cases, the contour package mistakingly interpreted the presence of isotherms which did not exist (such as a zero degree isotherm) and these should be ignored. In spite of these problems, the temperature profiles did provide a good indication of the heat front advance within the model. With the limitations in mind, the temperature profiles were used to explain the mechanisms involved in the oil recovery process for each experiment.

6.2 Base Steamflood

In Run 4, the model was saturated with 100% water and steamflooded. The purpose of this run was to examine the model and overall system operation, and to observe the general pattern of flow distribution. The temperature profiles for this run at 0.25, 0.50, 0.75 and 1.00 pore volumes of steam injected are presented in Appendix A as Figures 29, 30, 31, and 32, respectively. Each temperature profile clearly shows the heat distribution through the model, and examining them in series illustrates the progression of the heat front.

6.3 Continuous Steamfloods in Aberfeldy Model

Runs 5, 6, 7, 10, 17, 18, 19, and 22 were steamfloods conducted on a model with all pertinent parameters designed to simulate the Aberfeldy reservoir. Run 7 involved a

steamflood following a waterflood and will be discussed in a later section. Similarly, Runs 17, 18, 19, and 22 were designed to simulate a particular recovery scheme (slug runs) and also will be discussed in separate sections.

The remaining Aberfeldy runs (Runs 5, 6, and 10) were conducted with steam temperature and pressure of about 24 kPa and 65°C, respectively, and a steam quality of about 70%. The average steam flow rate was 230 cm³/min and the average initial oil saturation was 87.7%. Injection for each of these three runs was into the lower half of the reservoir while the production well was opened over the entire interval. Tables 9, 10, and 11 give a summary of the important experimental parameters of each run. Table 11 also details the recovery for Run 10 as a function of pore volumes of steam injected.

Run 5 was halted prematurely when the apparatus developed a leak after about 25 minutes of steam injection (0.45 pore volumes of steam injected). However, at this point, 6.6% of the original oil in place was recovered which is similar to the initial production response observed in Run 6. This represents an oil-steam ratio of approximately 0.13.

Figure 6 presents the cumulative recovery as a function of the pore volumes of steam injected for Runs 6 and 10, and plots of instantaneous oil and water production as a function of cumulative injection are given in Figures 7 and 8 for Runs 6 and 10, respectively. These figures indicate that following breakthrough (which was observed during the experiments to be at about 0.13 pore volumes injected), the

Table 9. Experimental Data for Run 5; Steamflood in
Aberfeldy Model

Type of Oil Used: Faxam-100 (208 mPa·s at 23°C)
Pore Volume: 14180 cm³
Porosity of Bead Pack: 33.76 %
Hydrocarbon Pore Volume: 12300 cm³
Initial Oil Saturation: 86.74 %
Irreducible Water Saturation: 13.26 %
Initial Model Temperature: 2.5°C
Water Feed Flow Rate: 199.6 cm³/min
Boiler Feed Flow Rate: 27.3 cm³/min
Total Flow Rate of Steam: 226.9 cm³/min
Volume of Steam Injected: 6320 cm³ (0.45 PV)
Volume of Oil Recovered: 810 cm³ (6.59 % OOIP)

Table 10. Experimental Data for Run 6; Steamflood in
Aberfeldy Model.

Type of Oil Used: Faxam-100 (208 mPa·s at 23°C)
Pore Volume: 13990 cm³
Porosity of Bead Pack: 33.31 %
Hydrocarbon Pore Volume: 12160 cm³
Initial Oil Saturation: 84.49 %
Irreducible Water Saturation: 15.51 %
Initial Model Temperature: 1.93°C
Water Feed Flow Rate: 200.2 cm³/min
Boiler Feed Flow Rate: 27.1 cm³/min
Total Flow Rate of Steam: 227.3 cm³/min
Volume of Steam Injected: 32710 cm³ (2.34 PV)
Volume of Oil Recovered: 2660 cm³ (21.89 % OOIP)

Table 11.   Experimental Data for Run 40; Steamflood in
Aberfeldy Model

Type of Oil Used: Faxam-100 (208 mPa·s at 23°C)
Pore Volume: 12700 cm³
Porosity of Bead Pack: 30.23 %
Hydrocarbon Pore Volume: 11680 cm³
Initial Oil Saturation: 92.00 %
Irreducible Water Saturation: 8.00 %
Initial Model Temperature: 4.07°C
Water Feed Flow Rate: 199.8 cm³/min
Boiler Feed Flow Rate: 30.3 cm³/min
Total Flow Rate of Steam: 230.1 cm³/min
Volume of Steam Injected: 26850 cm³ (2.114 PV)
Volume of Oil Recovered: 3677 cm³ (31.48 % OOIP)

Cumulative Total PV Injected (cm³)	Cumulative Total PV Injected (PV)	Cumulative Oil Produced (cm³)	Cumulative Oil Produced (%OOIP)	Oil-Steam Ratio (cm³/cm³)
1100	0.087	540	4.62	0.4909
2830	0.223	895	7.66	0.2052
4280	0.337	1245	10.66	0.2414
6085	0.479	1690	14.47	0.2465
7575	0.596	1897	16.24	0.1389
9265	0.730	2027	17.35	0.0769
10760	0.847	2234	19.13	0.1385
12550	0.988	2399	20.54	0.0922
14240	1.212	2624	22.47	0.1331
16050	1.264	2749	23.54	0.0691
17745	1.397	2859	24.48	0.0649
19535	1.538	2998	25.67	0.0776
21335	1.680	3162	27.07	0.0911
23135	1.822	3304	28.29	0.0789
24030	1.892	3381	28.95	0.0860
24950	1.965	3422	29.30	0.0446
26850	2.114	3677	31.48	0.1342

Two Continuous Steamfloods in Aberfeldy Model.
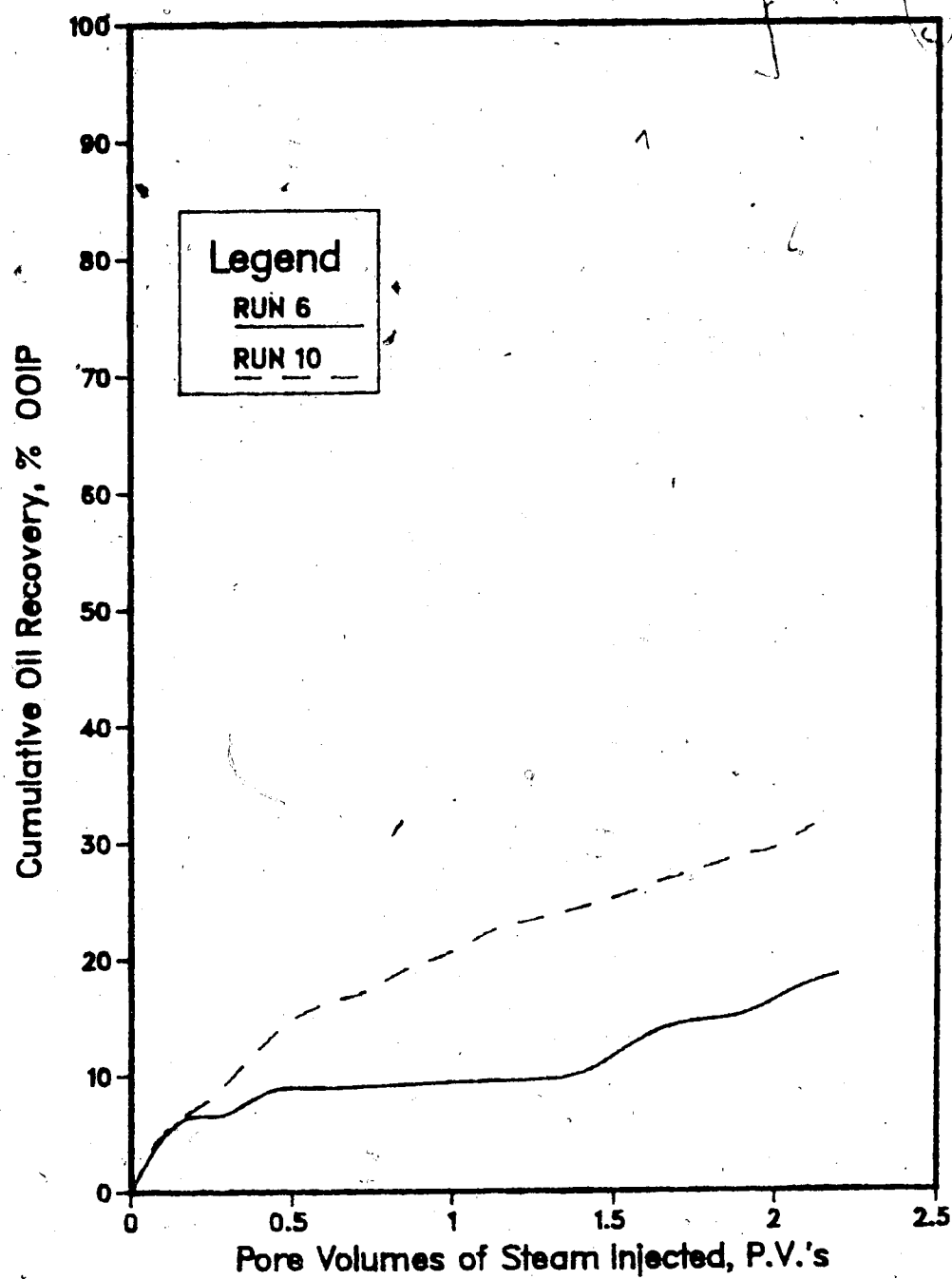
Figure 6. Comparison of the Recovery Response of Run 6 and Run 10.
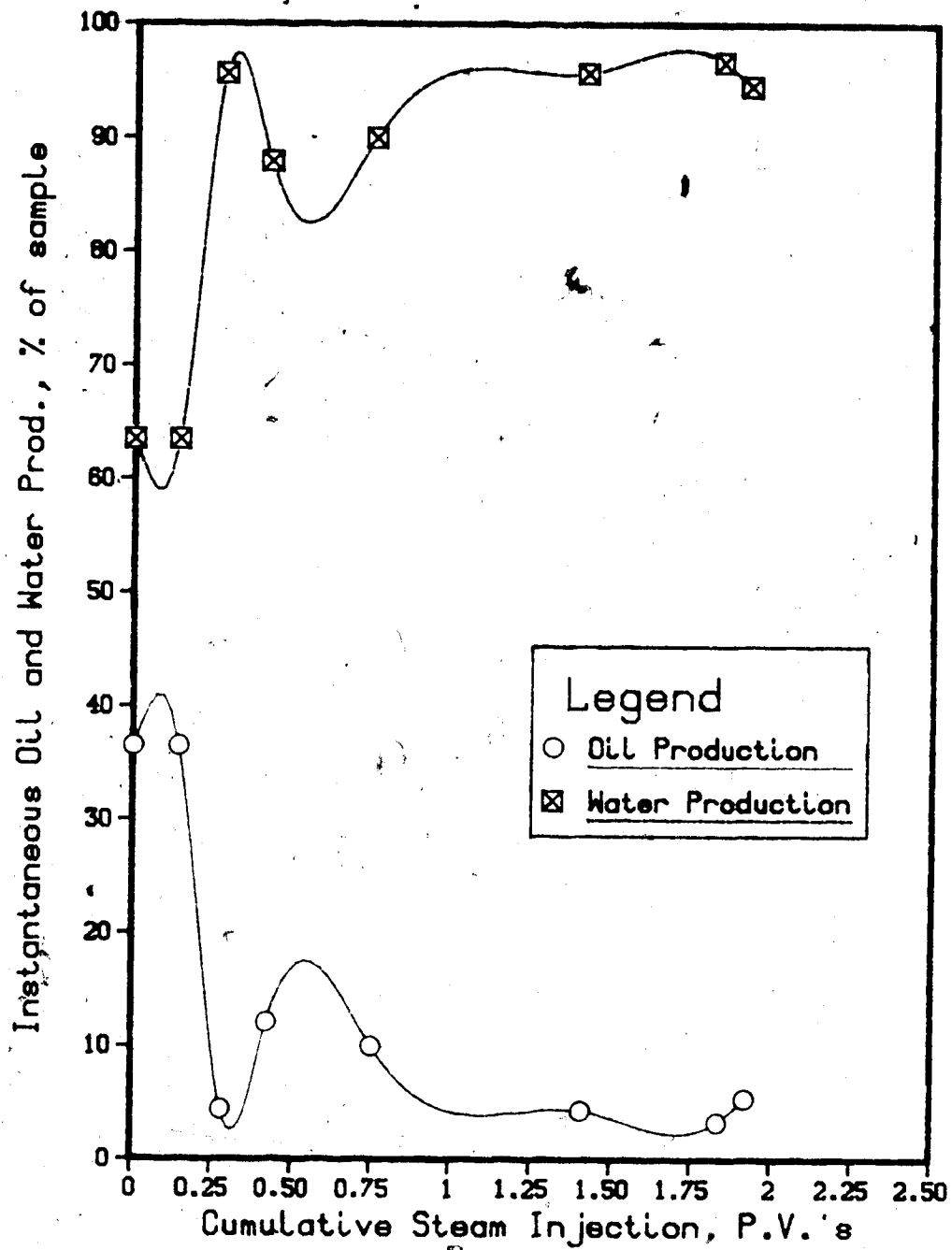
Figure 7.   Run 6, Instantaneous Oil and Water Production vs.
Cumulative Injection.
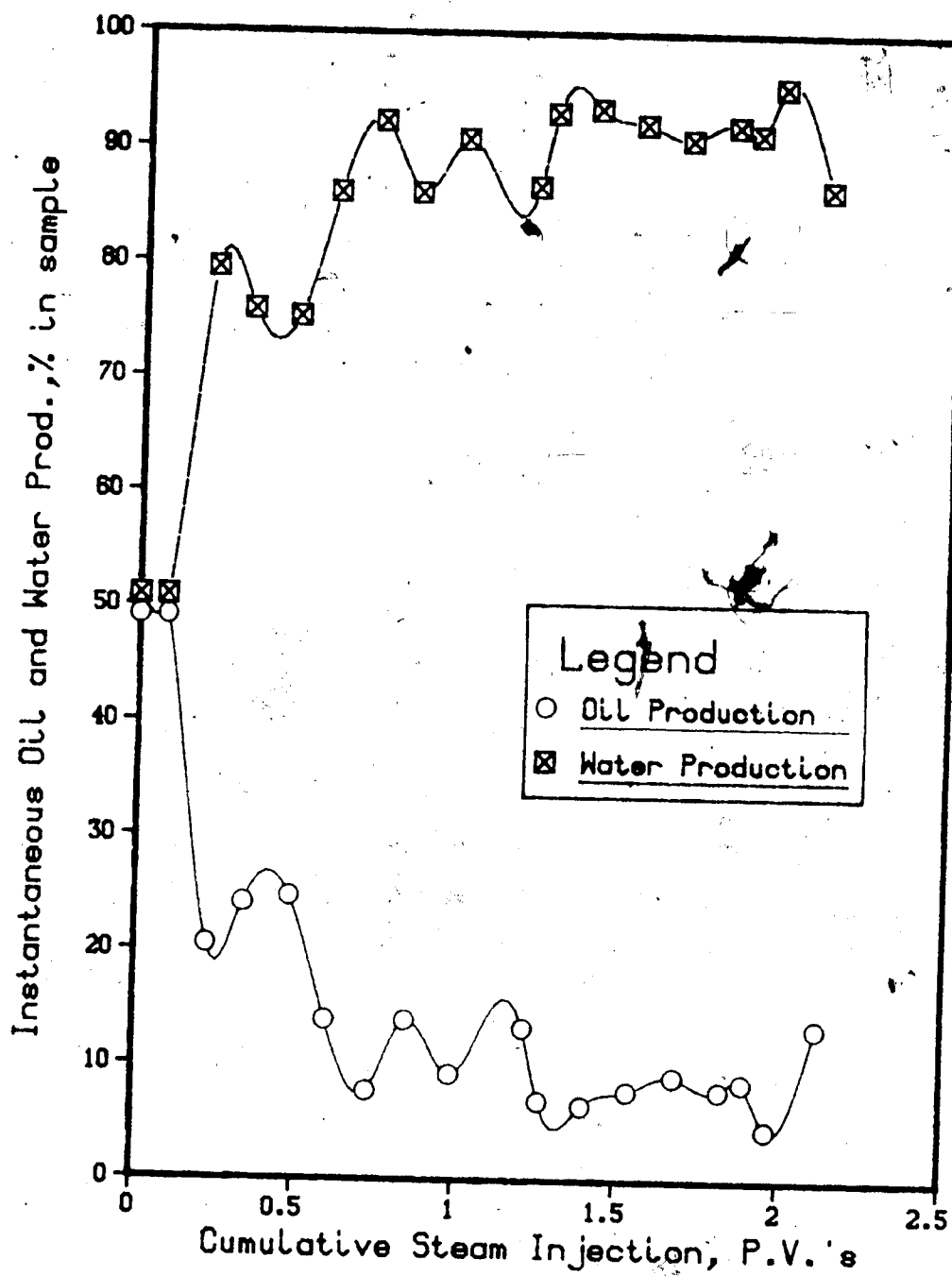
Figure 8. Run 10, Instantaneous Oil and Water Production vs. Cumulative Injection.

cumulative oil recovery still increased at an appreciable rate. This may be because the steam advance at this point was irregular, and pockets of oil were recovered sporadically. If the steam zone had advanced in the classical sweep pattern (as predicted by an assumption of frontal drive), there would be considerably less oil production after breakthrough.

The average oil-steam ratio for Run 10, at 2.114 pore volumes of steam injected, was 0.1369, and the recovery to this point was 31.48% of the original oil in place. The total oil recovery of Run 6 was considerably lower than that of Run 10 (21.9% OOIP after injecting 2.34 pv) which is illustrated by plotting the two recovery curves together, as done in Figure 6. However, it can be seen that the initial oil production response for the two runs was similar and that the production response only began to differ significantly after breakthrough.

Temperature profiles for Run 6 at 0.25, 0.50, 0.75, and 1.00 pore volumes of steam injected are presented in Appendix A as Figures 33, 34, 35, and 36, respectively, and those for Run 10 at 0.25, 0.50, 0.75, and 1.00 pore volumes of steam injected are presented in Appendix A as Figures 43, 44, 45, and 46, respectively. An examination of these temperature profiles shows considerable differences in the recovery response of Run 10, relative to that of Run 6. Figure 43, for 0.25 pore volumes injected, shows that the higher isotherms were advancing faster in the lower part of the model than in the upper part which is contrary to the expected trend, based on experiences with steam override.

The expected trend is observed in Figure 33 for Run 6 at a similar stage of the injection process, in that in this figure, the upper isotherms are advancing faster than the lower isotherms. Figures 44 and 45 for Run 10 at 0.50 and 0.75 pore volumes injected, respectively, show that the tendency for the lower isotherms to advance more rapidly than the upper isotherms persisted. Although the advance was relatively uniform in the upper part of the model (almost radial), it was highly irregular in the lower part, which may be indicative of hot water advance. With 0.75 pore volumes of steam injected, the 15°C isotherm had reached the producer in the upper layer, while in the lower layer, the 30°C isotherm had reached the producer. Upon the injection of 1.00 pore volumes of steam for Run 10, the temperature distribution in the lower layer was very irregular, but most of the formation had been heated to over 15°C.

If Run 10 had involved hot water injection at the outset (as opposed to steam), it is possible that the hot water zone would stay in the lower part of the model and that heating of the upper part of the reservoir would be accomplished only by convection. This is a reasonable possibility, especially when one considers the that the density of the water was higher than that of the oil, and that the injection well was completed over the lower half of the formation. Run 22 provides some support for this point of view in that it was designed and conducted as a hot waterflood in the initial stages of the run and its temperature profiles (given in Appendix A as Figures 76, 77,

78, and 79 for 0.25, 0.50, 0.75 and 1.00 pore volumes of hot water injected, respectively) show a trend similar to that of Run 10. Further details concerning Run 22 will be presented in a later section.

On the other hand, if steam was initially injected into the formation of Run 10 (as was intended), and the steam rapidly condensed, it is conceivable that the condensate segregated and eventually developed a path for the steam. Thus, it is possible that condensation of the steam led to steam channeling. Figure 9 shows the instantaneous oil-steam ratio as a function of cumulative oil production for Run 10. It shows that the initial period of clean oil production was relatively short compared to that of other runs (see Figures 16, 17, 19, 20, and 21) which suggests that a clear cut oil bank was not formed; rather, the displacement process consisted of rapid mobilization of the in-place oil due to the unstable advance in the lower portion of the model, and then the mobilized oil was displaced by steam.

6.4 Steamflood Following a Waterflood

Run 7 was comprised of a waterflood prior to a steamflood. The run was conducted with all experimental parameters designed to simulate the Aberfeldy prototype. During the run, the fluids were injected into the lower half of the reservoir with water injection at approximately 100 cm³/min and the subsequent steam injection at 225 cm³/min. The initial oil saturation was 90.4% and the model porosity was 31.0%. All pertinent experimental data for this run are

Continuous Steamflood in Aberfeldy Model.
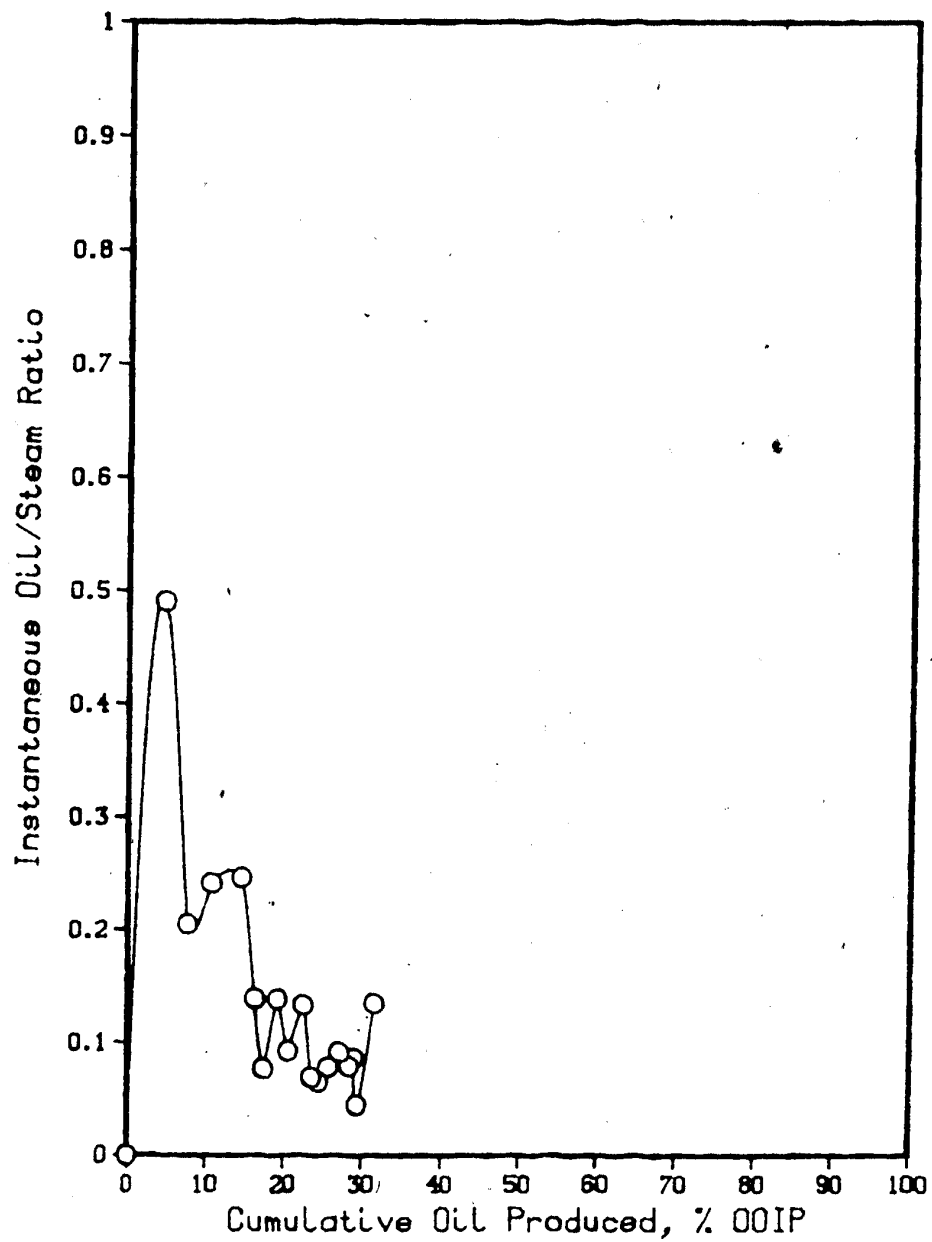
Figure 9. Run 10, Instantaneous Oil-Steam Ratio vs.
Cumulative Oil Production.

presented in Table 12.

In the first part of this run, water at the same temperature as the model (3°C) was injected. After injecting 1.17 pore volumes of water, at which point 22.5% of the in-place oil had been recovered, the injected water temperature was raised to the room temperature of 23°C. The waterflood was terminated at a water/oil ratio of approximately 6, at which time the oil recovery was 26.5% of the original oil in place and the average oil saturation in the model was 63.7%. The steamflood was started at this point. Figure 10 shows the cumulative oil recovery as a function of the volume of water and steam injected and indicates the points at which the injection process was altered.

The steamflood was continued until the cumulative pore volume of water injected was equal to 2.867 (including 1.05 pore volumes of steam injected), at which point the cumulative oil recovery was 32.40%. The incremental oil recovery by steam was 5.9% of the original oil in place (8.1% of the waterflood residual oil saturation), which represents a very low recovery for a steamflood. However, the injection of room temperature water into the model represents a warm waterflood in the prototype when scaling is applied, thus heat was injected into the formation in this phase of the operation. Nevertheless, the temperature profiles for this steamflood, given in Appendix A as Figures 37, 38, 39, and 40 for 0.25, 0.50, 0.75, and 1.00 pore volumes of steam injected, respectively, indicate a very uniform advance of the steam zone, again with condensate

Table 12.   Experimental Data for Run 7; Steamflood Following
a Waterflood in the Aberfeldy Model

Type of Oil Used: Faxam-100 (208 mPa·s at 23°C)
Pore Volume: 13040 cm³
Porosity of Bead Pack: 31.04 %
Hydrocarbon Pore Volume: 11420 cm³
Initial Oil Saturation: 90.41 %
Irreducible Water Saturation: 9.59 %
Initial Model Temperature: 3.0°C
Water Feed Flow Rate: (A) 96.9 cm³/min
                                      (B) 93.6 cm³/min
                                      (C) 197.7 cm³/min
Boiler Feed Flow Rate: (A) 0.0 cm³/min
                                      (B) 0.0 cm³/min
                                      (C) 27.6 cm³/min
Total Flow Rate of Steam: (A) 96.9 cm³/min
                                      (B) 93.6 cm³/min
                                      (C) 225.3 cm³/min
Volume of Water Injected: 15295 cm³ (1.1729 PV)
Volume of Oil Recovered: 2655 cm³ (22.52 % OOIP)

(A) Low Temperature Waterflood

Cumulative Total PV Injected (cm³)	Cumulative Total PV Injected (PV)	Cumulative Oil Produced (cm³)	Cumulative Oil Produced (% OOIP)	Oil-Water Ratio (cm³/cm³)
1610	0.124	1010	8.57	0.6273
3410	0.262	1415	12.00	0.2250
5240	0.402	1755	14.89	0.1858
7085	0.543	1990	16.88	0.1274
8905	0.683	2190	18.58	0.1099
10740	0.824	2305	19.55	0.0627
12505	0.959	2400	20.36	0.0538
14465	1.109	2540	21.54	0.0714
15295	1.173	2655	22.52	0.1386

(B) Room Temperature Waterflood

Cumulative Total PV Injected (cm³)	Cumulative Total PV Injected (PV)	Cumulative Oil Produced (cm³)	Cumulative Oil Produced (% OOIP)	Oil-Water Ratio (cm³/cm³)
17050	1.308	2740	23.24	0.0484
18910	1.450	2840	24.09	0.0538
20690	1.587	2920	24.77	0.0449
21840	1.675	3120	26.47	0.1739

(C) Steamflood

Cumulative Total PV Injected (cm³)	Cumulative Total PV Injected (PV)	Cumulative Oil Produced (cm³)	Cumulative Oil Produced (% OOIP)	Oil-Steam Ratio (cm³/cm³)
23750	1.821	3170	26.89	0.0262
25670	1.969	3240	27.48	0.0365
26655	2.044	3285	27.86	0.0457
27635	2.119	3340	28.33	0.0561
29635	2.273	3520	29.86	0.0900
33585	2.576	3720	31.55	0.0506
37385	2.867	3820	32.40	0.0263

Steamflood Following Waterflood in Aberfeldy Model.
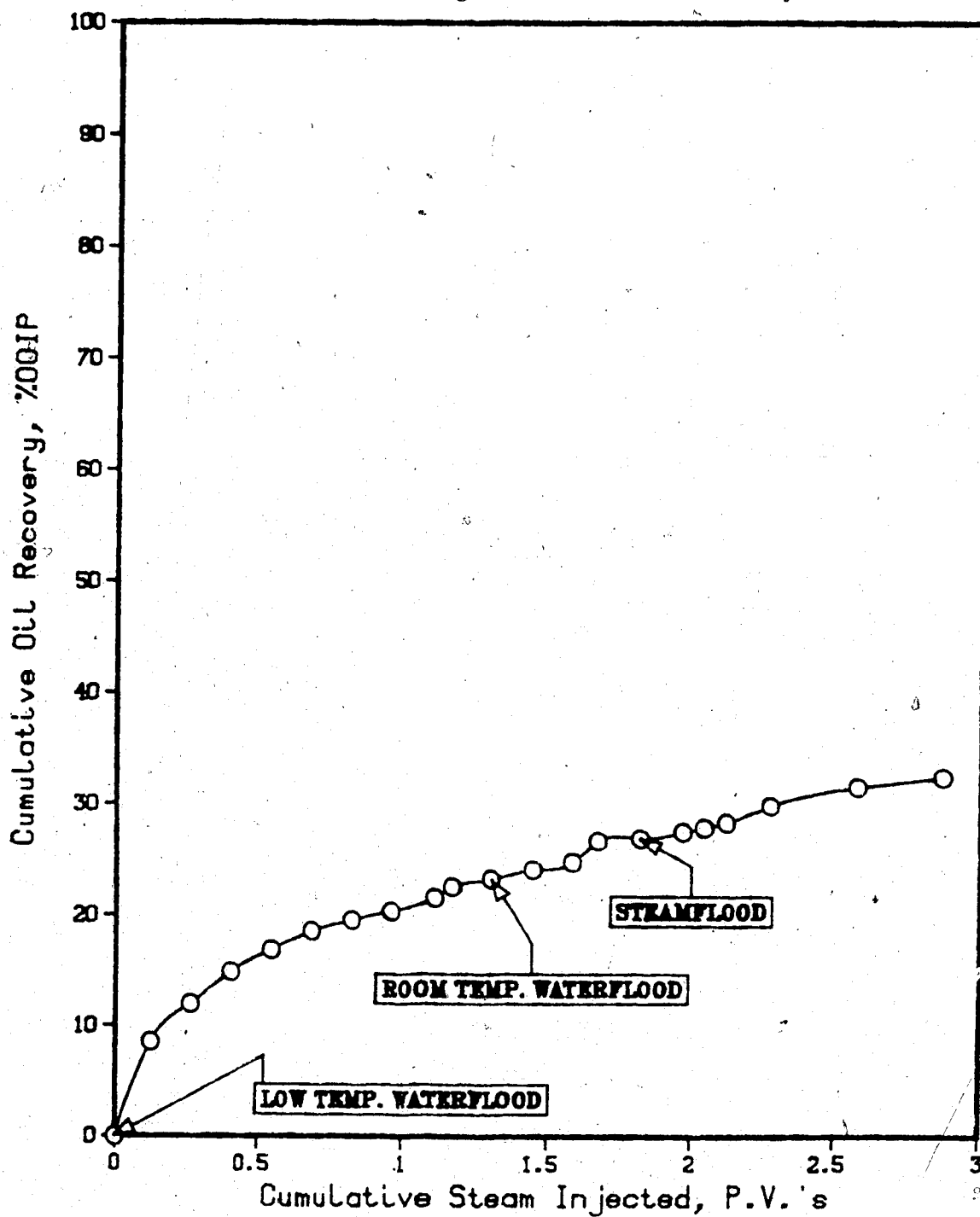
Figure 10. Run 7, Cumulative Recovery vs. PV Injected.

underride dominating the steam override.

Figure 11 shows the instantaneous oil and water production as a function of cumulative injection. The production response shown by this curve and by Figure 10 indicates that the ultimate recovery for Run 7, with an initially waterflooded porous medium, was similar to the that obtained in Run 10, and distinctly better than the recovery obtained for Run 6. It is believed that the waterflood helped to create adequate injectivity for steam, but at the same time it led to an inefficient utilization of the injected steam. Figure 12 shows the instantaneous oil-steam ratio for the steamflood portion of Run 7. The small increase seen in the oil-steam ratio curve at the point where steam injection is begun, further illustrates the poor response of the reservoir to steam injection.

6.5 Steamflooding a Highly Viscous Oil

Run 9 utilized a highly viscous oil, the viscosity - temperature relation for which is given in Table 6. Steam injection was over the lower half of the model wellbore at a rate of 228.8 cm^3/min. The initial oil saturation was 87.7 % and the model porosity was 32.9 %. The ultimate oil recovery observed in this run was very low. After 14000 cm^3 of steam (water equivalent) had been injected, only 200 cm^3 of oil had been produced (1.65 % of the original oil in place). Table 13 presents the experimental data for this run.

Figures 41 and 42 in Appendix A show the temperature profiles for Run 9 at 0.50 and 1.00 pore volumes of steam

Table 13. Experimental Data for Run 9; Steamflood in a
Heavy Oil Model

Type of Oil Used: Heavy Oil (9256.5 mPa·s at
                                         23°C)
Pore Volume: 13800 cm³
Porosity of Bead Pack: 32.85 %
Hydrocarbon Pore Volume: 12100 cm³
Initial Oil Saturation: 87.68 %
Irreducible Water Saturation: 12.32 %
Initial Model Temperature: 4.03°C
Water Feed Flow Rate: 199.0 cm³/min
Boiler Feed Flow Rate: 29.8 cm³/min
Total Flow Rate of Steam: 228.8 cm³/min
Volume of Steam Injected: 14000 cm³ (1.01 PV)
Volume of Oil Recovered: 200.0 cm³ (1.65 % OOIP)
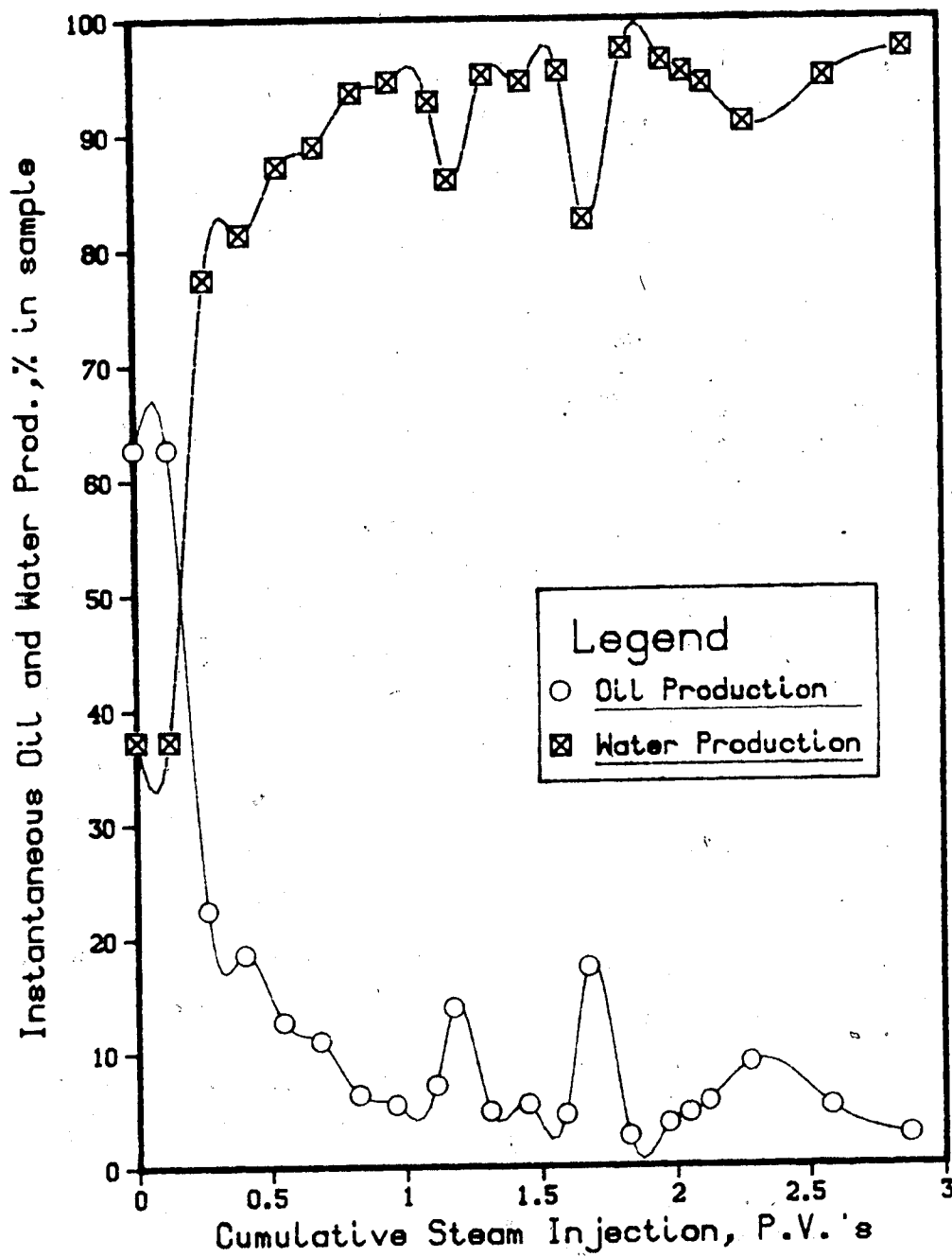
Figure 11. Run 7, Instantaneous Oil and Water Production vs. Cumulative Injection.

Steamflood Following Waterflood in Aberfeldy Model.
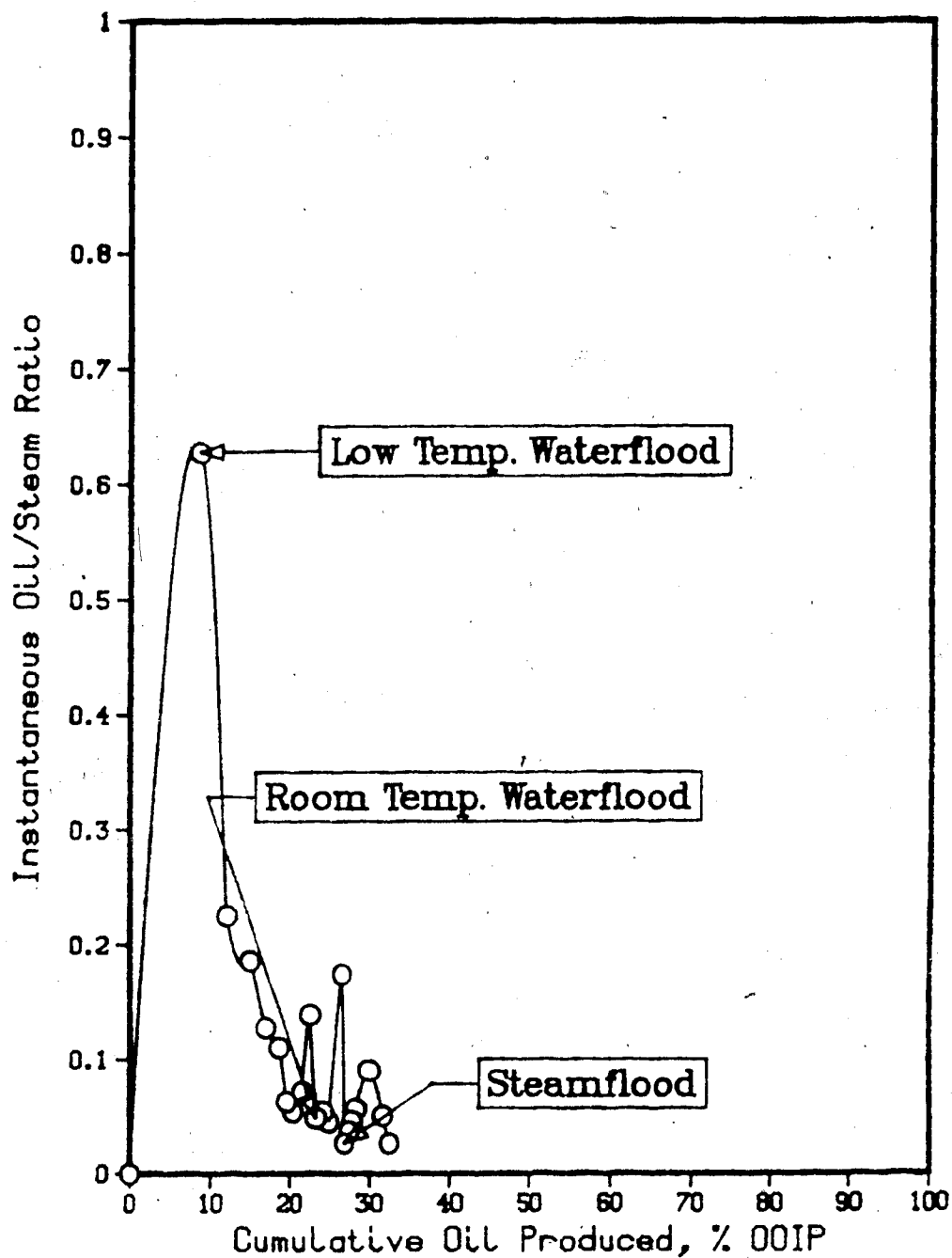
Figure 12. Run 7, Instantaneous Oil-Steam Ratio vs.
Cumulative Oil Production.

injected, respectively. It is interesting to note that, unlike the runs discussed previously, in this run the steam clearly sweeps the upper part of the model. This would indicate that steam override becomes more prominant as the viscosity of the model oil increases.

6.6 Light Oil Steamfloods

Runs 12 and 13 utilized a light oil (60 mPa·s at 23°C) to simulate a steamflood in a conventional oil reservoir. Tables 14 and 15 give the important experimental parameters for Runs 12 and 13, respectively, and also present a tabulation of the oil recovery for each run as a function of the volume of steam injected.

In Run 12, the production well was only opened over the lower half of the formation while in Run 13 the production well was opened over the entire interval. Oil recovery after the injection of about one pore volume of steam was 29.72% for Run 12 and 29.26% for Run 13. Figures 13 and 14 show the instantaneous oil and water production as a function of the cumulative steam injected for Runs 12 and 13, respectively. A comparison of the cumulative recovery behavior for the two runs is given in Figure 15. An examination of these figures shows the similarity between the two runs and indicates that the production interval had very little effect on the recovery response. The small departure in the curves may be due to the slight differences in the initial conditions for the experiments (See Tables 14 and 15).

Table 14. Experimental Data for Run 12; Steamflood in Light Oil Model

Type of Oil Used:	MCT-10 (60 mPa·s at 23°C)
Pore Volume:	14050 cm³
Porosity of Bead Pack:	33.45 %
Hydrocarbon Pore Volume:	12535 cm³
Initial Oil Saturation:	89.22 %
Irreducible Water Saturation:	10.78 %
Initial Model Temperature:	3.0°C
Water Feed Flow Rate:	199.3 cm³/min
Boiler Feed Flow Rate:	30.1 cm³/min
Total Flow Rate of Steam:	229.4 cm³/min
Volume of Steam Injected:	20170 cm³ (1.4356 PV)
Volume of Oil Recovered:	4130 cm³ (32.95 % OOIP)

Cumulative Total PV Injected (cm³)	Cumulative Total PV Injected (PV)	Cumulative Oil Produced (cm³)	Cumulative Oil Produced (%OOIP)	Oil-Steam Ratio (cm³/cm³)
920	0.066	870	6.94	0.9457
2770	0.197	1520	12.13	0.3514
4460	0.317	2305	18.39	0.4645
6280	0.447	2595	20.70	0.1593
7995	0.569	2875	22.94	0.1633
9885	0.704	3185	25.41	0.1640
11695	0.832	3355	26.77	0.0939
13465	0.958	3545	28.28	0.1073
15275	1.087	3725	29.72	0.0945
17035	1.213	3875	30.91	0.0852
18835	1.341	4035	32.19	0.0889
20170	1.436	4130	32.95	0.0712

Table 15.   Experimental Data for Run 13; Steamflood in Light
            Oil Model ·

Type of Oil Used: MCT-10 (60 mPa·s at 23°C)
Pore Volume: 12660 cm³
Porosity of Bead Pack: 30.14 %
Hydrocarbon Pore Volume: 11670 cm³
Initial Oil Saturation: 92.18 %
Irreducible Water Saturation: 7.82 %
Initial Model Temperature: 3.0°C
Water Feed Flow Rate: 199.3 cm³/min
Boiler Feed Flow Rate: 30.1 cm³/min
Total Flow Rate of Steam: 229.4 cm³/min
Volume of Steam Injected: 20920 cm³ (1.6524 PV)
Volume of Oil Recovered: 4145 cm³ (35.52 % OOIP)

Cumulative Total PV Injected (cm³)	Cumulative Total PV Injected (PV)	Cumulative Oil Produced (cm³)	Cumulative Oil Produced (%OOIP)	Oil-Steam Ratio (cm³/cm³)
1870	0.148	1345	11.53	0.7193
3800	0.300	1780	15.25	0.2254
5710	0.451	2210	18.94	0.2253
7450	0.588	2525	21.64	0.1810
9345	0.738	2820	24.16	0.1557
11275	0.891	3145	26.95	0.1684
13225	1.045	3415	29.26	0.1385
15155	1.197	3630	31.11	0.1114
17105	1.351	3800	32.56	0.0872
19060	1.506	3985	34.15	0.0946
20920	1.652	4145	35.52	0.0860
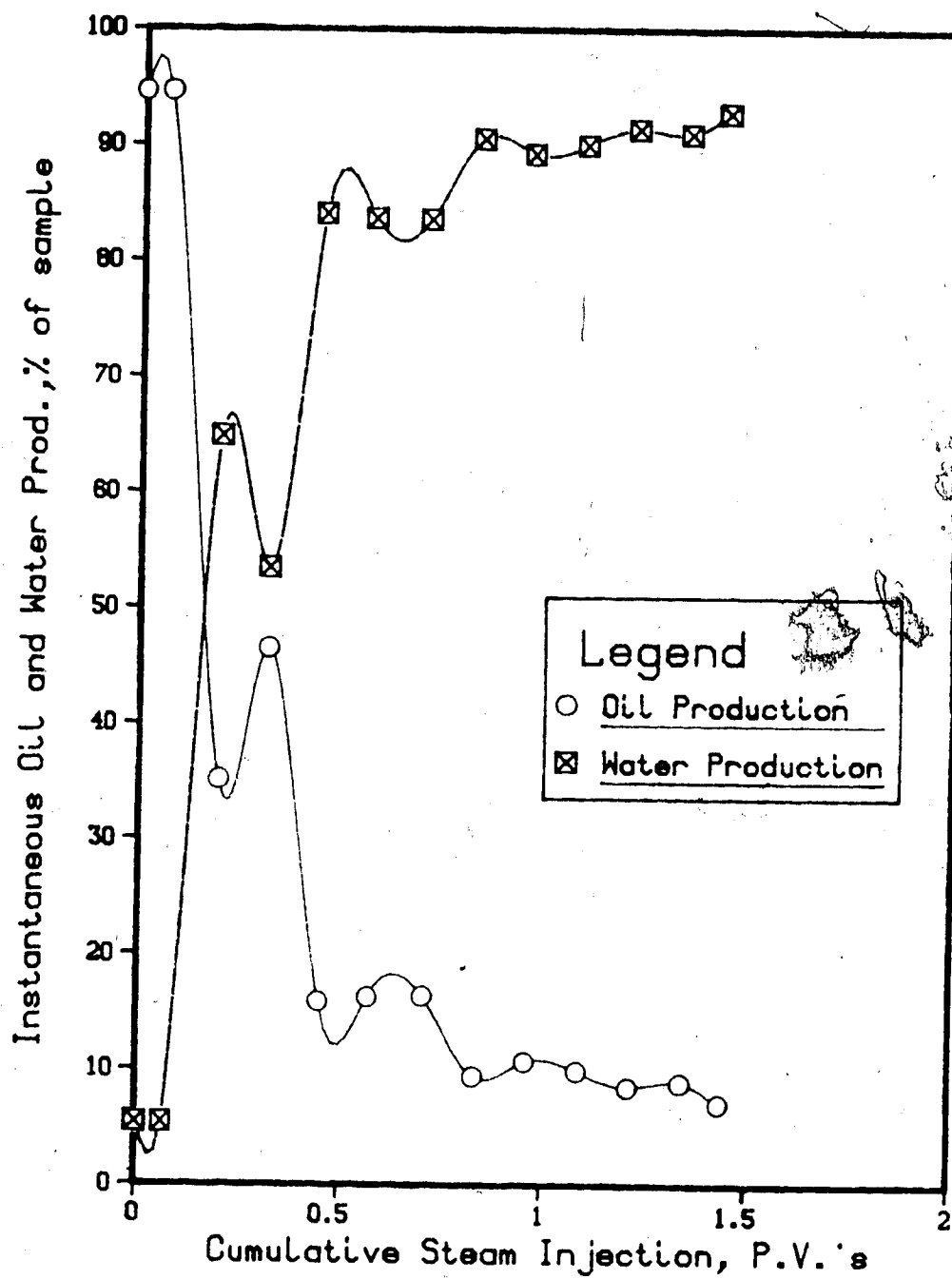
Figure 13. Run 12, Instantaneous Oil and Water Production vs. Cumulative Injection.
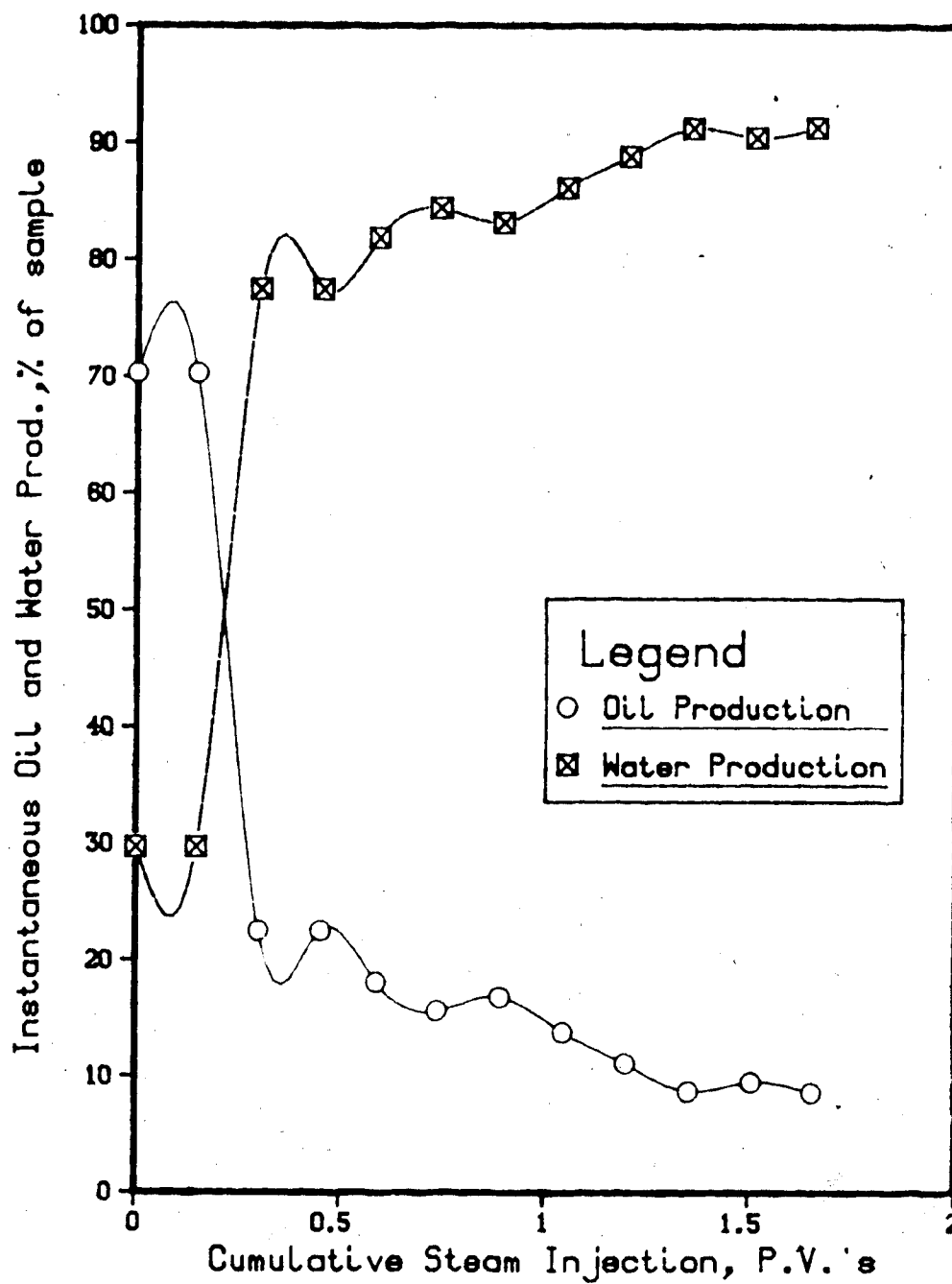
Figure 14. Run 13, Instantaneous Oil and Water Production vs. Cumulative Injection.

Two Steamfloods in Light Oil Models.
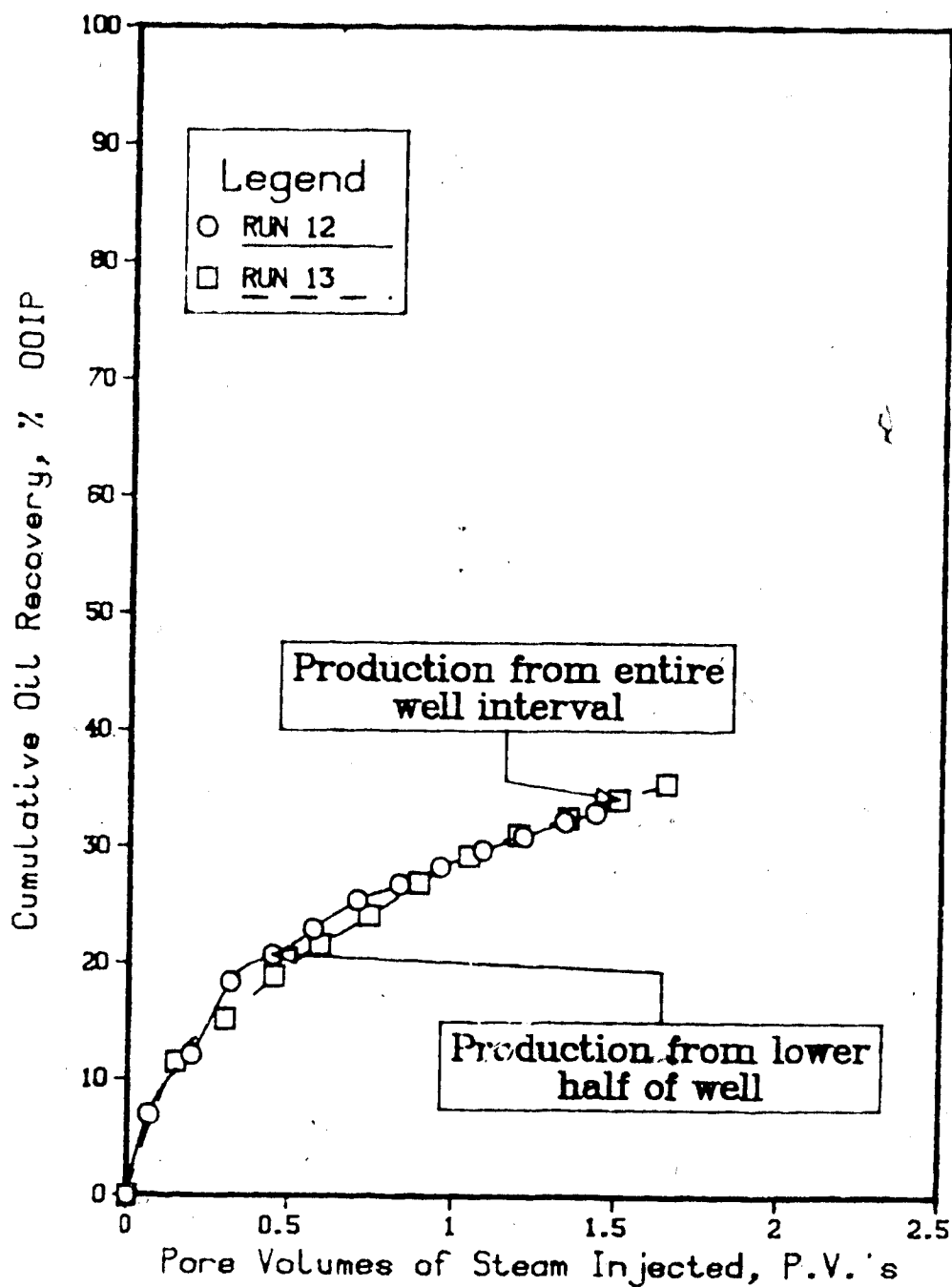
Figure   15.   Comparison of the Steamflood Recovery Response
of Run 12 and Run 13.

The temperature profiles for Run 12 at 0.25, 0.50, 0.75 and 1.00 pore volumes of steam injected are given in Appendix A as Figures 47, 48, 49, and 50, respectively, while those for Run 13 are given in Appendix A as Figures 51, 52, 53, and 54, respectively. A comparison of these temperature profiles with the profiles of previously discussed Aberfeldy model runs (in which the oil viscosity was 208 mPa·s at 23°C), immediately shows the much steeper temperature fronts, as indicated by the proximity of the isotherms. Figure 47 shows that at 0.25 pore volumes of steam injected into the model of Run 12, the higher temperature isotherms at the top and the base of the model are almost coincident, however, the lower temperature isotherms (e.g. 5 and 10°C) advance more rapidly in the lower part of the model. Thus, there is considerable evidence that a steam front advanced in the upper part of the formation while condensate segregated and flowed in the lower part. By the time one pore volume of steam had been injected into the model in Run 12 (Figure 50), the profile became more complex. It can be seen that the steam spreads areally over most of the formation, with a symmetrical temperature profile developing near the base of the sand as well. It can be seen that the heat advance in the upper zone was much slower than in the lower zone, further illustrating the condensate advance.

The temperature profiles for Run 13 (Figures 51, 52, 53, and 54) are similar to those of Run 12. The agreement between these temperature profiles and the figures showing the cumulative recovery responses of the two runs, serves to show the reproducibility of the results.

The oil recovery for Runs 12 and 13 was the highest observed of all the runs which were conducted as part of this work. The oil-steam ratio for Run 12 as a function of the cumulative oil production is shown in Figure 16 and that of Run 13 in Figure 17. The two curves are similar in shape, but a higher initial production response is observed in Run 12. However, the oil-steam ratio in both cases achieves a value of approximately 0.1 at 30% oil recovery. Note that the decline in the OSR for the peak value is sharper in the case of light oils, as would be expected on the basis of a frontal drive.

6.7 Bottom Water Steamflood

One run, Run 15, was conducted with a bottom water layer in the model. The bottom water layer was installed by freezing a measured volume of water into the lower layer of the the model, which had previously been packed with beads. (Extensive details of the process involved in installing the bottom water layer were given in a previous chapter.) It is believed that the layer of water was 0.43 inches thick (17.2% of the formation thickness). All important experimental parameters, as well as a tabulation of recoveries as a function of pore volumes of steam injected, are given in Table 19.

The bottom water model was steamflooded through the water zone at an injection rate of 228.6 cm³/min, with the production well open over the top half of the formation, Figures 55, 56, 57, and 58 in Appendix A show the temperature profiles for this run upon the injection of

Table 16. Experimental Data for Run 15; Steamflood in Aberfeldy Model With Bottom Water

Type of Oil Used: Faxam-100 (208 mPa·s at 23°C)
Pore Volume Oil Zone: 13136 cm³
Porosity of Bead Pack: 35.92 %
Hydrocarbon Pore Volume: 11520 cm³
Initial Oil Saturation: 87.70 %
Irreducible Water Saturation: 12.30 %
Initial Model Temperature: 3.0°C
Thickness of Water Layer: 0.4252 Inches
Water Feed Flow Rate: 199.5 cm³/min
Boiler Feed Flow Rate: 29.1 cm³/min
Total Flow Rate of Steam: 228.6 cm³/min
Volume of Steam Injected: 15895 cm³ (1.210 PV)
Volume of Oil Recovered: 355 cm³ (3.08 % OOIP)

Cumulative Total PV Injected (cm³)	Cumulative Total PV Injected (PV)	Cumulative Oil Produced (cm³)	Cumulative Oil Produced (%OOIP)	Oil-Steam Ratio (cm³/cm³)
1930	0.147	25	0.22	0.0130
3610	0.275	45	0.39	0.0119
5250	0.400	65	0.56	0.0122
7010	0.534	90	0.78	0.0142
8745	0.666	110	0.95	0.0115
10585	0.806	155	1.35	0.0245
12320	0.938	190	1.65	0.0202
14085	1.072	245	2.13	0.0312
15895	1.210	355	3.08	0.0608

Continuous Steamflood in Light Oil Model,
Production Well Completed Over Lower Half.
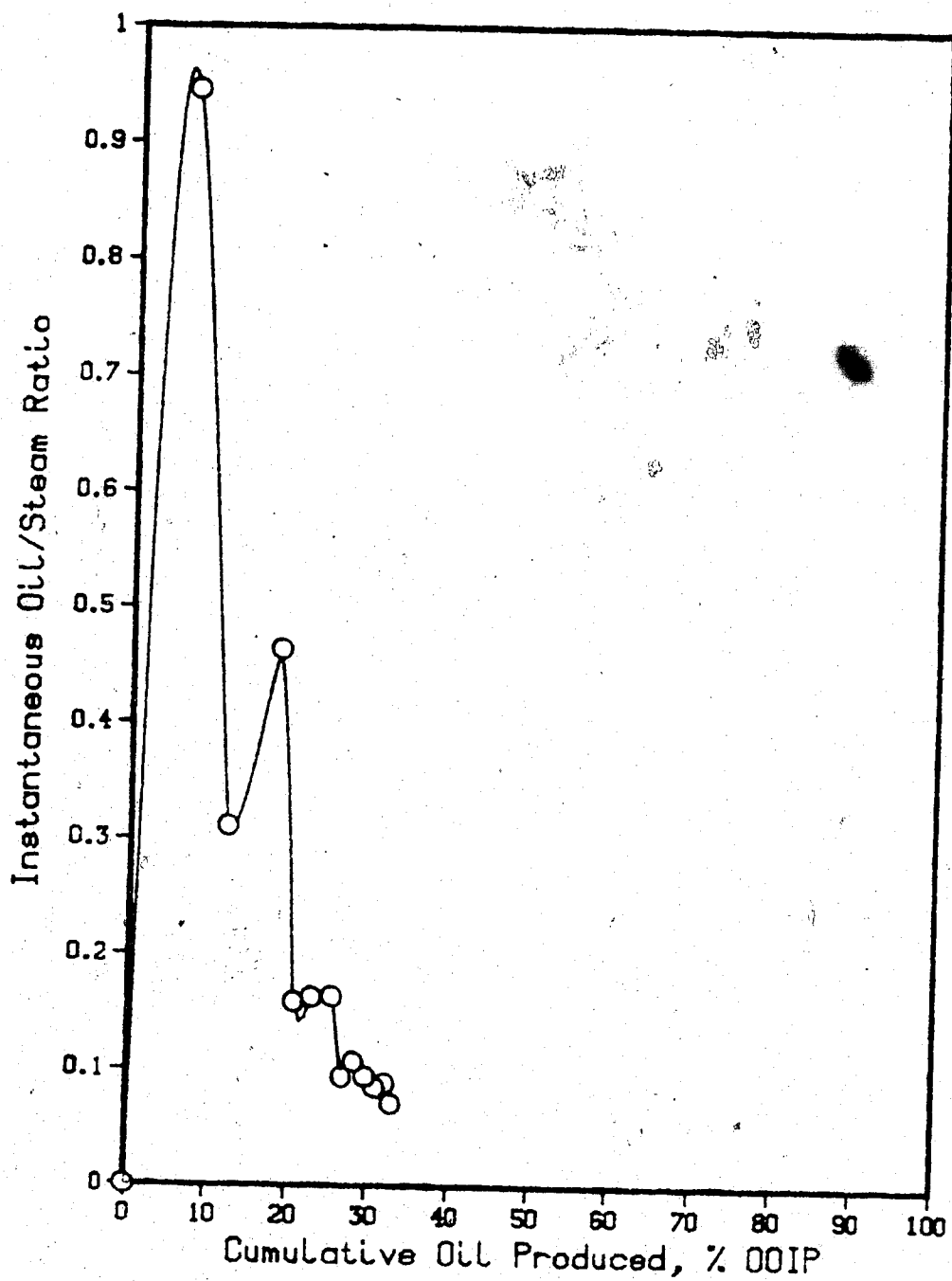
Figure 16. Run 12, Instantaneous Oil-Steam Ratio vs.
Cumulative Oil Production.

Continuous Steamflood in Light Oil Model,
Production Well Completed Over Upper Half.
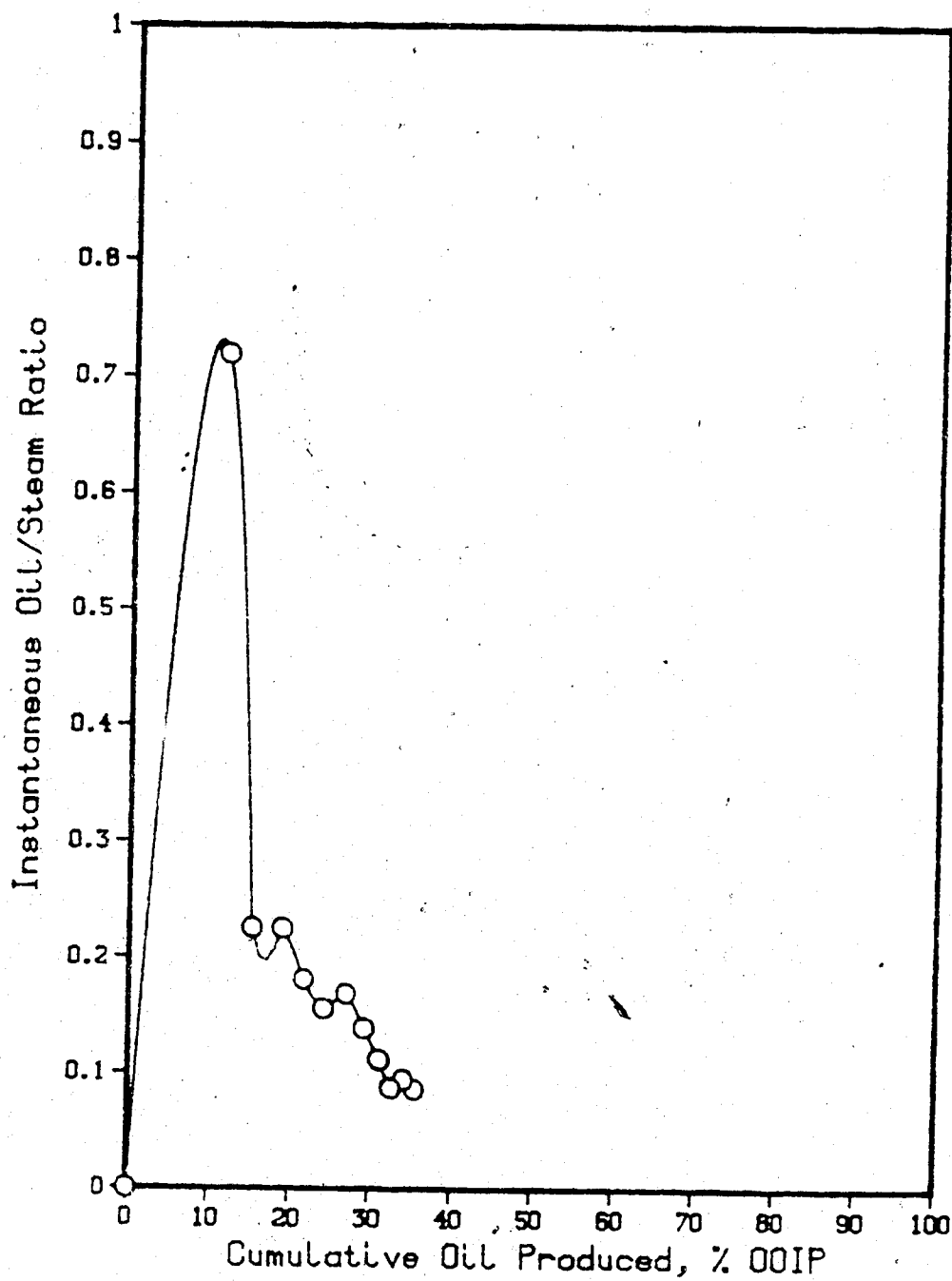
Figure 17. Run 13, Instantaneous Oil-Steam Ratio vs.
Cumulative Oil Production.

0.25, 0.50, 0.75, and 1.00 pore volumes of steam, respectively. A study of these temperature profiles indicates that the injected heat advanced rapidly in the bottom water layer. It can be seen that the 15 and 20°C isotherms in the upper part of the sand are virtually stationary while the heat advances unevenly in the water layer, which suggests that a hot waterflood occurred when the inje   steam condensed and the condensate migrated rapidly   o the highly conductive water layer.

As expected, the oil recovery for this run was poor, being 3.1% of the original oil in place after injecting 1.2 pore volumes of steam, as shown in cumulative oil recovery curve, given as Figure 18. Future runs in the continuation of this research will concentrate on minimizing the deleterious effects of the bottom water zone. In spite of the poor oil recovery, this run is considered to be successful, because it showed that a bottom water layer can be created in the vacuum model (note that Prats'[2] situation was very different), and that a steamflood can be conducted under such conditions. The observed behavior of the steamflood was according to expectations.

6.8 Steam Slug Runs

Runs 17, 18, and 19 were designed to test the steam slug process, and to ascertain the reproducibility of such experiments. As seen in Table 8 the initial oil saturation in each of these runs was close to 92%. Tables 17, 18, and 19 present the important experimental parameters for Runs 17, 18, and 19, respectively, and also give a tabulation of

Continuous Steamflood in a Bottom Water Aberfeldy Model.
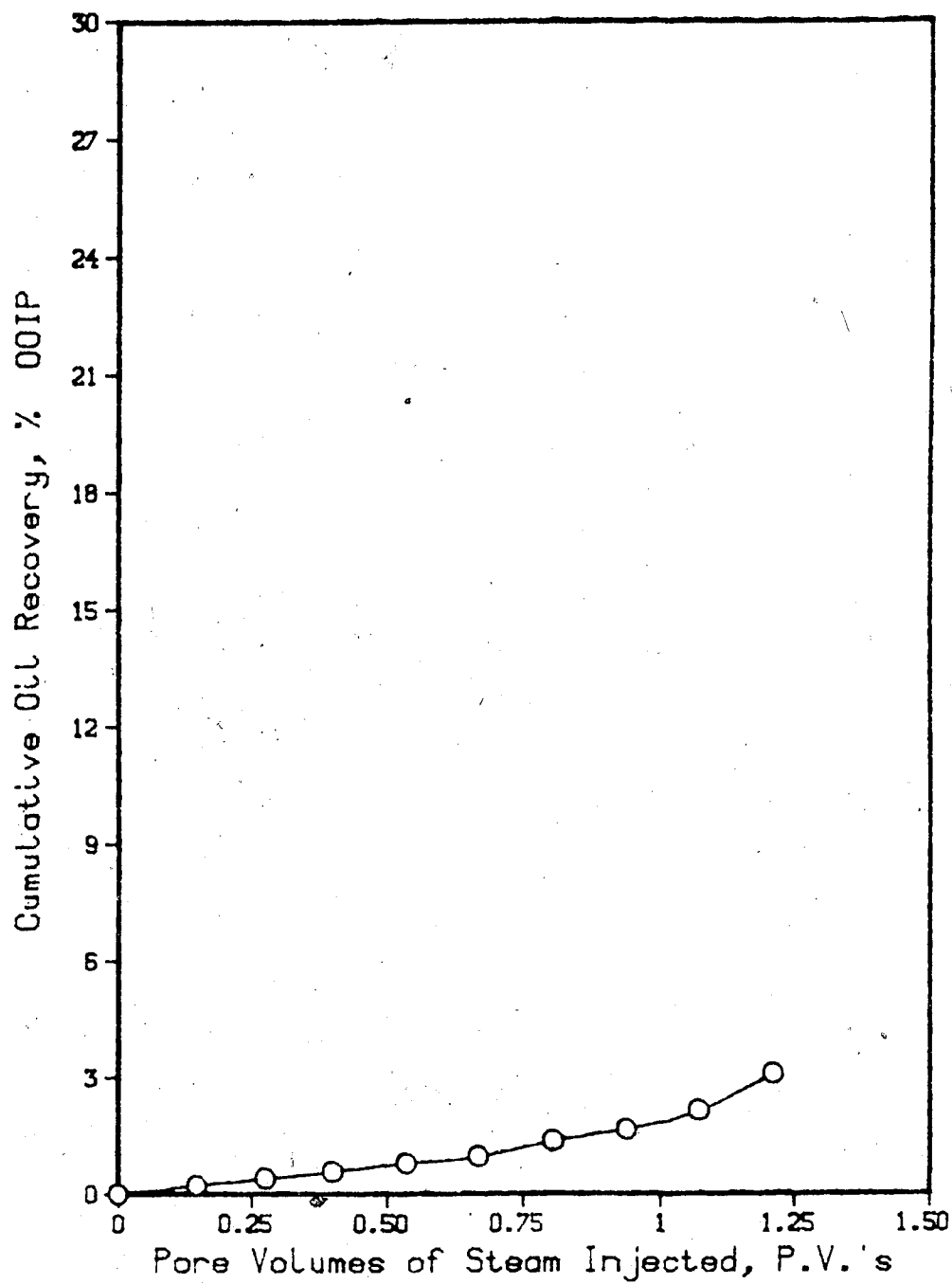
Figure 18. Run 15, Cumulative Oil Recovery vs. PV Steam Injected.

the oil recovery as a function of pore volumes of steam injected.

Steam injection for these runs was terminated at the point where a sharp drop in the oil-steam ratio was observed, and then water was injected. (Refer to Figures 19, 20, and 21 for the oil-steam ratio curves for Runs 17, 18, and 19, respectively.) The water was injected at 4°C to coincide with the scaling criteria; thus the water was at a temperature near the initial reservoir temperature.

Consider the temperature distribution plots for Run 17, given in Appendix A as Figures 59, 60, 61, 62, and 63, for injection to 0.25, 0.31 (start of cold waterflood), 0.50, 0.75, and 1.00 pore volumes, respectively. At 0.25 pore volumes of steam injected, it is seen that the advance of the steam front was nearly radial but there was considerable underrunning of the hot condensate. At the point where steam injection was terminated, and the cold waterflood was started (Figure 60), the temperature profile for the upper part of the model still shows approximately radial advance, but the lower part of the model shows a much more rapid heat (condensate) advance. Upon the injection of 0.50 pore volumes of water and steam (Figure 61), it can be observed that the heat had spread over most of the area in the lower part of the formation, but that the development of a heat bank in the upper part of the model still seemed to follow an approximately radial pattern. Injection of water to 0.75 pore volumes (Figure 62) appears to have totally condensed the steam, and it is seen that the model temperature became more constant. Further injection to 1.00 pore volumes

Table 17. Experimental Data for Run 17; Steam Slug Run in Aberfeldy Model

Type of Oil Used: Faxam-100 (208 mPa·s at 23°C)
Pore Volume Oil Zone: 13820 cm³
Porosity of Bead Pack: 32.90 %
Hydrocarbon Pore Volume: 12800 cm³
Initial Oil Saturation: 92.62 %
Irreducible Water Saturation: 7.38 %
Initial Model Temperature: 3.0°C
Water Feed Flow Rate: 198.7 cm³/min
Boiler Feed Flow Rate: 30.4 cm³/min
Total Flow Rate of Steam: 229.1 cm³/min
Flow Rate of Water Slug: 198.7 cm³/min
Volume of Steam Injected: 14250 cm³ (1.031 PV)
Volume of Oil Recovered: 3100 cm³ (24.22 % OOIP)

Cumulative Total PV Injected (cm³)	Cumulative Total PV Injected (PV)	Cumulative Oil Produced (cm³)	Cumulative Oil Produced (%OOIP)	Oil-Steam Ratio (cm³/cm³)
1910	0.138	1610	12.58	0.8429
3790	0.274	2070	16.17	0.2447
	COLD	WATER	INJECTION	
5670	0.410	2390	18.67	0.1702
7470	0.541	2590	20.23	0.1111
9320	0.674	2765	21.60	0.0946
11220	0.812	2925	22.85	0.0842
13100	0.948	3045	23.79	0.0638
14250	1.031	3100	24.22	0.0478

Table 18. Experimental Data for Run 18; Steam Slug Run in Aberfeldy Model

```
Type of Oil Used:              Faxam-100 (208 mPa·s at 23°C)
Pore Volume Oil Zone:          13880 cm³
Porosity of Bead Pack:         33.04 %
Hydrocarbon Pore Volume:       12770 cm³
Initial Oil Saturation:        92.00 %
Irreducible Water Saturation:  8.00 %
Initial Model Temperature:     3.0°C
Water Feed Flow Rate:          199.3 cm³/min
Boiler Feed Flow Rate:         30.1 cm³/min
Total Flow Rate of Steam:      229.4 cm³/min
Flow Rate of Water Slug:       199.3 cm³/min
Volume of Steam Injected:      20040 cm³ (1.444 PV)
Volume of Oil Recovered:       3940 cm³ (30.85 % OOIP)
```

Cumulative Total PV Injected (cm³)	Cumulative Total PV Injected (PV)	Cumulative Oil Produced (cm³)	Cumulative Oil Produced (%OOIP)	Oil-Steam Ratio (cm³/cm³)
1920	0.138	1490	11.67	0.7760
4000	0.288	2660	20.83	0.5625
	COLD	WATER	INJECTION	
5890	0.424	3035	23.77	0.1984
8040	0.579	3265	25.57	0.1070
9950	0.717	3450	27.02	0.0969
12175	0.877	3595	28.15	0.0652
14215	1.024	3720	29.13	0.0613
16080	1.159	3805	29.80	0.0456
18060	1.301	3875	30.34	0.0354
20040	1.444	3940	30.85	0.0328

Table 19. Experimental Data for Run 19; Steam Slug Run in Aberfeldy Model

```
Type of Oil Used:              Faxam-100 (208 mPa·s at 23°C)
Pore Volume Oil Zone:          13970 cm³
Porosity of Bead Pack:         33.26 %
Hydrocarbon Pore Volume:       12785 cm³
Initial Oil Saturation:        91.52 %
Irreducible Water Saturation:  8.48 %
Initial Model Temperature:     3.0°C
Water Feed Flow Rate:          199.8 cm³/min
Boiler Feed Flow Rate:         29.4 cm³/min
Total Flow Rate of Steam:      229.2 cm³/min
Flow Rate of Water Slug:       199.8 cm³/min
Volume of Steam Injected:      21800 cm³ (1.560 PV)
Volume of Oil Recovered:       3845 cm³ (30.07 % OOIP)
```

Cumulative Total PV Injected (cm³)	Cumulative Total PV Injected (PV)	Cumulative Oil Produced (cm³)	Cumulative Oil Produced (%OOIP)	Oil-Steam Ratio (cm³/cm³)
1905	0.136	1115	8.72	0.5853
4080	0.292	2135	16.70	0.4690
	COLD	WATER	INJECTION	
5970	0.427	2535	19.83	0.2116
8030	0.575	2840	22.21	0.1481
9990	0.715	3070	24.01	0.1173
11980	0.858	3260	25.50	0.0955
13845	0.991	3395	26.55	0.0724
15940	1.141	3515	27.49	0.0573
17780	1.273	3655	28.60	0.0761
19860	1.422	3755	29.37	0.0481
21800	1.560	3845	30.07	0.0464
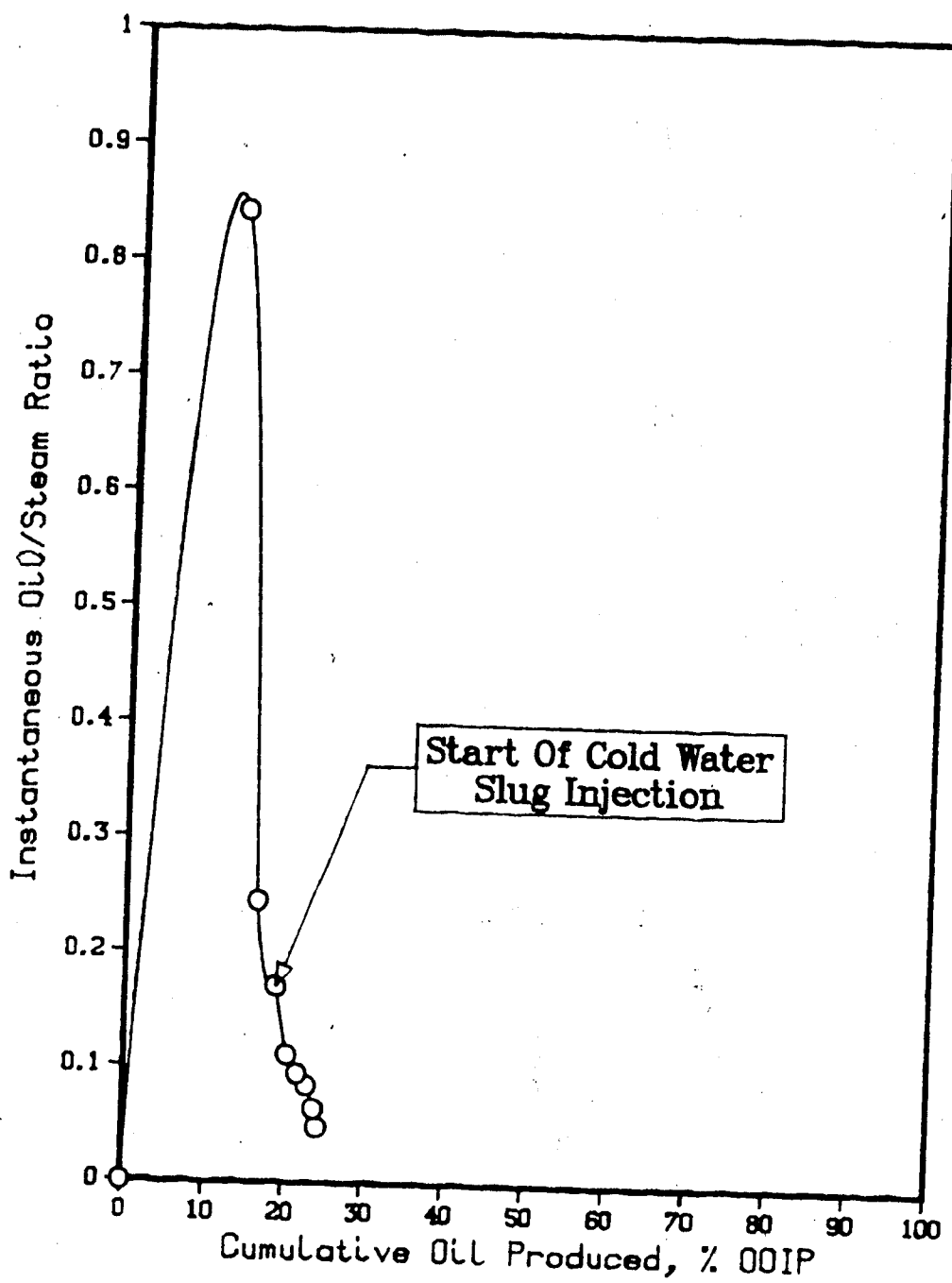
Figure 19. Run 17, Instantaneous Oil-Steam Ratio vs. Cumulative Oil Production.
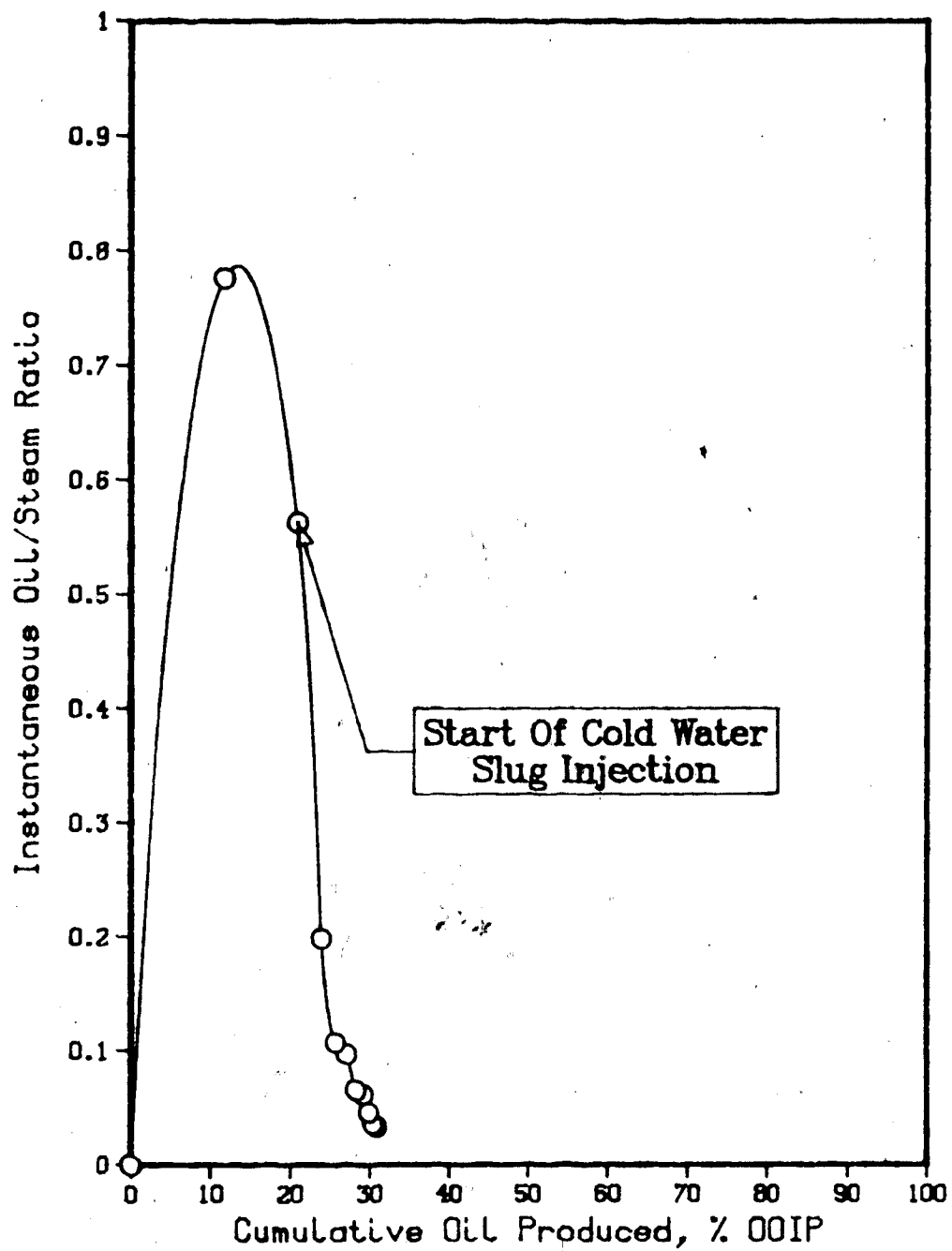
Figure 20.   Run 18, Instantaneous Oil-Steam Ratio vs.
Cumulative Oil Production.
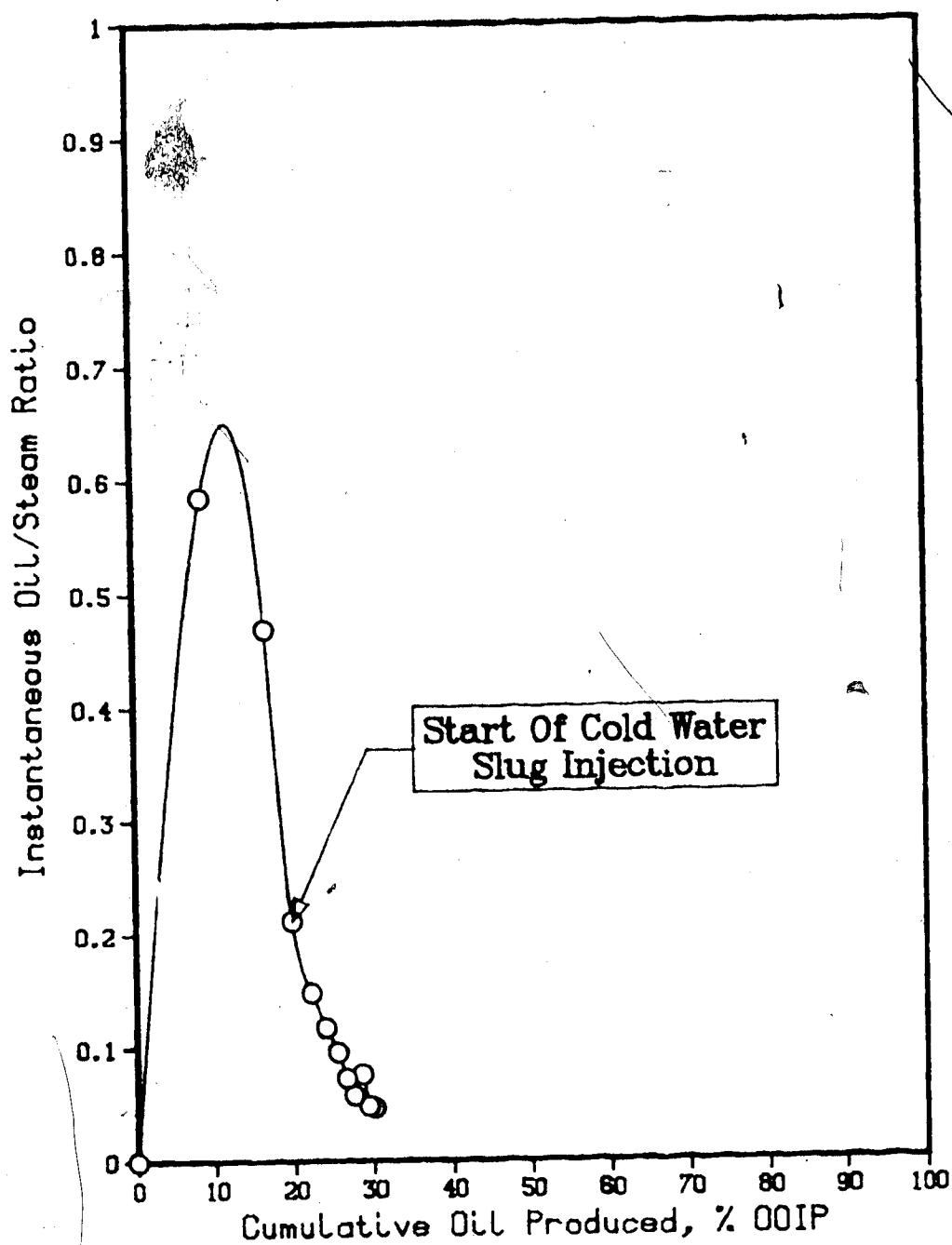
Figure 21. Run 19, Instantaneous Oil-Steam Ratio vs. Cumulative Oil Production.

(Figure 63) shows that the model temperature was about 10°C throughout.

The temperature profiles for Run 18, given in Appendix A as Figures 64, 65, 66, 67, 68, and 69, for the injection of 0.25, 0.30 (start of cold waterflood), 0.50, 0.75, 1.00, and 1.25 pore volumes of steam, depict a response very similar to that of Run 17. Run 18 was continued slightly longer than Run 17 and the final profile (Figure 69) shows that the heat distribution was highly asymmetrical, with a 15°C isotherm still present in the lower part of the formation. On the whole, the temperature profiles for Runs 17 and 18 show: (i) considerable slowdown of heat advance in the upper part of the formation with the injection of cold water and, (ii) more rapid and very uneven heat spreading in the lower part of the model. The former is symptomatic of steam condensation by the injected cold water, essentially bringing the steam zone to a halt until total condensation has occurred, while the latter is quite typical of a hot waterflood, characterized by fingering and unstable heat advance.

The temperature profiles for Run 19 are given in Appendix A as Figures 70, 71, 72, 73, 74, and 75, for 0.25, 0.28 (start of cold waterflood), 0.50, 0.75, 1.00, and 1.25 pore volumes of steam injected, respectively. These are sufficiently different than those of Runs 17 and 18 to show that even though the experimental conditions were similar, instabilities can play a significant role in modifying the temperature distributions in the upper and lower parts of the model. Possibly some perturbation during the steam

injection stage caused early departure from radial flow, with concomitant later distortion of temperature profiles. Nevertheless, the final recovery curves for all three runs are similar as can be seen in Figure 22. Similarities are also observed in the plots of instantaneous oil and water production as functions of cumulative injection. These plots are given as Figures 23, 24, and 25, for Runs 17, 18, and 19, respectively.

The final temperature profile for Run 19 at 1.25 pore volumes injected (Figure 75), and that of Run 18 (Figure 69), show a greater heat accumulation in the lower part of the formation than in the upper part. It has been hypothesized that the injected cold water condensed the steam zone at the top, and the condensate then dropped down and flushed out the oil.

On the whole, the steam slug process appears to be quite attractive because;

i.   it yields a good oil recovery,

ii.   it utilizes less steam than other variations of steam injection and thus is more economical in field operations,

iii. it promotes greater utilization of the injected heat with the injected water transporting heat from the swept zone into the colder parts downstream.

Three Slug Runs on Aberfeldy Model.
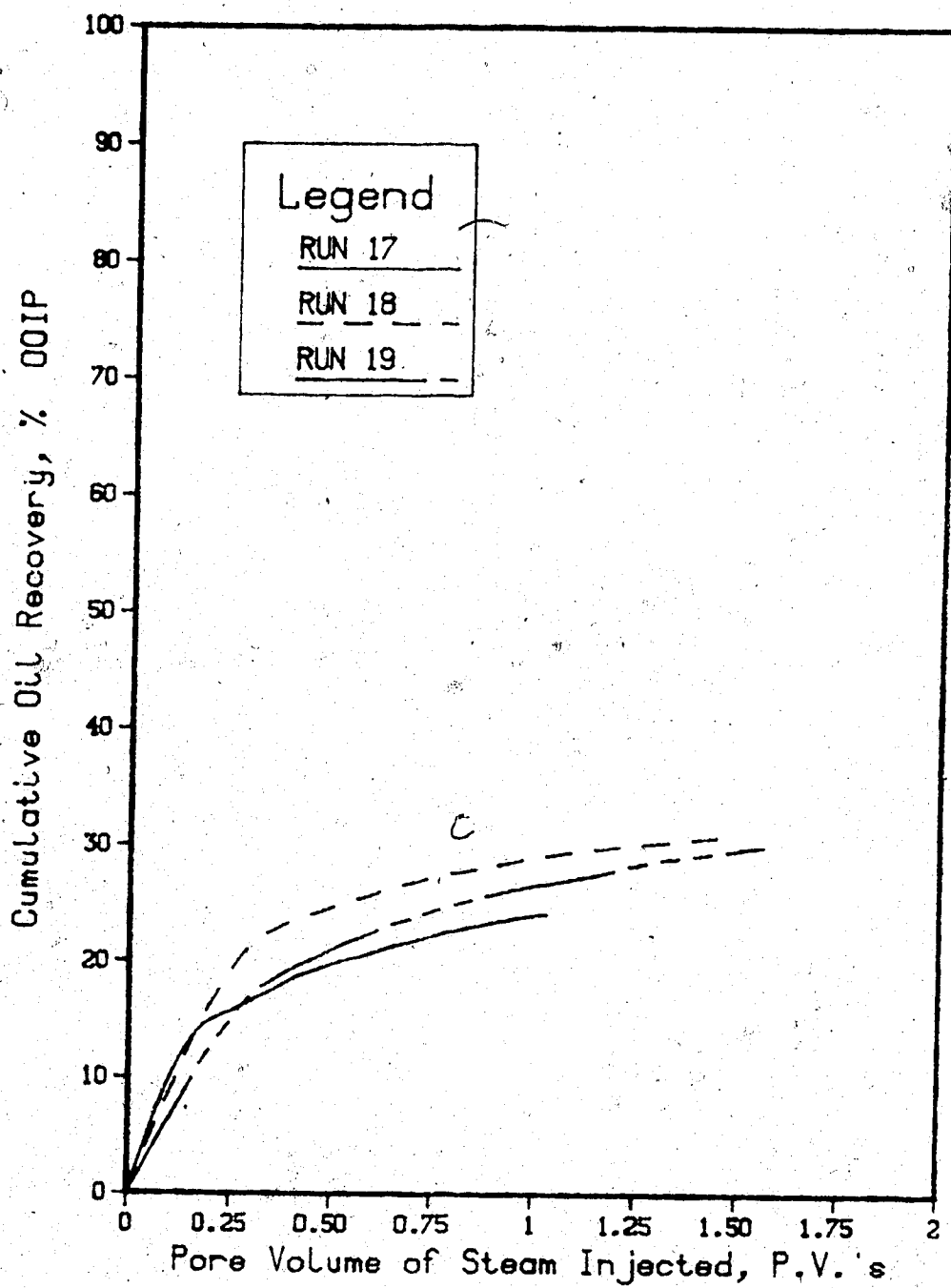
Figure 22. Comparison of the Recovery Responses of Runs 17,
18, and 19.
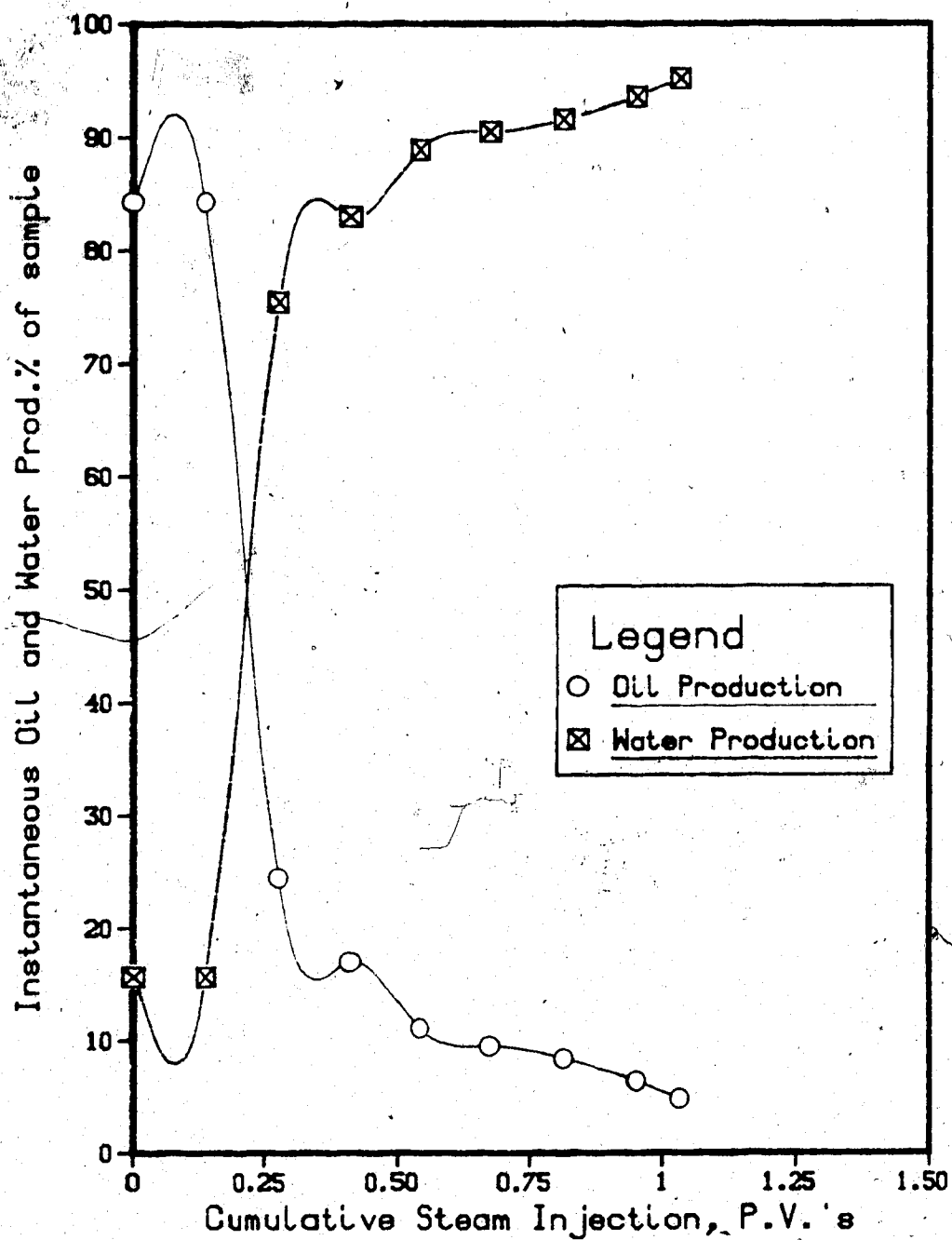
Figure 23. Run 17, Instantaneous Oil and Water Production vs. Cumulative Injection.
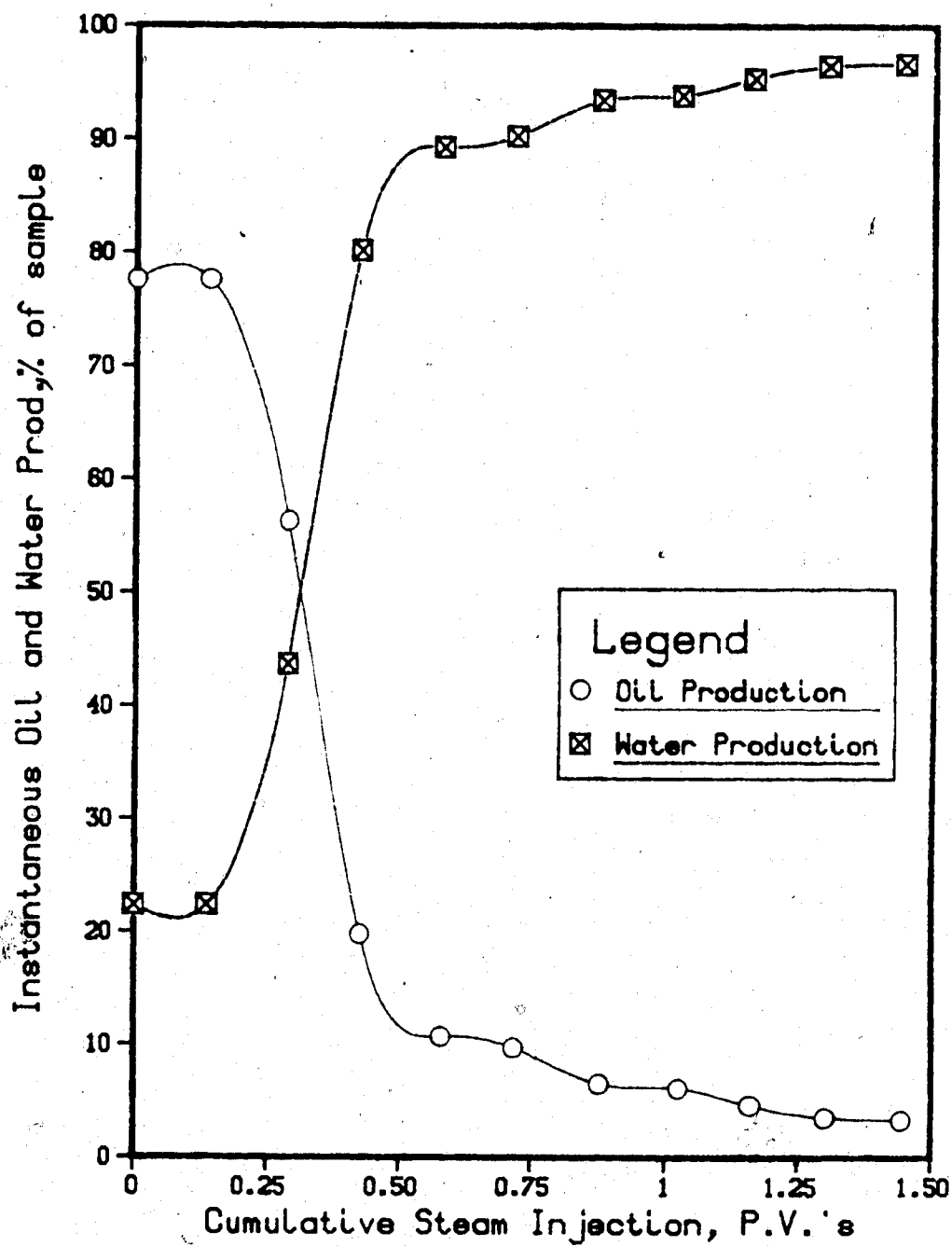
Figure 24. Run 18, Instantaneous Oil and Water Production
vs. Cumulative Injection.
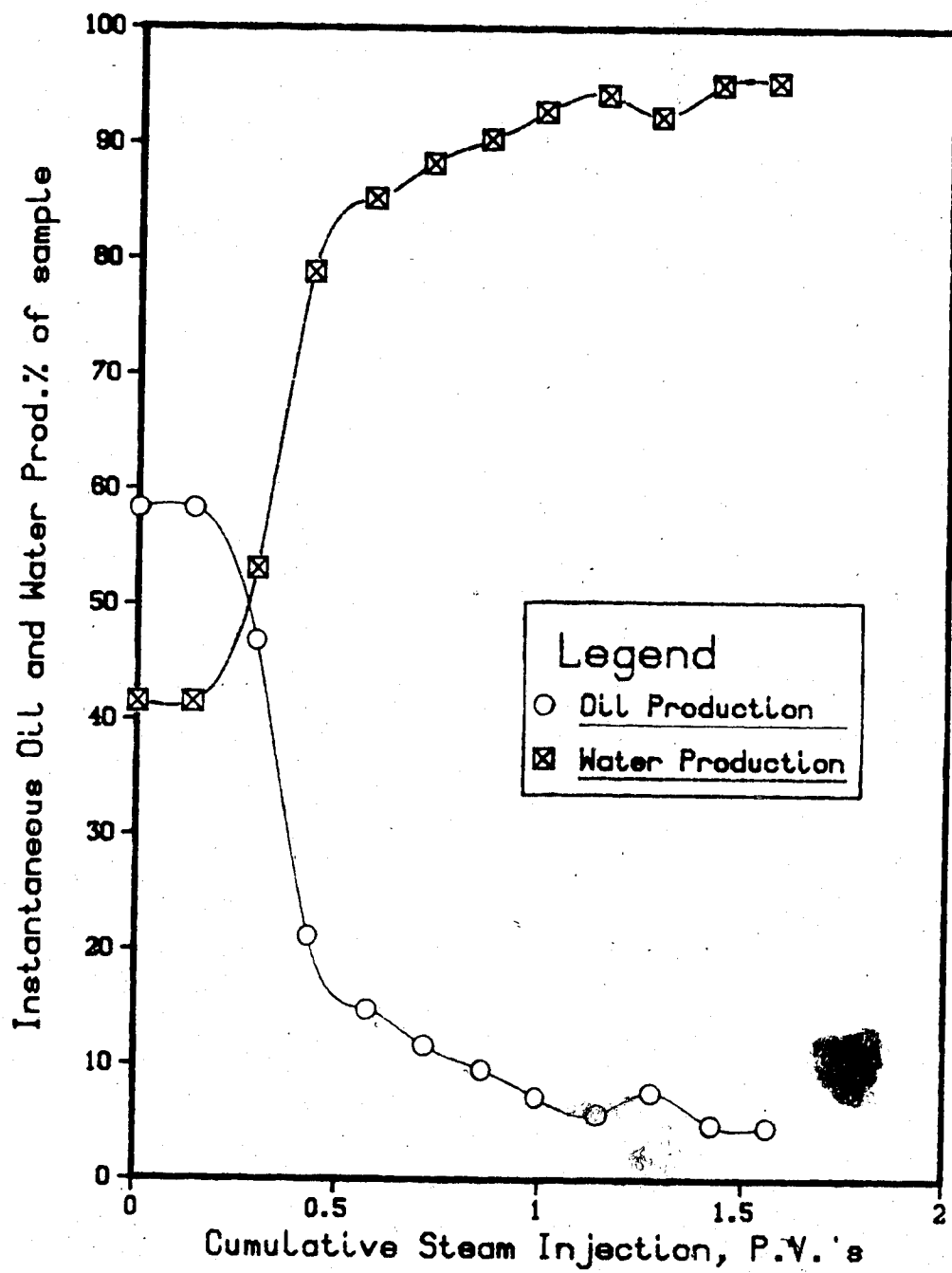
Figure 25. Run 19, Instantaneous Oil and Water Production
vs. Cumulative Injection.

6.9 Hot Water Slug Run

Run 22 was a hot water slug run which was conducted for the purpose of determining whether steam injectivity could be improved by an initial slug of hot water. The experimental parameters and a tabulation of the recovery response for this run are presented in Table 20. The water injection rate was 230.2 cm^3/min into the lower half of the formation.

The run was designed to inject approximately one half of a pore volume of hot water and gradually heat up the injected fluid until it became steam. However, the steam generating system was unable to gain heat at the rate required and thus it is questionable whether steam was injected at the later stages of the run.

Figure 26 shows the recovery response of Run 22. The sudden jump in the recovery curve at the injection of 0.8 pore volumes of water, could possibly be attributed to steam injection. It is possible that, although the boiler was not hot enough to generate superheated steam, the injected hot water flashed to steam when it encountered a low enough pressure within the model. A sudden increase in oil recovery is also observed in the oil-steam ratio curve, given as Figure 27, and in the instantaneous oil and water production curve given as Figure 28.

An inspection of the temperature profiles for this run (Given in Appendix A as Figures 76, 77, 78, and 79, for the injection of 0.25, 0.50, 0.75, and 1.00 pore volumes of water, respectively), shows that the heat advance occurred very quickly in the lower part of the formation. Figure 76

Table 20. Experimental Data for Run 22; Hot Water Slug Run
         in Aberfeldy Model

Type of Oil Used: Faxam-100 (208 mPa·s at 23°C)
Pore Volume Oil Zone: 14310 cm³
Porosity of Bead Pack: 34.07 %
Hydrocarbon Pore Volume: 12800 cm³
Initial Oil Saturation: 89.45 %
Irreducible Water Saturation: 10.55 %
Initial Model Temperature: 3.0°C
Water Feed Flow Rate: 199.3 cm³/min
Boiler Feed Flow Rate: 30.9 cm³/min
Total Flow Rate of Steam: 230.2 cm³/min
Volume of Steam Injected: 19377 cm³ (1.354 PV)
Volume of Oil Recovered: 3317 cm³ (25.91 % OOIP)

Cumulative Total PV Injected (cm³)	Cumulative Total PV Injected (PV)	Cumulative Oil Produced (cm³)	Cumulative Oil Produced (%OOIP)	Oil-Steam Ratio (cm³/cm³)
1950	0.136	1310	10.23	0.6718
3900	0.273	1640	12.81	0.1692
5961	0.417	1891	14.77	0.1218
7891	0.551	2101	16.41	0.1088
9851	0.688	2281	17.82	0.0918
11641	0.813	2651	20.71	0.2067
13401	0.936	2821	22.04	0.0966
15291	1.069	3021	23.60	0.1058
17437	1.219	3187	24.90	0.0774
19377	1.354	3317	25.91	0.0670

Hot Water Slug Run in Aberfeldy Model.
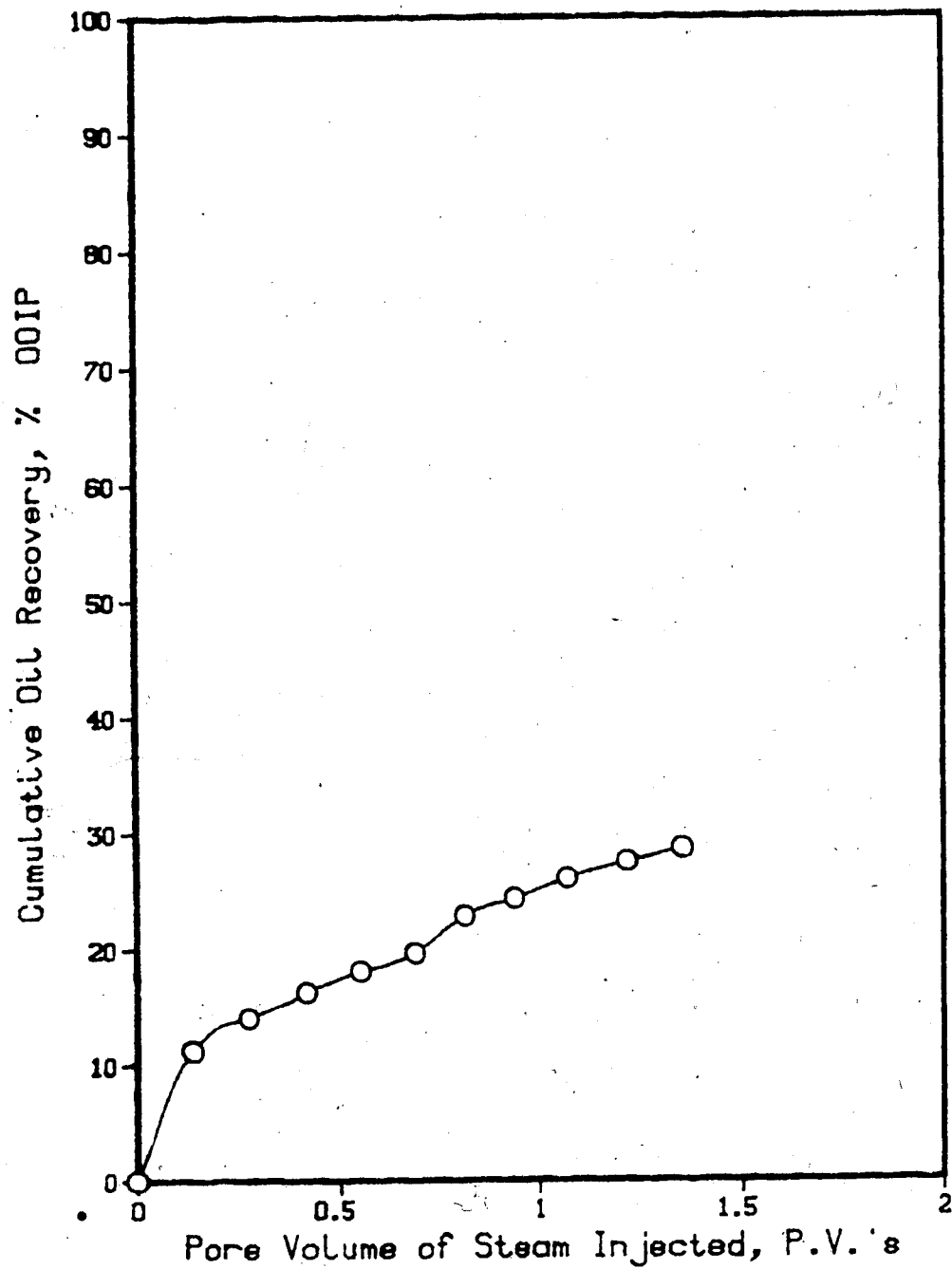
Figure 26. Run 22, Cumulative Oil Recovery vs. PV Injected.

Hot Water Slug Run in Aberfeldy Model.
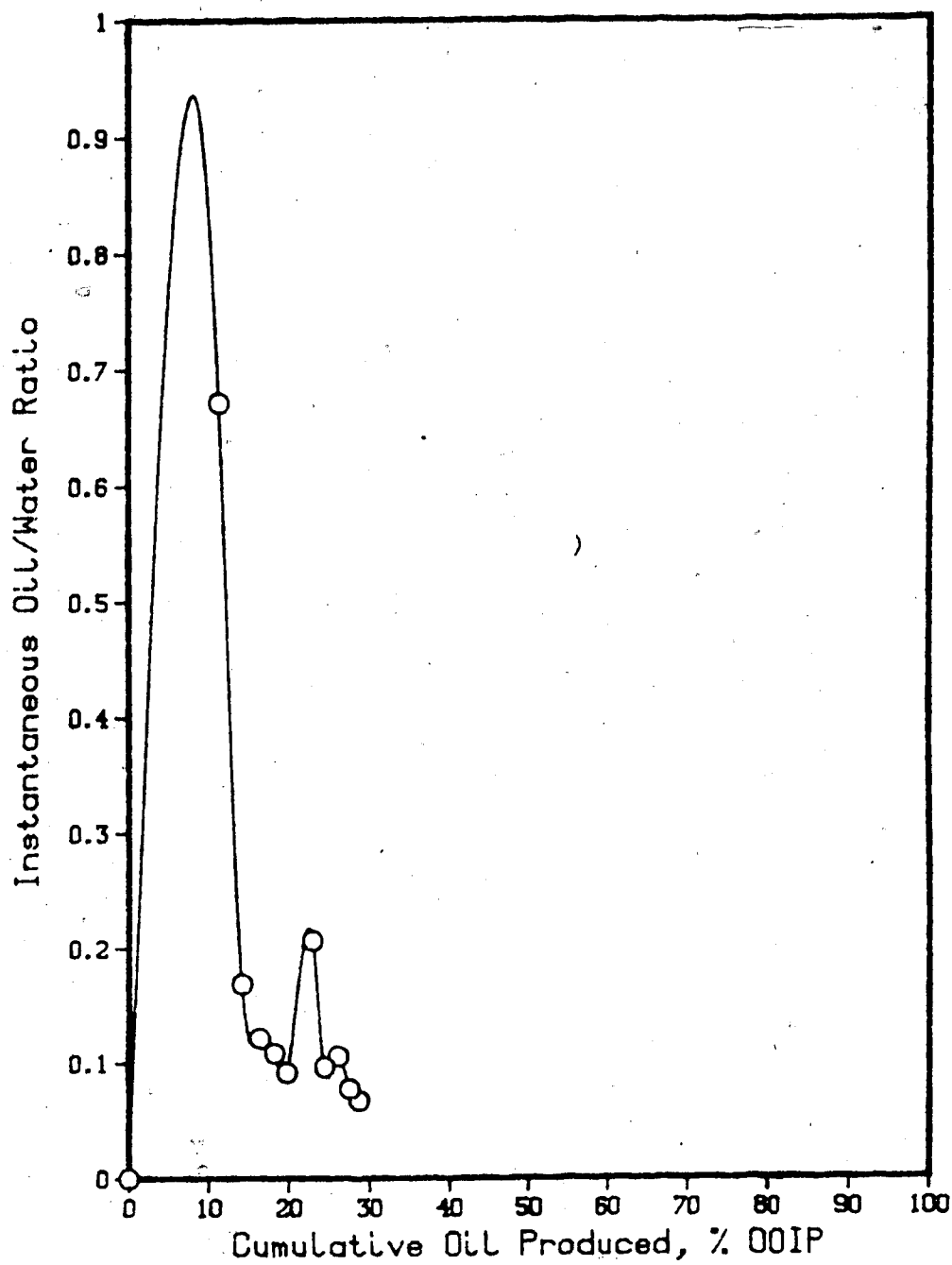
Figure 27. Run 22, Instantaneous Oil-Steam Ratio vs. Cumulative Oil Production.
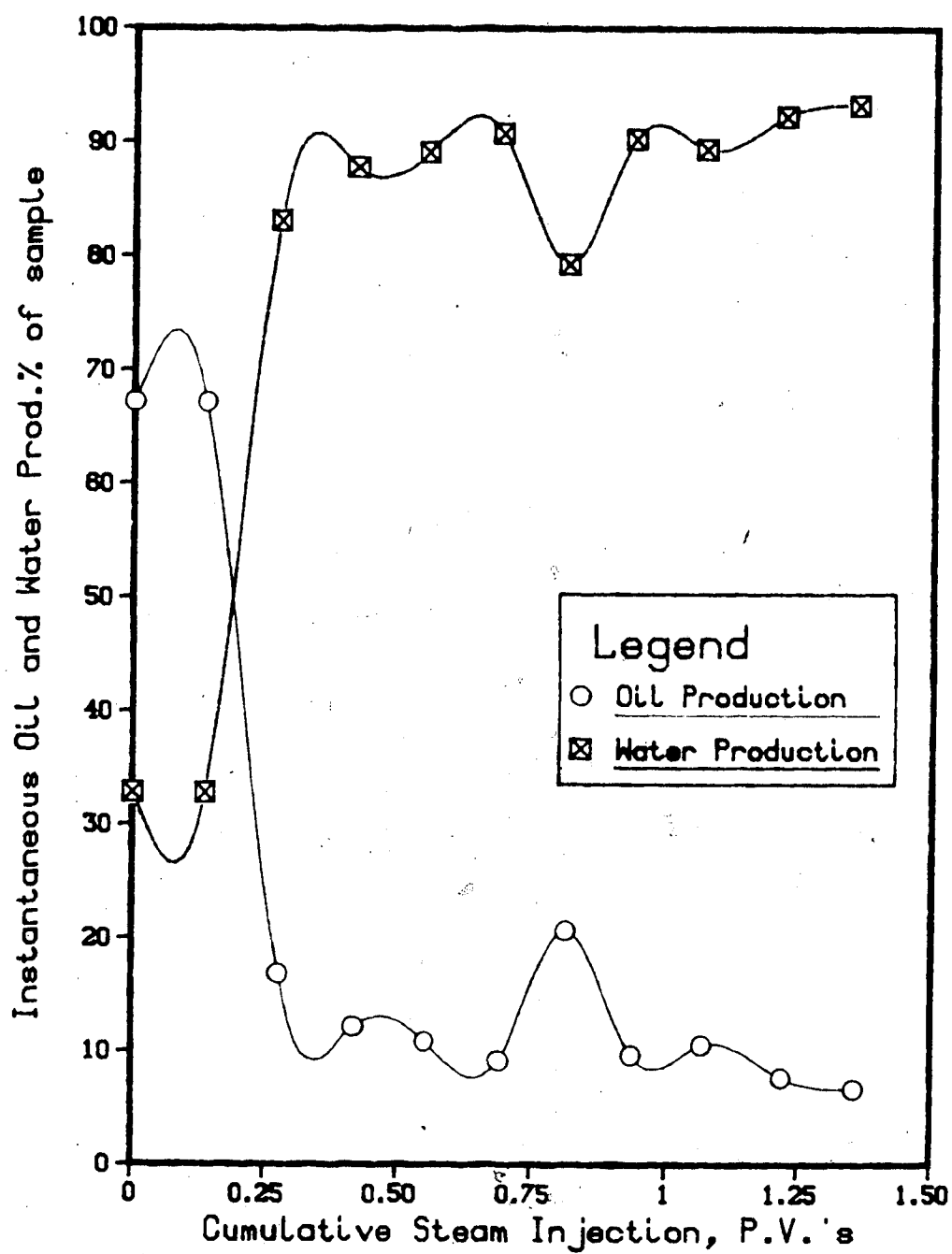
Figure 28. Run 22, Instantaneous Oil and Water Production
vs. Cumulative Injection.

shows that even upon the injection of only 0.25 pore volumes of hot water, the heated zone had advanced considerably in the lower part of the formation, while less movement had occurred in the upper part. Figure 77 at 0.50 pore volumes of steam injected shows the further advance of the hot zone in the lower layer. The sweep appears to be very efficient, extending almost radially. At 0.75 pore volumes injected (Figure 78) the isotherms begin to appear slightly irregular, and this nonuniformity becomes even more pronounced upon the injection of 1.00 pore volumes (Figure 79).

After 1.35 pore volumes of hot water had been injected, 25.9 % of the original oil in place had been recovered. This represented a recovery response quite similar to that obtained in the continuous steamflood experiments (Runs 6 and 10), but was considerably less than the average recovery observed in the steam slug runs (Runs 17, 18, and 19).

7. CONCLUSIONS

1. A low pressure, scaled steamflood model was designed, constructed, and tested for a variety of steamflood runs, and was found to be satisfactory for the purpose of conducting steamflood experiments.

2. Oil viscosity was observed to have a considerable influence on the type of steam drive developed. In the case of the Aberfeldy oil (208 mPa·s at 24°C; 1275 mPa·s at 24°C in prototype), the steam zone developed in the upper part of the formation, with steam condensate movement toward the base. In the case of a more viscous oil (9250 mPa·s at 24°C; 13085 mPa·s at 24°C in prototype), the steam zone development was clearly in the upper part of the sand. In the case of the light oil (60 mPa·s at 24°C; 25.6 mPa·s at 23°C in prototype), the steam zone development was closer to a frontal drive.

3. Based upon one run, it was concluded that bottom water has an extremely unfavorable effect on steamflood efficiency, with a cumulative recovery of only 3% for a water/oil zone thickness ratio of 5:1.

4. The steam slug process appears to be an efficient and practically viable recovery technique, with oil recovery of 30.9% of the original oil in place, for a 0.29 pore volume slug of steam, followed by the injection of 1.16 pore volumes of cold water. Among the techniques tested thus far, the steam slug process appears to be the best recovery process for the Aberfeldy crude.

5. The oil recovery observed for a steamflood in a light

128

oil model was higher than that of the Aberfeldy model, being 35.7% of the original oil in place, after the injection of 1.65 pore volumes of steam. Thus steamflooding may be a viable recovery method for light oils as well, although the flood performance needs to be examined for a variety of operating parameters, in particular, the oil saturation, because such reservoirs would normally be waterflooded first.

NOMENCLATURE

f_{sr} = Steam quality. (dimensionless)

h_{ss} = Enthalpy of saturated steam. (kJ/kg)

h_{wa} = Enthalpy of water. (kJ/kg)

k_m = Permeability in the model. (darcies)

k_p = Permeability in the prototype. (darcies)

k_{hm} = Thermal conductivity in the model. (kW/m·K)

k_{hp} = Thermal conductivity in the prototype. (kW/m·K)

L_m = Length of the model.

L_p = Length of the prototype.

L_v = Latent heat of vapourization. (kJ/kg)

M_m = Heat capacity in the model. (kJ/kg·K)

M_p = Heat capacity in the prototype. (kJ/kg·K)

P_m = Pressure in the model. (MPa or kPa)

P_p = Pressure in the prototype. (MPa)

$(P_p)_m$ = Production pressure in the model. (MPa)

$(P_p)_p$ = Production pressure in the prototype. (MPa)

r = Scaled radius of the well. (inches)

S_g = Saturation of gas. (dimensionless)

S_o = Saturation of oil. (dimensionless)

S_{or} = Residual oil saturation to steam. (dimensionless)

S_w = Saturation of water. (dimensionless)

t_m = Time in the model. (min)

t_p = Time in the prototype. (days)

T_m = Model temperature. (C)

T_p = Prototype temperature. (C)

T_{o_m} = Initial model temperature. (C)

130

T_{o_p} = Initial prototype temperature. (C)

w = Slit width of scaled well. (inches)

w_a = Mass rate of flow of the aqueous phase.

w_m = Injection rate into the model. (cm³/min)

w_p = Injection rate into the prototype. (m³/day)

w_s = Mass rate of flow of superheated steam.

w_{wi} = Total mass rate injected.

$\gamma(L)$ = Length scaling factor. (dimensionless)

$\gamma(\Delta P)$ = Pressure scaling factor. (dimensionless)

ρ = Density. (kg/m³)

ϕ_m = Porosity in the model. (dimensionless)

ϕ_p = Porosity in the prototype. (dimensionless)

μ = Viscosity. (mPa·s)

REFERENCES

1. "Annual Production Report", Oil and Gas Journal (April 2, 1984), 83-105.

2. Farouq Ali, S.M., "Steam Injection as a Method for Recovering Light Oil Crudes -- The Bradford Steamflood", Paper presented at the 1978 Eastern Regional Meeting of the Society of Petroleum Engineers held in Washington, D.C., November 10, 1978.

3. Farouq Ali, S.M., "Potential of Steamflooding for Recovering Light Oils", Paper presented at the meeting of the Petroleum Society of the Canadian Institute of Mining and Metallurgy held in Banff, Alberta, May 9-11, 1979.

4. Farouq Ali, S. M. and Meldau, R.F.: "Current Steamflood Technology", J.P.T., October 1979, 1332-1342.

5. Blevins, T.R., Duerksen, J.H., Ault, J.W.: "Light Oil Steamflooding -- An Emerging Technology," Paper presented at the 1982 SPE/DOE Third Joint Symposium on Enhanced Oil Recovery of the Society of Petroleum Engineers held in Tulsa, Oklahoma, April 4-7, 1982.

6. Farouq Ali, S.M.: "Steam Injection Theories--A Unified Approach", Paper presented at the 1982 California Regional Meeting of the SPE held in San Francisco, California (March 24-26, 1982).

7. Willman, B.T., Valleroy, V.V., Runberg, G.W., Cornelius, A.J., and Powers, L.W.: "Laboratory Studies of Oil Recovery by Steam Injection", J. Pet. Tech. (July, 1961), 681-690.

8. Marx, J.W. and Langenheim, R.H.: "Reservoir Heating by Hot Fluid Injection", Trans. AIME, (1959) vol. 216, 312-315.

9. Ozen, A.S. and Farouq Ali, S.M.: "An Investigation of the Recovery of the Bradford Crude by Steam Injection", J.P.T. (June 1969), 692-698.

10. Baker, P.E.: "An Experimental Study of Heat Flow in Steamflooding", S.P.E.J., (March 1969) 89-99.

11. Baker, P.E.: "Effect of Pressure and Rate on Steam Zone Development in Steamflooding", Paper presented at SPE-AIME 47th Annual Fall Meeting held in San

Antonio, Texas, Oct. 8-11, 1972.

12. El-Saleh, M.M. and Farouq Ali, S.M.: "Oil Recovery by a Water-Driven Steam Slug", SPEJ, (December, 1971), 351-355.

13. Hong, K.C.: "Guidelines for Converting Steamflood to Waterflood", Paper presented at the SPE 1985 California Regional Meeting, held in Bakersfield, California (March 27-29, 1985), 167-179.

14. Ault, J.W., Johnson, W.M., and Kamilos, G.N.: "Conversion of Mature Steamfloods to Low-Quality Steam and/or Hot-Water Injection Projects", Paper presented at the SPE 1985 California Regional Meeting, held in Bakersfield, California (March 27-29, 1985), 149-166.

15. Redford, D.A., Flock, D.L., Peters, E.J., and Lee, J.: "Laboratory Model Flow-Test Systems of In Situ Recovery From Alberta Oil Sands", Annual Meeting of Can. Chem. Soc., Montreal (1976).

16. Flock, D.L. and Lee, J.: "An Experimental Investigation of Steam Displacement of a Medium Gravity Crude Oil", Canadian Institute of Mining and Metallurgy, Special Volume No. 17, 386-394.

17. Farouq Ali, S.M. and Abad, B.: "Bitumen Recovery from Oil Sands, Using Solvents in Conjunction With Steam", J.C.P.T., (July-Sept., 1976).

18. Lee, J.L.: Experimental Investigation of Steamflooding Behavior in an Adiabatic Water-Saturated Core", M.Sc. Thesis, U. of Alberta (1977).

19. Farouq Ali, S.M. and Redford, D.A.: "Physical Modeling of In Situ Recovery Methods for Oil Sands", Canadian Institute of Mining and Metallurgy, Special Volume No. 17, 319-326.

20. Johnstone, R.E. and Thring, N.W.: "Pilot Plants, Models and Scale-Up Methods in Chemical Engineering", McGraw-Hill Book Co., New York (1957).

21. Geertsma, J., Croes, G.A., and Schwarz, N.: "Theory of Dimensionally Scaled Models of Petroleum Reservoirs", Trans. AIME, Vol. 207 (1956) 118-127.

22. Pujol, L. and Boberg, T.C.: "Scaling Accuracy of Laboratory Steamflooding Models", Paper presented at the California Regional Meeting of the Society of Petroleum Engineers held in Bakersfield (Nov. 8-10, 1972). SPE paper #4191.

23. Niko, H. and Troost, P.J.P.M.: "Experimental Investigation of Steam Soaking in a Depletion-Type Reservoir", J.P.T. (Aug., 1971), 1006-1014.

24. Perkins, F.M. and Collins, R.E.: "Scaling Laws for Laboratory Flow Models of Oil Reservoirs", Trans., AIME (1960), vol. 219, 383-385

25. Demetre, G.P., Bentsen, R.G., and Flock, D.L.: "A Multi-Dimensional Approach to Scaled Immiscible Fluid Displacement", JCPT, (July-August, 1982), 49-61.

26. Greenkorn, R.A.: "Flow Models and Scaling Laws for Flow Through Porous Media", Industrial and Engineering Chemistry (March, 1964), Vol. 56, No. 3, 32-37.

27. Loomis, A.G. and Crowell D.C.: "Theory and Application of Dimensional and Inspectional Analysis to Model Study of Fluid Displacements in Petroleum Reservoirs", Bureau of Mines Report RI6546 (1964).

28. Bentsen, R.G.: "Scaled Fluid-Flow Models With Permeabilities Differing From That of the Prototype", JCPT (July-September, 1976).

29. Rapoport, L.A.: "Scaling Laws for Use in Design and Operation of Water-Oil Flow Models", Trans., AIME (1955), vol. 204, 143-150.

30. Leverett, M.C., Lewis, W.B. and True, M.E.: "Dimensional-Model Studies of Oil-Field Behavior", Trans., AIME (1942), vol. 146, 175-193.

31. Pursley, S.A.: "Experimental Studies of Thermal Recovery Processes", Paper presented at the Heavy Oil Symposium, Maracaibo, Venezuala (1974).

32. Ehrlich, R.: "Laboratory Investigation of Steam Displacement in the Wabasca Grand Rapids A Sand", Paper presented at the Canada-Venezuela Oil Sands Symposium, Edmonton, Alberta (May 1977), 364-379.

33. Huygen, H.H.A.: "Laboratory Steamfloods in Half of a Five-Spot", Paper presented at the 51st Annual Fall Meeting of the Society of Petroleum Engineers of AIME held in New Orleans, (Oct. 3-6, 1976).

34. Huygen, H.H.A. and Lowry, W.E.: "Steamflooding Wabasca Tar Sand Through The Bottom Water Zone -- Scaled Lab Experiments", Paper presented at the 54th Annual Fall Meeting of the Society of Petroleum Engineers held in Las Vegas, (Sept. 23-26, 1979).

35. Singhal, A.K.: "Physical Model Studies of Inverted
        Seven-Spot Steamfloods in a Pool Containing a
        Lloydminster Type Heavy Oil", Petroleum Recovery
        Institute Research Report RR-38 (November, 1978).

36. Lo, H.Y.: "Laboratory Model Study of Steamflood Oil
        Recovery", Petroleum Recovery Institute Interim
        Report, IR-5, (March, 1977).

37. Stegemeier, G.L., Laumbach, D.D., and Volek, C.W.:
        "Representing Steam Processes With Vacuum Models",
        Paper presented at the 52nd Annual Fall Technical
        Conference and Exhibition of the SPE, held in Denver
        (Oct. 9-12, 1977).

38. French M.S. and Howard, R.L.: "The Steamflood Job,
        Hefner Sho-Vel-Tum", Oil and Gas Journal (July,
        1967), Vol. 65, No. 29, 64.

39. Afoeju, B.I.: "Conversion of Steam Injection to
        Waterflood, East Coalings Field", J.P.T. (Nov.
        1974), 1227-1232.

40. Hall, A.L. and Bowman, R.W.: "Operation and Performance
        of the Slocum Thermal Recovery Project , J.P.T.
        (April 1973), 402-408.

41. Stokes, D.D., Brew, J.R., Whitten, D.G., and Wooden,
        L.W.,: "Steam Drive as a Supplemental Recovery
        Process in an Intermediate Viscosity Reservoir,
        Mount Poso Field, California", Paper presented at
        the 47th Annual California Regional Meeting of the
        SPE held at Bakersfield, (April 13-15, 1977).

42. Prats, M.: "Peace River Steam Drive Scaled Model
        Experiments", 28th Annual Technical Meeting of the
        Petrol. Soc. of the CIM, Canada-Venezuala Oil Sands
        Symposium of 1977, Edmonton (May, 1977).

43. Stokes, D.D. and Doscher, T.M.: "Shell Makes a Success
        of Steamflood at Yorba Linda", Oil and Gas Journal
        (Sept. 2, 1974), 71-78.

44. Doscher, T.M.: "Scaled Physical Model Studies of the
        Steam Drive Process", First Annual Report (Sept.,
        1977 to Sept., 1978), U.S. Department of Energy,
        Contract DOE/ET/12075-1.

45. Yortsos, Y.C.: "Analytical Modeling of Oil Recovery by
        Steam Injection", Ph.D. Dissertation, California
        Institute of Technology (1979).

46. Doscher, T.M. and Huang, W.: "Steam-drive Performance

Judged Quickly From Use of Physical Models", Oil and Gas Journal (Oct. 22, 1979), 52-57.

47. Doscher, T.M. and Ghassemi, F.: "The Influence of Oil Viscosity and Thickness on the Steam Drive", JPT (February, 1983), 291-298.

48. Kimber, K. and Farouq Ali, S.M.: Paper in progress.

49. Prats, M.: Comment to the Discussion on Physical Modeling, CIM Special volume no. 17, p397.

50. Kasraie, M. and Farouq Ali, S.M.: "Heavy Oil Recovery in the Presence of Bottom Water", Paper presented at the 35th Annual Technical Meeting of the Petroleum Society of CIM held in Calgary (June 10-13, 1984).

51. Singh, B., Malcolm, J.D., and Heidrick, T.M.: "Injection-Production Strategies for Reservoirs Having a Bottomwater Zone", Paper presented at the SPE 1985 California Regional Meeting, held in Bakersfield (March 27-29, 1985).

52. Coats, K.H., Ramesh, A.B., and Winestock, A.G.: "Numerical Modeling of Thermal Reservoir Behavior", CIM Special Volume No. 17, 399-410.

53. Van Wylen, G.J. and Sonntag, R.J.: "Fundamentals of Classical Thermodynamics", Steam Tables.

54. CRC Handbook of Chemistry and Physics, 59 th Edition, page E-16.

55. CRC Handbook of Chemistry and Physics, 59 th Edition, 1978-1979, page F-1.

56. Currie, J.B. and Gregory, A.R.: "Homogeneously Distributed Particles", U.S. Patent 2,808,242 (Oct. 1, 1957).

57. Wygal, R.J.: "Construction of Models that Simulate Oil Reservoirs", SPE Journal, (December, 1963).

APPENDIX A: Temperature Profiles

138

FIGURE 29: TEMPERATURE PROFILE FOR
RUN 4: STEAMFLOOD ON WATER SATURATED MODEL
0.25 Pore Volumes of Steam Injected
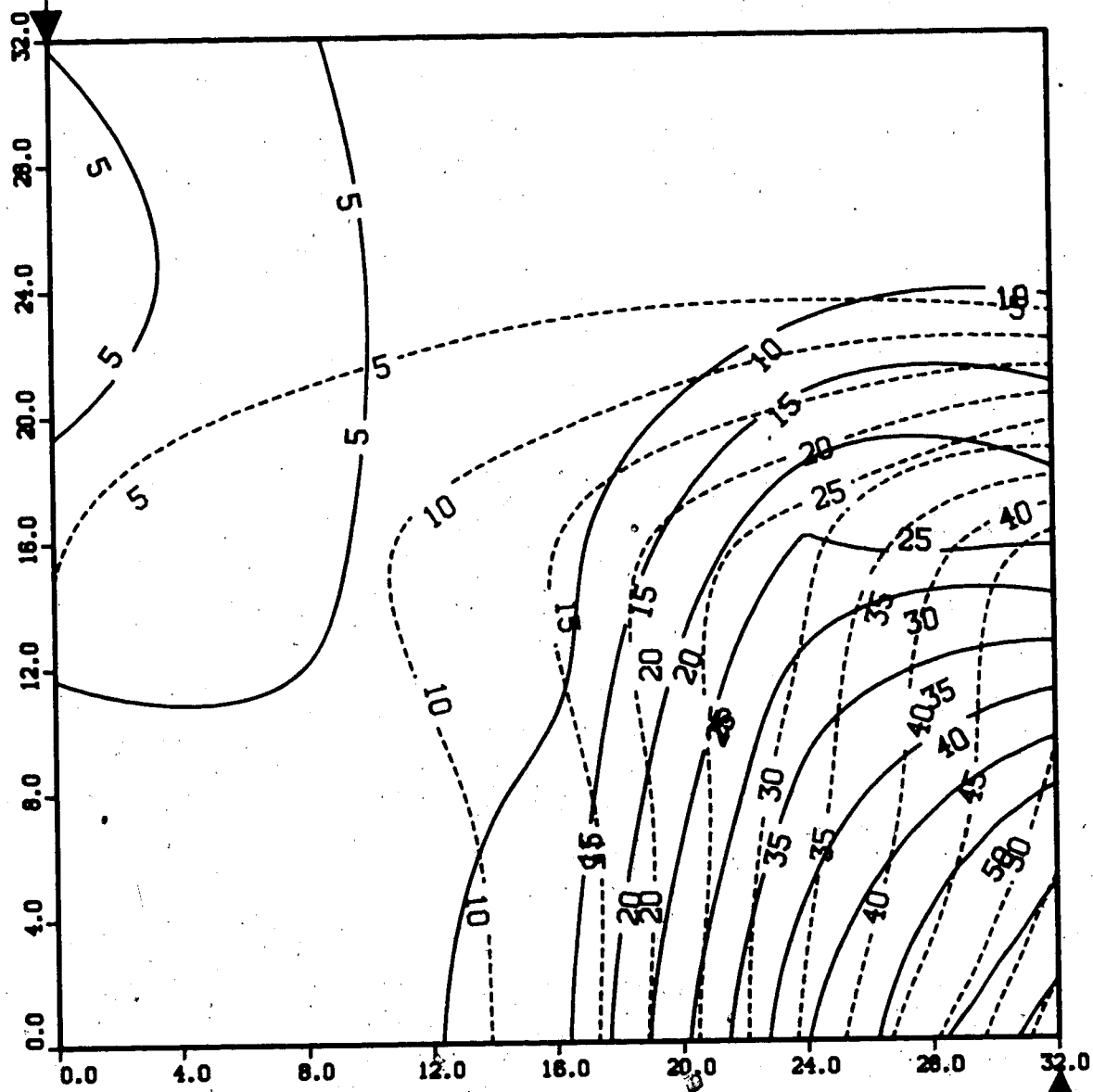
FIGURE 30: TEMPERATURE PROFILE FOR
RUN 4: STEAMFLOOD ON WATER SATURATED MODEL
0.50 Pore Volumes of Steam Injected
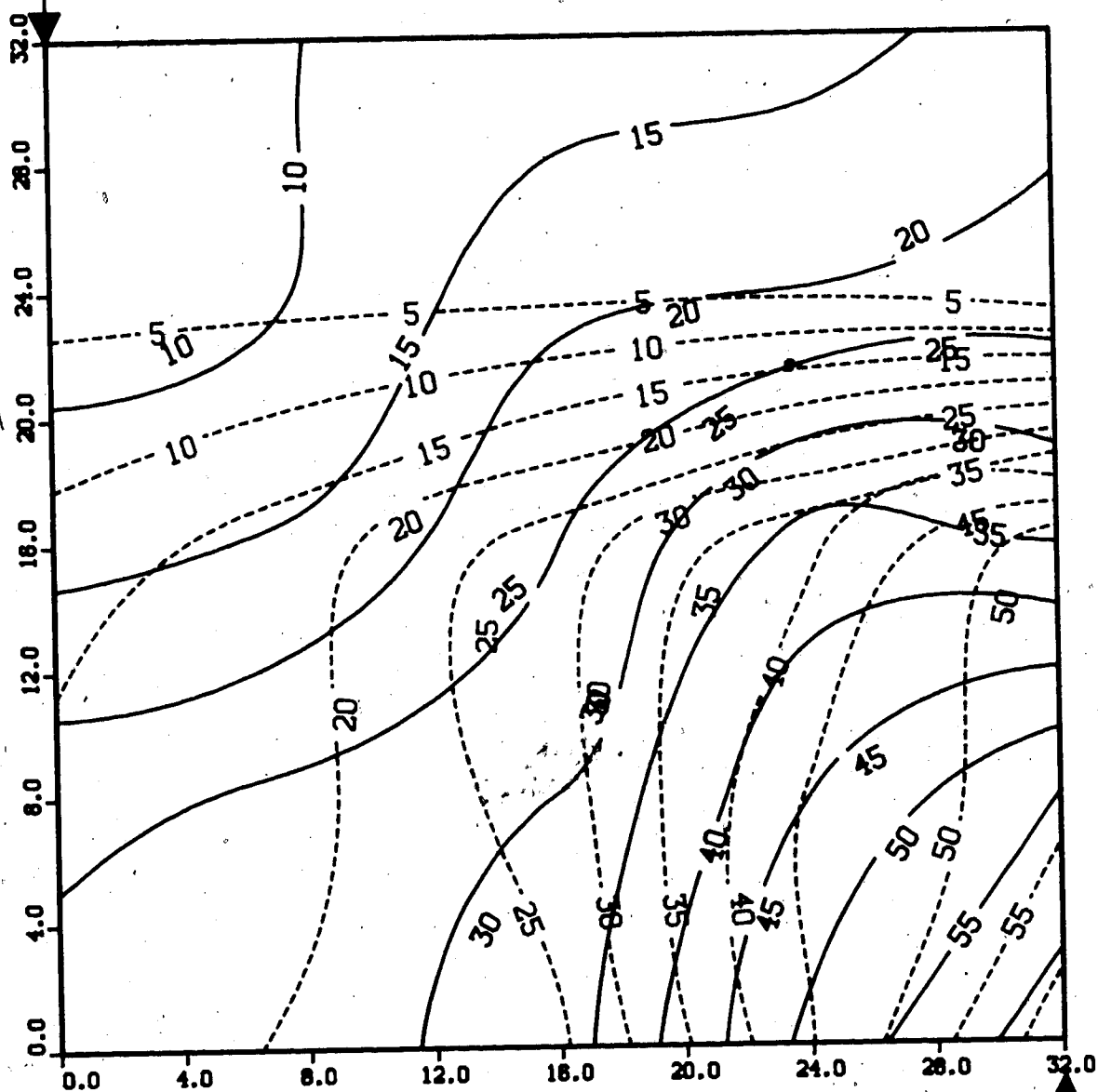
Production Well

Injection Well

Upper Model Temperature (C)
Lower Model Temperature (C)

FIGURE 31: TEMPERATURE PROFILE FOR
RUN 4: STEAMFLOOD ON WATER SATURATED MODEL
0.75 Pore Volumes of Steam Injected

Production Well
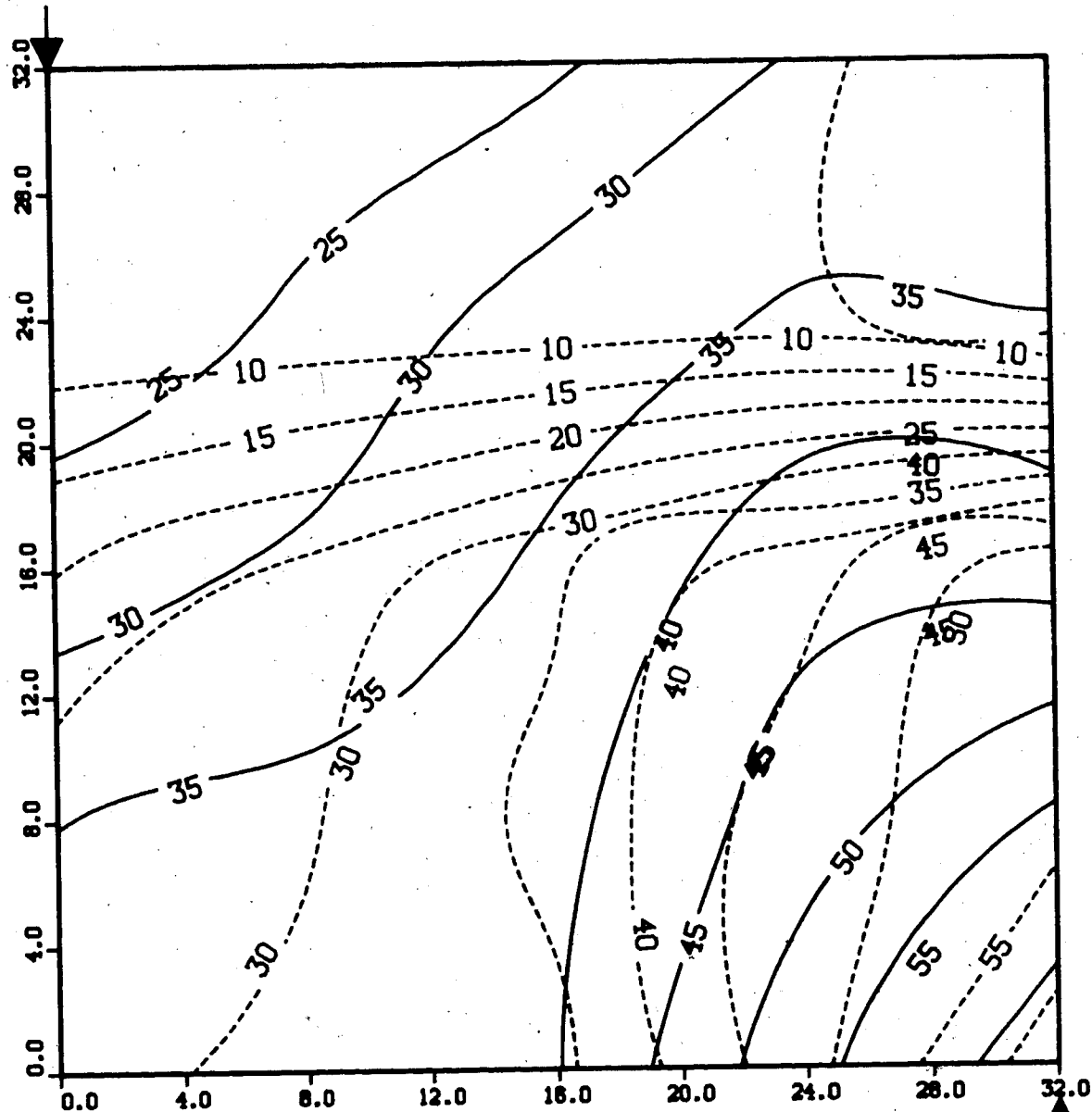
Injection Well

Upper Model Temperature (C)
Lower Model Temperature (C)

FIGURE 32: TEMPERATURE PROFILE FOR
RUN 4: STEAMFLOOD ON WATER SATURATED MODEL
1.00 Pore Volumes Injected
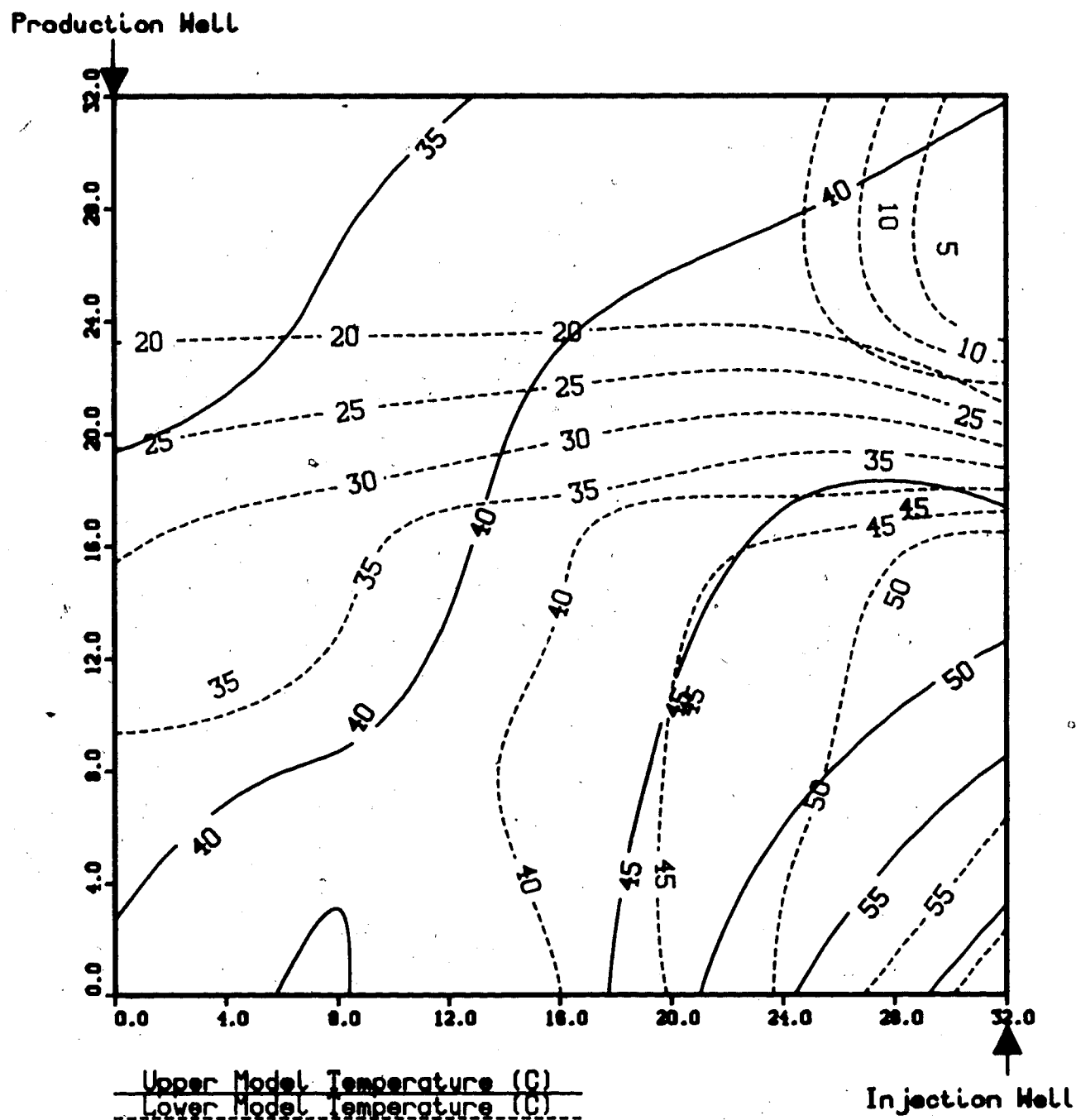
FIGURE 33: TEMPERATURE PROFILE FOR
RUN 6: CONTINUOUS STEAMFLOOD ON ABERFELDY MODEL
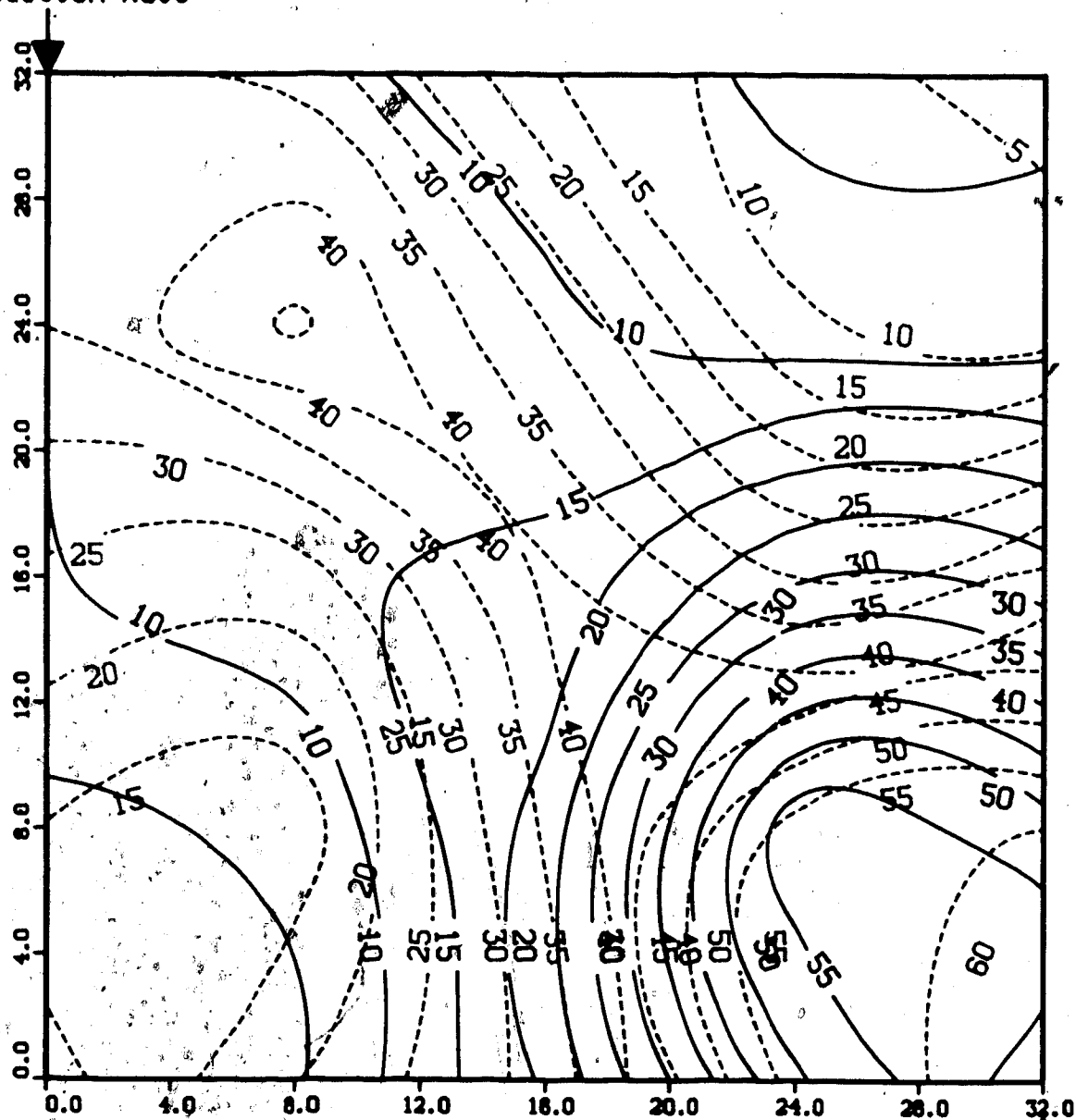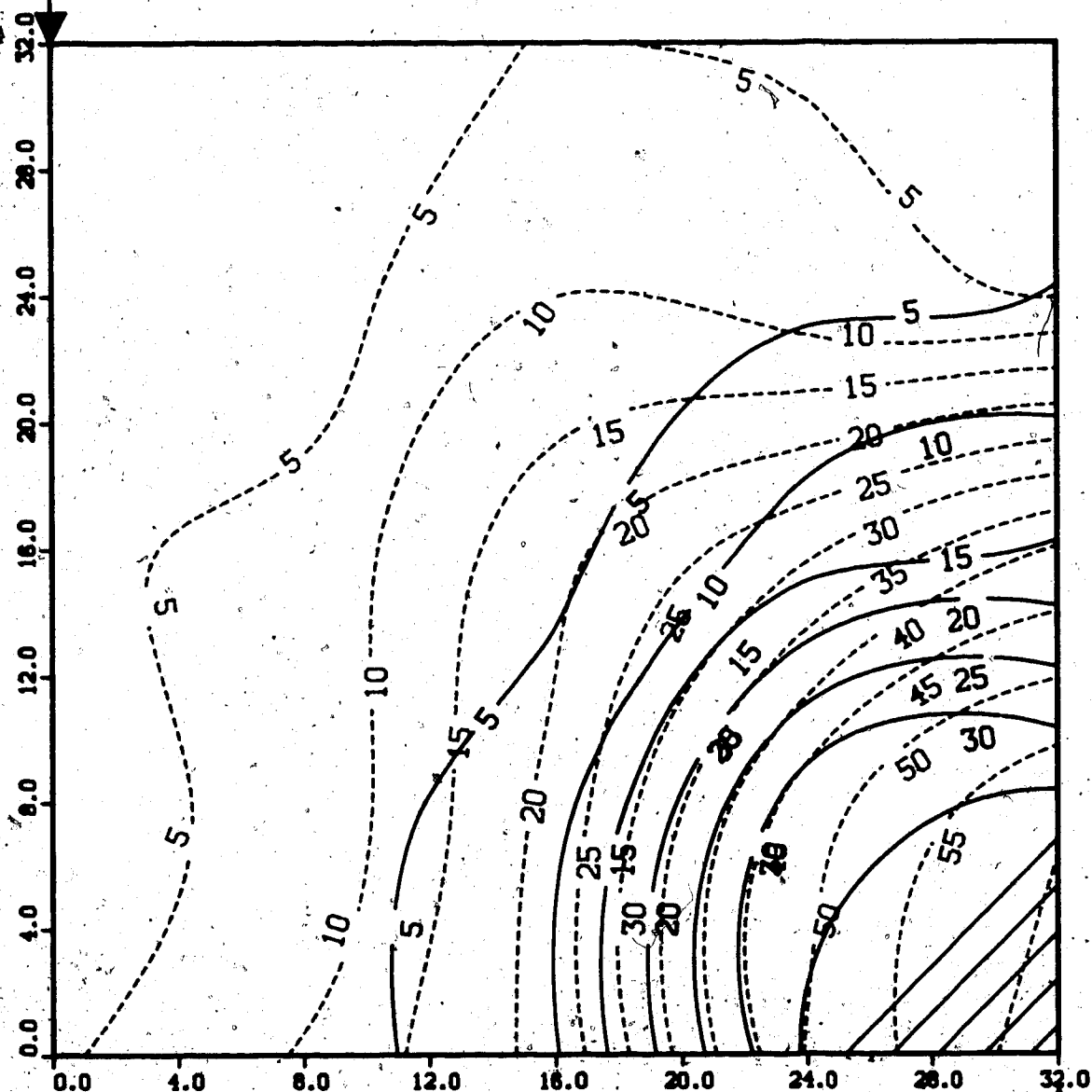### 0.25 Pore Volumes of Steam Injected

Production Well

Injection Well

Upper Model Temperature (C)
Lower Model Temperature (C)
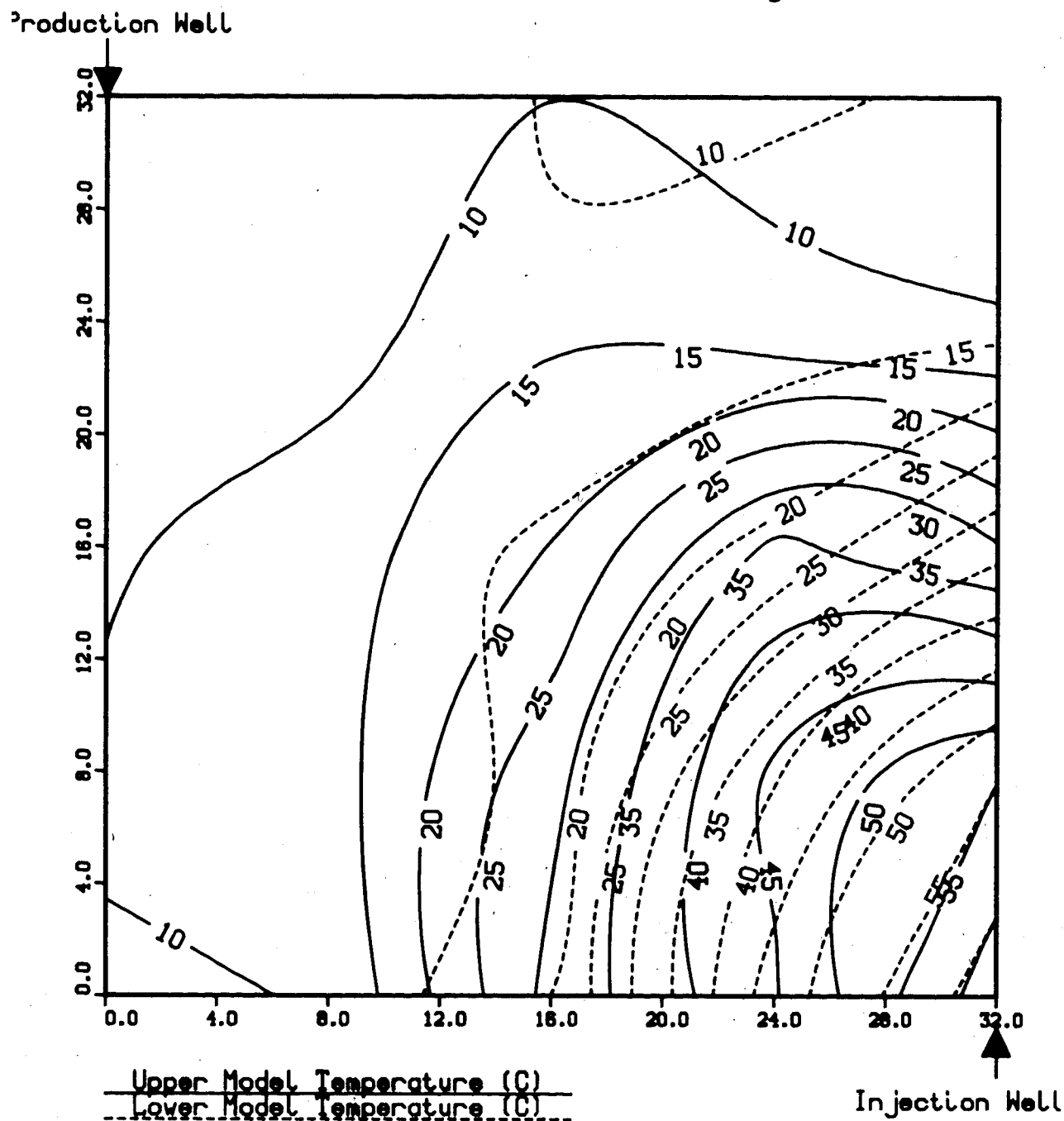
FIGURE 34: TEMPERATURE PROFILE FOR
RUN 6: CONTINUOUS STEAMFLOOD ON ABERFELDY MODEL
0.50 Pore Volumes of Steam Injected

Production Well
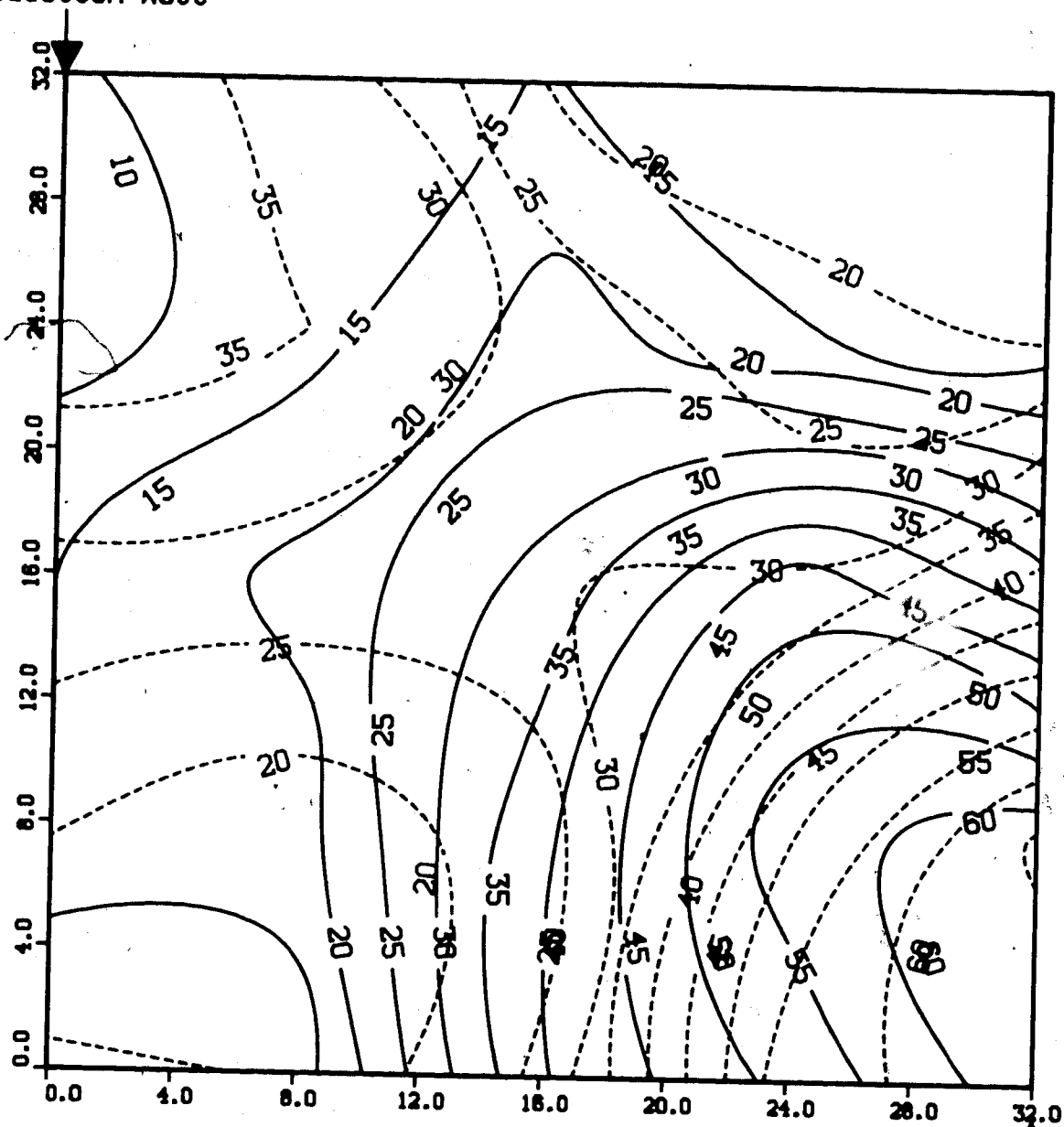
Injection Well

Upper Model Temperature (C)
Lower Model Temperature (C)

FIGURE 35: TEMPERATURE PROFILE FOR
RUN 6: CONTINUOUS STEAMFLOOD ON ABERFELDY MODEL
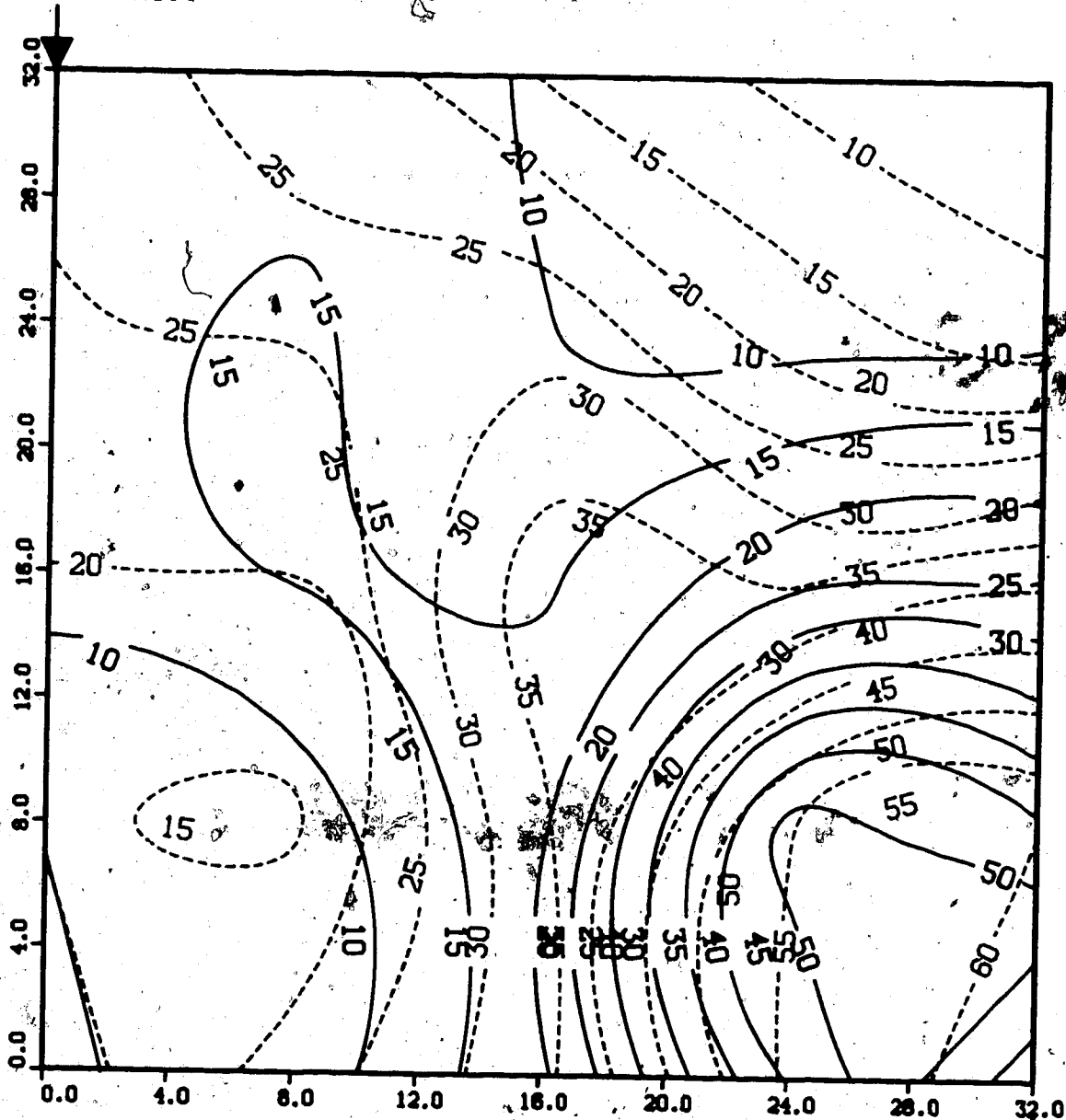### 0.75 Pore Volumes of Steam Injected

Production Well
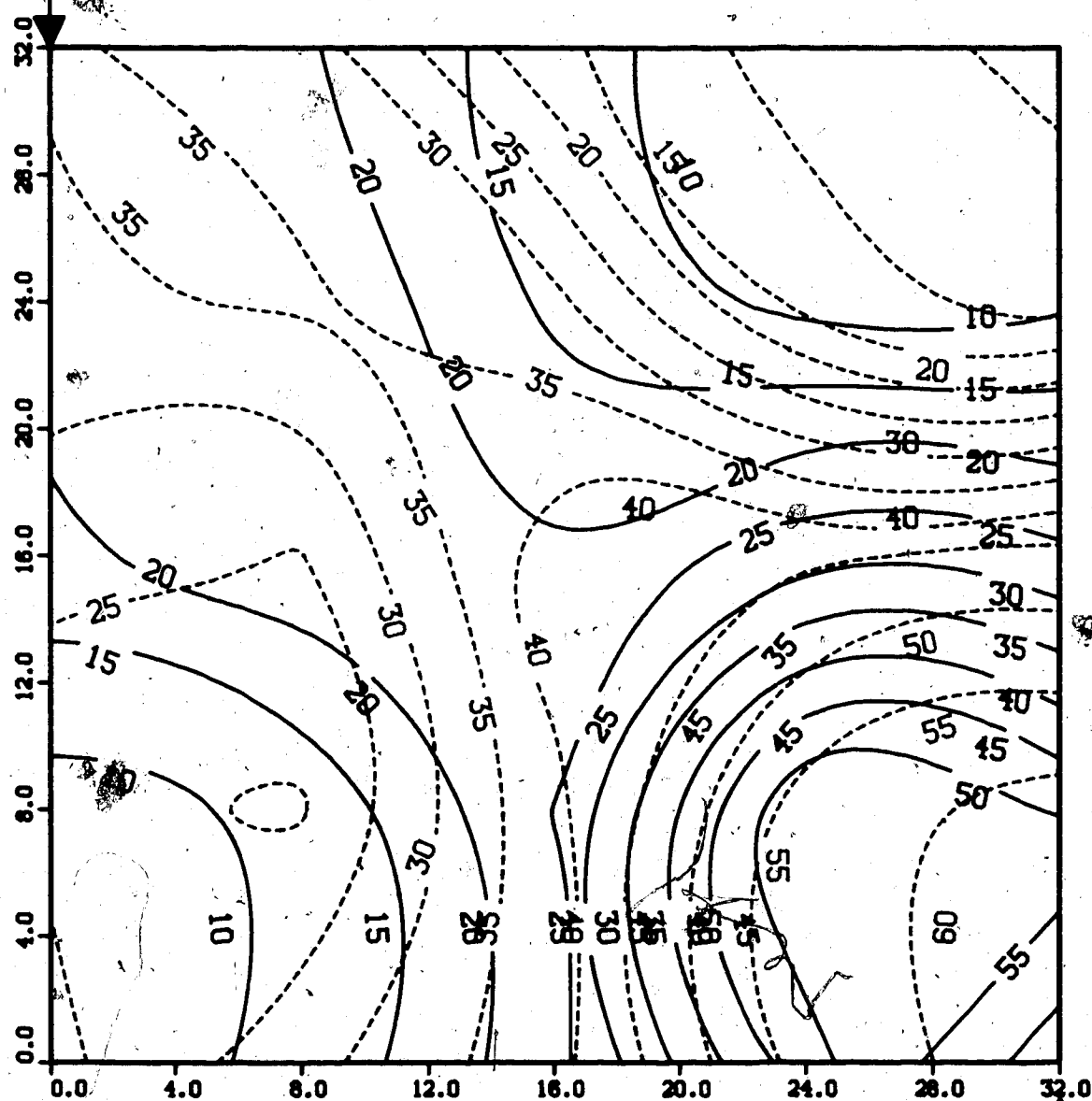
Upper Model Temperature (C)
Lower Model Temperature (C)

Injection Well
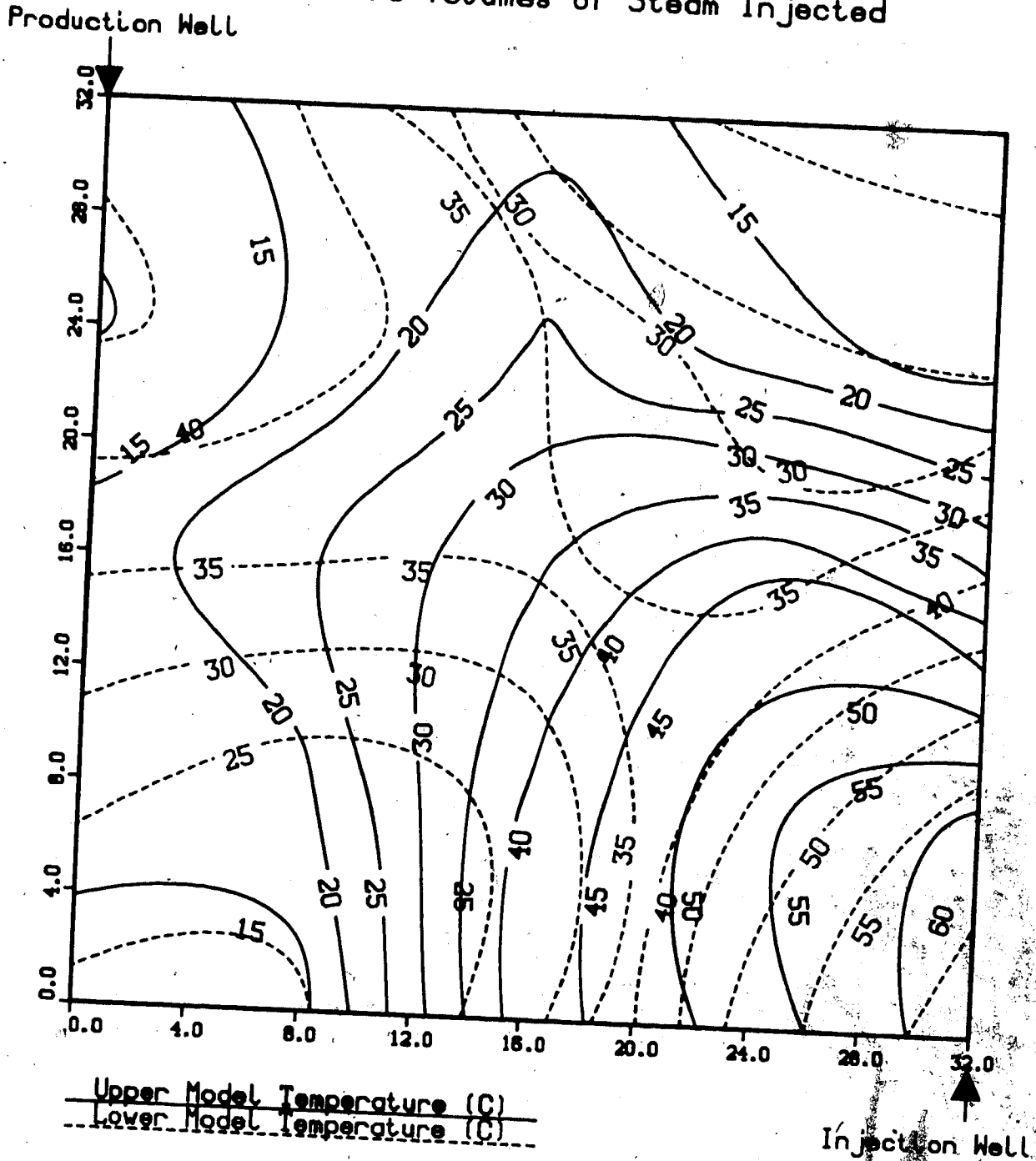
FIGURE 36: TEMPERATURE PROFILE FOR
RUN 6: CONTINUOUS STEAMFLOOD ON ABERFELDY MODEL
1.00 Pore Volumes of Steam Injected
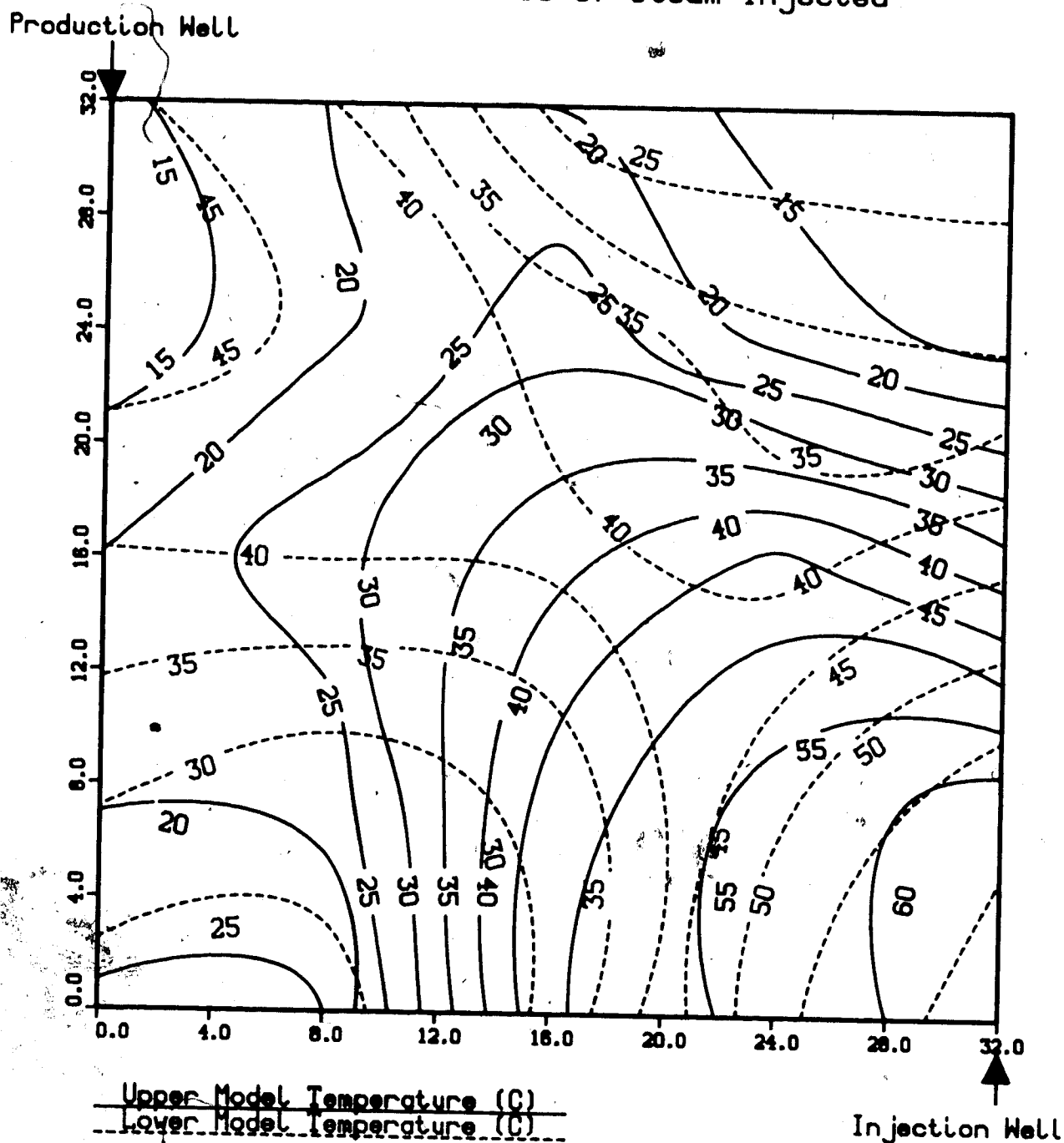
FIGURE 37: TEMPERATURE PROFILE FOR
RUN 7C: STEAMFLOOD IN ABERFELDY MODEL AFTER W.F.
0.25 Pore Volumes of Steam Injected
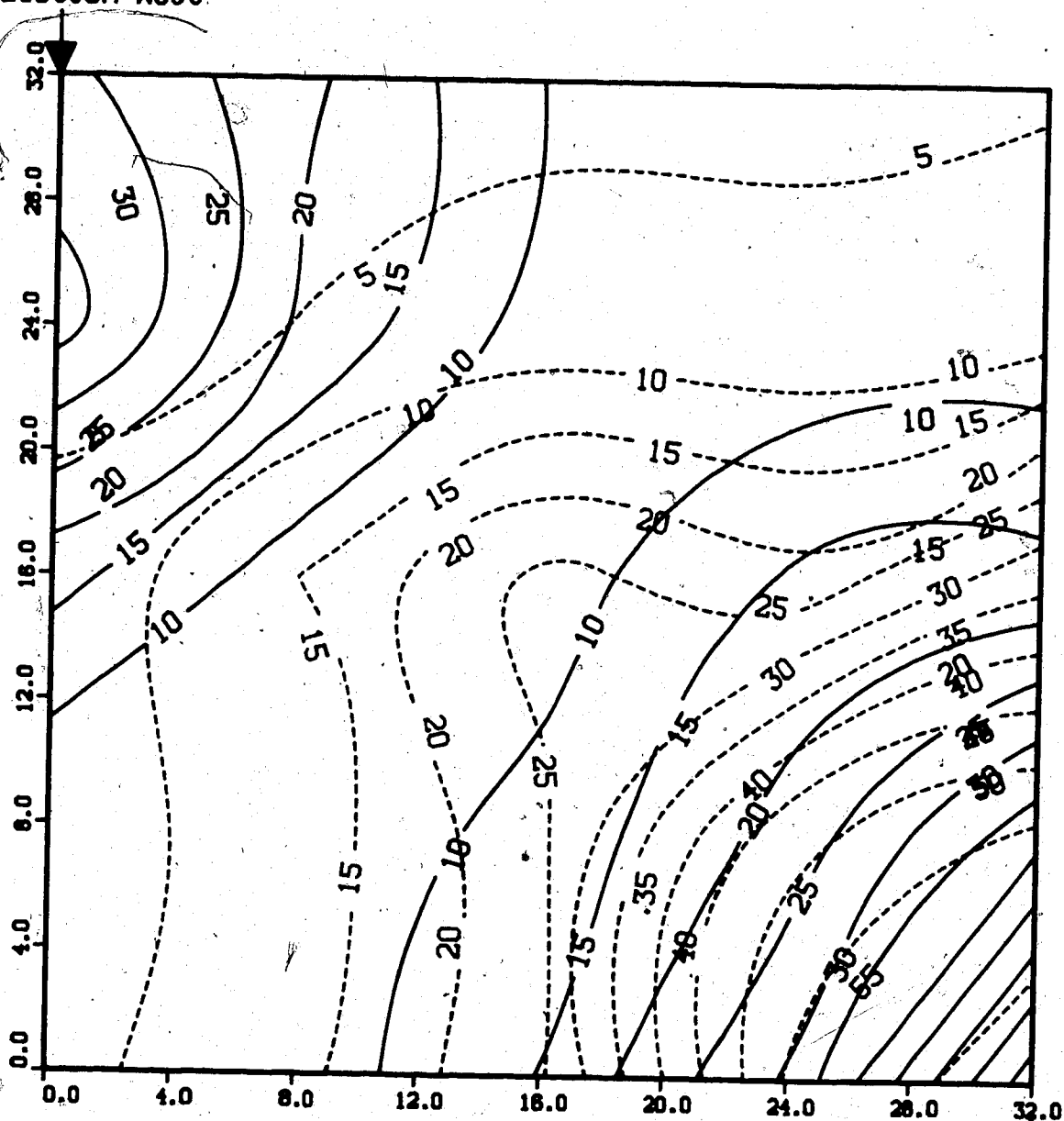
Production Well

Injection Well

Upper Model Temperature (C)
Lower Model Temperature (C)

FIGURE 38: TEMPERATURE PROFILE FOR
RUN 7C: STEAMFLOOD IN ABERFELDY MODEL AFTER W.F.

0.50 Pore Volumes of Steam Injected
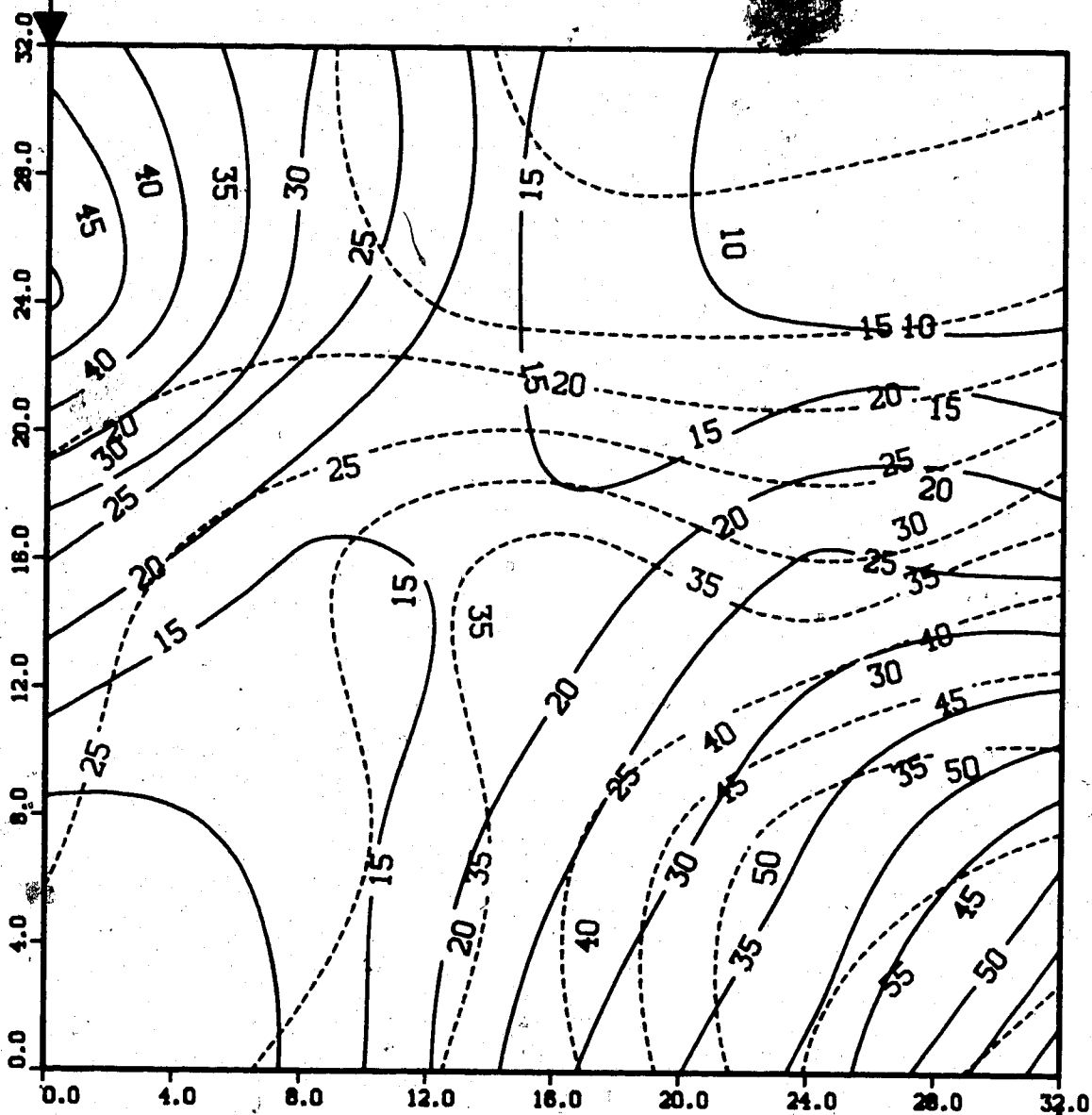
Production Well

Injection Well

Upper Model Temperature (C)
Lower Model Temperature (C)

FIGURE 39: TEMPERATURE PROFILE FOR
RUN 7C: STEAMFLOOD IN ABERFELDY MODEL AFTER W.F.
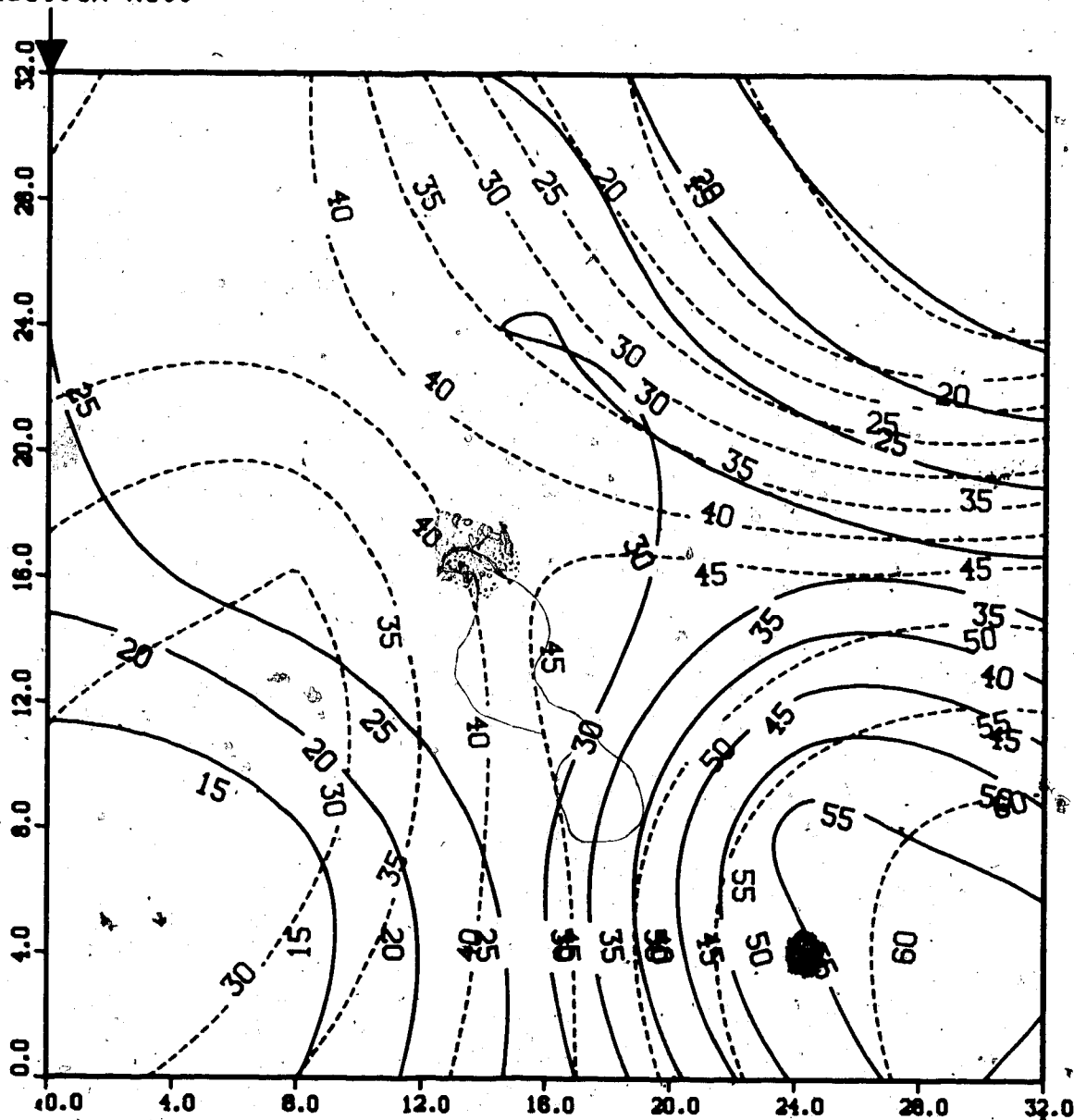### 0.75 Pore Volumes of Steam Injected
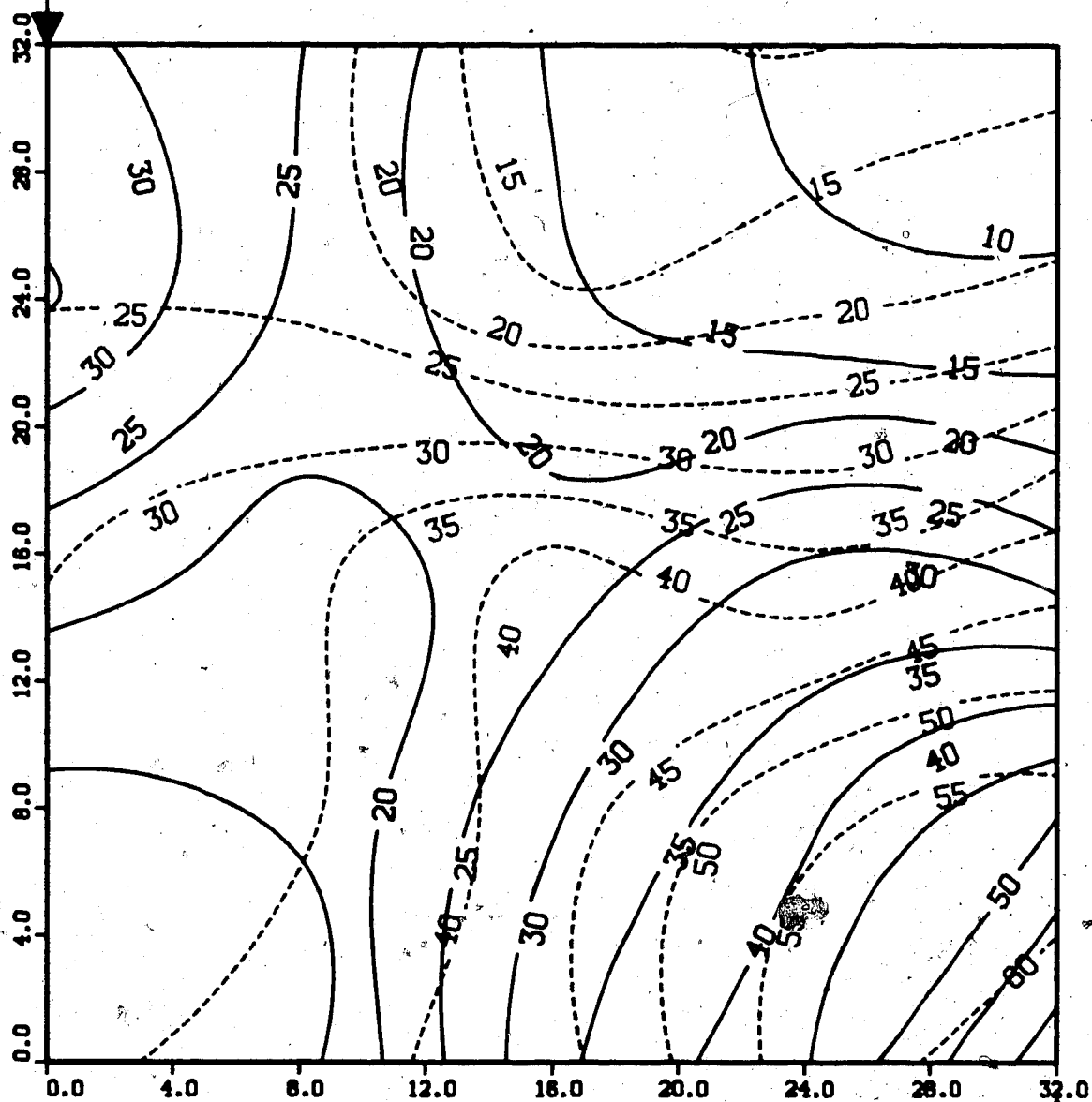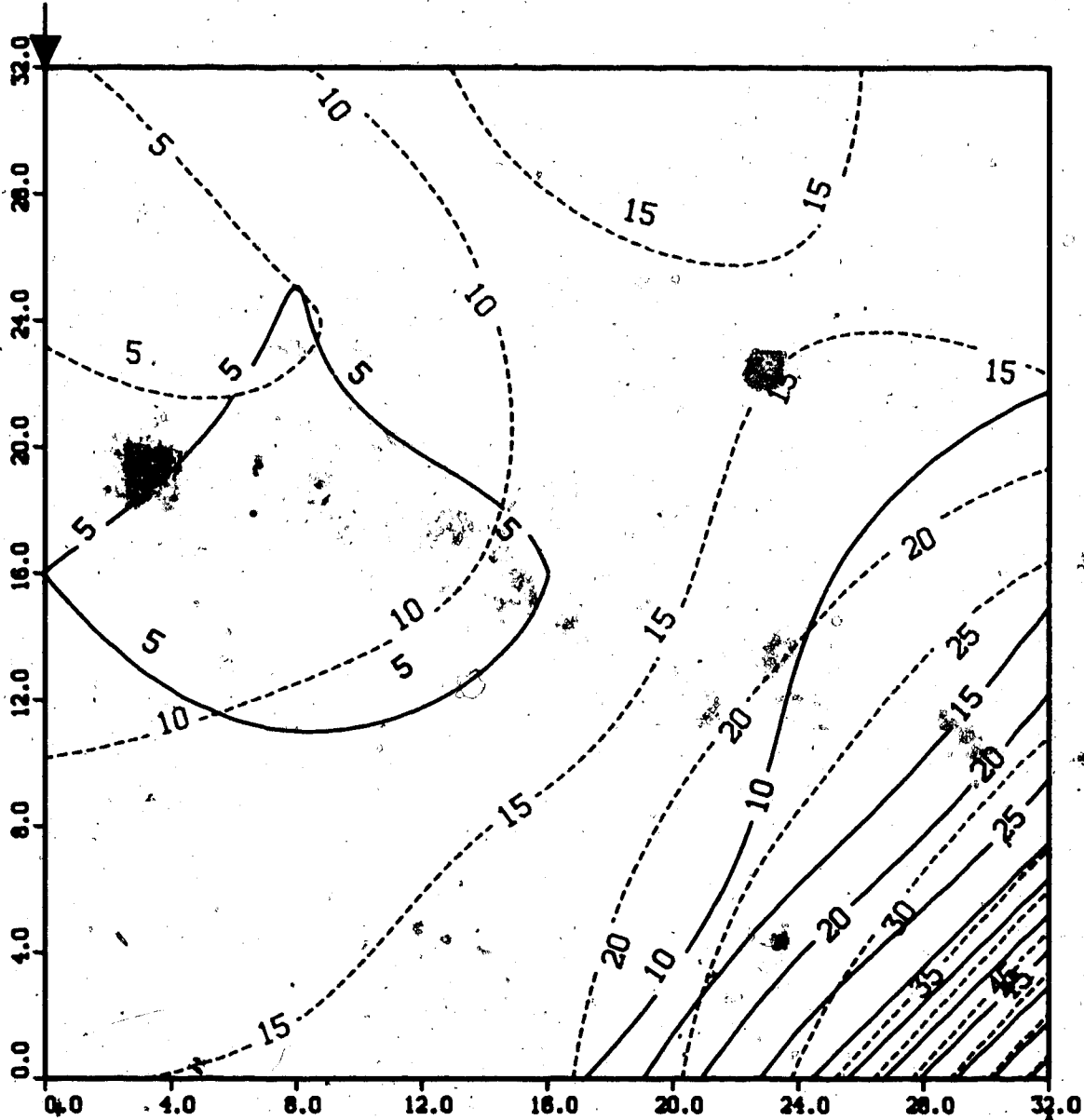
oduction Well

Upper Model Temperature (C)
Lower Model Temperature (C)

Injection Well

FIGURE 40: TEMPERATURE PROFILE FOR
RUN 7C: STEAMFLOOD IN ABERFELDY MODEL AFTER W.F.
1.00 Pore Volumes of Steam Injected
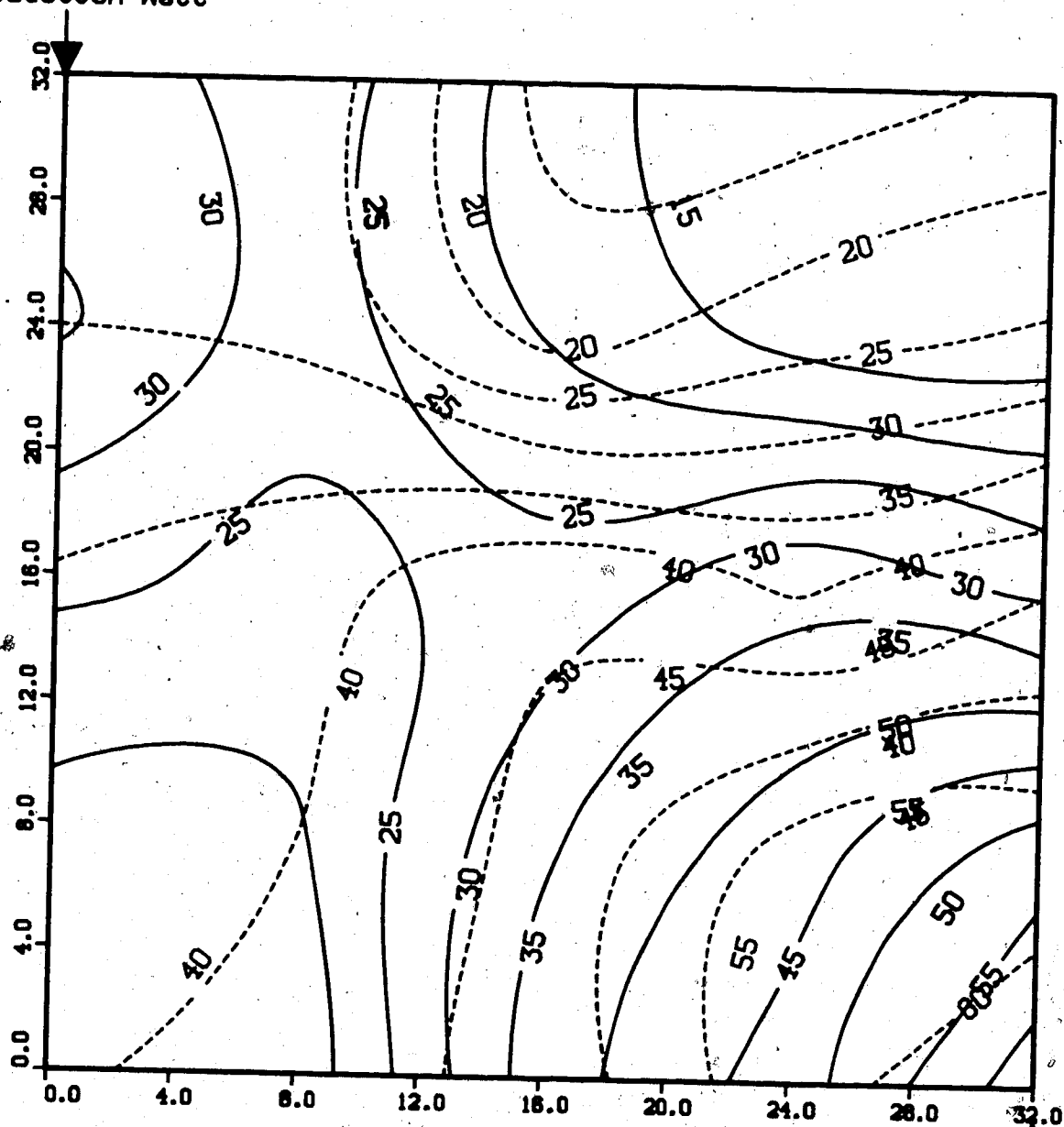
FIGURE 41: TEMPERATURE PROFILE FOR
RUN 9: STEAMFLOOD IN HEAVY OIL MODEL
0.50 Pore Volumes of Steam Injected
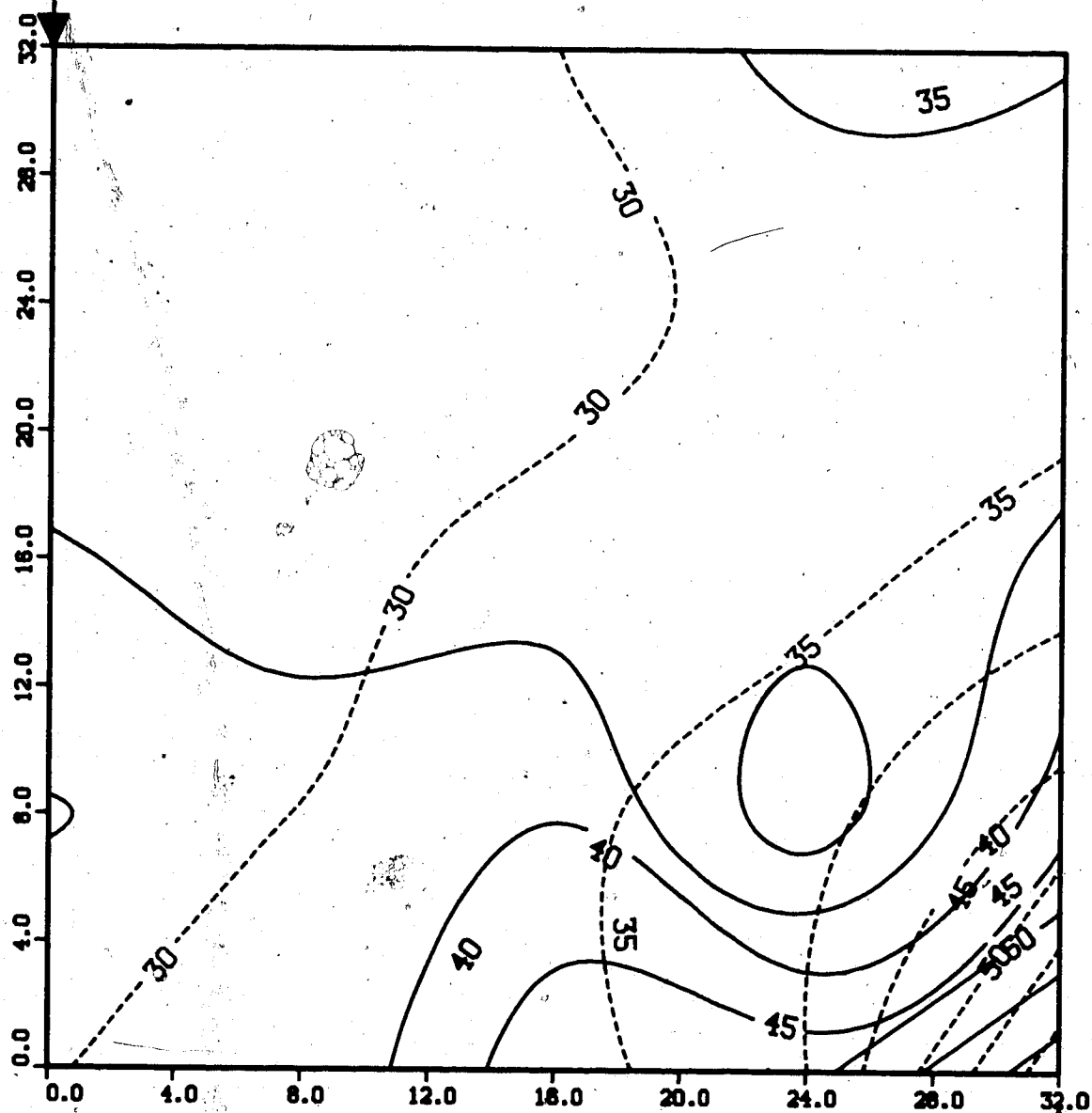
Production Well

Injection Well

Upper Model Temperature (C)
Lower Model Temperature (C)

FIGURE 42: TEMPERATURE PROFILE FOR
RUN 9: STEAMFLOOD IN HEAVY OIL MODEL
1.00 Pore Volumes of Steam Injected

152
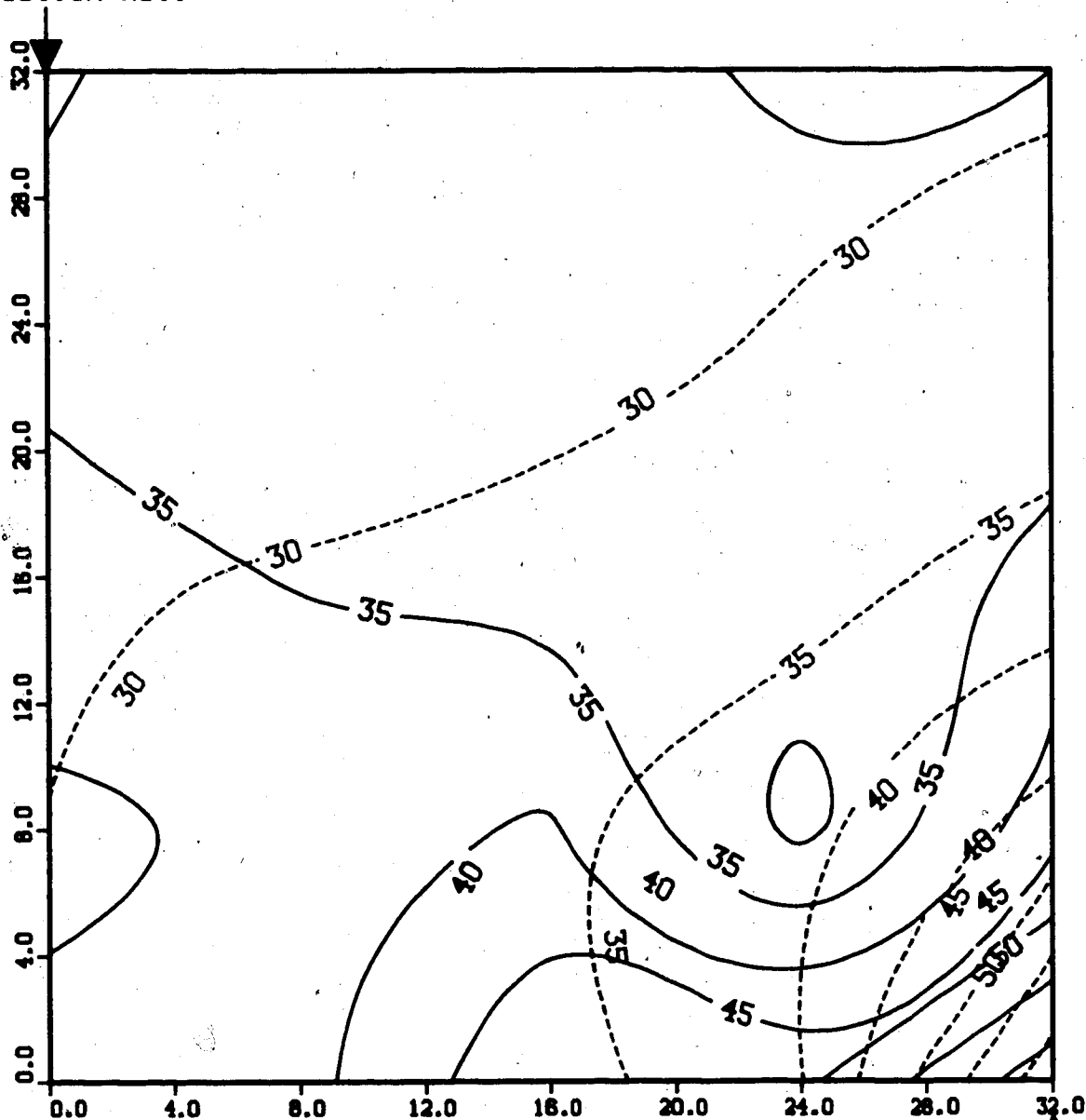
FIGURE 43: TEMPERATURE PROFILE FOR
RUN 10: CONTINUOUS STEAMFLOOD IN ABERFELDY MODEL
0.25 Pore Volumes of Steam Injected
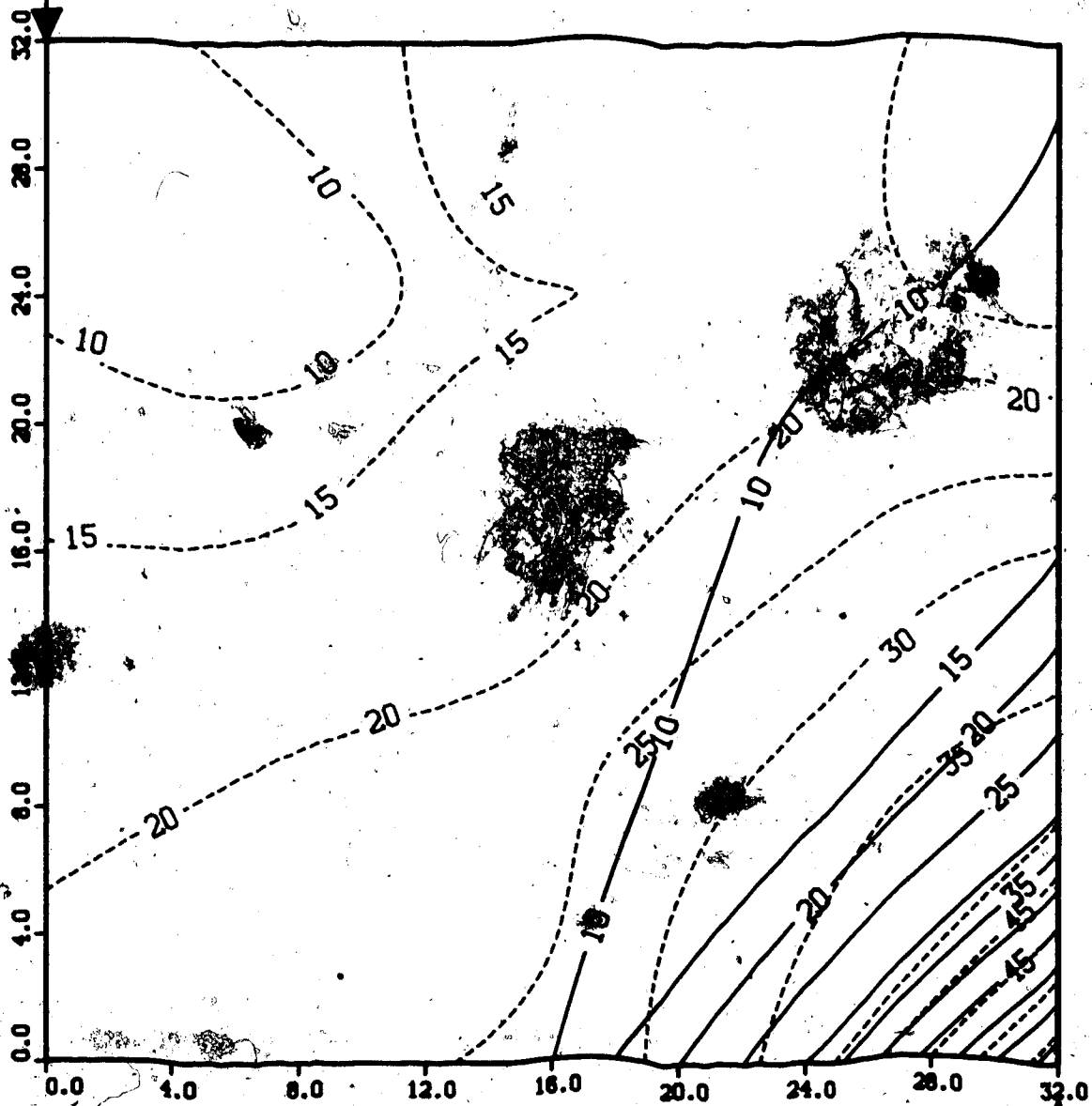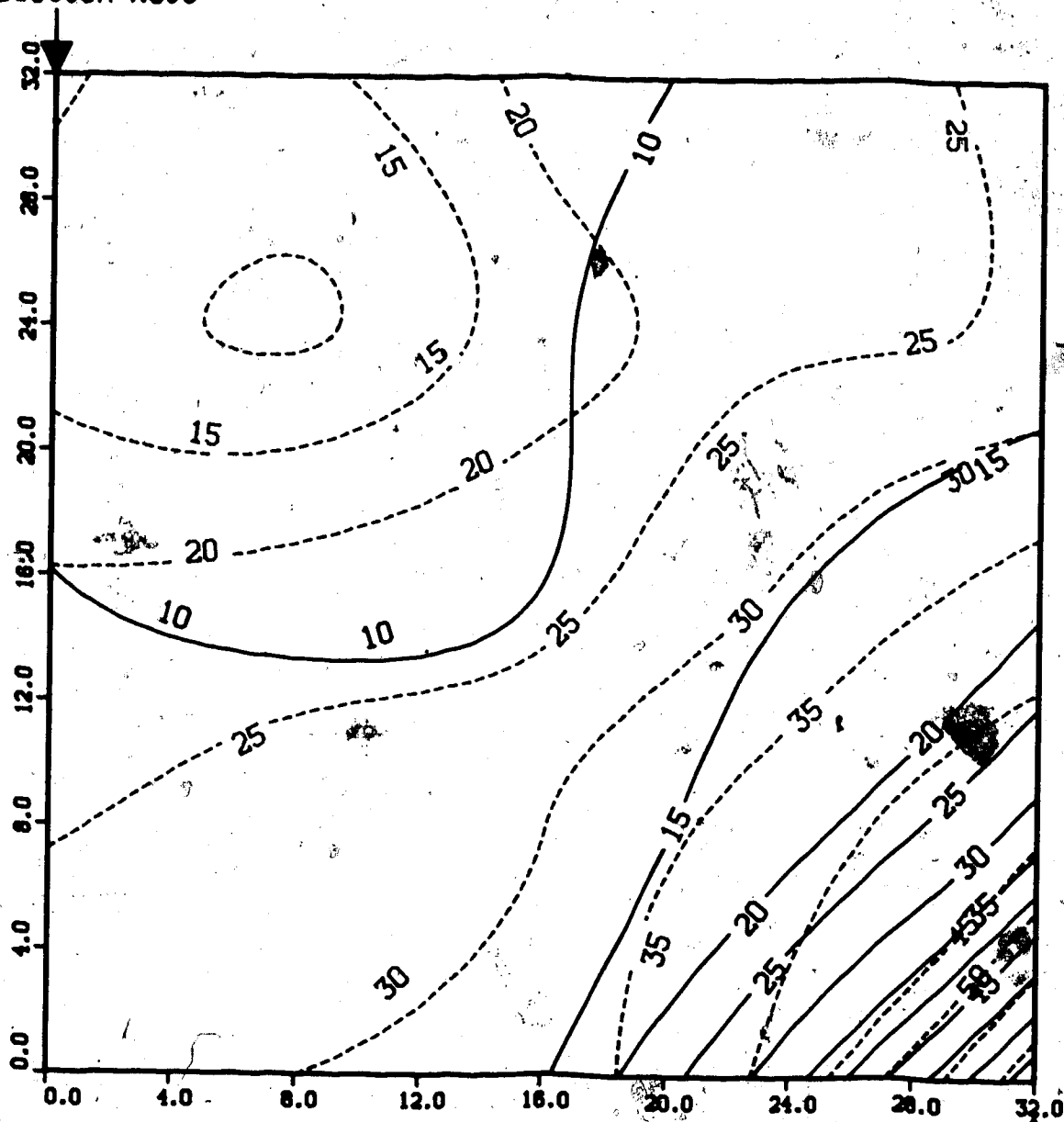
Production Well
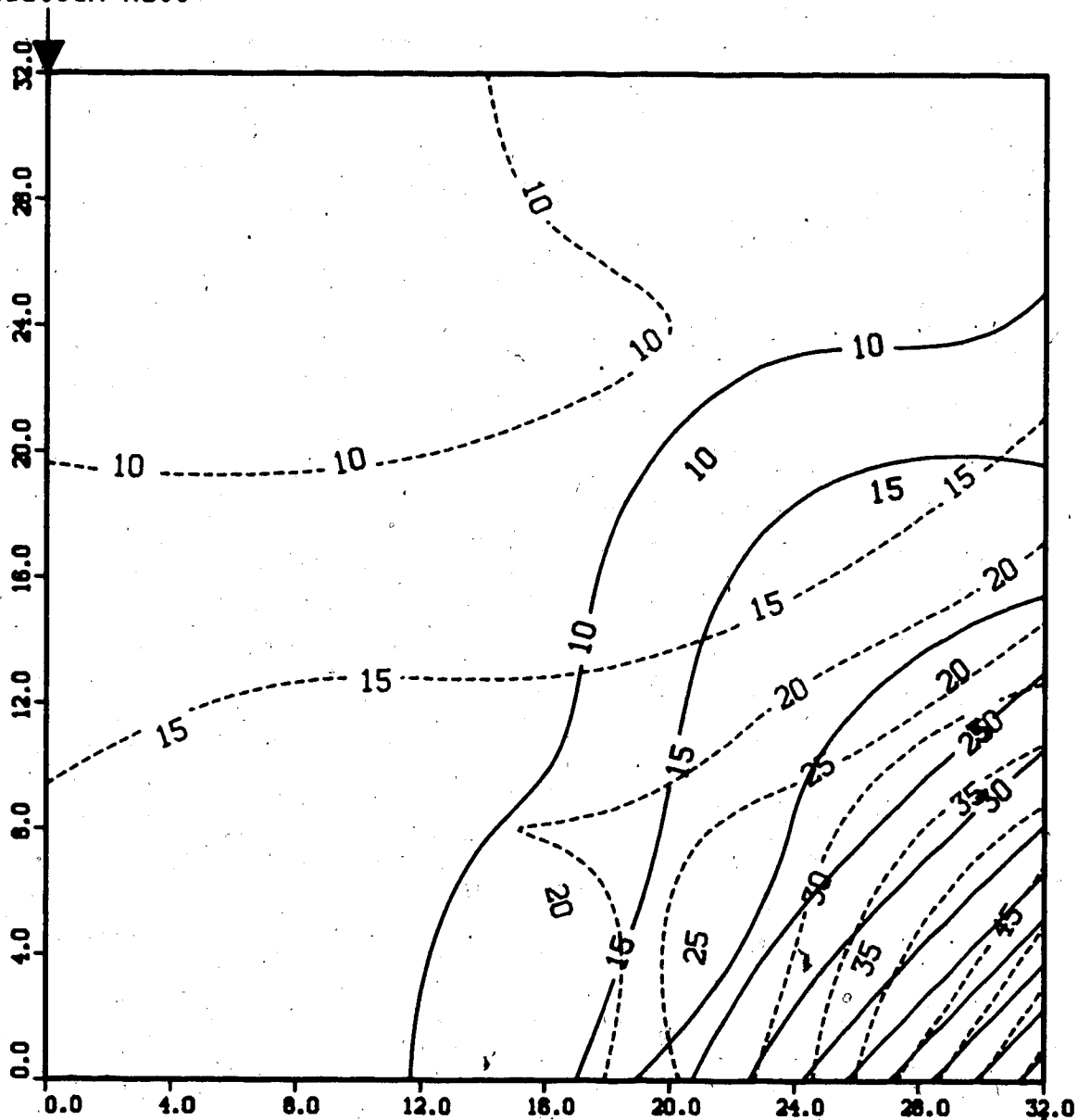
Upper Model Temperature (C)
Lower Model Temperature (C)

Injection Well

FIGURE 44: TEMPERATURE PROFILE FOR
RUN 10: CONTINUOUS STEAMFLOOD IN ABERFELDY MODEL
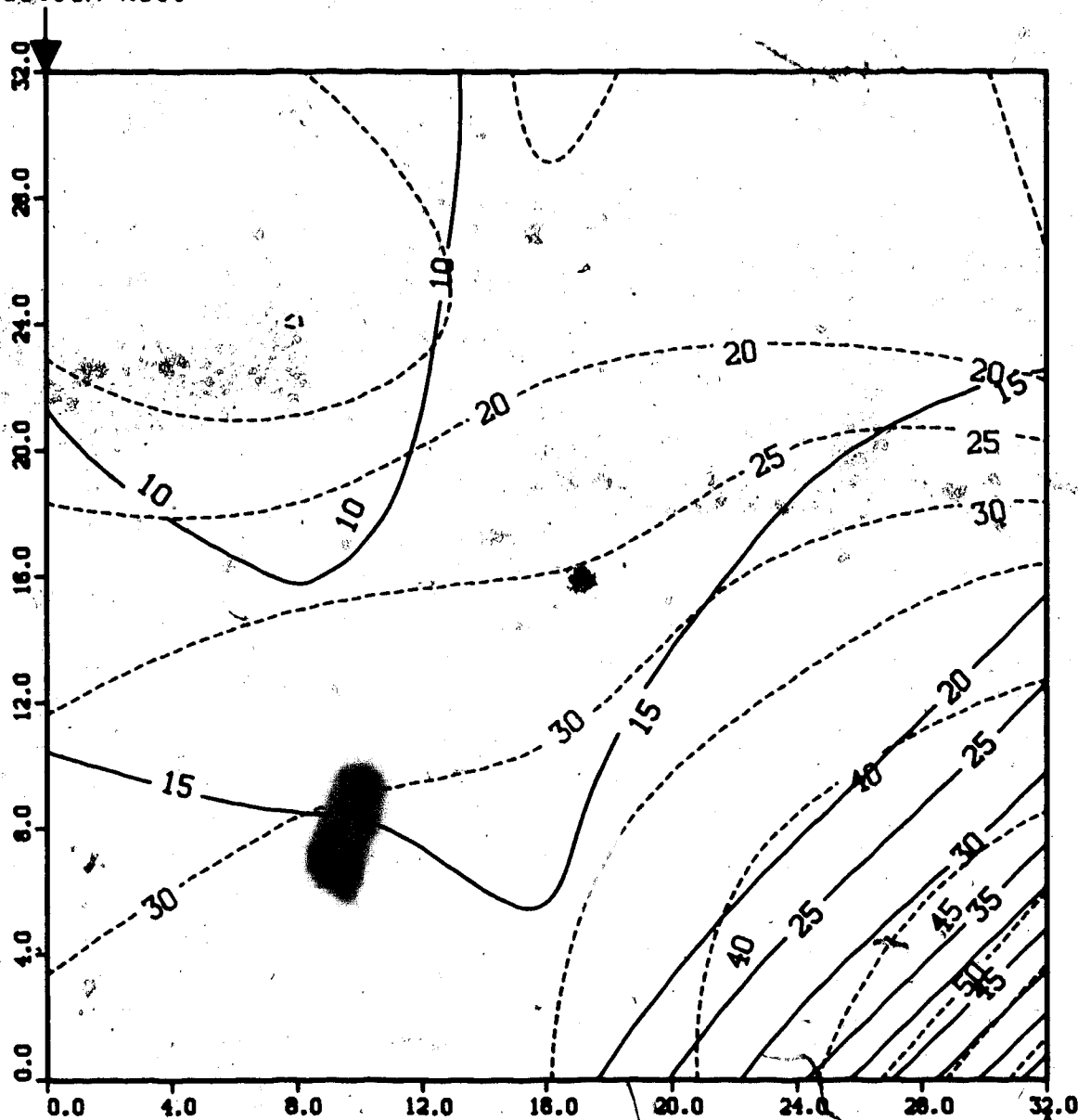### 0.50 Pore Volumes of Steam Injected

Production Well

Upper Model Temperature (C)
Lower Model Temperature (C)
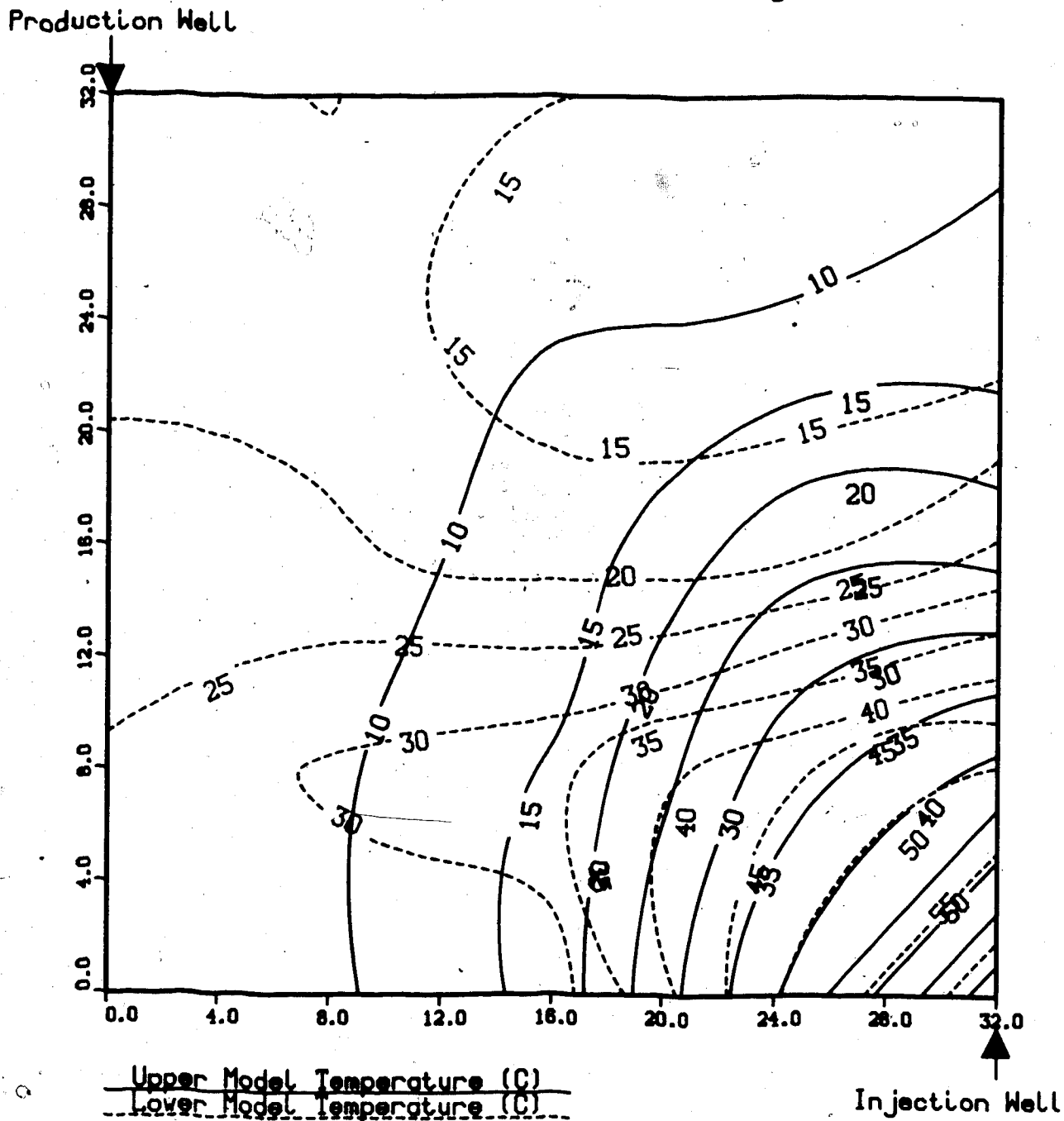
Injection Well

FIGURE 45: TEMPERATURE PROFILE FOR
RUN 10: CONTINUOUS STEAMFLOOD IN ABERFELDY MODEL
0.75 Pore Volumes of Steam Injected
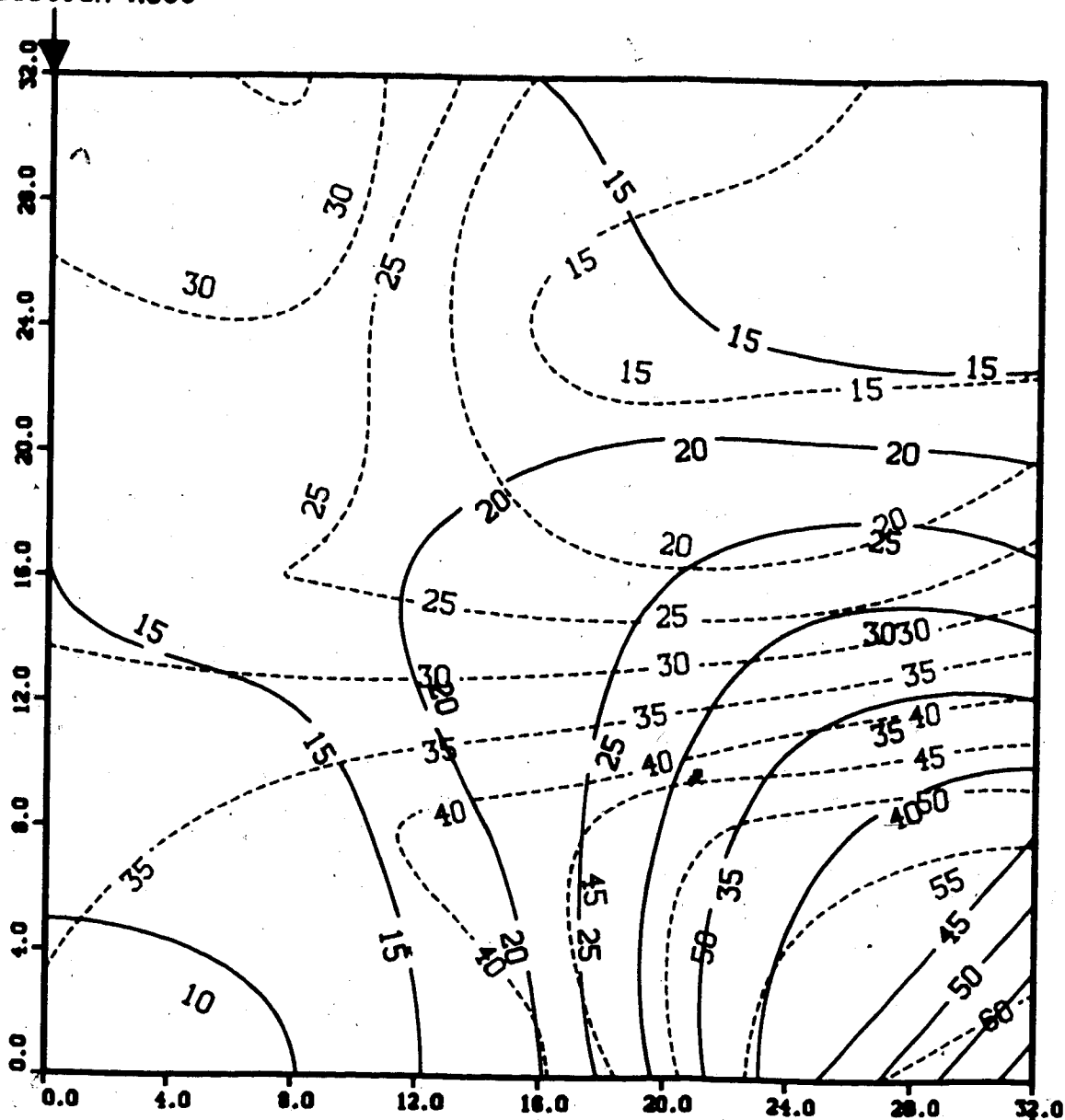
Upper Model Temperature (C)
Lower Model Temperature (C)

FIGURE 46: TEMPERATURE PROFILE FOR
RUN 10: CONTINUOUS STEAMFLOOD IN ABERFELDY MODEL
1.00 Pore Volumes of Steam Injected
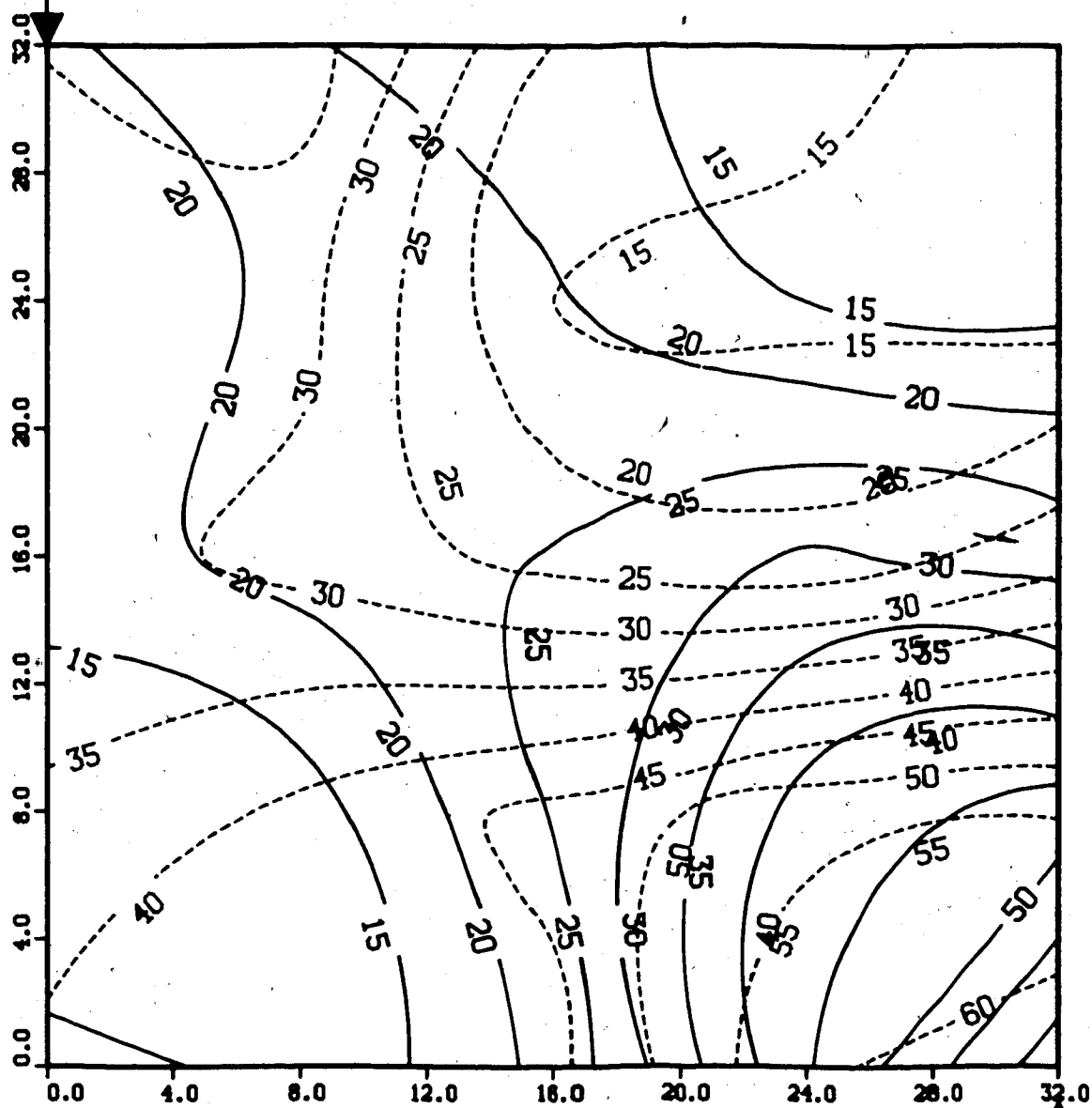
Upper Model Temperature (C)
Lower Model Temperature (C)

Production Well

Injection Well

FIGURE 47: TEMPERATURE PROFILE FOR
RUN 12: CONTINUOUS STEAMFLOOD IN LIGHT OIL MODEL
0.25 Pore Volumes of Steam Injected
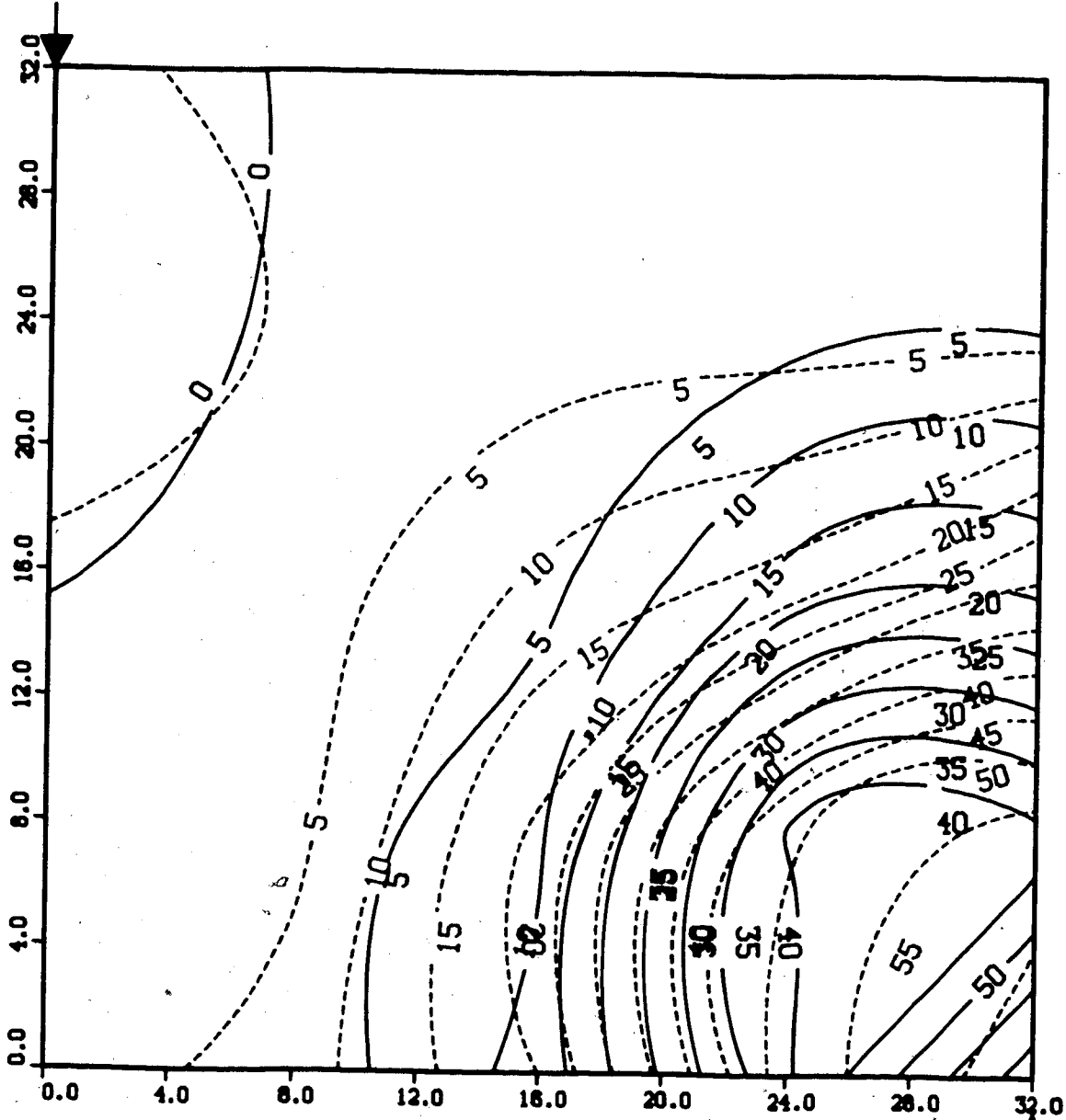
Production Well

Upper Model Temperature (C)
Lower Model Temperature (C)

Injection Well

FIGURE 48: TEMPERATURE PROFILE FOR
RUN 12: CONTINUOUS STEAMFLOOD IN LIGHT OIL MODEL
0.50 Pore Volumes of Steam Injected
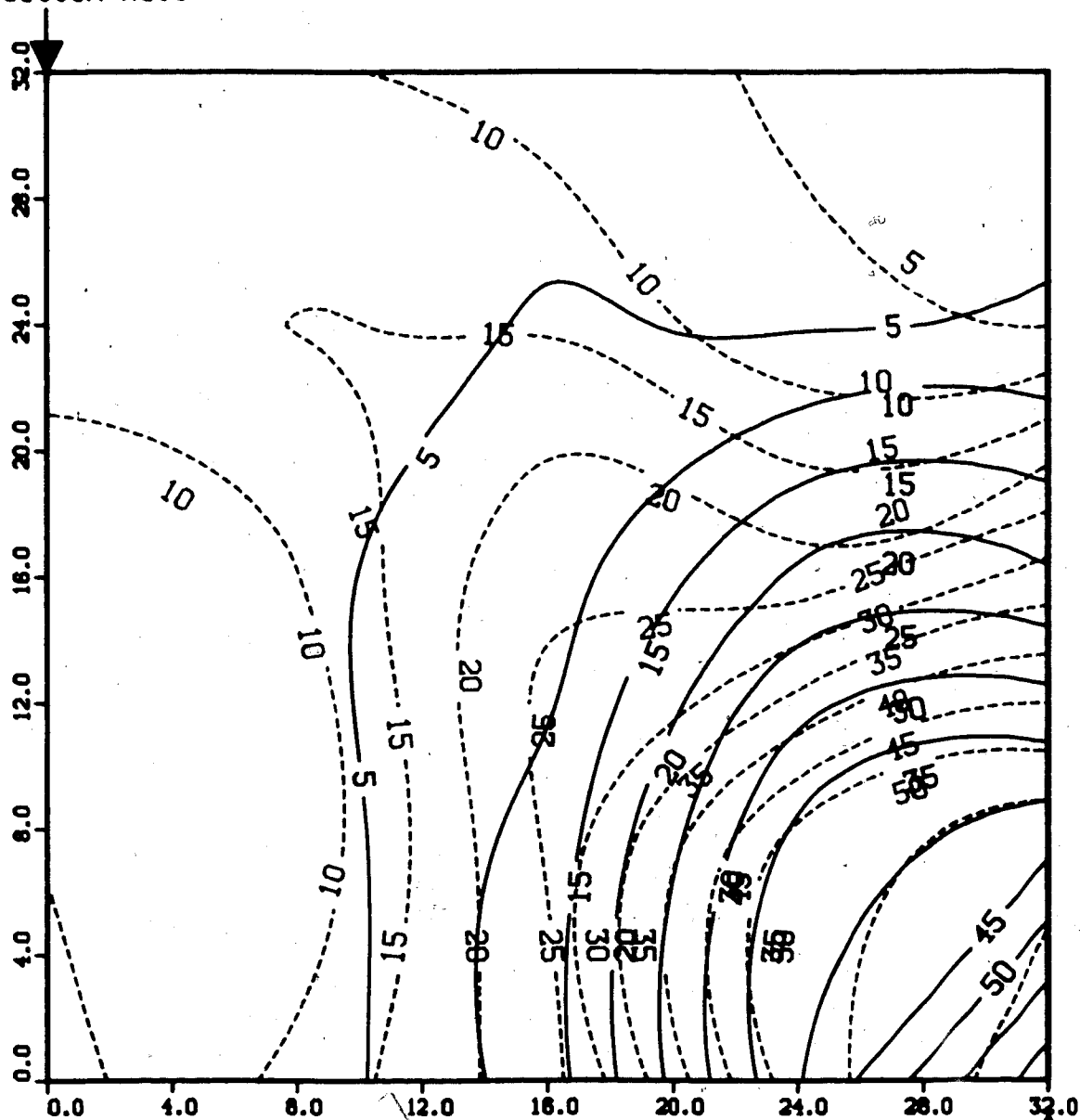
FIGURE 49: TEMPERATURE PROFILE FOR
RUN 12: CONTINUOUS STEAMFLOOD IN LIGHT OIL MODEL
0.75 Pore Volumes of Steam Injected
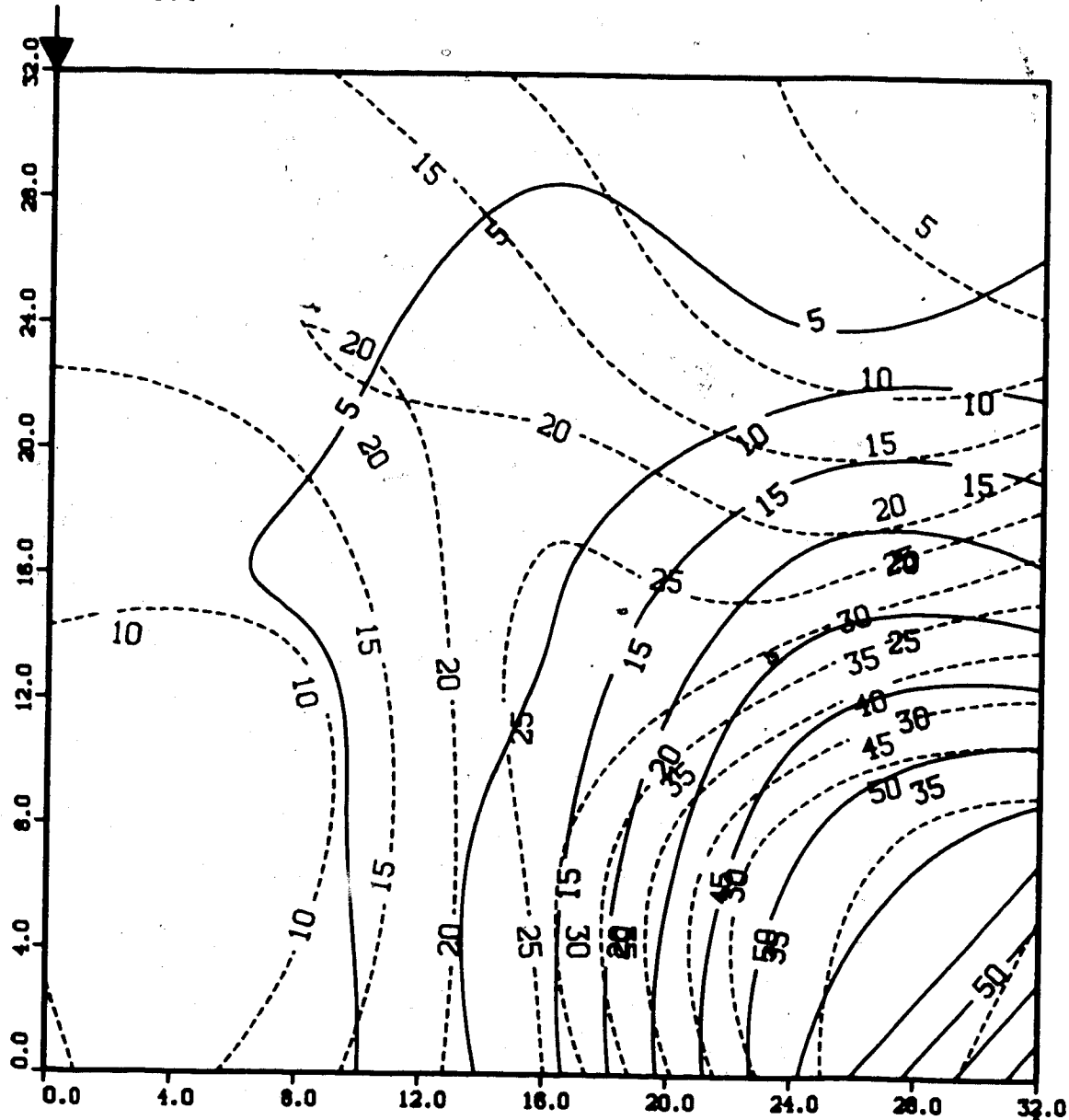
Production Well

Injection Well

Upper Model Temperature (C)
Lower Model Temperature (C)

FIGURE 50: TEMPERATURE PROFILE FOR
RUN 12: CONTINUOUS STEAMFLOOD IN LIGHT OIL MODEL
1.00 Pore Volumes of Steam Injected

Production Well

Injection Well

Upper Model Temperature (C)
Lower Model Temperature (C)

FIGURE 51: TEMPERATURE PROFILE FOR
RUN 13: CONTINUOUS STEAMFLOOD IN LIGHT OIL MODEL
0.25 Pore Volumes of Steam Injected

Production Well

Injection Well

Upper Model Temperature (C)
Lower Model Temperature (C)

FIGURE 52: TEMPERATURE PROFILE FOR
RUN 13: CONTINUOUS STEAMFLOOD IN LIGHT OIL MODEL
0.50 Pore Volumes of Steam Injected

FIGURE 53: TEMPERATURE PROFILE FOR
RUN 13: CONTINUOUS STEAMFLOOD IN LIGHT OIL MODEL
0.75 Pore Volumes of Steam Injected

Production Well

Upper Model Temperature (C)
Lower Model Temperature (C)

Injection Well

FIGURE 54: TEMPERATURE PROFILE FOR
RUN 13: CONTINUOUS STEAMFLOOD IN LIGHT OIL MODEL
1.00 Pore Volumes of Steam Injected

Production Well

Injection Well

Upper Model Temperature (C)
Lower Model Temperature (C)

164

FIGURE 55: TEMPERATURE PROFILE FOR
RUN 15: STEAMFLOOD IN BOTTOM WATER MODEL
0.25 Pore Volumes of Steam Injected

Production Well

Injection Well

Upper Model Temperature (C)
Lower Model Temperature (C)

FIGURE 56: TEMPERATURE PROFILE FOR
RUN 15: STEAMFLOOD IN BOTTOM WATER MODEL
0.50 Pore Volumes of Steam Injected

Production Well

Injection Well

Upper Model Temperature (C)
Lower Model Temperature (C)

FIGURE 57: TEMPERATURE PROFILE FOR
RUN 15: STEAMFLOOD IN BOTTOM WATER MODEL
0.75 Pore Volumes of Steam Injected

Production Well

Injection Well

Upper Model Temperature (C)
Lower Model Temperature (C)

FIGURE 58: TEMPERATURE PROFILE FOR
RUN 15: STEAMFLOOD IN BOTTOM WATER MODEL
1.00 Pore Volumes of Steam Injected

Production Well

Injection Well

Upper Model Temperature (C)
Lower Model Temperature (C)

FIGURE 59: TEMPERATURE PROFILE FOR
RUN 17: STEAM SLUG RUN IN ABERFELDY MODEL
0.25 Pore Volumes of Steam Injected
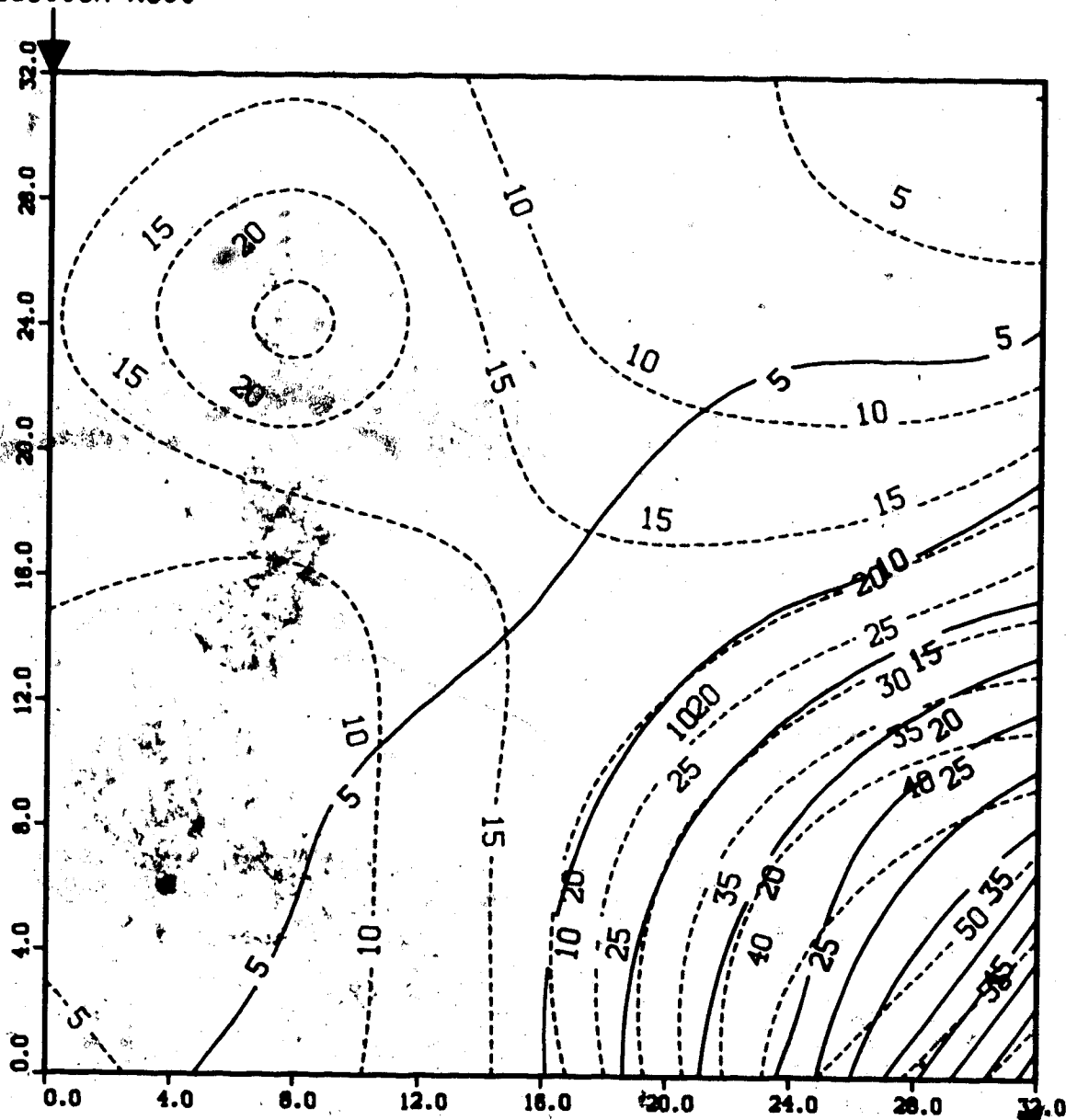
Production Well

Injection Well

Upper Model Temperature (C)
Lower Model Temperature (C)

FIGURE 60: TEMPERATURE PROFILE FOR
RUN 17: STEAM SLUG RUN IN ABERFELDY MODEL
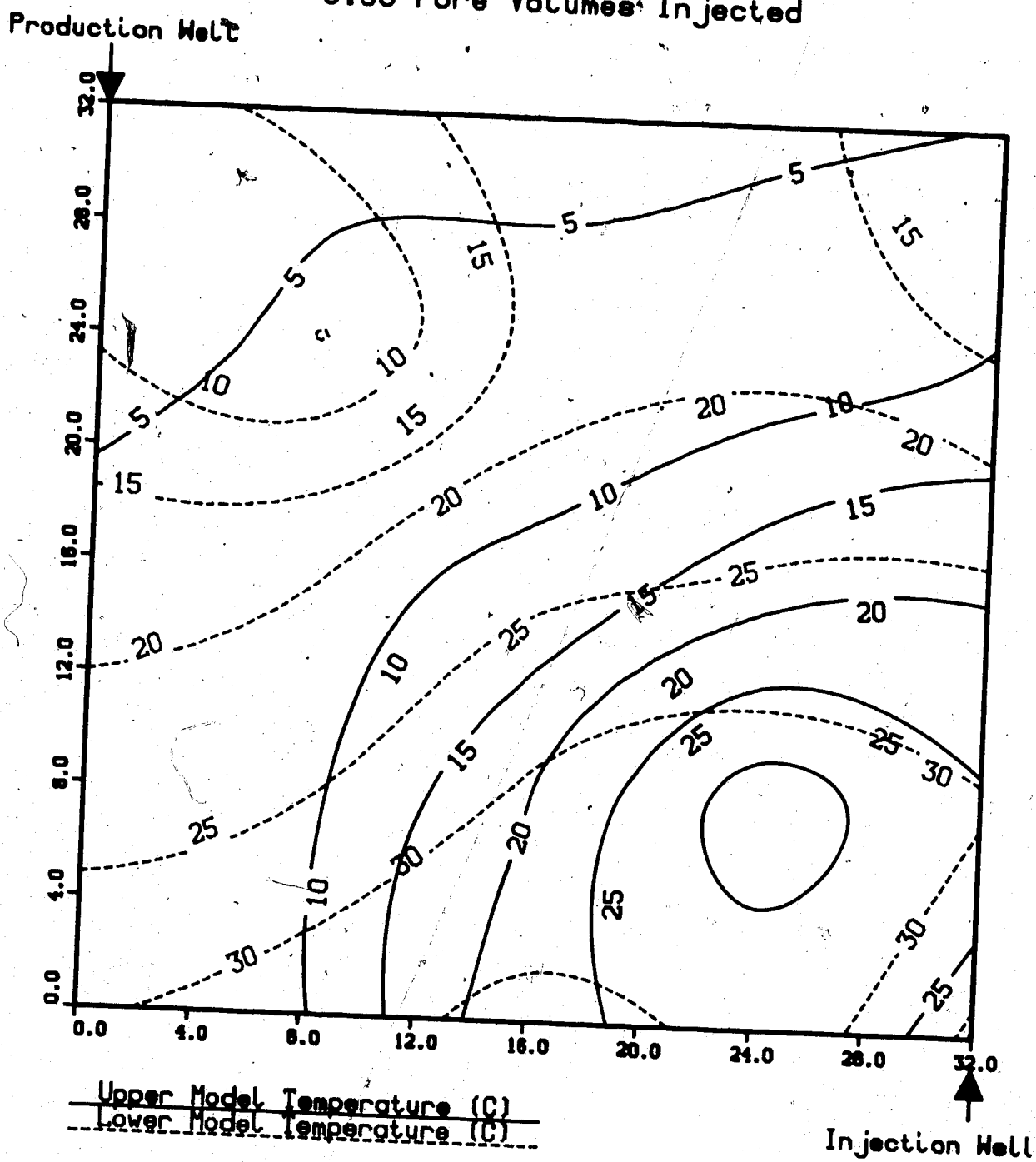### Start of Cold Water Injection (0.31 PV Inj.)

Production Well
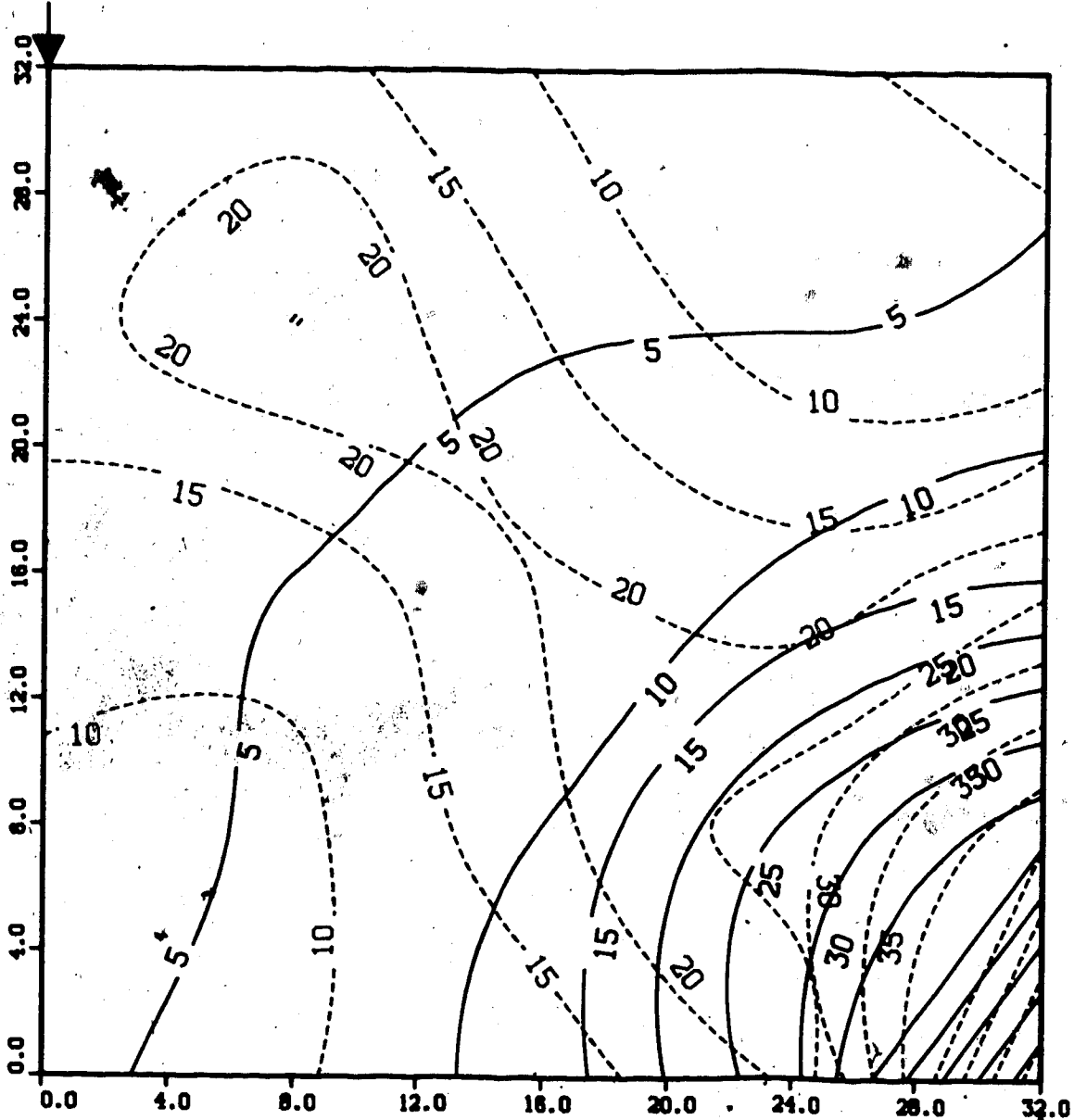
Injection Well
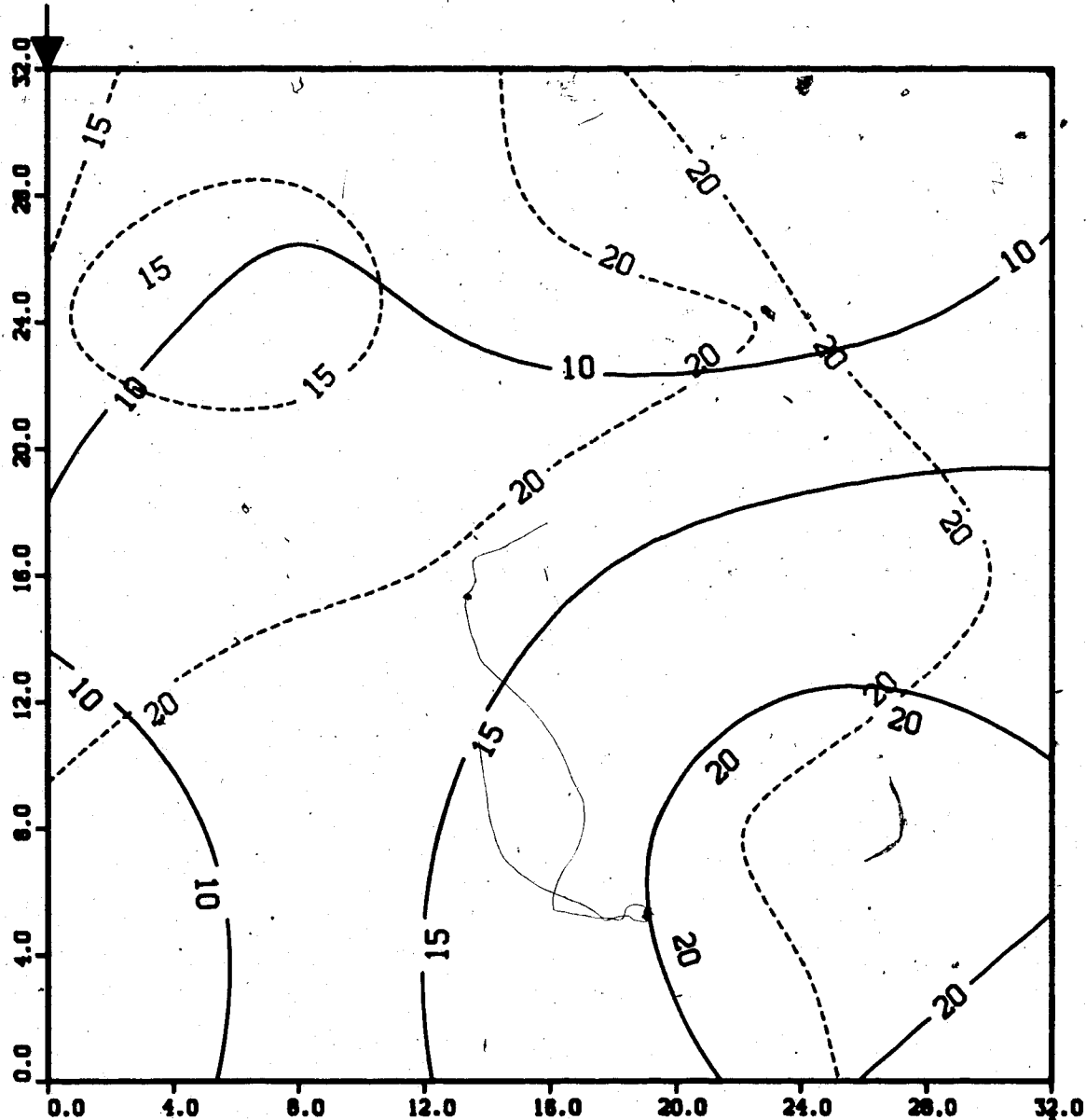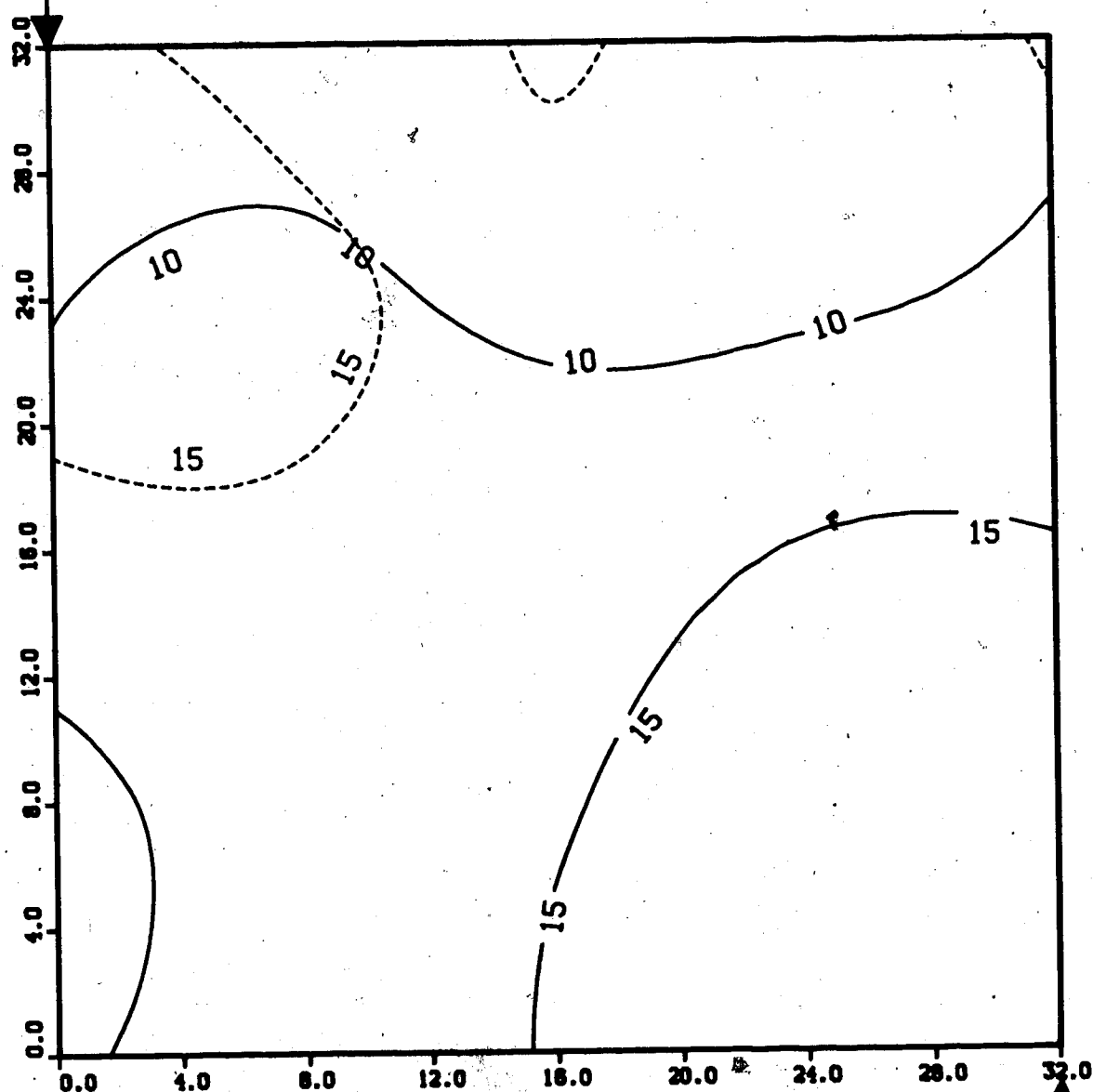
Upper Model Temperature (C)
Lower Model Temperature (C)

FIGURE 61: TEMPERATURE PROFILE FOR
RUN 17: STEAM SLUG RUN IN ABERFELDY MODEL
0.50 Pore Volumes Injected
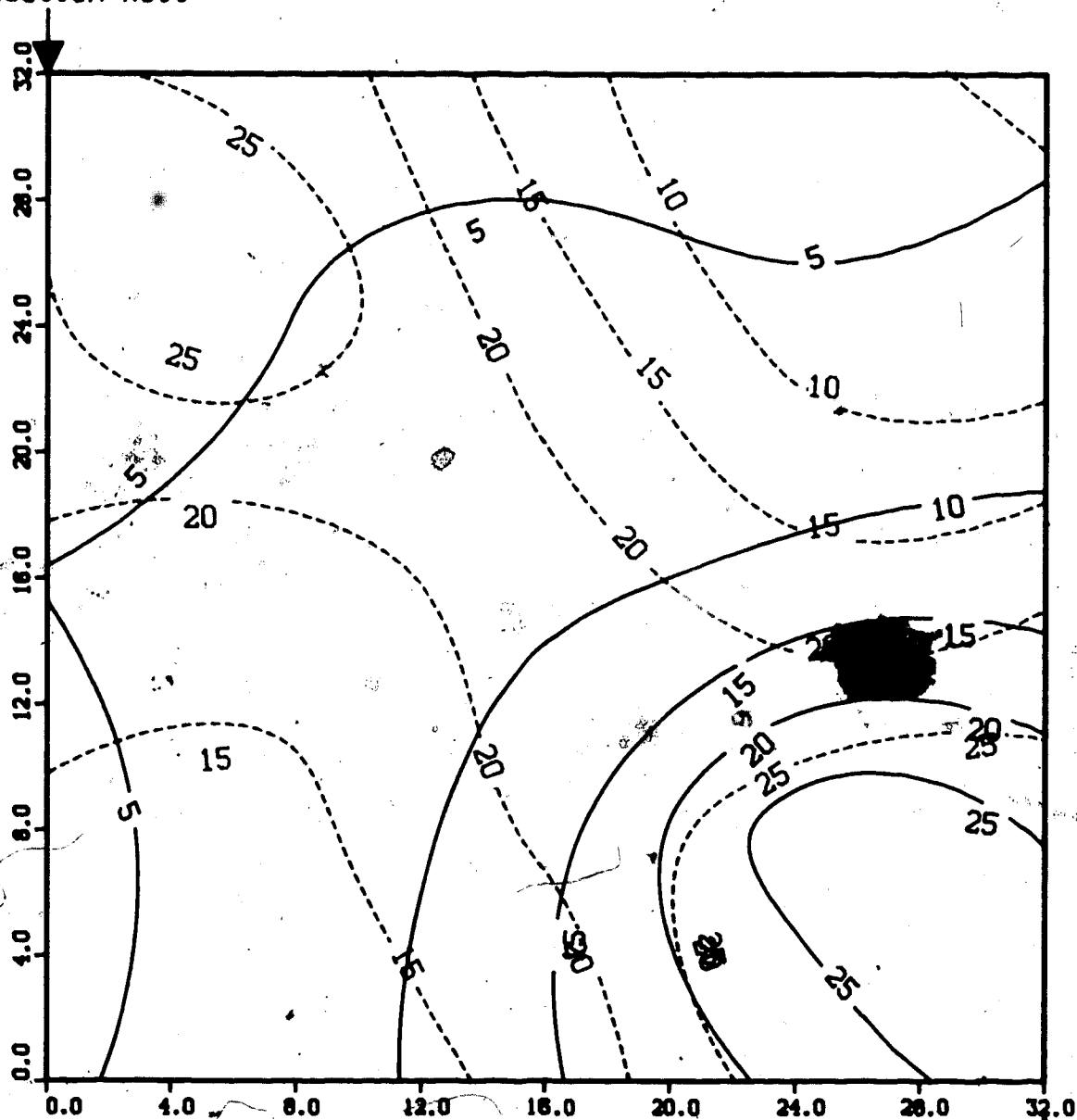
Production Well

Injection Well

Upper Model Temperature (C)
Lower Model Temperature (C)

FIGURE 62: TEMPERATURE PROFILE FOR
RUN 17: STEAM SLUG RUN IN ABERFELDY MODEL
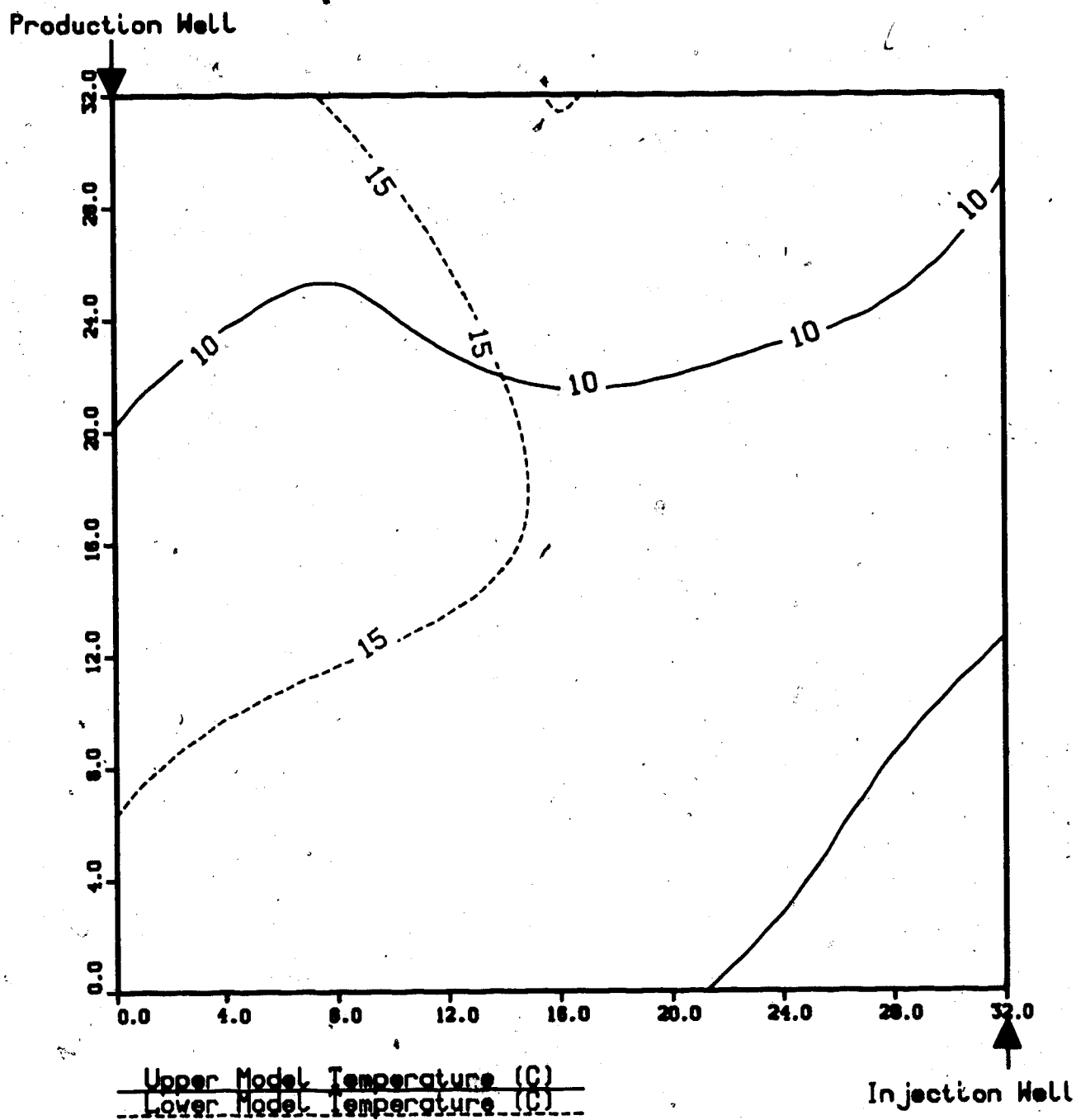### 0.75 Pore Volumes Injected

Production Well
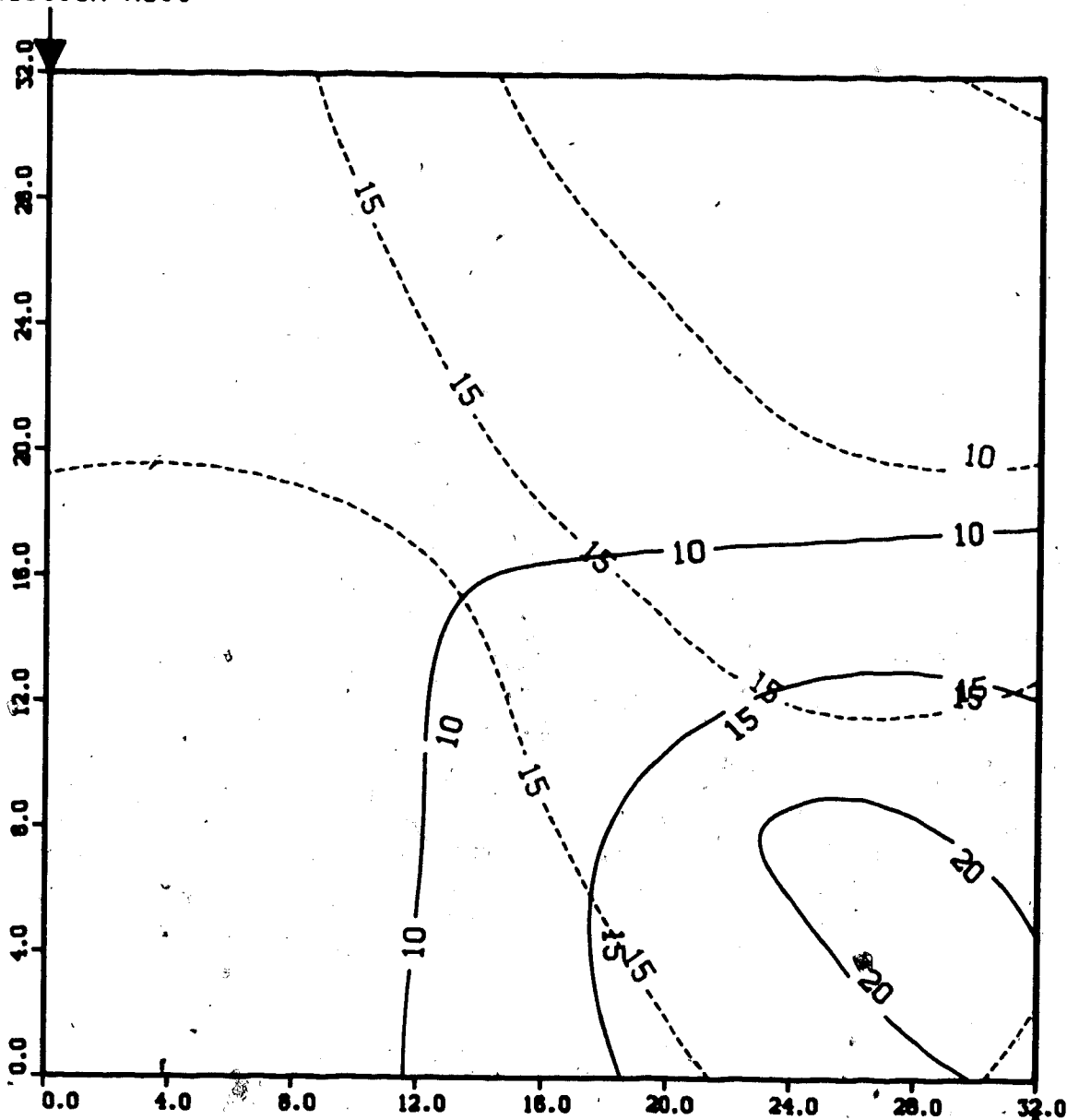
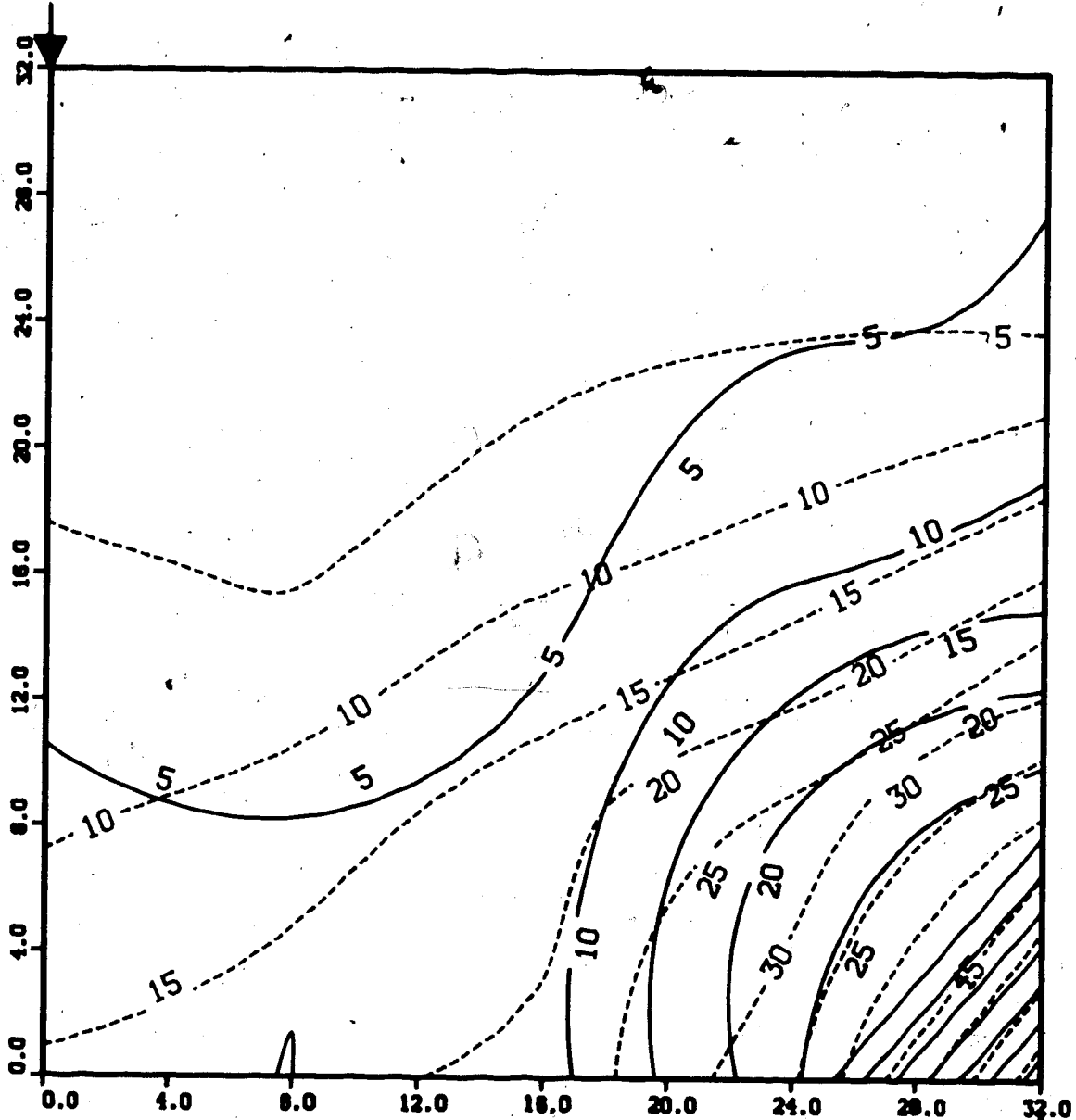Injection Well

Upper Model Temperature (C)
Lower Model Temperature (C)

FIGURE 63: TEMPERATURE PROFILE FOR
RUN 17: STEAM SLUG RUN IN ABERFELDY MODEL
1.00 Pore Volumes Injected

173
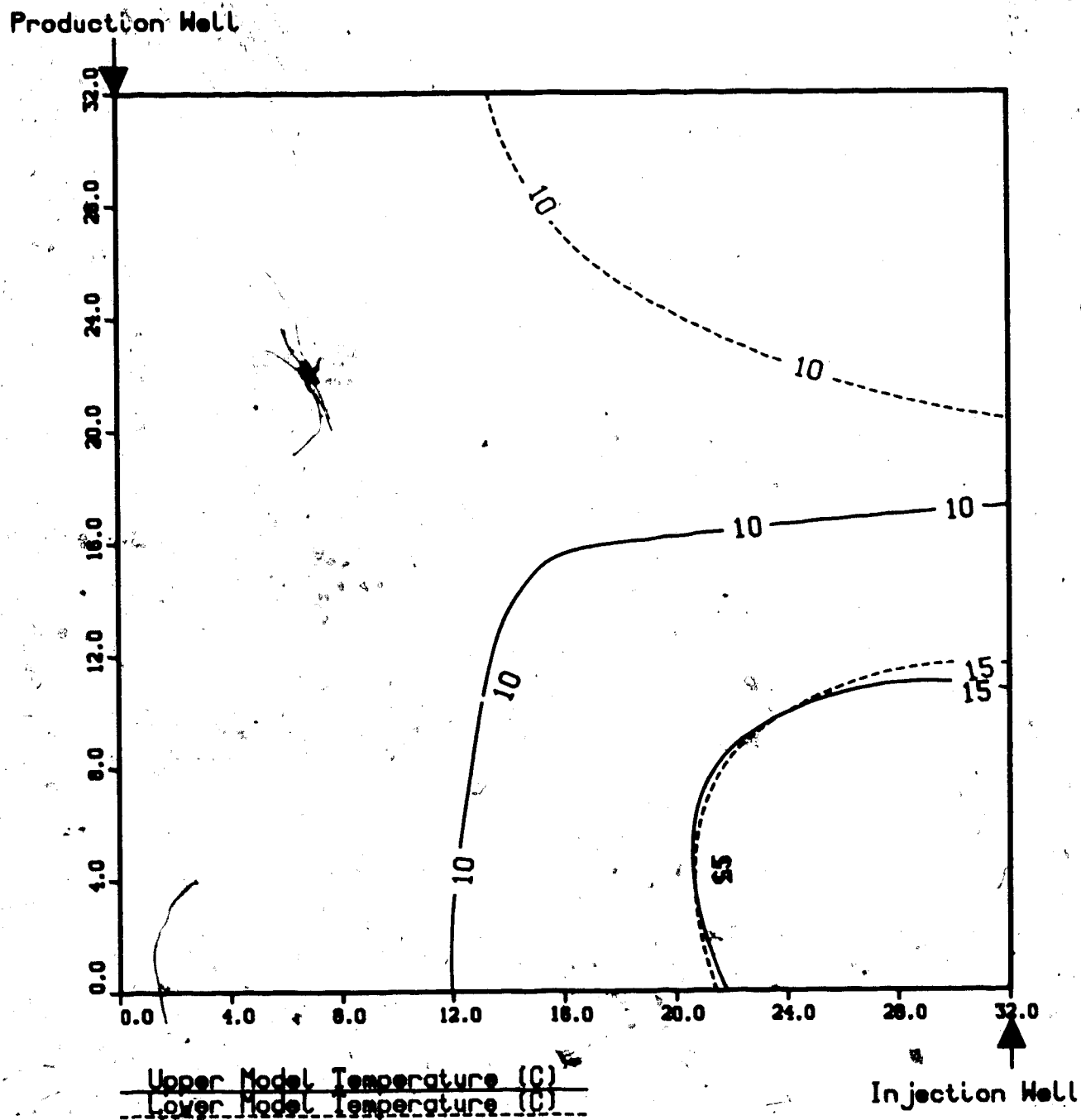
FIGURE 64: TEMPERATURE PROFILE FOR
RUN 18: STEAM SLUG RUN IN ABERFELDY MODEL
0.25 Pore Volumes of Steam Injected
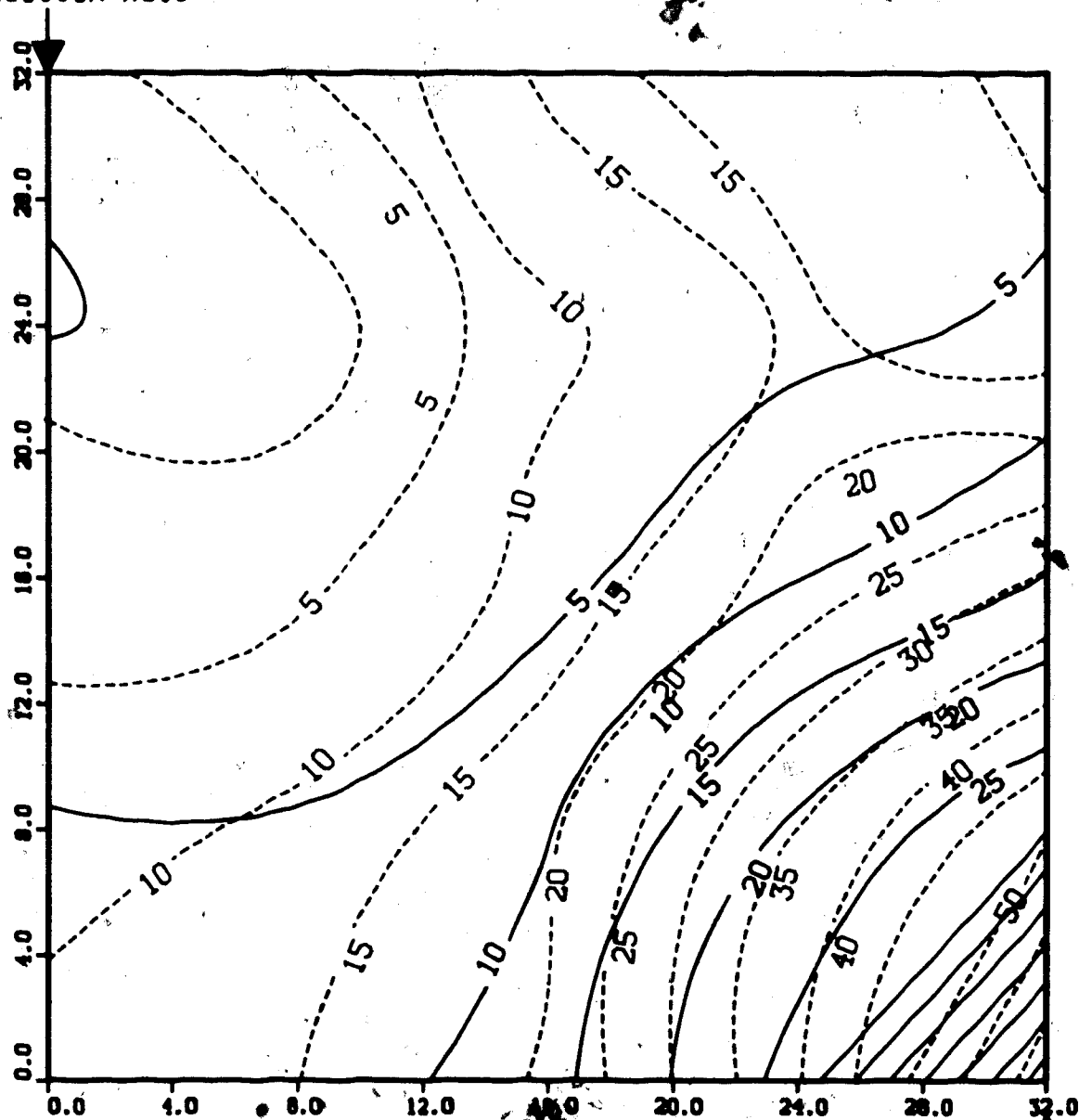
Production Well

Injection Well

Upper Model Temperature (C)
Lover Model Temperature (C)

FIGURE 65: TEMPERATURE PROFILE FOR
RUN 18: STEAM SLUG RUN IN ABERFELDY MODEL
Start of Cold Water Injection (0.30 PV Inj.)

Production Well

Injection Well
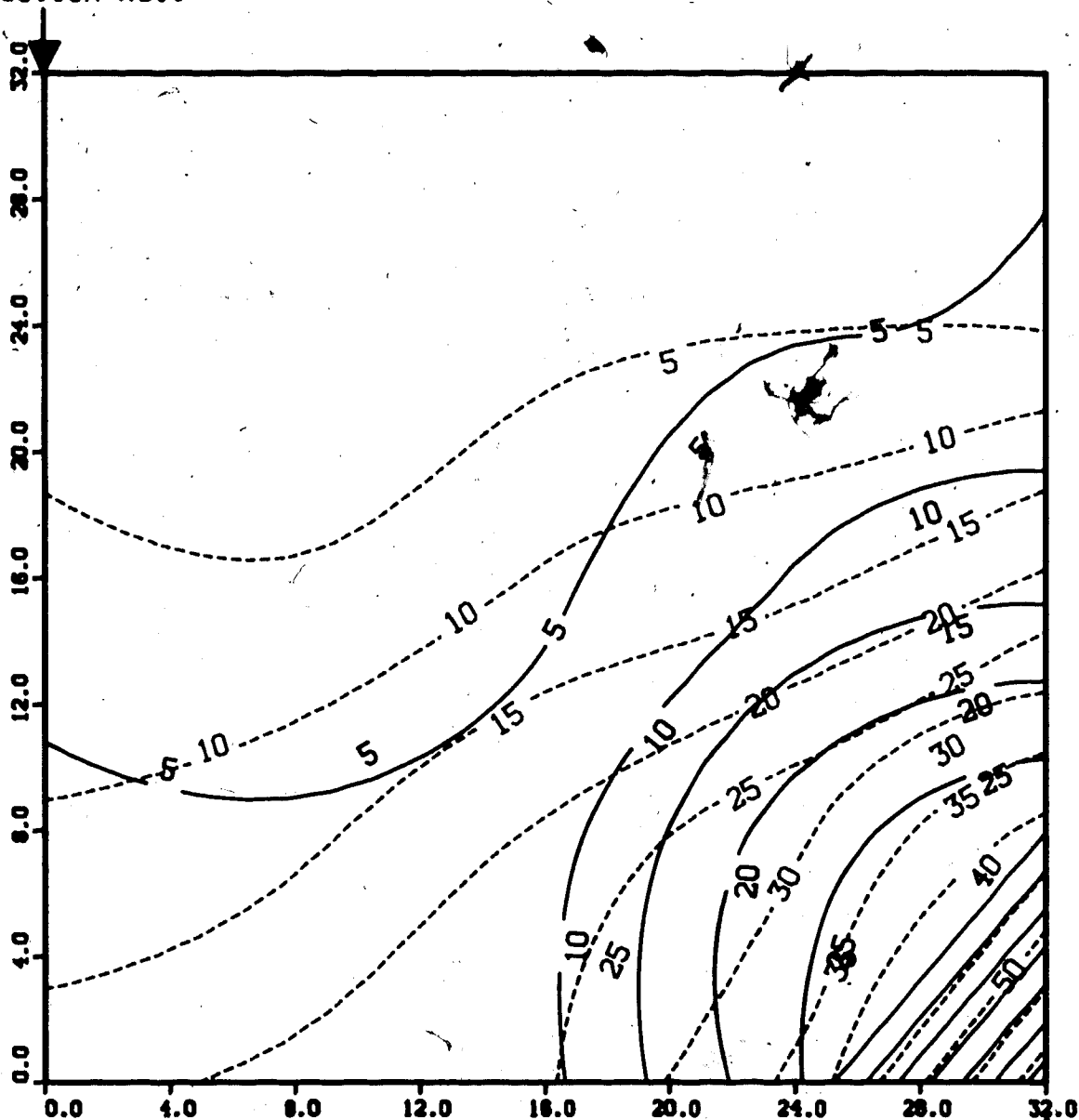
Upper Model Temperature (C)
Lower Model Temperature (C)

175
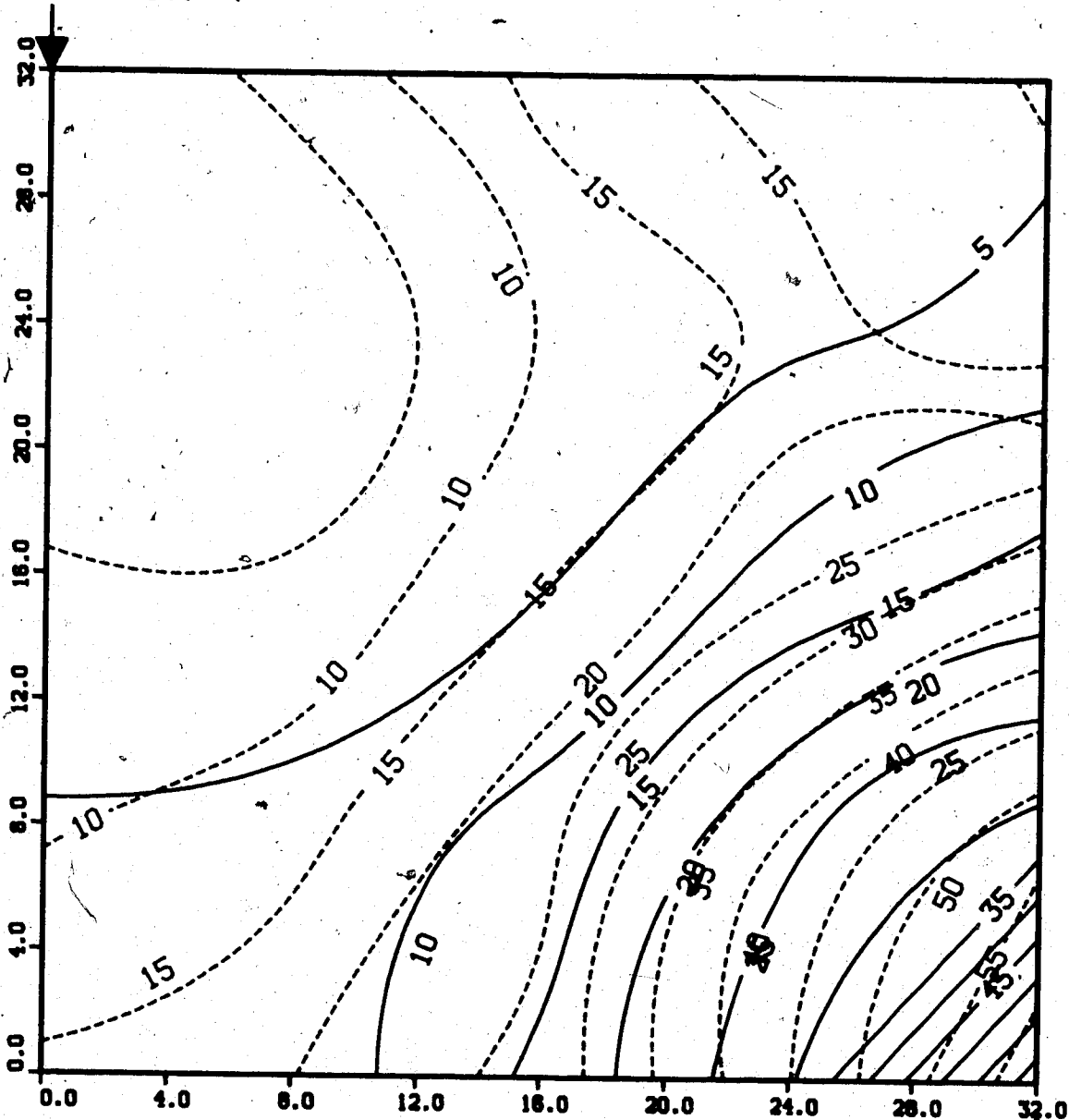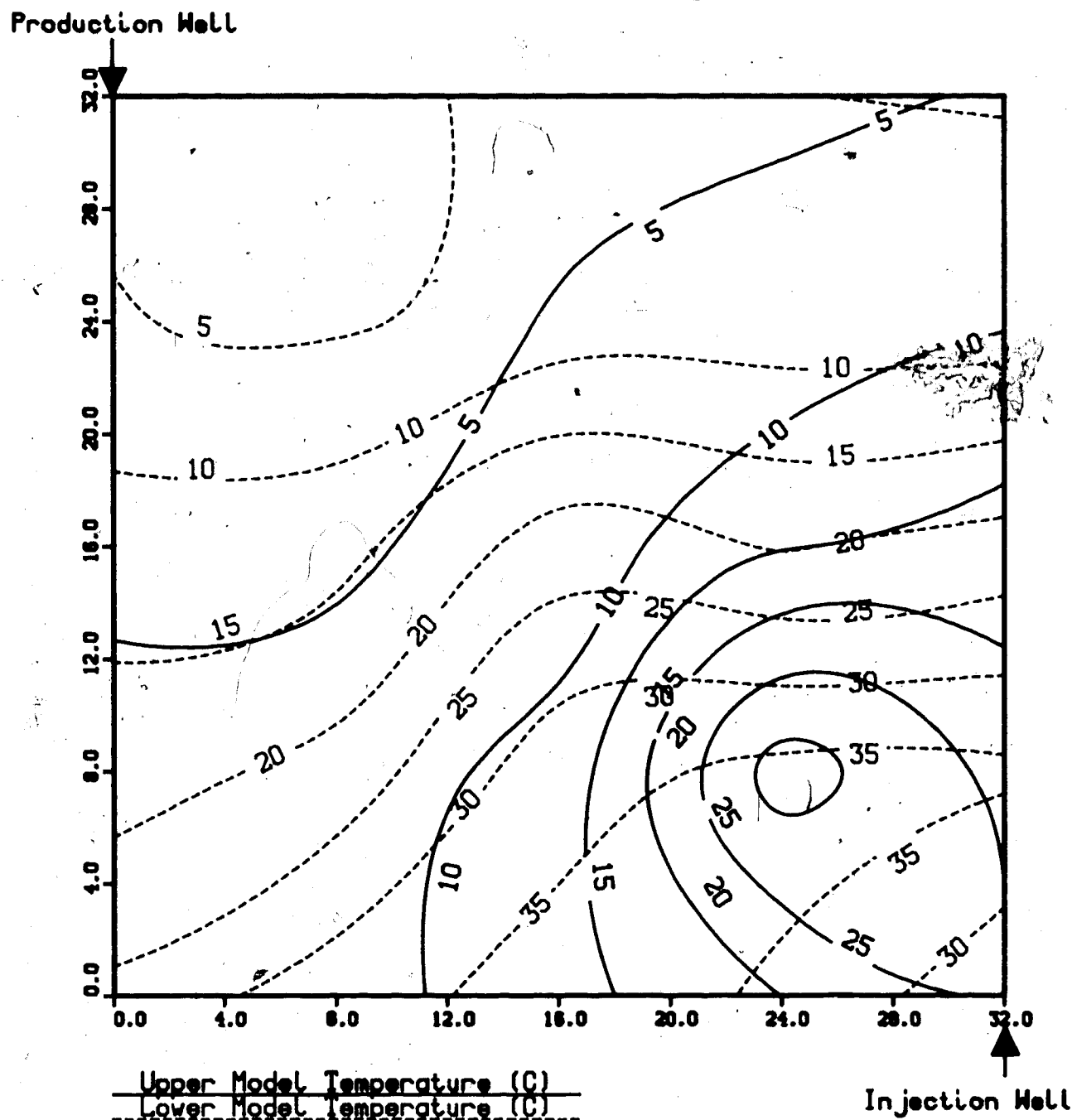

FIGURE 66: TEMPERATURE PROFILE FOR
RUN 18: STEAM SLUG RUN IN ABERFELDY MODEL
0.50 Pore Volumes Injected

FIGURE 67: TEMPERATURE PROFILE FOR
RUN 18: STEAM SLUG RUN IN ABERFELDY MODEL
0.75 Pore Volumes Injected

Production Well

Injection Well

Upper Model Temperature (C)
Lower Model Temperature (C)

FIGURE 68: TEMPERATURE PROFILE FOR
RUN 18: STEAM SLUG RUN IN ABERFELDY MODEL
1.00 Pore Volumes Injected

Production Well

Injection Well

Upper Model Temperature (C)
Lower Model Temperature (C)

FIGURE 69: TEMPERATURE PROFILE FOR
RUN 18: STEAM SLUG RUN IN ABERFELDY MODEL
1.25 Pore Volumes Injected

Production Well

Injection Well

Upper Model Temperature (C)
Lower Model Temperature (C)

FIGURE 70: TEMPERATURE PROFILE FOR
RUN 19: STEAM SLUG RUN IN ABERFELDY MODEL
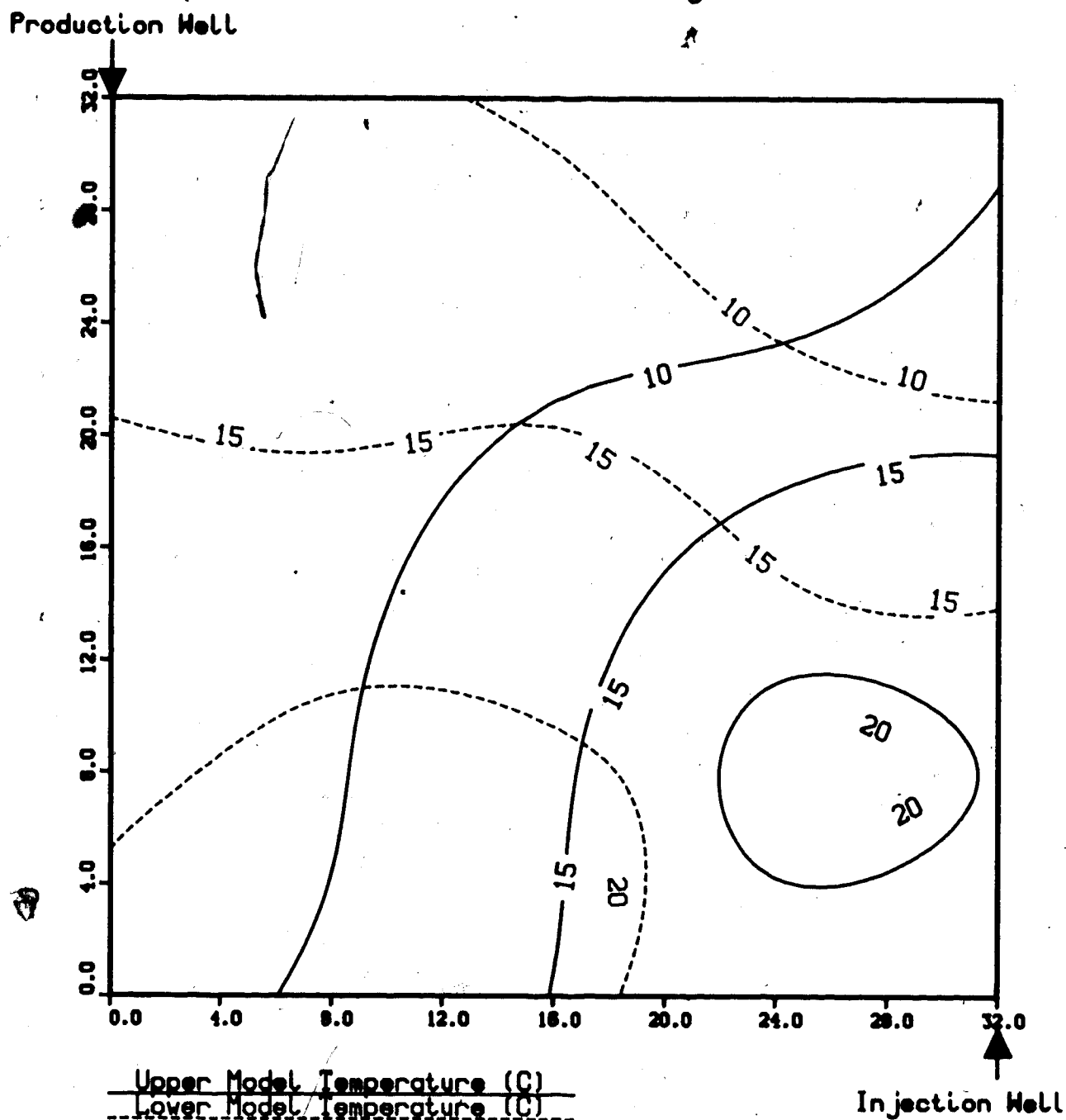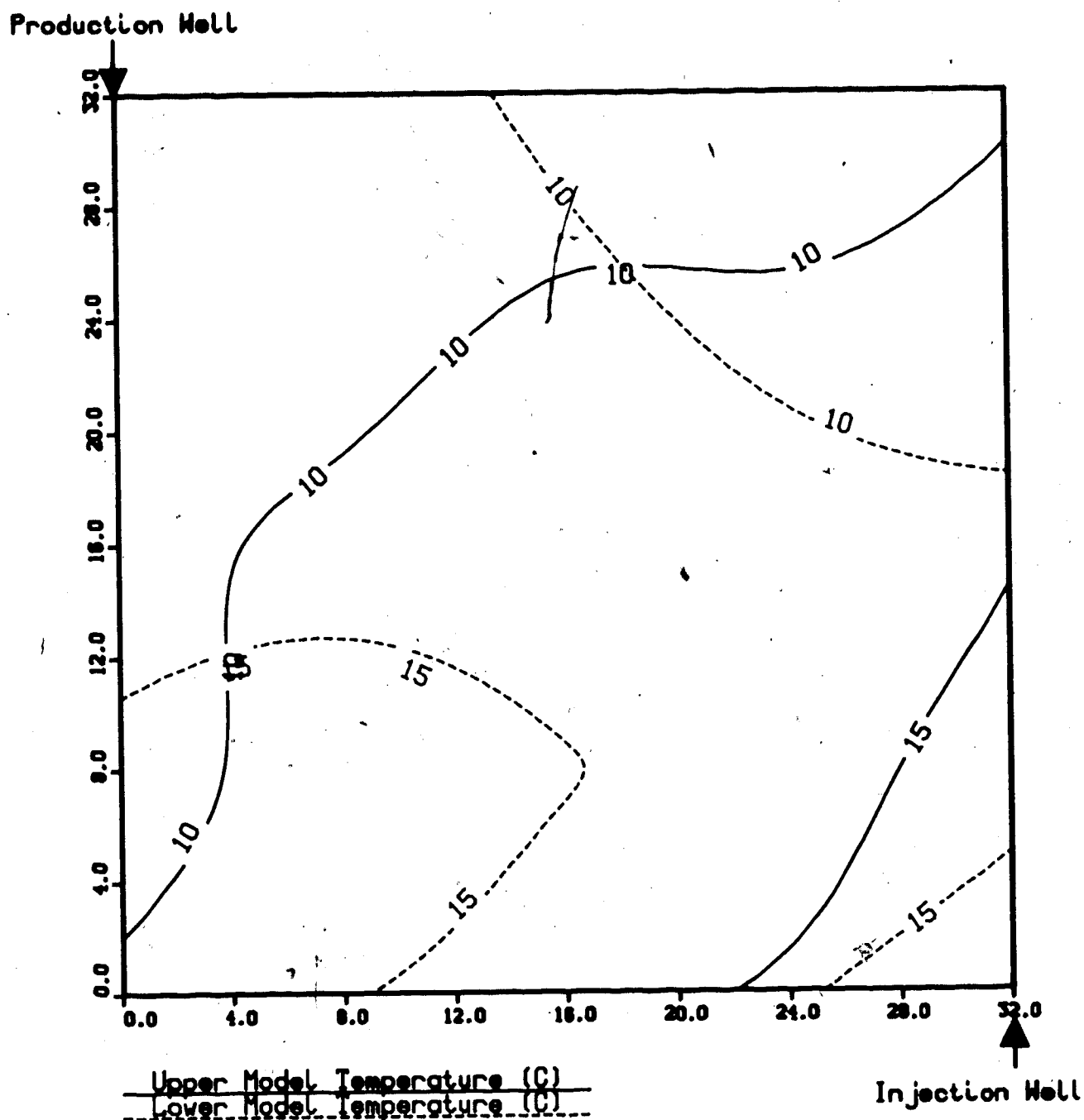### 0.25 Pore Volumes of Steam Injected

Production Well

Injection Well

Upper Model Temperature (C)
Lower Model Temperature (C)

FIGURE 71: TEMPERATURE PROFILE FOR
RUN 19: STEAM SLUG RUN IN ABERFELDY MODEL
Start of Cold Water Injection (0.28 PV Inj.)

Production Well

Injection Well

Upper Model Temperature (C)
Lower Model Temperature (C)

FIGURE 72: TEMPERATURE PROFILE FOR
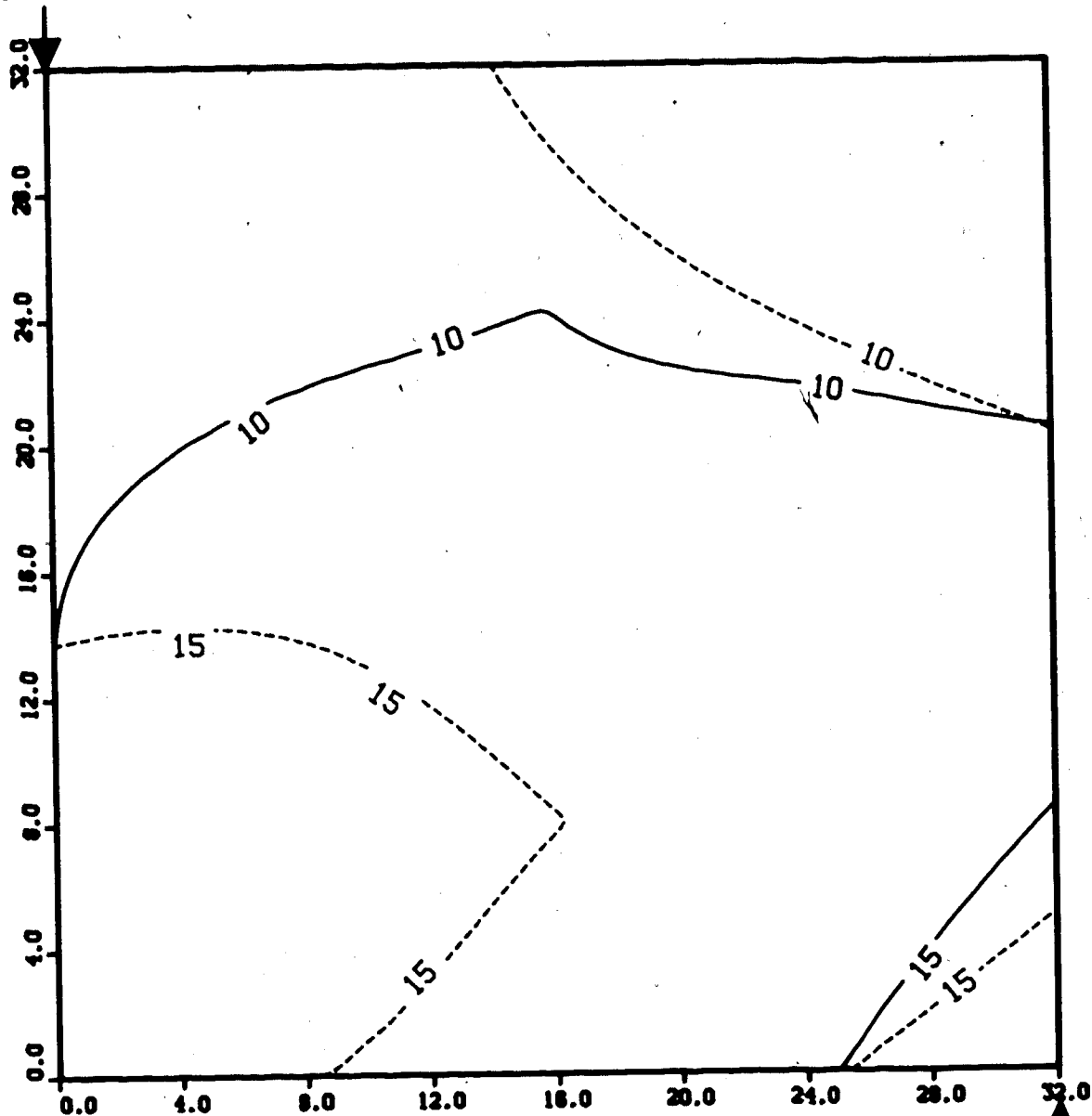## RUN 19: STEAM SLUG RUN IN ABERFELDY MODEL
0.50 Pore Volumes Injected

Production Well

Injection Well

Upper Model Temperature (C)
Lower Model Temperature (C)

FIGURE 73: TEMPERATURE PROFILE FOR
RUN 19: STEAM SLUG RUN IN ABERFELDY MODEL
0.75 Pore Volumes Injected

Production Well

Injection Well

Upper Model Temperature (C)
Lower Model Temperature (C)

FIGURE 74: TEMPERATURE PROFILE FOR
RUN 19: STEAM SLUG RUN IN ABERFELDY MODEL
1.00 Pore Volumes Injected

FIGURE 75: TEMPERATURE PROFILE FOR
RUN 19: STEAM SLUG RUN IN ABERFELDY MODEL
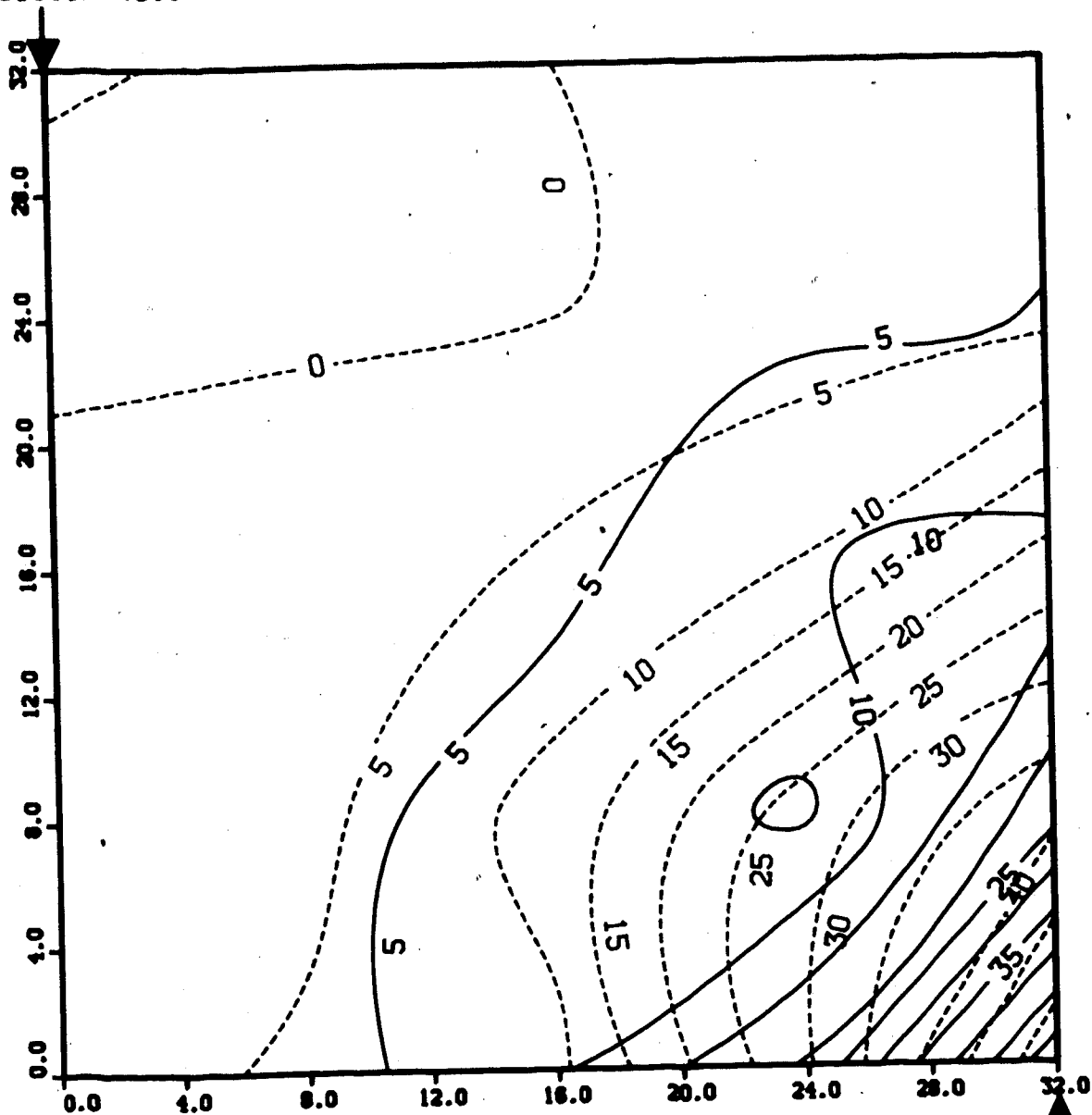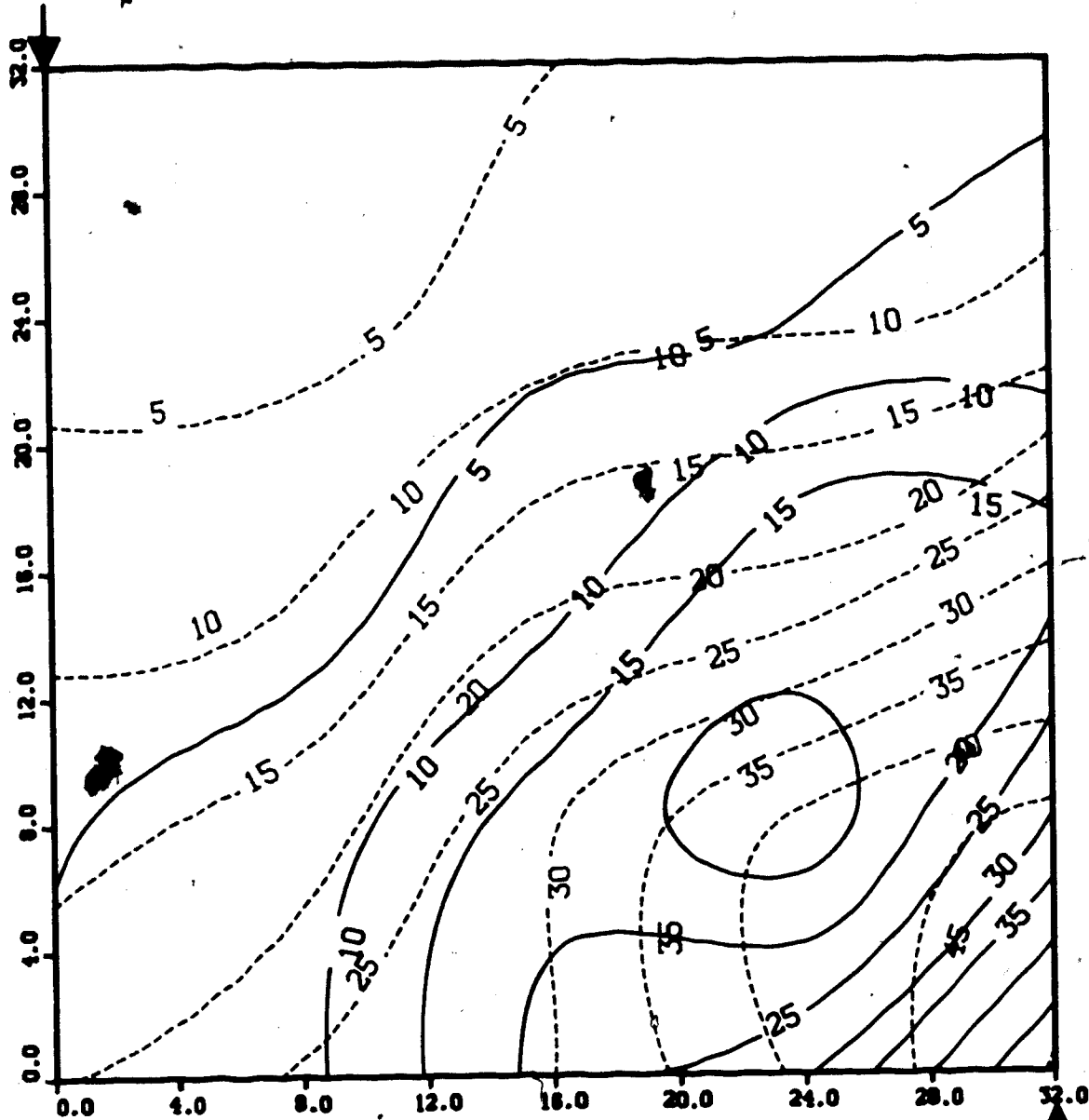### 1.25 Pore Volumes Injected

Production Well

Injection Well

Upper Model Temperature (C)
Lower Model Temperature (C)

FIGURE 76: TEMPERATURE PROFILE FOR
RUN 22: HOT WATER SLUG RUN IN ABERFELDY MODEL
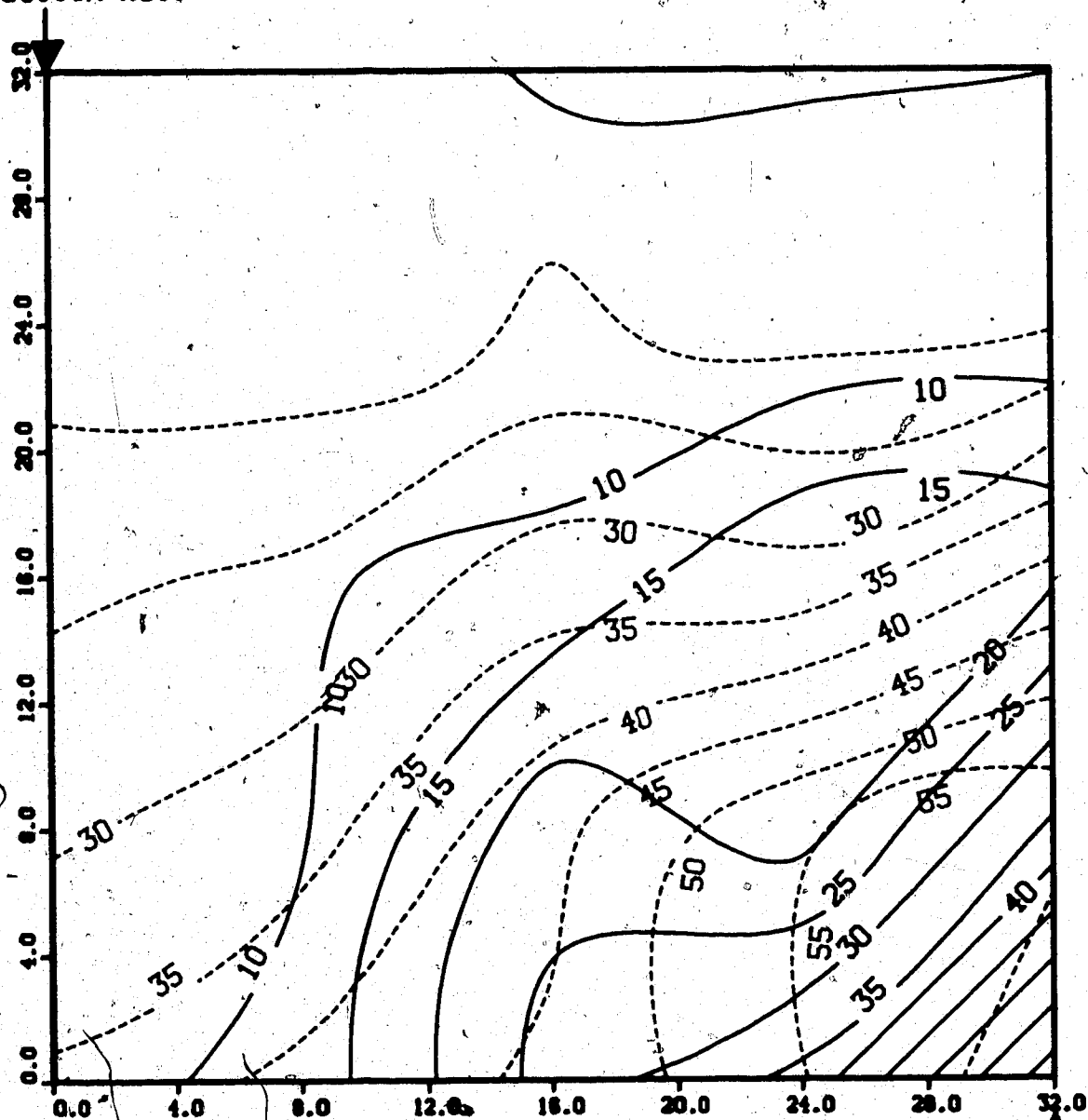### 0.25 Pore Volumes Injected

Production Well

Injection Well

Upper Model Temperature (C)
Lower Model Temperature (C)

FIGURE 77: TEMPERATURE PROFILE FOR
RUN 22: HOT WATER SLUG RUN IN ABERFELDY MODEL
0.50 Pore Volumes Injected

FIGURE 78: TEMPERATURE PROFILE FOR
RUN 22: HOT WATER SLUG RUN IN ABERFELDY MODEL
0.75 Pore Volumes Injected

FIGURE 79: TEMPERATURE PROFILE FOR
RUN 22: HOT WATER SLUG RUN IN ABERFELDY MODEL
1.00 Pore Volumes Injected

Production Well

Injection Well

Upper Model Temperature (C)
Lower Model Temperature (C)